

## Treatment of Lignin and Waste residues by Flash Pyrolysis

Final report

**Jensen, Peter Arendt; Trinh, Ngoc Trung; Dam-Johansen, Kim; Knudsen, Niels Ole; Sørensen, Hanne Risbjerg**

*Publication date:*  
2014

*Document Version*  
Publisher's PDF, also known as Version of record

[Link back to DTU Orbit](#)

*Citation (APA):*  
Jensen, P. A., Trinh, N. T., Dam-Johansen, K., Knudsen, N. O., & Sørensen, H. R. (2014). Treatment of Lignin and Waste residues by Flash Pyrolysis: Final report. Technical University of Denmark, Department of Chemical and Biochemical Engineering.

## DTU Library

Technical Information Center of Denmark

---

### General rights

Copyright and moral rights for the publications made accessible in the public portal are retained by the authors and/or other copyright owners and it is a condition of accessing publications that users recognise and abide by the legal requirements associated with these rights.

- Users may download and print one copy of any publication from the public portal for the purpose of private study or research.
- You may not further distribute the material or use it for any profit-making activity or commercial gain
- You may freely distribute the URL identifying the publication in the public portal

If you believe that this document breaches copyright please contact us providing details, and we will remove access to the work immediately and investigate your claim.

Energinet.dk project no. 010077

# **Final report: Treatment of Lignin and waste residues by flash pyrolysis**

**Peter Arendt Jensen<sup>1</sup>, Trung Ngoc Trinh<sup>1</sup>, Kim Dam-Johansen<sup>1</sup>, Niels Ole Knudsen<sup>2</sup>, Hanne Risbjerg Sørensen<sup>2</sup>.**

**\*1. Department of Chemical and Biochemical Engineering  
Technical University of Denmark  
Søltofts Plads, Building 229, DK-2800, Kgs. Lyngby, Denmark  
\*2. DONG Energy, Klippehagevej 22, 7000 Fredericia**

**CHEC no. R1401**

## Abstract

Lignin, sewage sludge and macroalgae (nonconventional biomasses) fast pyrolysis properties has been studied through experimental investigations on a laboratory Pyrolysis Centrifugal Reactor (PCR) and a model on lignin pyrolysis have been developed. Furthermore the nonconventional biomass pyrolysis properties were compared with the pyrolysis properties of wood and straw. The PCR treatment of sewage sludge provides an oil that can be used for energy purposes and a solid residue rich in organic nutrients that may be used as fertilizer product. By fast pyrolysis of lignin from the IBUS ethanol plant a bio-oil can be produced with oil yields of 36% (daf) and an oil energy recovery of 45%. This is a relatively low bio-oil yield compared to other feedstock's, however, it may increase the value of the lignin residual product, such that the lignin char is used for combustion on the ethanol plant, and the bio-oil is sold for use on heavy oil burners. The macroalgae is a promising feedstock with a high bio-oil yield of 54 wt% daf and an energy recovery of 76 % in the liquid oil. Detailed characterization of the pyrolysis products in the form of bio-oil, gas and char has been performed. The properties of slurries made of char and pyrolysis oil that potentially may be used as a feed for pressurized gasifiers has been investigated. It was shown that slurries made of mixtures of wood and bio-oil can be pumped into pressurized systems. A new patented version of the PCR rotor unit, which can be operated at low rotational speed was constructed. The new rotor systems should make it easier to make an up-scaling of the process.

## Table of contents

Abstract	2
List of appendixes	3
1.0 Introduction	4
2.0 Literature review	5
3.0 Sewage sludge pyrolysis	6
4.0 Lignin pyrolysis optimization.	7
5.0 Comparison of wood, straw, algae, and lignin pyrolysis.	9
6.0 Slurry made by bio-oil and char or wood property study	12
7.0 New rotor for the flash pyrolysis centrifuge process	13
8.0 Conclusions	14
Acknowledgement	15
References	16

## Appendices

A1. **Literature review.** Trung Ngoc Trinh, Peter Arendt Jensen, Kim Dam-Johansen.

A2. Journal Paper: Trinh, N. T.; Jensen, A. P.; Dam-Johansen. K.; Knudsen.N. O.; Sørensen, H. R.; Hvilsted. S. A. **Comparison of Lignin, Macroalgae, Wood and Straw Fast Pyrolysis.** *Energy Fuels*, **2013**, 27 (3), pp 1399–1409

A3. Journal Paper: Trinh, N. T.; Jensen, A. P.; Dam-Johansen. K.; Knudsen.N. O.; Sørensen, H. R. **Influence of the pyrolysis temperature on sewage sludge product distribution, bio-oil, and char properties.** *Energy Fuels*, **2013**, 27 (3), pp 1419–1427.

A4. Journal Paper: Trinh, N. T.; Jensen, A. P.; Sárossy, Z.; Dam-Johansen. K.; Egsgaard. H.; Knudsen.N. O.; Sørensen, H. R. **Fast pyrolysis of lignin using a pyrolysis centrifuge reactor.** *Energy Fuels*, **2013**, 27, 3802–3810.

A5. Journal Paper: Trinh, N. T.; Jensen, A. P.; Dam-Johansen. K.; Knudsen.N. O.; Sørensen, H. R.; Szabo. P. **Properties of slurries made of fast pyrolysis oil and char or beech wood.** *Biomass and Bioenergy*, **2014**, 61, 227 – 235.

A6. Report. Trung Ngoc Trinh, Peter Arendt Jensen, Kim Dam-Johansen. **Model of Lignin PCR pyrolysis.**

A7. Report. Trung Ngoc Trinh, Peter Arendt Jensen. **Preparation of Solid Rescience Sample for Fast Pyrolysis – This part is not included in the report – It is kept confidential based on a request from DONG Energy.**

A8. Report. Trung Ngoc Trinh, Peter Arendt Jensen, Kim Dam-Johansen, Rasmus Lundgaard Christensen. **Construction of new Pyrolysis Centrifuge Reactor**

## 1.0 Introduction

By flash pyrolysis organic materials can be converted to char, gas and oil. Pyrolysis is defined as the heating of materials in an atmosphere depleted of oxygen. Both biomass and many waste fractions can be pyrolyzed at temperatures from 300 to 600°C, and by using a high heating rate (flash pyrolysis) the yield of liquid (bio-oil) is maximized. The advantage of a flash pyrolysis process is that a high conversion efficiency of a solid biomass to a liquid bio-oil can be obtained, and that the process is relatively simple compared to other processes for conversion of biomass to a liquid fuel. Major limitations of the Bio-oil product is a high water content, a limited stability and that it cannot be directly treated on an oil refinery plant. In this project different types of feedstocks were pyrolyzed on a laboratory Pyrolysis Centrifuge Reactor to investigate the obtainable yields and to characterize the properties of the products of gas, char and bio-oil.

The original project objectives as described in the project proposal included studies on pyrolysis oil combustion properties, and pyrolysis of the solid product from the Renaissance process. The combustion properties of pyrolysis oil were investigated in another project (reference 1), so that subject was excluded. The obtained solid product from the Renaissance process was very difficult to grind, and it turned out that even with a complicated pretreatment, the product could not be feed to our experimental pyrolysis unit. It was therefore decided to put in more emphasis on other parts of the project, and to investigate also the pyrolysis properties of macro algae. The project objectives of the conducted project were the following:

- To investigate if lignin from the IBUS process can be converted to a pyrolysis oil and thereby a more valuable product could be provided.
- To investigate if different alternative solid fuels (including sewage sludge, algae and Renaissance solids) could be converted to bio-oil by flash pyrolysis and to determine the properties of the char, bio-oil and gas products.
- To investigate the properties of slurries made of pyrolysis oil and char with respect to viscosity and phase changes. Such slurries may be an attractive feedstock for pressurized gasification plants.

The project was conducted by performing the 7 work packets as listed below. The section 2 to 8 in this report summarizes the results of the work packets. Detailed descriptions of the project work and the results can be found in the appendixes.

WP1. Literature study. (Appendix A1)

WP2. Sewage sludge pyrolysis. (Appendix A3)

WP3. Lignin pyrolysis optimization. (Appendix A4 an A6)

WP4. Comparison of wood, straw, algae, and lignin pyrolysis. (Appendix A2)

WP5. Slurry bio-oil and char or wood property study. (Appendix A5)

WP6. Renaissance solid waste study. (Appendix A7)

WP7. New rotor for the flash pyrolysis centrifuge process. (Appendix A8)

Most of the project research work was conducted by Ph.D. student Trung Ngoc Trinh, and regular project meetings were held with participants from Inbicon and DTU. Much of the experimental work was done by using the DTU Pyrolysis Centrifuge Reactor (PCR) that has been developed in previous Ph.D. projects (Reference 1 and 2).

The PCR have a maximum input flow of approximately 2 kg solids per hour and is shown in Figure 1. The centrifugal reactor is made of stainless steel and has an inner diameter of 85 mm. The biomass is pushed

towards the heated reactor wall by a strong rotation of the gas. The gas rotation is obtained by rotation of central internal rotor. The reactor tube is electrically heated by four independent heating zones along the reactor length. The pyrolysis of solids takes place inside the reactor, whereby char, bio oil and gas are produced. Large char particles are removed by a change-in-flow separator, whereas fine char particles are collected by a cyclone. The vapor products are condensed in a bubble chamber filled with isopropanol as a condensing solvent. The temperature in the bubble chamber is controlled to be 30 – 40 °C by means of a cooling water system. Light oil fractions and aerosols are further condensed by a coalescer filled with Rockwool. A recycled gas flow maintains a desired gas residence time in the reactor. The gas is pumped back to a pre-heater and heated up to around 400 °C before being fed back to the reactor. The gas products are dried by a water condenser and filtered to remove liquid before coming to a gas meter.

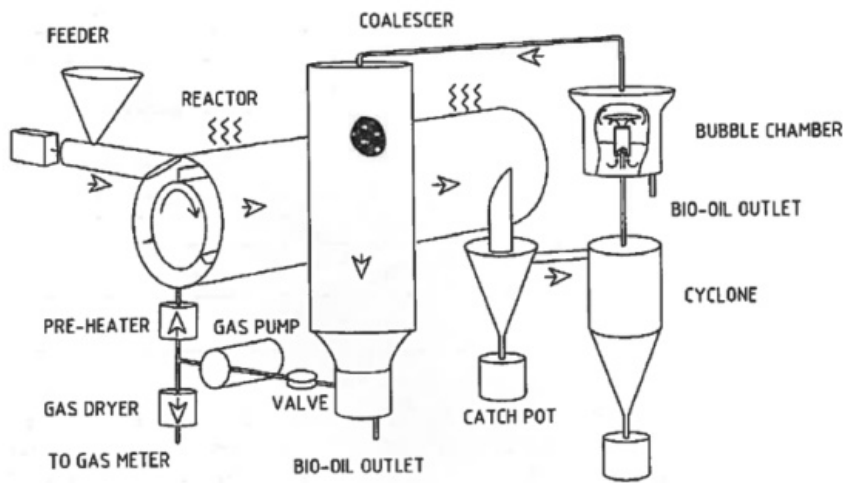


Figure 1. Sketch of the pyrolysis centrifugal reactor (PCR).

## 2.0 Literature review

As part of the project a literature review was conducted and it can be seen in Appendix 1. A short resume of the review is provided here.

The fast pyrolysis technologies are close to commercialization using different reactor types such as bubbling fluidized bed, circulating fluidized bed, and ablative reactors; however, none of the reactor types demonstrates significant superiority to the others in terms of market attractiveness and technology strength. A wide range of biomass feedstock from wood, agriculture, industrial by-products, waste products and algae have been investigated for use in the fast pyrolysis process. The reported results show that the ash content (especially the potassium content) and the feedstock lignin content influence the bio-oil yield, such that a high content of lignin and alkali metal causes a low bio-oil yield. The pyrolysis conditions (temperature, heating rate and reactor gas residence time) are found to have a strong influence on the product distribution. A reactor temperature range of 450 – 550 °C and a reactor gas residence time of less than 2 s are believed to be optimal conditions for obtaining maximum bio-oil yield. The majority of fast pyrolysis studies have been

performed using feedstock's as wood and straw, while the use of alternatives like lignin, sewage sludge and algae only have been investigated to a limited extent.

The bio-oil has been considered as a potential fuel for boilers, gas turbines and internal combustion engines. The bio-oil have a relatively high oxygen and water content, is acidic and can contain trace amounts of S, Cl and alkali metals, which makes the oil difficult to applied in engines and turbines without upgrading. Furthermore the aging (phase separation and increase of viscosity) is a challenge in the context of storage and also for the application of the bio-oil in boilers. In bio-refinery concepts producing transportation fuel from biomass, fast pyrolysis is considered a main component for densification of biomass and production of bio-oil. Possible bio-oil upgrading technologies for the production of transport fuel involve hydro treating, gasification and fluid catalytic cracking. These technologies are in the early stages of demonstration with upgrading oil properties showing promising prospects for transport fuel production.

### 3.0 Sewage sludge pyrolysis

Sewage sludge produced from wastewater treatment plant consists of a mixture of undigested organics (plant residue, paper, oils, food, and fecal material), microorganism and inorganic materials. Traditionally, the most common way to manage sewage sludge disposal are land filling and agricultural reuse. However some heavy metals are toxic to plants and may also be transferred to human through their presence in crops. Therefore, the legislation of the European Union (directive 86/278/CEE) was issued to qualify sewage sludge used in agriculture, and heavy metal threshold values must be fulfilled regarding the accumulation of sewage sludge on land. Several European countries have even stricter regulations. As a result, the disposal of sewage sludge is becoming of increasing concern in European, where sewage sludge disposal was estimated to be 40% for land filling and 37% for farmland applications in 2008. However, since environmental standards may become stricter in the future, the sewage sludge proportion used on farmland will probably be reduced. Consequently treatment cost of sludge disposal will increase.

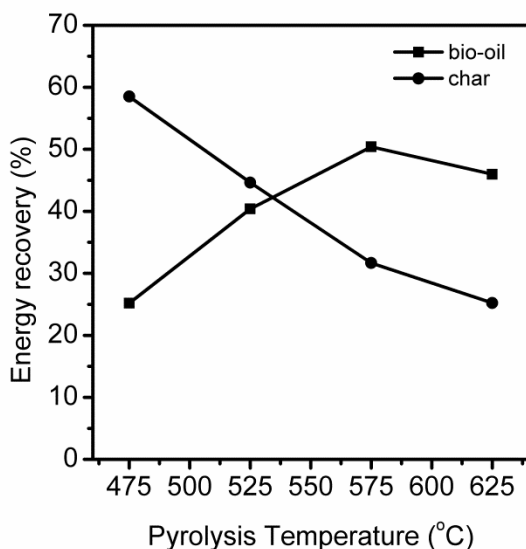


Figure 2. Energy recovered in bio-oil and char compared to the feedstock sewage sludge.

Fast pyrolysis may be used for sewage sludge treatment with the advantages of a significant reduction of the solid waste volume and production of a bio-oil that can be used as fuel. A study of the influence of reaction temperature on sewage sludge pyrolysis has been carried out using the pyrolysis centrifugal reactor at reactor temperature of 475 to 625 °C, and a detailed description of the study is provided in appendix A3. Maxima of both organic oil yield of 41 wt % dry ash free feedstock basis (daf) and a sludge oil energy recovery of 50 % were obtained at 575 °C as can be seen on Figure 2. The sludge bio oils water-insoluble fraction, molecular weight distribution, higher heating value (HHV), and thermal behaviors were found to be considerably influenced by the applied pyrolysis temperatures. The sludge oil properties obtained at the optimal reactor temperature of 575 °C were a HHV of 25.5 MJ/kg, a water-insoluble fraction of 18.7 wt%, a viscosity of 43.6 mPa.s at 40 °C, a mean molecular weight of 392 g/mol, and a metal concentrations lower than 0.14 wt % on dry basis (db). Less optimal oil properties with respect to industrial applications were observed for oil samples obtained at 475 and 625 °C. Char properties of the 575 °C sample were an ash content of 81 wt % and a HHV of 6.1 MJ/kg db. 95 % of the sewage sludge phosphorus content was recovered in the char. The solid waste amount (char compared to sludge) was reduced to 52% on bulk volume basis at the pyrolysis temperature of 575 °C. It is seen that the fast pyrolysis process provides a promising method to reduce cost for land filling, and produce a bio-oil that can be used as a fuel. It should however be kept in mind, that high sulfur and nitrogen contents of the sludge oil compared to conventional bio-oil from biomass may limit the further industrial applications of the sludge oil. Also, If the sludge char is used on farmland, the heavy metal contents of the char limited by Directive 86/278/CEE1 must be adequately taken into account.

#### **4.0 Lignin pyrolysis optimization.**

Lignin, with a typical biomass weight fraction of 15 – 33 wt%, is the second most abundant component in biomass and may account for up to 40 % of the biomass energy content. Today lignin is mainly produced by the pulp and paper industry. In the near future it is expected also to appear as a by-product in the second generation bio-ethanol industry based on lignocelluloses. Previously a fluid bed study on fast pyrolysis of lignin have shown that a liquid oil can be produced. However plugging/agglomeration in the fuel feeder system of a fluidized bed reactor and condenser have been observed and is probably due to a low melting point of lignin and high molecular mass of lignin oil. The objectives of this work were to provide detailed knowledge on the lignin fast pyrolysis process and the properties of the obtained lignin bio-oil.

In this study the pyrolysis properties of the residual lignin rich product from Inbicons IBUS process (ethanol production based on straw feed) were investigated by experiments on the PCR apparatus (Further details of the study can be found in Appendix 4). The IBUS product had a water content of 4.7 wt % (as received) an ash content of 12 wt % (db) and a lignin content of 69.5 wt % (db) and other organic constituents of 18,5 wt % (db) (mainly cellulose). For simplicity reasons this product is in the following called lignin. It was investigated how changes in operation conditions as feeding rate, reactor temperature and reactor gas residence time influenced the obtained yields and the product properties.

The IBUS lignin sample was successfully pyrolyzed on the pyrolysis centrifuge reactor without plugging of the feeder equipment. However, after an hour of operation plugging at the cooling nozzle in the condenser unit was observed. The effects of pyrolysis conditions as temperature (450 – 600 °C), reactor gas residence time (0.9 and 4.2 s) and feed rate (4.1 - 10.4 g/min) on trends of product yields were reasonably similar to those of wood fast pyrolysis. On Figure 3 is shown the yields of organics (the bio-oil yield excluding water),



reaction water, char and gas. The optimal pyrolysis conditions of the lignin PCR to obtain a maximal organic oil yield is a temperature of 550 °C, a short reactor gas residence time (0.8 s) and a feed rate of 5.6 g/min. The maximal organic oil yield of 34 wt% db (bio-oil yield of 43 wt% db) is, however, much lower than that of wood fast pyrolysis. The bio oil energetic yield compared to the fuel was 45%. The char contained nearly all the ash from the lignin and the char produced at 550°C had an ash content of 27 wt% (db). The produced gas was mainly containing CO and CO<sub>2</sub> with smaller amounts of hydrogen and hydrocarbons. GC-MS analysis of the lignin oil was conducted. Yields of syringol, p-vinylguaiacol and o-guaiacol obtained maximal values of 0.62, 0.67 and 0.38 wt% db, at a pyrolysis temperature of 500 - 550 °C. Molecular mass distributions indicate that a higher content of the lignin derivatives is formed in the lower temperature range (450 – 500 °C) and formation of oligomer/polymer species taken place above 600 °C.

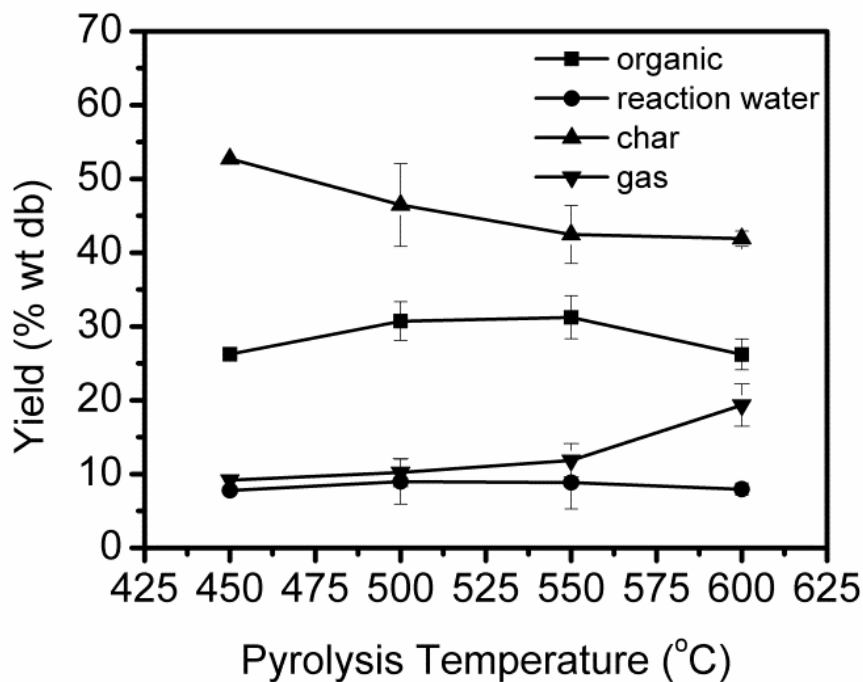


Figure 3: The effect of pyrolysis temperature at a reactor gas residence time of  $0.8 \pm 0.07$  s and a feed rate of 10.4 g/min.

A model study on the behavior of the lignin in the PCR pyrolysis unit was also conducted (see appendix 6). A previously developed model (reference 1) was used and only feedstock related parameters were changed based on kinetic values of lignin pyrolysis found in the literature. An acceptable fit between simulated and experimental data is obtained by only modification of the ratio of gas and char selectivity  $\lambda_g$  to be 0.55. ( $\lambda_g$  is the fraction of gas relative to char of the products that are not oil). The modification of the  $\lambda_g$  value is probably influenced by the presence of alkali and by using lignin from a bio-ethanol plant.

The established model was used to investigate the effect of changed rotational speed and thereby changed centrifugal acceleration (G) influence on the product fractions. An increasing G from  $2 \cdot 10^3$  to  $15 \cdot 10^3$  results in considerable changes in product fractions: a decrease of unconverted lignin fraction and an increase of organic oil, pyrolytic char and gas fractions. However, the change is less important with a further increasing of G. The optimal temperature for maximal organic oil fraction moves down with an increase of the G value. The organic fraction enhances from 4 to 33 wt% daf when G increases from  $2 \cdot 10^3$  to  $15 \cdot 10^3$  and obtain 39

wt% daf at a G of  $30 \times 10^3$ . The result suggests that a maximal organic oil yield of approximately 39 wt% daf could be obtained. However this is not confirmed by experiments.

In order to obtain an organic oil yield above 30 wt% daf (an unconverted lignin fraction below 12 wt% daf at 550 °C) the lignin PCR pyrolysis has to operate with a G of above  $10 \times 10^3$ . It means that the rotor has to perform at least 14800 rpm to obtain such an organic oil yield. The heat transfer rate of the biomass is considerably influenced by the centrifugal force in the current reactor, leading to the consequence that a high organic oil yield can only be obtained if a high rotor speed is used. Thereby the reactor probably has a problem which is related to a high rotor speed when it is scaled up. A new reactor design that could use both mechanical and centrifugal forces for increasing the heat transfer rate and this should be considered to obtain a high degree of organic oil yield with a low rotor speed.

## 5.0 Comparison of wood, straw, algae, and lignin pyrolysis.

Wood is often found to be an optimal feedstock for fast pyrolysis with a bio-oil yield of 70 – 75 wt%. However, other biomass feedstock may be applicable. Among the forms of non-conventional biomass: macroalgae and lignin may be attractive materials for fast pyrolysis due to their low price and non-competitiveness with food crops. Macroalgae may be cultivated in coastal areas. The species *Ulva lactuca* is considered as a potential macroalgae for production of biofuel. It can produce up to 45 tons dry/ha/year and has a content of carbohydrates of up to 60% of dry matter. Macroalgae contain large amounts of alkali metals and chlorides. This will probably cause slagging, fouling and aerosol formation related problems if the algae is used directly in combustion and gasification plants. However, fast pyrolysis is performed at a lower temperature compared to combustion or gasification, and it is believed that the process may not be significantly disturbed by the ash. On till this project was conducted studies of macroalgae pyrolysis were only carried out in low heating rate fixed bed reactors. These studies showed bio-oil yields of 15 – 52 wt% daf (13 – 47 wt% on as received basis) obtained from various macroalgae species. Fixed bed reactors have a lower solids heating rate than that of fast pyrolysis reactors, and this probably lead to a low bio-oil yield when macroalgae is pyrolyzed in a fixed bed reactor.

A comparative study of the fast pyrolysis properties of wood and straw with lignin and algae to investigate obtainable yields as well as product properties were conducted. The pyrolysis of the wood, straw, lignin and algae were performed on the PCR with constant operation conditions: an rotor speed of 8870 rpm, a gas residence time of 0.8 second, a total experimental time of 60 - 90 minutes, feed consumption of 350 - 750 g biomass for each run, feeding rates of 340 – 990 g/hour and a reactor temperature of 550°C. The experiments were performed twice with each biomass to ensure reproducible pyrolysis products determinations. The operations of the PCR reactor using wood, straw and algae were smooth and the experiments were carried out within 90 minutes operation time. While the operation of the PCR using lignin was difficult, blocking of the nozzle connecting the cyclone and the bubble chamber took place after 60 minutes operation. The obtained mass balance closures were in the range of 96 – 99 wt% for the wood, straw and algae PCR pyrolysis and 93 – 96 wt% for the lignin PCR pyrolysis tests.

A comparison of the energy fraction recovered in bio-oil, char and gas is shown in Figure 4. The pyrolysis of macroalgae showed promising results with a bio-oil yield of 65 %wt daf (organic oil yield of 54 wt% daf) and an energy recovery in the bio-oil of 76%. These results are similar to that of wood pyrolysis. The pyrolysis of lignin has a lower bio-oil yield of 47 wt% daf and an energy recovery in the bio-oil of 45 %. The

obtained oils and chars were carefully characterized with respect to pH, density, elemental contents, HHV, thermal behaviors, phase separation and aging, elemental contents, and particle size distribution. The HHV of wood, straw, lignin and algae oils were 24.0, 23.7, 29.7 and 25.7 MJ/kg db, respectively. The lignin and macroalgae oil properties were relatively different to those of the straw and wood bio-oil with respect to carbon content, oxygen content, HHV, mean molecular weight, viscosity and thermal behavior. The main differences observed in the product yields and the bio-oil properties can be partially explained by differences of the biomass compositions especially differences with respect to ash, lignin and extractive contents of the biomasses.

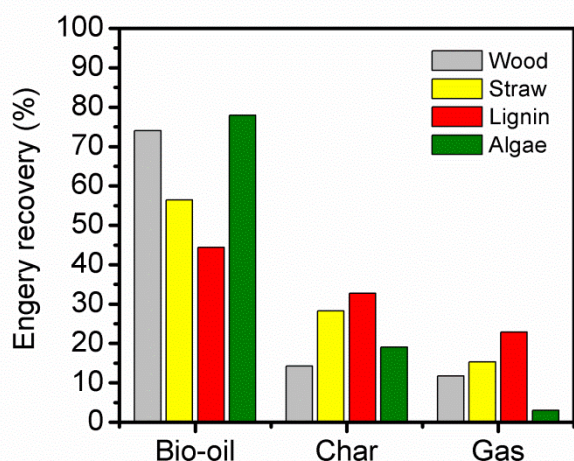


Figure 4. The energy recovery of gas, bio-oil and char.

High feedstock ash content do not disturb the PCR process. Most metals are contained in the chars at a pyrolysis temperature of 550 °C. Therefore when the bio-oils are used in boilers or gasifiers slagging, fouling and aerosol formation problems will be minimized. The relative distribution based on concentration measurements on char and bio-oil are shown in Table 1. In the case of Cl and S a large fraction can be found in the bio-oil. For the other elements the maximum fraction found in the bio oil is 8.1 %K in the case of straw.

Table 1. The relative element distribution in bio-oil and char of ash forming species (%)

		Al	Ca	Fe	K	Mg	Na	P	Si	Cl	S
Wood	Char	97.5	93.6	96.7	95.0	96.0	nd	98.2	99.2	nd	nd
	Bio-oil	nd	0.5	3.1	3.9	1.7	nd	nd	nd	nd	nd
Straw	Char	97.2	97.6	95.2	90.1	95.1	98.8	96.9	98.4	66.5	52.9
	Bio-oil	3.0	2.3	5.8	8.1	4.4	7.5	2.0	0.3	6.1	38.2
Lignin	Char	99.9	92.2	92.4	93.5	96.1	95.1	94.1	93.2	54.3	25.0
	Bio-oil	nd	nd	0.3	4.0	nd	4.7	nd	nd	nd	43.8
Algae	Char	93.9	97.1	90.6	97.9	96.1	94.3	95.2	93.2	40.0	75.3
	Bio-oil	0.2	0.1	2.6	0.9	3.2	4.1	1.0	nd	25.0	15.8

*nd: not detected in the samples*

With a high proportion of small size particles, a HHV of 19 – 21 MJ/kg db and being almost free of chloride and sulfur, the wood char and lignin char are considered also as promising fuels for gasification or combustion, whereas the straw and algae chars contained high amounts of macro nutrients such as N, P, K, N, S, Ca, and especially the high K content could makes these chars valuable as raw materials for fertilizer production or to be used as bio-chars that can be spread on fields.

## 6.0 Slurry made by bio-oil and char or wood property study

Entrained flow pressurized gasification has the capability for converting biomass to a tar free syngas with a high concentration of H<sub>2</sub> and CO. However, feeding solid biomass with a low bulk density into a pressurized system is not trivial. Because of the low bulk density a high amount of auxiliary gases shall be used in the hoppers and this cause a reduced efficiency, high complexities and high costs. In contrast pumping of viscous slurries such as bio-oil-char mixtures into a high pressure reactor is known to be a simple and reliable technology and a large auxiliary gas supply is not needed. Very limited published knowledge on slurries made of char and bio-oil form fast pyrolysis reactors are available, so the objective of this study was to provide data on slurries of char or wood and bio-oil with respect to material properties that are important with respect to pumping of the slurries.

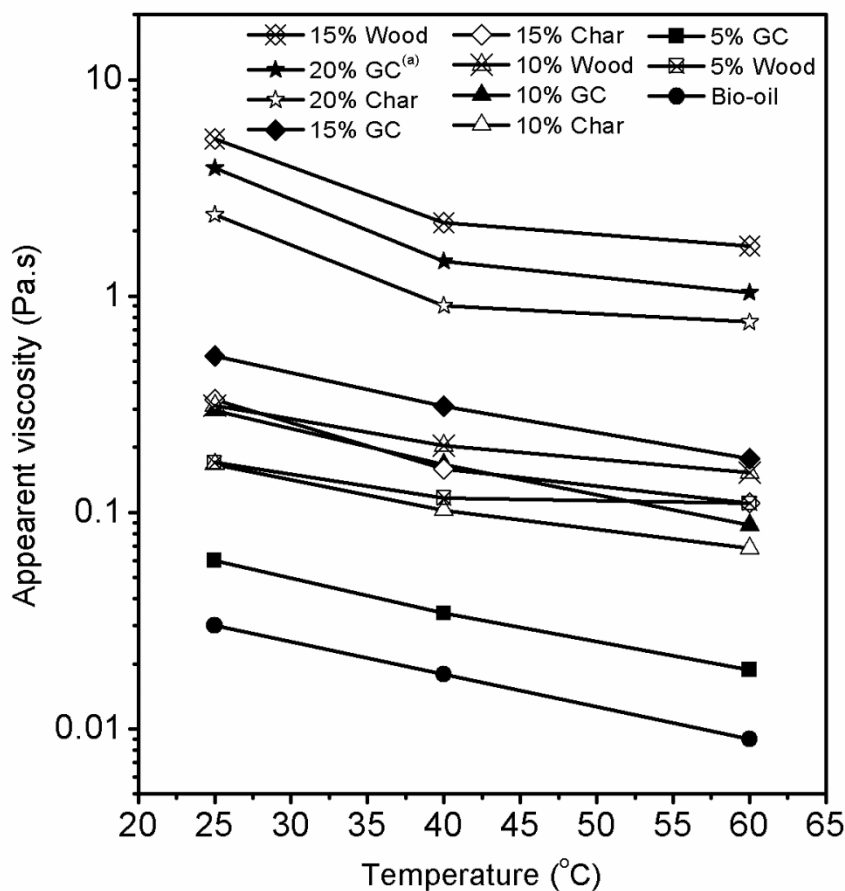


Figure. 6: Effect of temperature and char loading on bioslurry viscosity at shear rate of 100 s<sup>-1</sup> (a Ground char)

Bio-oil and char were produced from pyrolysis of Danish beech wood on the PCR at a reactor temperature of 550 °C (for further information see Appendix 5). Bioslurry samples with the wood, char and ground char were prepared by mixing the bio-oil with the wood, char and ground char, respectively. No additional additives were used. The slurry samples were investigated with respect to phase changes, viscosity and composition. Phase transitions of the bioslurry samples with solid loadings in a range of 0 to 25 wt% was evaluated based on visual observations. The slurry samples with char and grinded char transform from liquid to a past phase (liquid-paste form) at the solid loadings of 15 – 20 wt% and become totally solid phase when the solid concentration is 25 wt%. The wood slurry samples have the phase transition at lower solid loadings. 10 - 15 wt% wood solids for the liquid to paste change and 15 – 20 wt% for the paste to solid change. It is anticipated that the solid forms are difficult or even impossible to pump into a pressurized reactor. Thus the slurries with solid char loading of 20 wt% and wood solid loading of 15 wt% were used for rheological and pump properties investigations. The apparent viscosities (determined at a shear rate of 100 s<sup>-1</sup>) of the slurry samples shown on Figure 6 were found to be considerably impacted by solid loading level (0 - 20 wt%) and temperature (25 - 60 °C). At similar solid levels the char slurry sample had the lowest viscosity and the wood sample the highest viscosity. A slurry sample with 20 wt% ground char loading (having a d<sub>80</sub> of 118 µm) was pumped successfully into a pressurized chamber (0 - 6 bar) while plugging appeared when using a slurry sample with 15 wt% char loading (having a d<sub>80</sub> of 276 µm). Thus, the ground char slurry might be considered as a promising feedstock for feeding by pumping into a pressurized gasifier.

The slurries with 5 - 20 wt% solid loading obtained volumetric energy densities of 21 - 23 GJ/m<sup>3</sup>, consequently resulting in a considerable volumetric energy densification (4.5 - 5 times) when compared to beech wood. The wood, char and ground char slurry samples had similar C, H and O contents to that of the beech wood and had low N (< 0.4 wt%), S (< 0.03 wt%) and Cl (< 0.1 wt%) contents.

## 7.0 New rotor for the flash pyrolysis centrifuge process

The PCR concept was developed in an attempt to obtain some advantages when compared to fluid bed reactors or circulating fluid bed reactors. The PCR can use relatively large particle sizes due to a high heating rate created by a strong centrifuge force, the PCR is a compact design, and it can use a low flow rate of carrier gas and still obtain a short gas residence time. The compact design may also make it possible to construct a mobile pyrolysis unit that can operate in-situ on a farmer's field. Thus a high power consumption for grinding biomass to a suitable size and a large amount of recirculated carrier gas is probably reduced in this concept. A first version of the lab scale PCR set-up was developed by Bech et al.<sup>1</sup> The PCR set-up is described in section 1 and Figure 1 of this report.

The old PCR rotor construction is a cylindrical core that has attached three blades that induce a strong rotation of the gas in the reactor, the gas then moves the particles and thereby create a centrifugal force on the particles. The typical rotation level used during the PCR experiments has been 15000 - 18000 rpm. However, when the PCR unit is up-scaled to a larger size a higher amount of rotational energy will be stored in the reactor during operation. Also the risk of feeding of stones or metal pieces to the reactor will increase. This could be dangerous if the rotor crashes and the stored rotational energy is released to the surroundings. A new design of the rotor system is therefore proposed, that can obtain a high force on the biomass particles towards the reactor wall, and thereby high heat transfer at low rotational speed. A patent is submitted by DTU on the proposed new design. In Figure 7 the new design is shown. The Rotor contains three rows of movable blades that during rotation of the rotor press the biomass particles towards the heated reactor tube.

Because the blades have a much higher weight than the single particles they ensures a higher force on the particle against the wall during operation (at a similar rpm level). A detailed description of the reactor system can be found in Appendix 8.

The new lab scale PCR set-up has been constructed and is ready for trial tests. It is expected that the new PCR can obtain a high bio-oil yield at a low rotor speed (less than 2800 rpm). In a new project (*Advanced technology foundation project. Biomass for the 21st century: Integrated bio refining technologies for shipping fuels and bio based chemicals*) the new PCR set up is used for lignin pyrolysis, and it has been observed to function well at low rotational speeds.

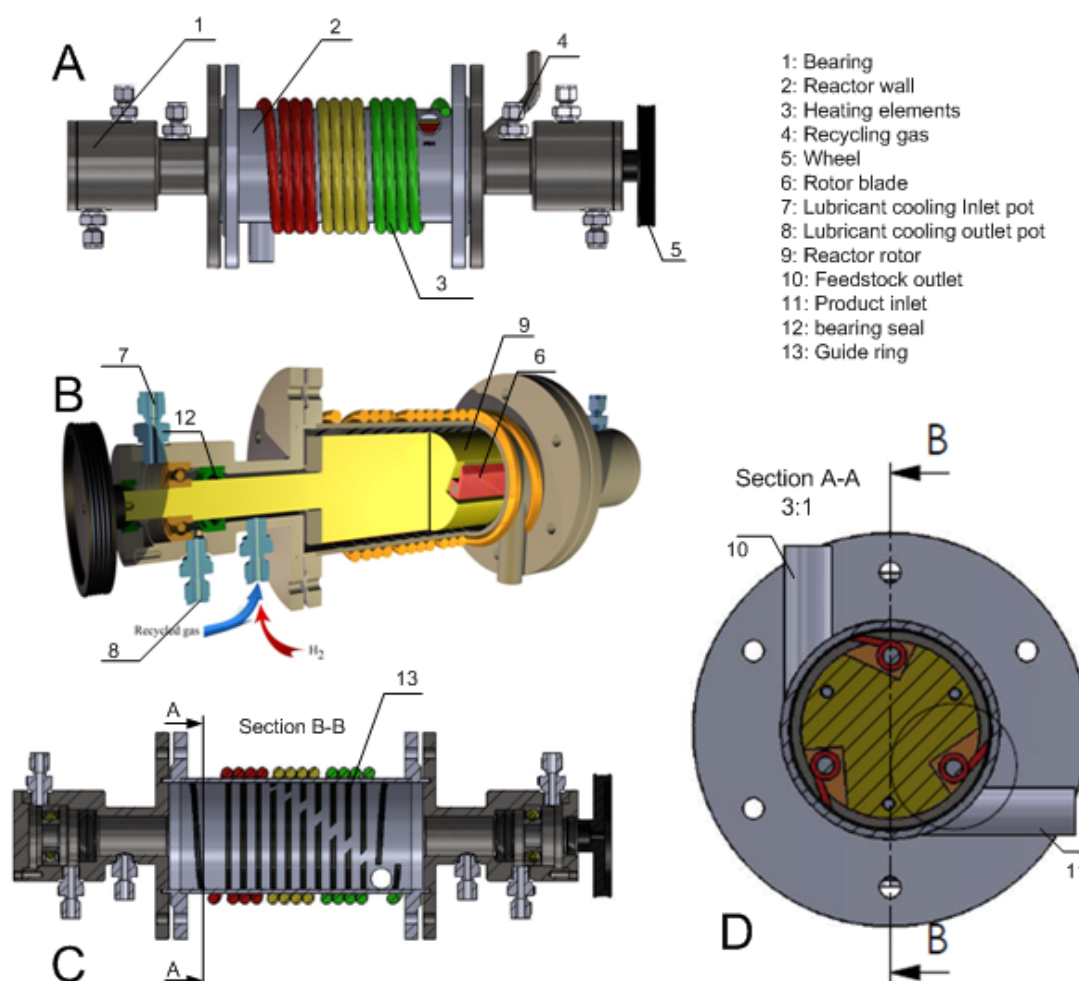


Figure 7: Modified pyrolysis centrifuge reactor (A: overview of PCR reactor, B: cut-view of reactor, C: cut-view of reactor without rotor (front view), D: cut-view of reactor (side view)).

## 8.0 Conclusions

Understanding of nonconventional biomass (lignin, sewage sludge, macroalgae) fast pyrolysis properties has been gained through literature studies, experimental investigations on a laboratory Pyrolysis Centrifugal Reactor (PCR) and mathematical modeling. Furthermore slurries made of char and pyrolysis oil has been

investigated. Such slurries may be used as a feed for pressurized gasifiers. A new version of the PCR rotor unit that can be operated at low rotational speeds was constructed. This makes it easier to up scale the PCR process to pilot and commercial scale units.

A study of the influence of reaction temperature on sewage sludge pyrolysis was done using the PCR at reactor temperature of 475 to 625 °C. Maxima of both organic oil yield of 41 wt % dry ash free feedstock basis (daf) and sludge oil energy recovery of 50 % were obtained at 575 °C. The sewage sludge waste bulk volume (the char compared to the sludge) was reduced with 52 % by pyrolysis at 575 °C. The PCR treatment of sewage sludge thereby provides a bio-oil that can be used for energy purposes and a solid residue rich in inorganic nutrients that may be used as a fertilizer product.

In this study the pyrolysis properties of the residual lignin rich product from Inbicons IBUS process (ethanol production based on straw feed) were investigated by experiments on the PCR apparatus. The optimal pyrolysis conditions of the lignin PCR to obtain a maximal organic oil yield is a temperature of 550 °C, a short reactor gas residence time (0.8 s) and a relatively low feed rate of 5.6 g/min. The maximal organic oil yield of 34 wt% db (bio-oil yield of 43 wt% db) is; however, lower than that of wood fast pyrolysis. A mathematical model of the PCR pyrolysis was modified so the lignin pyrolysis process could be modelled. An acceptable fit between simulated and experimental data is obtained with only small modifications. The model showed that a maximum pressure of the lignin particles toward the hot reactor surface shall be used to obtain a maximum oil yield. The fast PCR pyrolysis of the lignin rich residual product may increase the value of the lignin residual product, such that the lignin char is used for combustion on the local ethanol plant, and the bio-oil is sold externally for use on heavy oil burners.

A broad range of different feed stocks were pyrolyzed on the PCR making comparisons of the obtainable yields and product properties possible. The lignin and sewage sludge PCR pyrolysis provided organic oil yields of 36 and 41 wt% daf, and oil energy recoveries of 45 and 50%, respectively. While the macroalgae PCR pyrolysis showed promising results with an organic oil yield of 54 wt% daf and an oil energy recovery of 76 %. The lignin, macroalgae and sewage sludge (nonconventional biomasses) have bio-oil properties with a lower oxygen content, higher viscosity, higher HHV and higher mean molecular mass when compared to those of conventional biomasses (wood and straw). A high level of nitrogen (4.0 – 9.6 wt% db) and sulfur (0.8 – 1.8 wt% db) contents of macroalgae and sewage sludge oils compared to conventional bio-oil was observed. The lignin, macroalgae and sewage sludge bio-oils obtain low metal concentrations (less than 0.27 wt%). High-ash biomasses do not disturb the PCR process. Almost all metals are contained in the chars at the pyrolysis temperature of 550 - 575 °C. Therefore when the bio-oils are used in boilers or gasifiers slagging, fouling and aerosol formation problems will probably be minimized. The pyrolysis temperature has a considerable effect on the product distributions of the lignin and sewage sludge PCR pyrolysis, as well as on their bio-oil properties with respect to molecular mass distribution, identified GC-MS component compositions, water-insoluble fraction, viscosity, and HHV. With a high proportion of small size particles, a HHV of 21 MJ/kg db and being almost free of chloride and sulfur, the lignin char is considered as a promising fuel for gasification or combustion, whereas macroalgae and sewage sludge chars contained high amounts of ash (67 - 80 wt% db) and high amounts of macronutrients of N, P, K, Mg, S and Ca that could make the chars most valuable as raw materials for fertilizer production.

As part of this project it was originally the plan to conduct flash pyrolysis studies on solid residue from the Renaissance process. Because of problems with the laboratory pyrolysis of the solid residue this part was not conducted..

The fast pyrolysis process can be used as a process to densify biomass. A bio-oil is mixed with char or wood to produce a bioslurry that may be used as feedstock for a pressurized gasification process. Bio slurries of bio-oil produced from wood PCR pyrolysis mixed with wood, char or grinded char obtained a volume energy density of 21 – 23 GJ/m<sup>3</sup> and a volumetric energy densification factor of 4.5 – 5 (when compared to beech wood). Their apparent viscosities were significantly influenced by solid loading (0 – 20 wt %) and temperature (25 – 60 °C). The slurry samples with 10 wt% char (having d<sub>80</sub> of 276 µm) and 20 wt% grinded char (having d<sub>80</sub> of 118 µm) were successfully pumped into a pressurized reactor (0 - 6 bar).

The old PCR rotor construction is a cylindrical core that has attached three blades, which induce a strong rotation of the gas in the reactor. The gas then moves the particles and thereby creates a centrifugal force on the particles. The typical rotation level used during the PCR experiments has been 15000 - 18000 rpm. However, when the PCR unit is up-scaled to a larger size a higher amount of rotational energy will be stored in the reactor during operation, which makes the equipment dangerous. A new patented PCR rotor have therefore been developed that can operate at lower speeds.

### **Acknowledgment**

Financial support of this project and the PhD study of Trung Ngoc Trinh by DONG energy A/S, Energinet.dk and DTU are gratefully acknowledged.

### **References**

1. Norazana Ibrahim, Bio-oil from Flash Pyrolysis of Agricultural Residues. Ph.D. thesis. Technical University of Denmark, Department of Chemical Engineering. 2012.
2. Niels Bech. In Situ Flash Pyrolysis of Straw. Ph.D. thesis. Technical University of Denmark, Department of Chemical Engineering. 2008.
3. Trung Ngoc Trin. Fast Pyrolysis of lignin, macroalgae and sewage sludge. Ph.D. thesis. Technical University of Denmark, Department of Chemical Engineering. 2013.



February, 2014, DTU

**Appendix A1**  
**Literature review**

**Energinet.dk project no. 010077**

**Treatment of Lignin and waste residues by flash pyrolysis**

**Trung Ngoc Trinh, Peter Arendt Jensen, Kim Dam-Johansen.**

*Department of Chemical and Biochemical Engineering*

Technical University of Denmark

Søltofts Plads, Building 229, DK-2800 Lyngby, Denmark

**CHEC no. R1401**

The combustion of fossil fuel is responsible for the majority of CO<sub>2</sub> emissions which causes the climate change effects. The demand for energy is continuously rising and is dependent on the use fossil fuel. As an alternative, bio-oil is an option; it is CO<sub>2</sub> neutral and has low sulfur content. Furthermore, when used in diesel engines bio-oil is found to generate less than 50% NO<sub>x</sub> emission and lower SO<sub>x</sub> emissions compared to diesel oil.<sup>1,2</sup>

Biomass fast pyrolysis is a thermal conversion technology. Pyrolysis of biomass at temperatures of 400 - 600 °C without presence of oxygen can convert a large fraction of the biomass to bio-oil, and smaller fractions of char and gas. Wood, agricultural waste, industrial residues and algae are used as feedstock for fast pyrolysis processes. Bio-oil yield obtained from various biomass sources are in the range of 30 – 75 wt% db.<sup>3-18</sup> Wood, having a low ash content and a lignin content of 20 – 30 wt% db,<sup>3,8-10,14,18</sup> is often found to provide a high bio-oil yield of 70 – 75 wt% db.<sup>1,3</sup>

Bio-oil typically contains 20 – 35 wt% water, has a pH of 2 – 4, a higher heating value (HHV) of 16 – 19 MJ/kg and viscosity of 10 – 100mPa.s,<sup>1,20,21</sup> and sometimes shows instabilities (phase separation and oil viscosity increase by aging).<sup>22,23</sup> Although bio-oil is close to being a commercial fuel used for combustion in boilers, diesel engines and gas turbines, it is still not a realistic candidate as a substitute for liquid transportation fuel. The use of bio-oil upgrading technologies may be the next step to produce a liquid transportation fuel or chemicals.

Bio-oil is not a realistic liquid transportation fuel substitution and bio-oil upgrading is a next important step for liquid transportation fuel production or chemical production. Bio-oil is possible for use as a feedstock for gasification processes to produce syngas (and then synthesize syngas into transport fuel) or for hydrodeoxygenation (HDO) or catalyst cracking processes to produce bio-crude oil for conventional refinery.

## **2.1 Fast pyrolysis technology development**

### **2.1.1 Principle of fast pyrolysis**

Pyrolysis is defined as thermal decompositions of biomass in an absence of oxygen whereby vapors, char and gas products are formed. The temperature, the heating rate and vapor residence time have significant influence on the product yield distribution of the pyrolysis process. By applying the different temperatures, heating rates and vapor residence times, the pyrolysis processes can be divided into torrefaction, carbonization, intermediate pyrolysis and fast pyrolysis which show the different gases, liquids and solid

yields<sup>2</sup> (see Table 2.1). Torrefaction favors char production (a char yield of 80 wt% db) and takes place at a low process temperature (290 °C), low heating rate (less than 100K/s) and long vapor residence (10 – 60 minutes)<sup>20</sup> whereas fast pyrolysis is used to obtain a maximum liquid product yield (a yield of 68 – 75 wt% db). Fast pyrolysis typically takes place at a reactor temperature of 500°C, a high heating rate (1000 K/s) and a vapor residence time of 1 s.

Table 2.1: Typical product yields obtained by different modes of pyrolysis of wood<sup>20</sup>

Mode	Conditions	Product yields (wt% db)		
		Liquid	Solid	Gas
Fast pyrolysis	~ 500°C, short hot vapor residence time ~ 1s	75%	12%	13%
Intermediate	~ 500°C, short hot vapor residence time ~ 10 -30 s	50% in 2 phases	25%	25%
Carbonization (slow)	~ 400°C, long vapor residence hours ~ days	30%	35%	35%
Torrefaction (slow)	~ 290°C, solid residence time ~ 10 – 60 mins	0% unless condensed, then up to 5%	80%	20%

In order to produce a high bio-oil yield (often 68 – 75 wt% db as received for woody biomass) the fast pyrolysis processes are designed to meet the following requirements:

- A high heating rate and high heat transfer rate to biomass particles. Typically the fast pyrolysis technology can obtain feedstock heating rates of 700 – 10,000 K/s.
- Short hot gas residence times (typically less than 2 s) to minimize secondary reactions which cause a reduction of the bio-oil yield. This is achieved by short gas reactor residence time and rapid cooling of vapors to collect the oil.
- The reactor temperature is controlled in the range of 450 – 600 °C. At this stage the decomposition of biomass is complete and secondary reactions of the bio-oil to form gas and char is minimized.
- 

### 2.1.2 Reactor configuration

Fast pyrolysis processes have been explored over the last twenty five years and many different fast pyrolysis reactor types, such as bubbling fluidized bed, circulating fluidized bed, rotary cone, auger and ablative reactor technologies, have been developed, and are close to commercialization.<sup>2,24</sup> The main difference among these technologies is that the reactors use different heat transfer methods to gain a high heating rate. In order to reduce feedstock preparation cost and the operational cost of fast pyrolysis while at the same time obtaining a high bio-oil yield, the reactor designs attempt to

meet the following targets: using large particle sizes and low flow rate of carrier gas while still maintaining a gas residence time of less than 2 s and a high biomass particles heating rate. The advantages and disadvantages of each reactor design have been reviewed by Bulter et al.<sup>23</sup> and Bridgwater<sup>2</sup> and they are summarized in this report.

### **Bubbling fluidized bed reactor (BFB)**

This technology is well understood and is based on the commercial development of the petrochemical fluidized bed technology. The typical configuration of a BFB pyrolysis process is shown in Figure 2.1. The BFB is simple in construction and operation and provides good heat transfer to biomass particles due to a high solids density of heat carrier (sand) in the reactor. The process often results in a good performance with a high bio-oil yield of 70 – 75 wt% db for wood.<sup>1,9</sup> The residence time of solid particles and vapors is controlled by the fluidized gas flow rate and as a result a high level of inert gas flow is required for the operation of the fluidized bed, leading to high operational cost. The vapor has a lower residence time than solid particles. Char does not accumulate in the reactor bed and is separated by cyclones. Vapor is condensed in a cooling system to form bio-oil. Gas is often recycled into the reactor to maintain a given reactor gas residence time and extra gas is combusted to provide heat to the reactor.

The early development of this process was carried out at the University of Waterloo (Canada)<sup>20</sup> and many companies have selected the process for further development. Examples are Dynamotive who has built the two largest plants of 100 t/d and 200 t/d in Canada<sup>24</sup> and Wellman, Biomass Engineering Ltd, Union Fenosa, Fortum and Metso who have been operating pilot plants with capacities of 75 – 400 kg/h.<sup>23</sup>

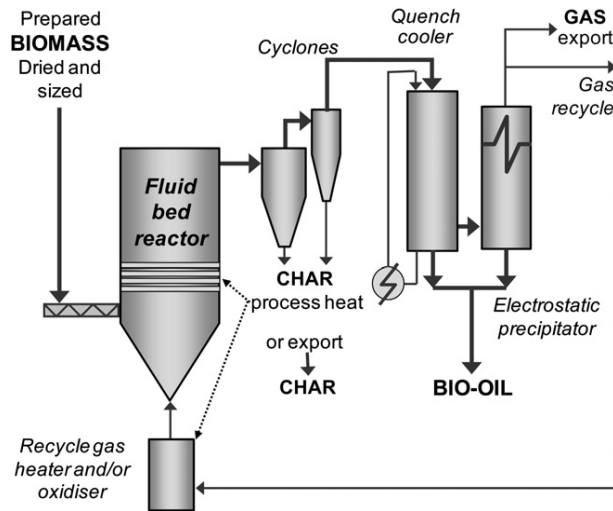


Figure 2.1: The bubbling fluid bed reactor<sup>20</sup>

### Circulating fluidized bed reactors (CFB)

Basically, the circulating fluidized bed reactors have many features similar to those of the bubbling fluidized bed reactor. The principle of a CFB is shown in Figure 2.2. Biomass is fed to a reactor where there is extensive contact between the hot sand and the biomass particles. The sand, char and vapors are discharged from the reactor. The char and sand are collected in cyclones and the char then combusted in a combustor. In order to maintain a constant pyrolysis temperature in the reactor, heat for the pyrolysis reactor is supplied by recirculation of heated sand. The process is usually performed at a high gas flow rate, and this probably causes an elevated char content in the collected bio-oil. The advantage of this technology is that it is suitable for very large throughputs compared to other technologies.<sup>20</sup>

The first circulating fluidized bed reactor was developed by the University of Western Ontario in the late 1970s and early 1980s. So far Ensyn (Canada) has several plants with the largest facility having a capacity of 100 t/d in Renfrew (Canada). They have built nine plants in Malaysia and their largest plant of 400 t/d in Alberta (Canada).<sup>24</sup> Enverget, a joint venture between Honeywell/UOP and Ensyn, and a Finnish consortium involving Metso, Fortum, UPM and VTT operated some CFB plants with capacities of several tons per day for research purposes. Enverget attempts to improve the bio-oil to be a blend feedstock for refining processes. The Finnish consortium is focused on developing a new concept based on CHP/bio-oil production.<sup>24</sup>

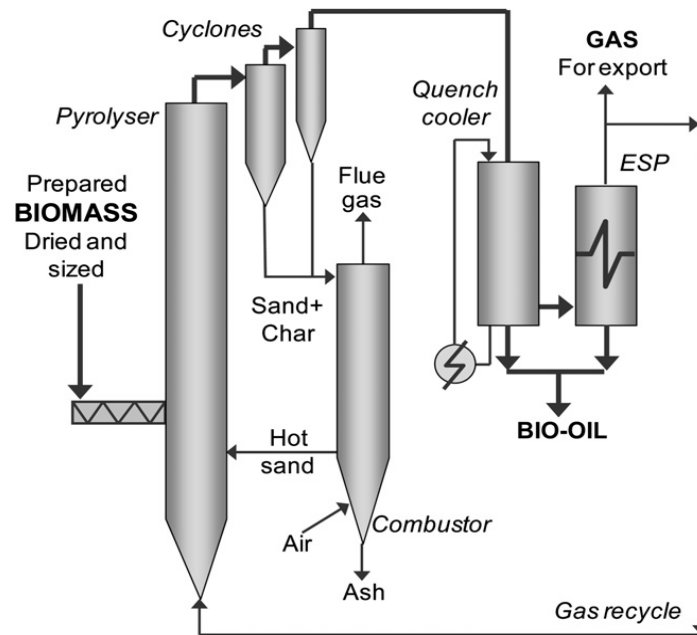


Figure 2.2: The circulating fluid bed reactor<sup>20</sup>

### Rotary cone reactor (RCR)

The rotary cone reactor was developed based on a new concept where the requirement for carrier gas in the pyrolysis reactor is much less than for the bubbling fluid bed or the circulating fluidized bed technology and this probably reduces the operational cost of the process. The original version of the technology was developed on a merely ablative principle by Twente University (The Netherlands) and later on the technology was modified to a sand-transported-bed-rotating cone reactor.<sup>19</sup> The principle of the technology is shown in Figure 2.3. Biomass and hot sand are in contact inside the reactor based on mechanical mixing which leads to fast heating of the biomass particles. Char separation, char combustion, circulation of heated sand and bio-oil collection of the rotary cone technology are similar to that of the circulating fluidized bed technology.

BTG (The Netherlands) has continued the development of the original version thereby achieving significant improvement of the technology. Operational experiences with the rotary cone reactor were obtained in a 50 t/d plant in Malaysia that was commissioned in 2006, but the plant is no longer in operation.<sup>24</sup> A 120 t/d plant was erected to produce bio-oil, electricity, process stream and aqueous organic acids from industrial wastes<sup>23</sup> and is operated under an EMPYRO European project (in Hengelo, the Netherlands).<sup>24</sup>

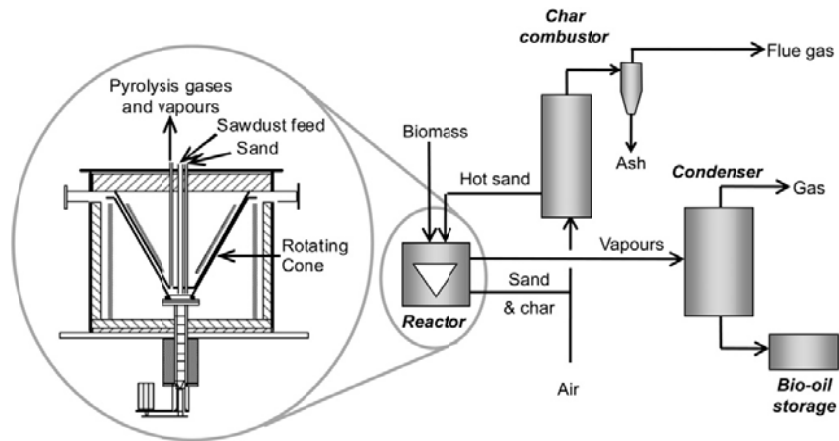


Figure 2.3: The rotator cone reactor<sup>20</sup>

### Auger bed reactor (ABR)

ABRI-Tech has developed the auger bed reactor which uses a hot, high-density heat carrier (sand) to convert biomass into bio-oil.<sup>24</sup> The reactor design is an improvement of the Lurgi-Ruhrgas twin-screw mixer reactor.<sup>24</sup> The principal of the reactor concept is shown in Figure 2.4. Biomass is mixed with hot sand in a double-screw reactor where the pyrolysis reaction takes place. Through the contact between hot sand and biomass the biomass particles can gain a high heating rate. The sand is heated in a combustor and recycled into the screw reactor as in the rotary cone reactor.

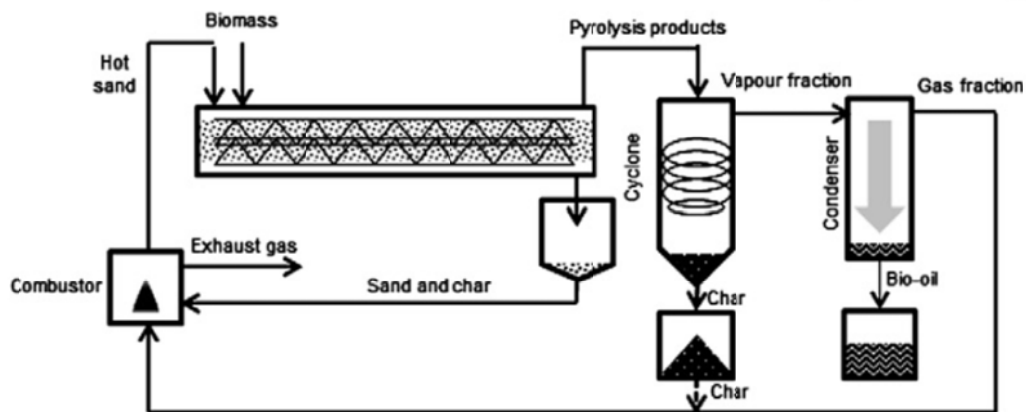


Figure 2.4: The auger reactor<sup>2</sup>

ARBI-Tech is in the process of building plants between 1 t/d and 50 t/d and they are expected to be operational soon.<sup>24</sup> So far Renewable Oil International LLC (USA) has built 4 units, which use the ABR technology, and the largest capacity is 4.8 t/d. In comparison a 12 t/d plant has been constructed by Lurgi-Ruhrgas using a twin screw mixer pyrolysis reactor for bioslurry production that is used as a feedstock for gasification process.<sup>24</sup>

## Ablative reactor

As the fundamental principle of an ablative reactor, the pyrolysis reactions are limited by the rate of heat transfer through a biomass particle. Consequently, small particles are required in most of the fast pyrolysis technologies and the ablative reactor is another concept used for fast pyrolysis. By pressing the material particles down on a hot surface and moving them across the heated surface of a reactor wall, the biomass gains a rapid heating rate. The biomass is pressed onto the hot reactor wall by mechanic and/or centrifuge force. Thus the biomass melts when it reaches 400 – 600 °C and consequently formation of char and vapours that can be condensed to form liquid and gases. The principle of the ablative reactor is shown in Figure 2.5. The pyrolysis products are collected in the same way as in the other processes. Relatively large biomass particles can be used because the reaction rates are not limited by internal heat transfer in the biomass particles.<sup>24</sup> However, since heat carriers are not used in this technology, the heat supply to the reactor surface could limit the capacity of the reactor. The main advantage of this concept is a compact design that does not use heat carriers and where the flow of inert gas is much lower compared to BFR or CBR and that the technology can also treat relatively large biomass particles.

An early design of an ablative reactor was developed by the CNRS laboratories in Nancy (France).<sup>25</sup> The National Renewable Energy Laboratory (NREL) and Aston University (USA) continued the development of the reactor type<sup>25</sup> obtaining bio-oil yields of 70 – 75 wt% for wood. PyTec built a 6 t/d plant in northern Germany in 2006 and a 50 t/d plant designed for the use of bio-oil for power generation.<sup>20,24</sup>

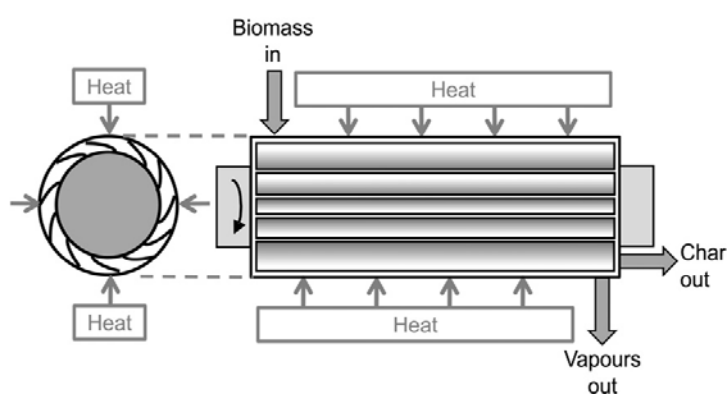


Figure 2.5: The ablative reactor<sup>19</sup>




### 2.1.3 Global status of the technology

Different fast pyrolysis processes have been developed globally and successful projects involving the bubbling fluidized bed technology, the circulating fluidized bed technology, the rotary cone technology, the auger technology and the ablative technology are close to commercialization (see Table 2.2 and Table 2.3). Some plants with capacities from a few t/d up to 200 t/d are successfully operated. The largest plant of 400 t/d was announced to be erected in Alberta with Tolko Industries LTD.<sup>26a</sup>

Table 2.2: Overview of fast pyrolysis reactor characteristics for bio-oil production<sup>26b</sup>

Property	Status <sup>a</sup>	Bio-oil yield on db	Complexity	Feed size specification	Inert gas requirements	Specific reactor size	Scale up	Gas quality
Fluid bed	Commercial	75 wt %	Medium	High	High	Medium	Easy	Low
Circulating fluid bed	Commercial	75 wt %	High	High	High	Medium	Easy	Low
Rotating cone	Demonstration	70 wt %	High	High	Low	Low	Medium	High
Entrained flow	Laboratory	60 wt %	Medium	High	High	Medium	Easy	Low
Ablative	Laboratory	75 wt %	High	Low	Low	Low	Difficult	High
Screw	Pilot	60 wt %	Medium	Medium	Low	Low	Medium	High
Vacuum	None	60 wt %	High	Low	Low	High	Difficult	Medium

<sup>a</sup>commercial (48-400t/d), demonstration (4.8 - 28t/d), laboratory (0.48-4.8t/d), pilot (24-480kg/d)

 Favourable feature       Moderate feature       Unfavourable feature

The overview of fast pyrolysis reactor characteristics for bio-oil production is summarized in table 2.2.<sup>26b</sup> Although the fluid bed reactor, circulating bed reactor and ablative reactor obtain the highest bio-oil yield (75 wt% db), they are some disadvantages such as small particle size and large inner gas requirements for the fluid bed reactor, circulating bed reactor or difficulty in scaling up for ablative reactor. The commercial potential of these reactors has been evaluated in the context of market attractiveness<sup>27</sup> and technology strength.<sup>26b,27</sup> The evaluation indicates that although no single reactor has emerged as being vastly superior to the others certain reactors are more suitable for commercial operation than the others, bubbling fluid beds, circulating fluid beds and auger pyrolysis reactors show a strong technology basis and high market attractiveness. Ensyn Technologies, Dynamotive, KIT, BTG, Pytec, Kurgi and ROI are leading companies in developing fast pyrolysis technologies. So far the fast pyrolysis of biomass is at an early stage of commercialization and it may be a focal point of the biorefinery concept.

Table 2.3: Summary of the technology developments of fast pyrolysis (2011)<sup>24</sup>

Company	Technology	Developments
Dynamotive	BFB	Several plants, largest is 200 t/d, West Lorne (CAN)
Ensyn	CFB	Several plants, largest is 100 t/d plant, Renfrew (CAN); construction of 400 t/d plant in High Level, Alberta (CAN) with Tolko Industries Ltd. announced; construction of nine plants in Malaysia by 2015 announced
BTG	RCR	120 t/d plant in Hengolo (NLD) announced production of bio-oil, electricity, organic acids
B-O H N.V.	RCR	Largest plant is 12 t/d. Construction of two 5 t/d plants underway in NLD and BEL
Biomass Eng.	BFB	4.8 t/d facility (UGBR)
KIT/Lurgi	Auger	12 t/d pilot plant in Karlsruhe (GER)
Pytec	Ablative	6 t/d plant (GER), 50 t/d plant is being designed
ARBI-Tech	Auger	50 t/d plant to be commissioned soon
ROI	M.Auger	Four units. Largest 4.8 t/d
Agri-Therm	M. BFB	Three units constructed 1 – 10 t/d
Anhui Yineng	M.FB	Three 14 t/d units constructed (CHI)
Metso Consort	CFB	7.2 t/d pilot plant, Tampere (FIN)

## 2.2 Biomass fast pyrolysis.

### 2.2.1 The effect of biomass compositions.

The main biomass components are celluloses, hemicelluloses and lignin. Their proportions vary for different biomass species. Biomass pyrolysis causes in fact thermal decomposition of these components and thereby the behavior of fast pyrolysis and the pyrolysis products are influenced by these component proportions.<sup>1,21,24,30,31</sup>

Cellulose is a linear polymer of  $\beta - (1 \rightarrow 4) - D$ - glucopyranose units. Cellulose has a molecular weight of  $10^6$  or more g/mol and the basic repeating unit of the cellulose polymer is two glucose anhydride units, a cellobiose unit, (see Figure 2.6A). Hemicellulose is a mixture of various polymerized monosaccharides such as glucose, mannose, galactose, xylose, arabinose, 4-O-ethyl glucuronic acid and galacturonic acid residues (see Figure 2.6B). Cellulose degradation during pyrolysis takes place at  $240 - 335 \text{ }^\circ\text{C}$ <sup>1,19</sup> and produces mostly anhydrocellulose and levoglucosan;<sup>1</sup> while the thermal decomposition of hemicelluloses takes place at  $200 - 260 \text{ }^\circ\text{C}$ .<sup>1,19</sup> Lignin is a three-dimensional, highly branched, polyphenolic substance that appears as an amorphous cross-linked resin with no exact structure (see Figure 2.6C).<sup>1,19</sup> Consequently, the lignin is difficult to decompose and provides a higher char yield than celluloses and hemicelluloses. The thermal decomposition of lignin takes place at a broad temperature range of  $280 - 500 \text{ }^\circ\text{C}$ .<sup>1,19</sup>

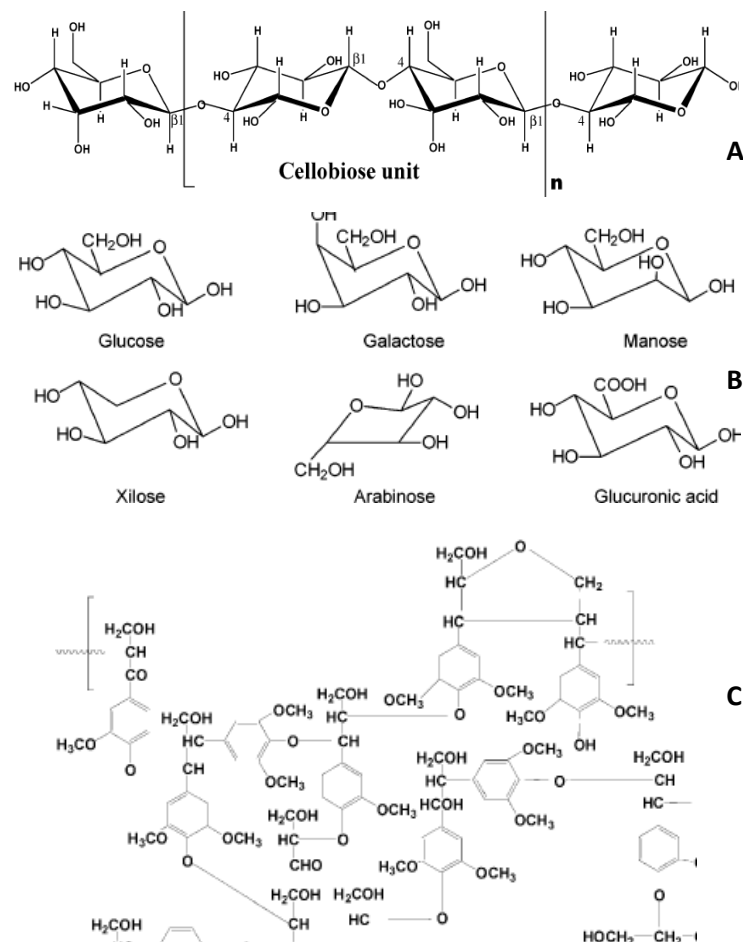


Figure 2.6: Chemical structure of cellulose (A), main components of hemicelluloses (B), partial structure of a hardwood lignin molecule from European beech (C)<sup>1</sup>

The bio-oil yield and the organic oil yield obtained from biomass fast pyrolysis have been found to be influenced by the ash and lignin contents of the biomass. A high lignin content or ash content in biomass gives a lower bio-oil yield.<sup>21,28,29</sup> The ash content of virgin lignocellulosic biomasses is 0.1 – 9 wt% and this is found to have a significant effect on the pyrolysis processes. Generally speaking, an increase of the biomass ash content generates higher char and gas yields but a lower bio-oil yield. Oasmaa et al.<sup>21</sup> discovered that the organic oil yield decreased from 65 to 42 wt% db when the ash content in lignocellulose biomass increased from 0.1 to 4 wt% (see Figure 2.7). Alkali metals in ash, especially potassium, acting as catalysts are considered a major contributor.<sup>30,31</sup> However, not all inorganic ash forming elements cause decreased bio-oil production. Silicon and also some other metals seem to be inactive in the pyrolysis process. At the moment a full knowledge of the effect of ash on pyrolysis is not available.

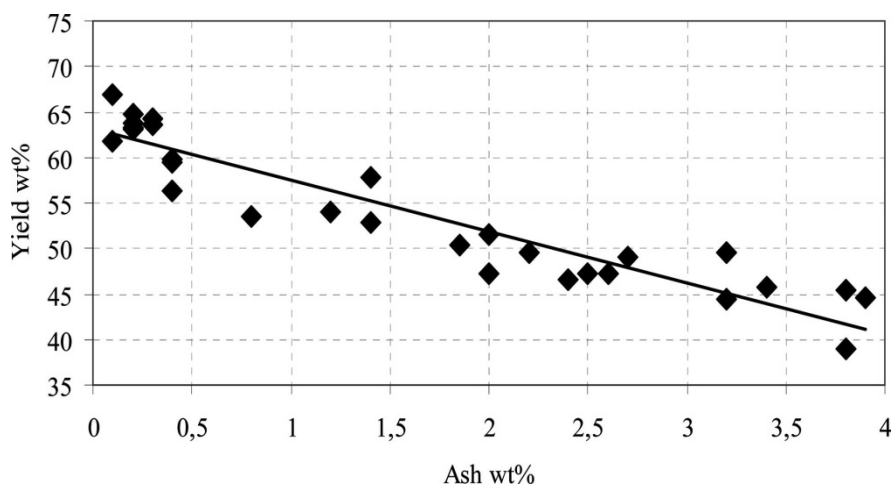


Figure 2.7: Effect of ash content on the organic oil yield in pyrolysis biomass<sup>21</sup>

### 2.2.2 Biomass fast pyrolysis.

A wide range of biomass resources (wood, agriculture products, industrial by-products, waste products and algae) are being investigated as feedstock for fast pyrolysis. Table 2.4 summarizes pyrolysis studies with respect to biomass components (cellulose, hemicellulose and lignin), ash content, potassium content, pyrolysis technology and pyrolysis temperature in addition to yields of pyrolysis oil and char.<sup>28,29,31-44</sup> Wood biomass has a low ash content of 0.4 – 3.5 wt% db (especially a low potassium content of 0.04 – 0.39 wt% db) and a lignin content of 16 – 30 wt% daf.<sup>30,31,36-38,40</sup> This probably means that fast pyrolysis of woody biomass in many cases provides a high bio-oil yield of 57 – 77 wt% daf.<sup>30,31,36-38,40</sup> Consequently, wood is an optimal feedstock for bio-oil production. Most studies of wood fast pyrolysis are conducted using fluidized bed reactors, and optimal pyrolysis temperatures have been found to be in the range of 450 – 510 °C.<sup>30,31,36-38,40</sup> Straw and grass are known as fuels with a high potassium content that causes fouling, slagging and corrosion if in boilers.<sup>30,31,36-38</sup> This limits to some degree the use of straw and grass in the high temperature processes in boilers or gasifiers. It seems to be difficult to make general assumptions as regards agricultural biomass pyrolysis since biomass compositions and ash contents are influenced by husbandry practices, seasonal harvest, level of maturity, and species. However, the bio-oil yield from agricultural fast pyrolysis seems to be lower than that of woody biomass; bio-oil yields of 38 – 61 wt% daf have been found for wheat straw fast pyrolysis.<sup>39-43</sup> These results are obtained with ash contents of 4.4 – 6.2 wt% db and potassium contents of 0.96 – 1.50 wt% db. Jung et al.<sup>42</sup> reported a bio-oil yield of 72 wt% daf for rice straw (having a lignin content of 27 wt% and a potassium content of 0.9 wt%) in a fluidized bed reactor at 491 °C.

Due to a high content of carbohydrates of up to 60% dry matter also macroalgae are considered a potential energy fuel.<sup>45</sup> The utilization of algae for energy recovery is, however, difficult due to a high ash content (10 – 40 wt%).<sup>44,45</sup> The share of macroalgae (*ulva lactuca*) coal co-firing (a maximum of 20 wt% *ulva lactuca*) has a limited impact on slagging, catalyst deactivation, corrosion, emissions and residue quality (fly ash, bottom ash gypsum). Fast pyrolysis is performed at a lower temperature (450 – 550 °C) compared to combustion or gasification, and it is believed that the pyrolysis can process a high ash-feedstock. Some initial studies of macroalgae pyrolysis have been carried out to evaluate the potential of algae oil production. A bio-oil yield of 47 – 50 wt% daf conducted in a pyrolysis fixed-bed reactor was reported for macroalgae.<sup>44</sup> Thus fast pyrolysis of macroalgae may be a promising method to utilize a high ash-feedstock to obtain a bio-oil product.

Lignin is the third most abundant biomass component (in wood and straw) and is a complex, amorphous cross-linked and three-dimensional, highly branched polymer.<sup>1</sup> Lignin may be obtained as a by-product from paper production or from second generation ethanol plants. Studies have been conducted on lignin fast pyrolysis<sup>28,29</sup> and initial results show that the bio-oil yields obtained from the lignin pyrolysis are much lower than that of typical biomasses.<sup>28,29</sup> In addition, fast pyrolysis of highly concentrated lignin material is reported to be more difficult than that of wood and straw because of blockages at the feeder, condenser and electrostatic precipitator units.<sup>29</sup>

The treatment of sewage sludge by fast pyrolysis has been demonstrated to be an alternative to incineration, agricultural use or landfill.<sup>32-36</sup> The fast pyrolysis process can considerably reduce the volume of solid waste, and produce bio-oil. There seems to be a large variation in the ash content of sewage sludge (23 – 48 wt% db) which may be the reason for the wide range of bio-oil yields obtained (39 – 68 wt% daf).<sup>32-36</sup> The sewage sludge generated in a wastewater treatment plant consists mostly of a mixture of undigested organics (plant residue, paper, oils, food, and fecal material) and inorganic materials which means that the optimal pyrolysis temperature (450 – 550°C) is almost identical to that of wood and straw.

Table 2.4: The relationship of biomass components, ash content and potassium content of biomasses and bio-oil and char yields (the bio-oil yields are excluding the feedstock water content but including the reaction water contribution).

Sample	Content (wt% daf) <sup>(a)</sup>			Ash content (wt% db)	K content (wt% db)	Yield (wt% daf) <sup>(b)</sup>		Tech <sup>(c)</sup> -Temp	Ref
	Cel	Hem	Lig			Bio-oil	Char		
<b>Wood</b>									
Beech	46	30	22	0.7	0.12	67	10	FBR, 470°C	31
Spruce	47	21	29	0.4	0.04	67	10	FBR, 470°C	31
Iroko	55	19	30	3.5	0.39	54	23	FBR, 470°C	31
<i>Albizia</i>	52	20	29	1.8	0.27	58	17	FBR, 470°C	31
Poplar aspen	42	31	16	0.4	-	77	14	FBR, 500°C	40
Willow	-	-	20	1.3	0.20	70	20	FBR, 507°C	30
Pine	49	37	30	0.2	0.09	65	10	FBR, 474°C	36
White oak	55	16	25	2.0	0.15	57	22	FBR, 450°C	37
Mallee	-	-	-	0.2	-	63	18	FBR, 450°C	38
<b>Agriculture</b>									
Wheat straw	42	24	21	6.0	1.50	61	23	PCR, 550°C	41
Rice straw	44	30	27	8.9	0.92	72	41	FBR, 491°C	42
Wheat straw	-	-	8	6.3	0.96	54	34	FBR, 509°C	39
Wheat straw	43	42	17	4.6	-	56	26	FBR, 550°C	40
Wheat straw	39	16	14	4.4	-	38	15	FBR, 500°C	43
Corn cob	45	30	21	1.2	0.54	58	15	FBR, 470°C	31
Switchgrass	-	-	10	4.3	0.07	67	21	FBR, 500°C	30
Reed canary grass	-	-	11	5.1	0.15	63	18	FBR, 502°C	30
<i>Dactylis glomerata</i>	-	-	13	7.5	2.67	56	30	FBR, 500°C	30
<i>Festuca arundinacea</i>	-	-	8	7.3	2.40	51	29	FBR, 510°C	30
<i>Lolium perenne</i>	-	-	6	6.2	2.01	57	27	FBR, 503°C	30
<b>Industrial by-products</b>									
ETEK lignin	~50	-	~50	0.2 – 0.6	0.02	58	27	FBR, 530°C	29
ALM lignin	<0.2	<2	94	1.1 – 1.3	0.04	31	49	FBR, 530°C	29
Alcell lignin	0	0.1	96	0	-	39	43	FBR, 500°C	28
Granit lignin	-	-	90	<2	-	48	39	FBR, 500°C	28
<b>Marine</b>									
<i>Undaria</i>	-	-	-	29	0.57	46	20	PTR, 500°C	44
<i>Laminaria</i>	-	-	-	31.2	10.25	46	17	PTR, 500°C	44
<i>Pophyra</i>	-	-	-	11.6	3.87	50	31	PTR, 500°C	44
<b>Waste products</b>									
Sewage sludge	-	-	-	42.5	-	68	21	FBR, 450°C	33
Sewage sludge	-	-	-	40	-	52	21	FBR, 550°C	32
Sewage sludge	-	-	-	41	-	64	21	FBR, 550°C	32
Sewage sludge	-	-	-	23	-	28	42	FBR, 525°C	34
Activated sewage sludge	-	-	-	25.0	-	58	14	SCR, 500°C	35
Dewatered digested sludge	-	-	-	47.5	-	51	16	SCR, 500°C	35
OLDA sludge	-	-	-	23.7	-	39	21	SCR, 500°C	35

(a) Cel: Cellulose, Hem: Hemicellulose, Lig: Lignin. <sup>(b)</sup>The bio-oil yield on daf was calculated from available data. <sup>(c)</sup>FBR: fluidized bed reactor, TBR: transport bed reactor, PCR: pyrolysis centrifuge reactor, PTR: packed tube reactor, SCR: the semi-continuous pyrolysis reactor

### 2.2.3 Effect of pyrolysis conditions

Numerous studies have investigated the effect of temperature on pyrolysis product distributions.<sup>7,8,30</sup> Generally speaking, an increase of the gas yield and a decrease of the char yield with increasing pyrolysis temperature are observed for biomass pyrolysis; increasing pyrolysis temperature also promotes tar formation. However, high reactor temperatures cause further cracking of organic vapor compounds (tar). This will lead to a reduction of the bio-oil yield. Toft<sup>30</sup> investigated optimal temperatures that provide a maximum organic oil yield for various typical biomasses and found that the optimal temperature is in the range of 450 – 550 °C (see Figure 2.8). The bio-oil yield is found to be significantly decreased at a temperature of 550 °C in a fluidized bed reactor. Furthermore, since fast pyrolysis takes place at high temperatures, considerable dehydrogenation/aromatization take place eventually resulting in the production of large polynuclear aromatic hydrocarbons.<sup>47</sup> Elliot<sup>47</sup> proposed a reaction pathway of these compounds before quenching as shown in Figure 2.9. When the pyrolysis temperature is higher than 600 °C, alkyl groups are cleaved from phenolics thereby then resulting in cyclization reactions. Polycyclic aromatic hydrocarbons (PAH) are formed at 700 °C. Many authors studying fast pyrolysis<sup>9,37,38,46,48</sup> have concluded that the pyrolysis temperature is the most important parameter for fast pyrolysis, thus careful control of the temperature is necessary to obtain maximum organic oil production and bio-oil quality.

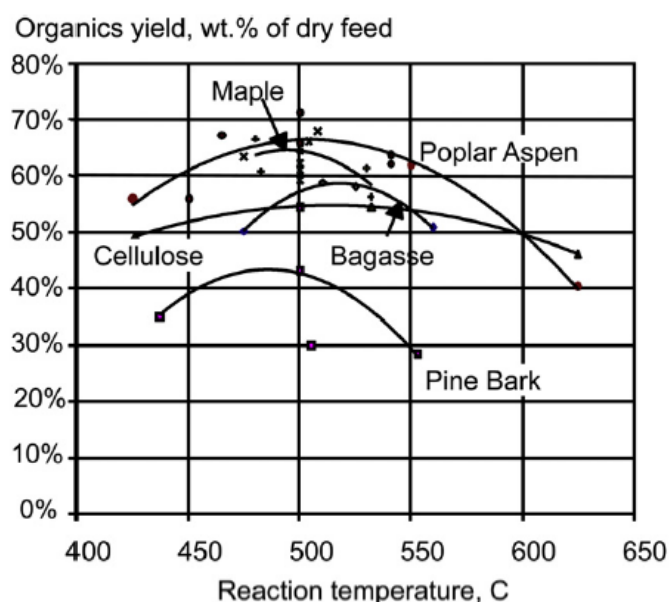


Figure 2.8: Organic oil yield of various biomass types<sup>30,46</sup>

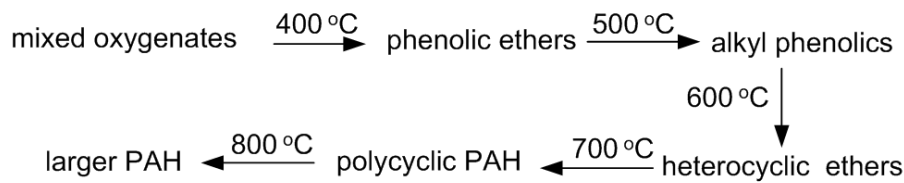


Figure 2.9: The relationship between the development of PAHs and pyrolysis temperature<sup>47</sup>

In biomass fast pyrolysis, the gas residence time needs to be less than two seconds in order to obtain the maximum bio-oil yield.<sup>1,20</sup> The thermal cracking reactions of the organic oil, secondary reactions, take place when vapors travel for a long time at high temperatures. The secondary reactions transform large molecular weight species into small species of vapors and non-condensable gases, resulting in a decrease of organic oil yield. Scott et al.<sup>49</sup> investigated the effect of vapor residence time of sorghum bagasse pyrolysis in a fluid bed reactor and the results showed that the bio-oil yield decreased from 75 to 60 wt % db when the vapor residence time increased from 0.2 to 0.9 s at 525 °C and Fagbemi et al.<sup>59</sup> and Boroson et al.<sup>39</sup> showed a significant decrease of bio-oil yield when the vapor residence time was increased from 0.8 to 4 s at a temperature range of 500 – 900 °C in a fixed-bed reactor.

The heating rate has a large influence on the pyrolysis product distributions. Many fast pyrolysis reactor types, such as bubbling and circulating bed reactors, ablative reactors, auger reactors and rotating cone reactors achieve heating rates of 700 – 1500 K/s<sup>7,26c</sup> which is much higher than that of fixed-bed reactors having a heating rate less than 100 K/min.<sup>1</sup> This leads to fast pyrolysis reactors often obtain high bio-oil yields of 65 - 75 wt% db (for wood) that is typically 1.9 ~ 2.8 times higher than that of slow pyrolysis (at heating rate of less than 100 K/s).<sup>1</sup> A bio-oil yield is found to increase from 28 to 36 wt% daf and a char yield decrease from 47 to 34 wt% daf when a heating rate increase from 2 to 100 K/s for beech trunkbars pyrolysis<sup>1</sup>

### 2.3 Bio-oil properties

Bio-oil is considered a fuel that can be used in boilers, diesel engines and gas turbines or it may be further processed to be used as a transportation fuel. Bio-oil is different from mineral oil which has required modifications of standard methods or the development of new methods for bio-oil characterization. Extensive work has been carried out to characterize the physical and chemical properties of bio-oil<sup>1,20,21,30,50,51</sup> and the guidelines for several analytic methods are summarized in



Table 2.5. Bio-oil is usually a dark brown and viscous although freely flowing liquid. Typical oil properties are summarized in Table 2.6 and compared with petroleum fuels.<sup>1</sup> Bio-oil contains about 20 – 30 wt% water that cannot be completely separated by atmospheric distillation.<sup>19</sup> If the bio-oil is heated to 210 °C (under vacuum pressure) to remove water and light organic fractions, polymerization rapidly takes place to form solid residues and eventually around 50 wt% solid residue is produced.<sup>52</sup> High water and oxygenated organic contents cause a low heating value for the bio-oil. The bio-oil lower heating value (LHV)<sup>2</sup> of 13 – 18 MJ/kg is much lower than for conventional petroleum oils (40 – 43 MJ/kg). However, the bio-oil density<sup>1,2,19</sup> of 1.05 – 1.3 kg/dm<sup>3</sup> is higher than that of petroleum fuels (around 0.72 - 0.96 kg/dm<sup>3</sup>). This means that the bio-oil has an energy content of 38 – 42% of the fuel oil on mass basis and 48 – 70% on volumetric basis. Bio-oils from wood and straw are also found to have lower nitrogen and sulfur contents than petroleum oils and low metals contents.<sup>53</sup> Bio-oil contains around 3 – 9 wt% acid including formic acid, acetic acid and propionic acid<sup>31</sup> which gives a low pH level of 2 – 3.8.<sup>1,2,19</sup> Because bio-oil contains a large number of oxygenated compounds,<sup>1,19</sup> it is immiscible with petroleum fuels but well miscible with ethanol and methanol. Viscosity is an important parameter for fuel applications. The use of a highly viscous oil leads to an increase of pumping cost. The oil viscosity varies from 25 cP up to 1000 cP,<sup>1,19</sup> depending on the water content and pyrolytic lignin content (see the method to determine pyrolysis lignin in Table 2.5).

Table 2.5: Analytical methods for physical and chemical properties of bio-oil<sup>1,20</sup>

Analysis	Unit	Methods/equipment
Water	wt%	ASTM E203, Karl-Fischer titration.
Solids	wt%	MeOH-DCM-insolubles, 1 µm filter, sample size 1 -15 g.
Metals	wt%	XRF, ICP, AAS.
Stability	°C	80°C, 24 hours, measure the viscosity and water content.
Homogeneity (phase separation)	wt%	7-days standing test, measure the water content at top, middle and bottom positions.
Flash point	°C	ASTM D93.
Ash	wt%	EN 7, ASTM D1102-84
CHN	wt%	ASTM D 5291, elemental analyzer.
Sulfur and chlorine	wt%	ICP
Viscosity (20, 40°C)	cSt mPas	Cannon Fenske glass capillaries. Rotational viscometry.
Density (15°C)	Kg/dm <sup>3</sup>	ASTM D 4052.
Pour point	°C	ASTM D 97.
HHV	MJ/kg	DIN 51900.
Pyrolytic lignin fraction	wt%	Add 60 mL oil to 1L ice-cooled water under stirring, filter and dry precipitate below 60°C.
pH	pH unit	pH meter.
Chemical components	wt%, %peak	Gas chromatography – mass spectrometry (GC-MS), dilute samples in ethanol.
Molecular mass distribution and average molecular mass	g/mol	Gel permeation chromatography (GPC), use THF as diluted solvent and polystyrene as calibration standard samples.

Table 2.6: Typical properties of wood pyrolysis bio-oil and mineral oils<sup>2,52</sup>

Analysis	Pyrolysis liquids	Light fuel oil (tempera 15)	Heavy fuel oil	Aviation fuel (JP-4)
Water, wt%	20 – 30	0.025	0.1	0
Solids, wt%	<0.5	0	0.2 – 1.0	0
Ash, wt%	<0.2	0.01	0.03	n.a
Carbon, wt%	32 – 48	86.0	85.6	80 – 83
Hydrogen, wt%	7 – 8.5	13.6	10.3	10 – 14
Nitrogen, wt%	<0.4	0.2	0.6	n.a
Oxygen, wt%	44 – 60	0	0.6	n.a
Sulfur, wt%	<0.05	<0.18	2.5	<0.4
Vanadium, ppm	0.5	<0.05	100	<0.6
Sodium, ppm	38	<0.01	20	n.av.
Calcium, ppm	100	n.a	1	n.av.
Potassium, pp,	220	<0.02	1	<1.5
Chloride, ppm	80	n.a	3	n.a
Stability	Unstable	Stable	Stable	Stable
Viscosity, cSt	15 – 1000 at 40°C	3.0 – 7 at 40 °C	351 at 50 °C	0.88 at 40 °C
Density (15°C), kg/dm <sup>3</sup>	1.05 – 1.30	0.89	0.94 – 0.96	0.72
Flash point, °C	40 – 110	60	100	-23
Pour point, °C	- 10 to -35	-15	21	<-48
Conradson Carbon Residue, wt%	14 – 23	9	12.2	n.a
LHV, MJ/kg	13 – 18	40.3	40.7	43.2
pH	2 – 3.8	Neutral	n.a	n.a
Distillability	Not totally distillable <sup>(a)</sup>			

<sup>(a)</sup> Up to 50 wt% distillation residue from bio-oil under vacuum pressure at 210°C

Bio-oil is often divided into three main fractions: water (20 - 30 wt%)<sup>1</sup>, water soluble (60 – 70 wt%) and water insoluble fraction (9-27 wt%)<sup>1,31,48,51</sup> (also called the pyrolytic lignin fraction).<sup>1,19</sup> These fractions can be partially separated by condensation at different cooling temperatures in a fast pyrolysis process. Pollard et al.<sup>50</sup> studied a separation of the bio-oil fractions by five serial condensers at different condensing temperature from 85 °C to 15 °C. The results show that 63.3 wt% the water and 0.74 wt% the pyrolytic lignin fraction were obtained in a low cooling temperature condenser (15 °C) while only 6.6 wt% of the water and 44.2 wt% of the pyrolytic lignin fraction appeared using a high cooling temperature condenser (85 °C).

GC-MS has been employed to identify about 300 chemical compounds in bio-oil that mainly comes from the water soluble fraction.<sup>31</sup> The detectable compounds identified contain 33 – 44 wt% of a whole bio-oil and include acids, nonaromatic aldehydes, nonaromatic ketones, furans, pyrans, sugars, benzenes, catechols, lignin derived phenols, guaiacols and syringols.<sup>31</sup> A summary of the major detectable chemical compounds in fast pyrolysis oils from beech, spruce, iroko, *Albizia* and corn cob oils<sup>31</sup> is presented in Table 2.7. The acetic acid (2.5 – 8.5 wt% db), hydroxyacetaldehyde (5.1 – 9.8 wt% db), nonaromatic ketones (4.2 – 10.2 wt% db), hydroxypropanone (2.7 – 4.7 wt% db) and levoglucosan (1.1 - 4.5 wt% db) appear in high concentrations compared to the other compounds in a bio-oil from a fluid bed reactor at a temperature of 465 - 470°C.

Table 2.7: GC-MS detected components in bio-oils (wt % db)<sup>31</sup>

No.	Components	Beech	Spruce	Iroko	Albizia	Corn cob
	<b>Acids</b>	<b>8.2</b>	<b>2.6</b>	<b>6.7</b>	<b>7.1</b>	<b>9.1</b>
1	Acetic acid	8.0	2.5	6.1	6.8	8.5
2	Propionic acid	0.2	0.1	0.6	0.3	0.6
	<b>Nonaromatic aldehydes</b>	<b>10.3</b>	<b>11.3</b>	<b>9.1</b>	<b>9.1</b>	<b>7.3</b>
3	Acetaldehyde, hydroxy-	7.9	9.8	7.0	6.7	5.1
4	Propionaldehyde, 3-hydroxy	1.4	0.9	0.8	1.0	0.9
5	Butanal or propanal	1.0	0.6	1.3	1.4	1.4
6	Nonaromatic ketones	5.1	4.2	8.1	5.8	10.2
7	Acetol (hydroxypropanone)	2.7	2.4	4.3	3.1	4.7
8	Butanone, 1-hydroxy-2-	0.3	0.2	0.6	0.4	1.3
9	Cyclopentene-1-one, 2-	0.2	0.1	0.3	0.2	0.4
10	Cyclopentene-1-one, 2-hydroxy-2-	1.2	0.9	1.4	1.2	1.9
11	Cyclopentene-3-one, 2-hydroxy-1-methyl-1-	0.5	0.3	1.1	0.6	1.3
	<b>Furans</b>	<b>2.4</b>	<b>2.5</b>	<b>2.8</b>	<b>2.7</b>	<b>3.3</b>
12	Furanone, 2(5H)-	0.6	0.5	0.7	0.6	0.6
13	Furaldehyde, 2-	0.6	0.4	0.5	0.6	1.0
14	Furaldehyde, 5-(hydroxymethyl)-, 2-		0.3			
15	Furan-x-on, x,x-dihydro-x-methyl-	0.3	0.2	0.2	0.2	0.2
16	Butyrolactone, γ-	0.1	0.1	0.2	0.2	0.2
17	Butyrolactone, 2-hydroxy-, γ-	0.3	0.4	0.5	0.4	0.5
18	Lactone derivative	0.3	0.3	0.3	0.5	0.4
	<b>Pyrans</b>	<b>1.9</b>	<b>1.8</b>	<b>0.7</b>	<b>1.2</b>	<b>1.3</b>
19	Maltol (pyran-4-one, 3-hydroxy-2-methyl-			0.2	0.1	0.3
20	Pyran-4-one, 3-hydroxy-5,6-dihydro-, (4H)-	1.5	0.9	0.5	1.0	0.9
21	Pyran-4-one, 2-hydroxymethyl-5-hydroxy-	0.3	0.9	0.1	0.1	0.1
	<b>Sugars</b>	<b>3.3</b>	<b>5.3</b>	<b>2.3</b>	<b>2.6</b>	<b>3.4</b>
22	Anhydro-β-D-arabinofuranose, 1,5-					0.4
23	Anhydro-β-D-xylfuranose, 1,5-	0.2				0.6
24	Anhydro-β-D-glucopyranose, 1,6-	2.4	4.5	1.1	1.4	1.2
25	Dianhydro-R-D-glucopyranose, 1,4:3,6-	0.2	0.1	0.3	0.2	0.4
26	Anhydrosugar unknown	0.5	0.8	1.0	0.5	0.9
27	Benzenes	0.1	0.1	0.1	0.1	0.1
28	Toluene	0.1	0.1	0.1	0.1	0.1
29	Catechols	<0.0	<0.0	0.4	0.1	0.3
30	Hydroquinone (benzene, 1,4-dihydroxy-)	<0.0		0.3	0.1	0.2
31	Lignin-derived phenols	0.2	0.4	0.9	0.4	3.6
32	Phenol	<0.0	0.1	0.2	0.1	0.3
33	Cresol	<0.0	0.1	0.3	<0.0	0.3
34	Phenol, 4-ethyl-			<0.0	<0.0	0.3
35	Phenol, 4-vinyl-			0.3	<0.0	2.5
36	Benzaldehyde, 4-hydroxy-					0.1
	<b>Guaiacols (methoxy phenols)</b>	<b>1.4</b>	<b>4.0</b>	<b>4.0</b>	<b>2.7</b>	<b>3.5</b>
37	Guaiacol	0.2	0.4	0.8	0.5	0.5
38	Guaiacol, 4-methyl-	0.1	0.4	0.3	0.2	0.2
39	Guaiacol, 4-ethyl-	<0.0	0.1	0.1	0.1	0.2
40	Guaiacol, 4-vinyl-	0.1	0.4	0.7	0.4	1.7
41	Guaiacol, 4-allyl- (eugenol)	0.1	0.2	0.1	0.1	0.1
42	Guaiacol, 4-propyl-		<0.0	<0.0	<0.0	<0.0
43	Guaiacol, 4-propenyl-cis (isoeugenol)	0.2	0.3	0.3	0.2	0.1
44	Guaiacol, 4-propenyl-(trans) (isoeugenol)	0.2	0.5	0.6	0.4	0.2
45	Vanillin	0.2	0.5	0.3	0.2	0.3
46	Phenylacetaldehyde, 4-hydroxy-3-methoxy-	0.1	0.3	0.2	0.1	
47	Coniferyl alcohol, isomer of		0.2	0.1	0.1	
48	Phenylethanone, 4-hydroxy-3-methoxy-	0.1	0.3	0.3	0.2	0.1
49	Guaiacyl acetone	<0.0	0.1	0.1	<0.0	0.1
50	Coniferylaldehyde	0.1	0.2	0.2	0.2	<0.0
	<b>Syringols (dimethoxy phenols)</b>	<b>3.0</b>	<b>&lt;0.0</b>	<b>3.0</b>	<b>3.3</b>	<b>1.2</b>
51	Syringol	0.5		0.7	0.6	0.3
52	Syringol, 4-methyl-	0.2		0.2	0.2	0.1
53	Syringol, 4-vinyl-	0.3		0.5	0.5	0.2
54	Syringol, 4-allyl-	0.1		0.2	0.1	0.1
55	Syringol, 4-(1-propenyl)-, trans	0.3		0.3	0.4	0.2
56	Syringaldehyde	0.3		0.2	0.3	<0.0
57	Acetosyringone	0.2		0.2	0.2	0.1
58	Sinapaldehyde (trans)	0.5		0.3	0.5	
	<b>Total</b>	<b>36.3</b>	<b>32.7</b>	<b>38.7</b>	<b>35.7</b>	<b>44.0</b>

The pyrolytic lignin fraction consists of a majority of oligomeric/polymer fractions and holocellulose derivatives that is not easily quantified by GC-MS. The pyrolytic lignin consists of a high molecular mass of 95 to 6900 g/mol.<sup>54,55</sup> The pyrolytic lignin content is 8.5 – 27 wt% of a whole bio-oil<sup>1,31,48,51</sup> and this has considerable influence on the viscosity and stability of bio-oil. Mullen et al.<sup>56</sup> investigated the pyrolytic lignin fraction from various bio-oils by Gel Permeation Chromatography (GPC) (see Table 2.8). The study found that 40 – 45 wt% of the pyrolytic lignin are monomers, dimers and trimers having molecular masses of 95 – 477 g/mol, 43 – 22 wt% are compounds having molecular masses of 478 – 1526 g/mol and 17 – 33 wt% are compounds with molecular masses higher than 1526 g/mol.

Table 2.8: Approximate molecular weight distribution of pyrolytic lignin<sup>56</sup>

Mw range		Barley straw	Barley hulls	Switchgrass	Soy straw	Oak
94-185	Monomers	11.2 <sup>(a)</sup>	8.4	8.6	7.3	12.9
186-318	Dimers	19.5	19.4	23.7	22.7	28.9
319-477	Trimers	12.8	11.8	15.8	14.8	17.0
478-636	Tetramers	7.5	7.0	8.4	8.5	8.7
636-763	Pentamers	4.0	3.9	4.2	4.6	4.4
764-915	Hexamers	3.3	3.3	3.3	3.9	3.4
916-1068	Heptamers	2.4	2.4	2.3	2.8	2.3
1069-1220	Octamers	1.8	1.8	1.7	2.1	1.5
1221-1373	Nonames	1.4	1.4	1.3	1.6	1.1
1374-1526	Decamers	1.1	1.1	1.0	1.3	0.8
1526-	>10-mers	30.4	33.2	24.8	25.4	16.5
	Mn <sup>(b)</sup>	358	393	361	319	304
	Mw <sup>(c)</sup>	4996	6896	4502	4461	2566

*a) wt% on a whole pyrolytic lignin. b) The weight average molecular weight. c) Number average molecular weight*

Oasma and Peacocke<sup>20</sup> reviewed the influence of the physical and chemical properties of bio-oil on storage, handling, processing and applications (see Table 2.9). The behavior of bio-oil is found to be quite different to that of petroleum oils. Phase separation, low heating value, high oxygen content, low pH value, poor distillation behavior and high viscosity are challenges to overcome when utilizing bio-oil in industrial applications. The contents of H, C, O, N and S of bio-oil are depended on biomass compositions. Thus bio-oil quality is influenced by not only pyrolysis conditions but also biomass compositions.

Table 2.9: Characteristics of bio-oil<sup>20</sup>

Characteristic	Cause	Effects
Acidity or low pH	Organic acids from biopolymer degradation	Corrosion of vessels and pipework
Aging	Continuation of secondary reactions including polymerization	Slow increase in viscosity from secondary reactions such as condensation  Potential phase separation
Alkali metals	Nearly all alkali metals report to char so not a big problem  High ash feed  Incomplete solids separation	Catalyst poisoning  Deposition of solids in combustion  Erosion and corrosion  Slag formation  Damage to turbines
Char	Incomplete char separation in process	Aging of oil  Sedimentation  Filter blockage  Catalyst blockage  Engine injector blockage  Alkali metal poisoning
Chlorine	Contaminants in biomass feed	Catalyst poisoning in upgrading
Color	Cracking of biopolymers and char	Discoloration of some products such as resins
Contamination of feed	Poor harvesting practice	Contaminants notably soil act as catalysts and can increase particulate carry over.
Poor distillability	Reactive mixture of degradation products	Typically, bio-oil cannot be distilled to a maximum of 50%.  Liquid begins to react at temp below 100 °C and substantially decomposes above 100 °C at atmospheric pressure
High viscosity		Gives high pressure drop increasing equipment cost  High pumping cost  Poor atomization
Low H:C ratio	Biomass has low H:C ratio	Upgrading to hydrocarbons is more difficult
Materials incompatibility	Phenolics and aromatics	Destruction of seals and gaskets
Miscibility with hydrocarbons is very low	Highly oxygenated nature of bio-oil	Will not mix with any hydrocarbons so integration into a refinery is more difficult

Nitrogen	Contaminants in biomass feed High nitrogen feed such as proteins in wastes	Unpleasant smell Catalyst poisoning in upgrading NOx in combustion
Oxygen content is very high	Biomass composition	Poor stability Non-miscibility with hydrocarbons
Phase separation or inhomogeneity	High feed water High ash in feed Poor char separation	Phase separation Partial phase separation Layering Poor mixing Inconsistency in handling, storage and processing
Smell or odor	Aldehydes and other volatile organics, many from hemicellulose	While not toxic, the smell is often objectionable
Solids	See also Char Particulates from reactor such as sand Particulates from feed contamination	Sedimentation Erosion and corrosion Blockage
Structure	The unique structure is caused by the rapid de-polymerization and rapid quenching of the vapors and aerosols	Susceptibility to aging such as viscosity increase and phase separation
Sulfur	Contaminants in biomass feed	Catalyst poisoning in upgrading
Temperature sensitivity	Incomplete reactions	Irreversible decomposition of liquid into two phases above 100 °C. Irreversible viscosity increase above 60 °C Potential phase separation above 60 °C
Toxicity	Biopolymer degradation products	Human toxicity is positive but small Eco-toxicity is negligible
Viscosity	Chemical composition of bio-oil	Fairly high and variable with time Greater temperature influence than hydrocarbons
Water content	Pyrolysis reactions Feed water	Complex effect on viscosity and stability: Increased water lowers heating value, density, stability, and increase pH Affects catalysts

Bio-oil is sometimes found to be characterized by phase separation and an increase of viscosity (aging) during storage. The aging results in difficulties with storage, processing and trading. Radical groups that are present in a fresh bio-oil combine with each other or other compounds and consequently form high molecular mass compounds and water.<sup>22,57</sup> The changes of chemical compounds cause instabilities of bio-oil.<sup>22</sup> Garcia-Perez et al.<sup>22</sup> proposed a physical model of aging of bio-oils with multiphase complex structures. Bio-oil is believed to contain char particles, waxy materials, aqueous droplets, and micelles formed of heavy compounds in a matrix of hollocellulose-derived compounds and water (see Figure 2.10). The waxy material has a tendency to crystallize and deposit on the upper layer while heavy components have a tendency to form networks at the bottom layer, probably causing phase separation and increase of oil viscosity during storage.

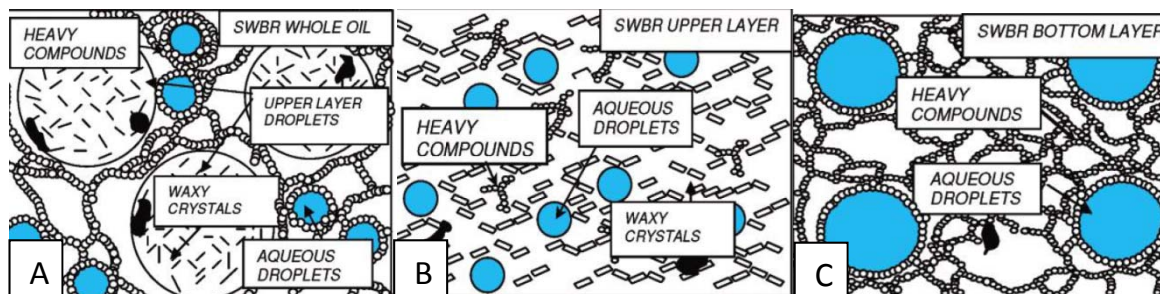


Figure 2.10: A physical model illustrating bio-oil multiphase structure of softwood bark residues (SWBR) (A: whole bio-oil, B: upper layer, C: bottom layer).<sup>22</sup>

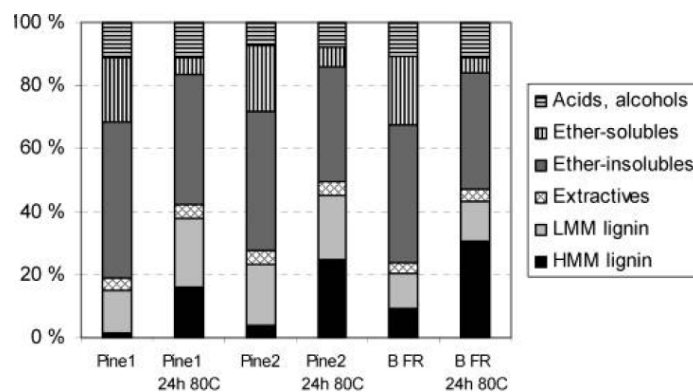


Figure 2.11. Chemical changes of forestry residue pyrolysis liquids (two pine and one brown) in the accelerated aging test at 80°C for 24 hours.<sup>23</sup> The pyrolytic lignin includes low molecular mass (LMM) lignin and high molecular mass (HMM) lignin.

In addition to this, the changes of the macro-chemical family distributions of bio-oil may also cause oil viscosity increase and phase separation. Oasmaa et al.<sup>23</sup> studied the storage stability of pine and brown forest residue oils in an accelerated aging test at 80°C for 24 hours, which corresponds to a

year of room-temperature storage.<sup>23</sup> The results demonstrated that an increase of the pyrolytic lignin fraction and a decrease of both the ether insoluble fraction (sugar fraction) and the ether soluble fraction (aldehydes, ketones, furans, phenols, guaiacols) took place after the aging test (Figure 2.11). Norazana<sup>57</sup> investigated the effect of straw and wood oil aging on viscosity and water content at various storage temperatures. She found a viscosity increases from 48 to 122 cP for wood oil and from 25 to 65 cP for straw oil at a storage for 1 day at a temperature of 80°C (see Figure 2.12) while the water content increased from 16.4 to 17.3 wt% for wood oil and 17.3 to 19.3 wt% for straw oil.

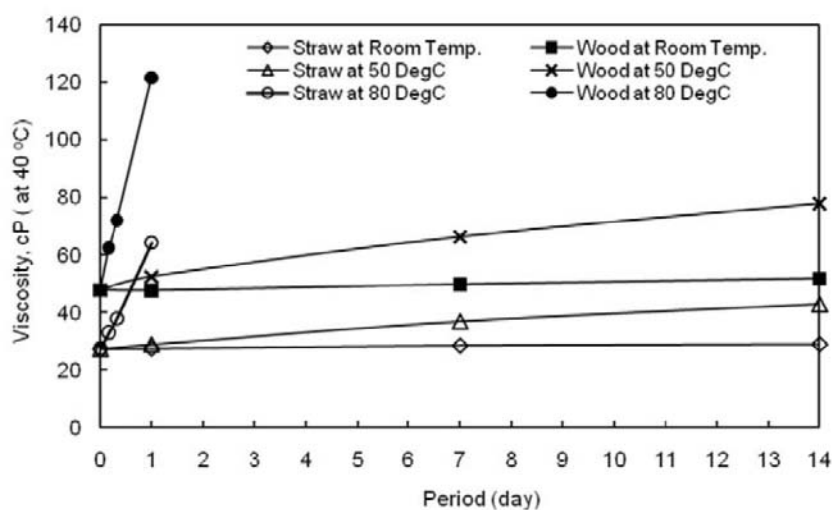


Figure 2.12: The effect of the aging on wood and straw oil viscosities at various storage temperatures.<sup>57</sup> The wood and straw oils were produced on the PCR at 525 – 550°C.

## 2.4 The kinetics and modeling of fast pyrolysis.

Biomass consists of three major constituents: cellulose, hemicellulose and lignin. In a pyrolysis reactor a large number of reactions take place, including biomass volatilization, vapor cracking, partial oxidation, repolymerization and condensation. The selectivity of these reactions determines the formation of gas, liquid and char products and the reactions are controlled by parameters such as the heating rate of the solid particles, reactor pyrolysis temperature, reactor gas residence time and reactor solid particle residence time. The pyrolysis process includes hundreds of elementary reactions and therefore it is not possible to model it in detail, but often a type of kinetic model which can be used to describe the yield of gas, char and tar is wanted. Thus reaction rates and their kinetic parameters of biomass pyrolysis are often based on schemes that describe the pyrolysis products production (char, gas and tar) and intermediates of biomass. To approach a fast pyrolysis



biomass model, a combination of the primary reactions and secondary reactions are proposed by many authors<sup>16,4-6</sup>

Multi-state mechanisms of primary pyrolysis are used to predict the formation rate and yields of reaction products and solid and gas-phase intermediates. The Broido-Shafizadeh scheme proposed by Bradbury et al.<sup>58</sup> and later modified by Miller et al.<sup>59</sup> is used to predict the formation of final products and intermediates for biomass pyrolysis (see Figure 2.13). The Broido-Shafizadeh scheme is generally accepted today and some authors<sup>7,8</sup> use it to study the behavior of biomass fast pyrolysis. The reaction rates of biomass melting to form activated biomass are proposed to be described by a first order reaction in the reactant mass fraction.<sup>4</sup> The melting of biomass to form activated biomass assumes that the chemical composition does not change but modifies only the physical properties.<sup>9</sup> The decomposition of activated biomass to generate tar, char and gases is the next step. Multistep, first-order, irreversible Arrhenius reactions are used for all kinetic parameters of the Broido-Shafizadeh scheme. The kinetic parameters reported for pyrolysis of cellulose,<sup>4,10,58</sup> hemicellulose,<sup>4</sup> lignin,<sup>4</sup> pine wood<sup>7</sup> and red oak<sup>8</sup> are summarized in Table 2.10. Biomass reactions are often based on superposition of cellulose, hemicellulose, and lignin reactions as proposed by Agrawal et al.<sup>4</sup> The simulated results show good agreement with experimental char yields for beech, cherry and oak wood determined using TGA at heating rates of 5 – 80 K/min,<sup>4</sup> for TGA pyrolysis of lignin at temperatures between 673 and 1073 K<sup>49</sup> and for pyrolysis of red oak particles in a fluid bed reactor.<sup>8</sup>

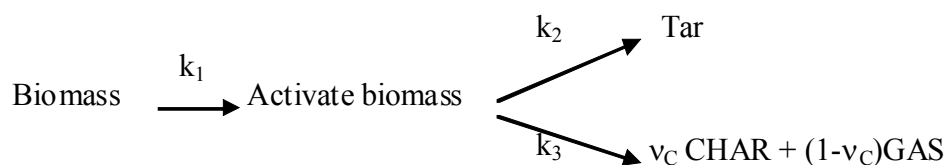


Figure 2.13: Multi-step mechanism of primary wood pyrolysis<sup>4,58</sup>

Secondary reactions lead to cracking of tar at temperatures above 500 °C<sup>9,46</sup> given sufficiently long residence time and cause decreased tar yield and increased gas yield. The secondary reactions are known to involve cracking, re-polymerization and condensation reactions.<sup>5</sup> Reactions to form permanent gases and a refractory condensable tar<sup>9</sup> (which may be a tar or some combination of water-soluble organic compounds) are assumed to appear as competitive secondary reactions (see Figure 2.14).<sup>9,60</sup> However, the amount of refractory tars is considered to be negligible when the

temperature is sufficiently high. So far the understanding of the pathways of refractory tar fraction is still qualitative.<sup>60</sup>

Table 2.10: Kinetic constants for multi-step mechanism of cellulose, hemicelluloses and lignin<sup>4</sup>

Biomass	Kinetic constants: A (s <sup>-1</sup> ), E(kJ/mol)	Reactor	Ref
Cellulose	$k_1=2.80 \times 10^{19} \exp(-242.4/RT)$ $k_2=3.28 \times 10^{14} \exp(-196.5/RT)$ $k_3=1.30 \times 10^{10} \exp(-150.5/RT)$ $v_c=0.35$	TGA, heating rate 5-80K/min	4,10,58
Hemicellulose	$k_1=2.10 \times 10^{16} \exp(-186.7/RT)$ $k_2=8.75 \times 10^{15} \exp(-202.4/RT)$ $k_3=2.60 \times 10^{11} \exp(-145.7/RT)$ $v_c=0.60$		4
Lignin	$k_1=9.60 \times 10^8 \exp(-107.6/RT)$ $k_2=1.50 \times 10^9 \exp(-143.8/RT)$ $k_3=7.70 \times 10^6 \exp(-111.4/RT)$ $v_c=0.75$		4
Pine wood	$k_1=2.80 \times 10^{19} \exp(-240/RT)$ $k_2=6.79 \times 10^9 \exp(-140/RT)$ $k_3=1.30 \times 10^{10} \exp(-150/RT)$ $v_c=0.35$	PCR <sup>a</sup>	7,11
Pine wood	Kinetic constants from cellulose, hemicelluloses and lignin components	TGA, heating rate 1000K/min	4
Beech, oak, cherry wood	Kinetic constants from cellulose, hemicelluloses and lignin components	TGA, heating rate 1000K/min	4
Red oak	Kinetic constants from cellulose, hemicelluloses and lignin components of ref 33	FBR <sup>b</sup>	4,18

<sup>a)</sup> Pyrolysis centrifuge reactor. <sup>b)</sup> Fluid bed reactor.



Figure 2.14: A global mechanism for the secondary reactions of vapor-phase tarry species<sup>4</sup>

The secondary reactions are less investigated and their kinetic constants are mostly evaluated based only on the cracking process. The reaction rates are proposed to be specified Arrhenius expressions and are assumed to be linearly dependent on mass concentration of the vapor tar (see Table 2.11). Many authors studying biomass pyrolysis have suggested an activation energy in the narrow range of 80 – 110 kJ/mol.<sup>9</sup>

Table 2.11: Kinetic constants for the global reactions of tar cracking summarized by Di Blasi<sup>9</sup>

Reactor; atmosphere	Primary pyrolysis: material; heating conditions	Secondary pyrolysis: temperature; vapor residence time	Kinetic law A (s <sup>-1</sup> ); E (kJ/mol)
Continuous vortex reactor + tubular reactor; steam	Softwood sawdust; 898K	923–1098K; <1 s	$r = -1.55 \times 10^5 \exp(-87.6/RT) \rho_T^{(a)}$
Continuous, bubbling fluidized-bed reactor; nitrogen	0.6–1.1mm thick poplar; 723–823K	723–823K; 0.5–0.7 s	$r = -4.28 \times 10^6 \exp(-107.5/RT) \rho_T$
Series-connected, tubular reactors; helium	20mm deep bed of sweetgum hardwood powder; 0.2K/s up to 723K	773–1073K; 0.9–2.2 s	$r = -10^{4.8} \exp(-93.3/RT) \rho_{TV}^{(b)}$
Batch, fluidized-bed reactor; nitrogen	3–4 g of almond shells, 0.3–0.5mm thick; 978–1123K	978–1123K	$r = -4.5 \times 10^6 \exp(-110.1/RT) \rho_T$
Continuous ultrapyrolysis reactor; nitrogen	Cellulose powder; 923–1173K	923–1173K; 0.05–0.9s	$r = -1.1 \times 10^6 \exp(-100.8/RT) \rho_T$
Two-zone tubular reactor; helium	15 g of milled refuse-derived fuel; 773–1173K	773–1173K; 6–22 s	$r = -4.1 \times 10^4 \exp(-100.8/RT) \rho_T$
Batch, fluidized bed reactor; nitrogen	0.8–5 g of municipal waste; 973–1123K	973–1073K; <5 s	$r = -1.9 \times 10^6 \exp(-99.5/RT) \rho_T$
Pyroprobe 1000 + tubular reactor packed with	1mg of Kraft lignin (Eucalyptus wood) powder;	673–1033K;	$r = -4.138 \times 10^3 \exp(-84.7/RT) \rho_T$

quartz particles; helium	300 K/s up to 973K		
Cyclone reactor; mixture of helium/ argon and steam	0.2–1mm thick beech wood particles; 793–1327K	793–1327K; 0.04–0.15s	$r = -5.9 \times 10^7 \exp(-123.5/RT) \rho_T$
Tubular reactor+packed-bed (metallic rings) reactor; helium	20–30 g of wood, straw, coconut shells powder; 673–1173K	673–1173K; 0.3–0.4 s	$r = -4.34 \exp(-23.4/RT) \rho_T$
TGA+tubular quartz reactor; nitrogen	500 mg of spruce wood (0.5–1mm thick particles); 5 K/min up to 1323K	873–1073K; 0.5–2 s	$r_I = -3.076 \times 10^3 \exp(-66.3/RT) \rho_{T(I)}$ ; $r_{II} = -1.13 \times 10^3 \exp(-109/RT) \rho_{T(II)}$ ;
Tubular, two zone, batch reactor; steam	100–300 mg of cellulose, cherry wood, yellow pine powder; 773K	773–1023K; 0.5–12 s	$r = -3.57 \times 10^{11} \exp(-204/RT) \rho_T$ ; (cellulose); E (cherry wood) = 98.6; E (yellow pine) = 101
Continuous fixed-bed reactor+tubular reactor; nitrogen	10–40 mm thick spruce and fir particles; 653K	773–1273K; <0.2 s	$r = -4.0 \times 10^4 \exp(-76.6/RT) \rho_T$
Tubular reactor+perfectly stirred reactor; argon	1 g of beech wood sawdust; 820K	836–1303K; 0.3–0.5 s	$r = -1.9 \times 10^3 \exp(-59/RT) \rho_T$
Pyrolysis centrifuge reactor, recycled gas <sup>7</sup>	Wood, straw	723 - 898 K, <2 s	$r = -4.3 \times 10^6 \exp(-108/RT) \rho_T$

<sup>a</sup> $\rho_T$  and <sup>b</sup> $\rho_{TV}$  are the total and reactive mass concentration of vapor-phase tar, respectively

Bech et al.<sup>7</sup> developed a model that includes the primary pyrolysis reaction, secondary reaction and a shrinkage mechanisms for pine wood pyrolysis in a pyrolysis centrifuge reactor (PCR), a type of ablative reactor. The kinetics of the solid-phase primary and secondary reactions is modeled using the Broido-Shafizadeh scheme<sup>6</sup> and cracking of organics (see Figure 2.14). Biomass particles travel and are heated in a plug flow reactor (see Figure 2.15). Large particles may not be completely converted before they are discharged from the reactor whereby the collected solids are a mixture of char and unconverted biomass. The vapors generated during the primary reaction enter the plug flow gas-phase and are further cracked to permanent gas.

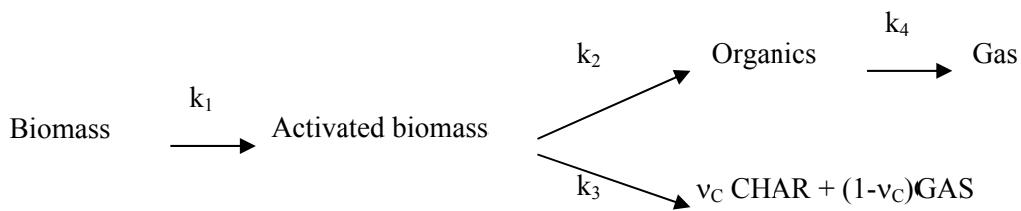


Figure 2.14: The Broido-Shafizadeh model for pyrolysis<sup>6</sup>

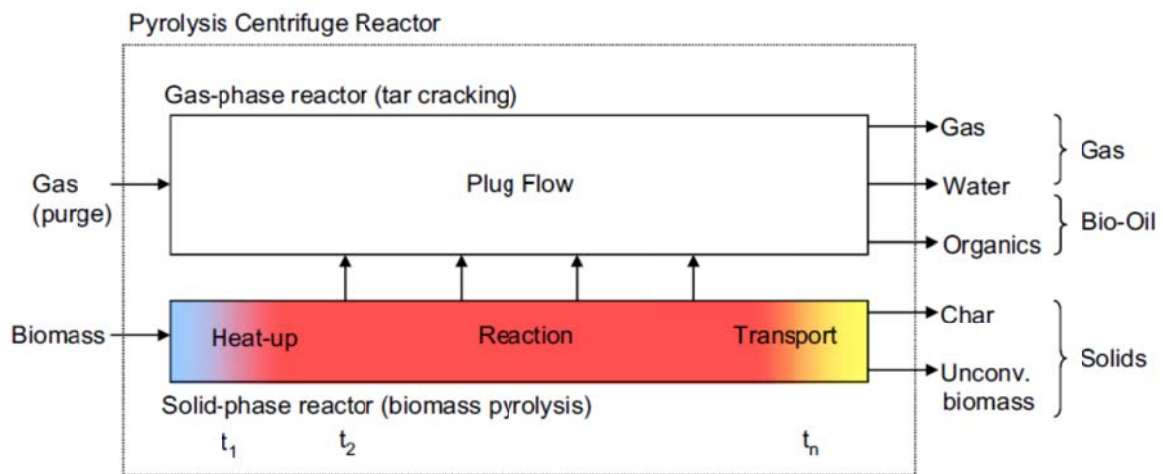


Figure 2.15: Model outline and convention for reactor streams<sup>7</sup>

The primary pyrolysis reaction within the particle leads to a movement of the surface toward the centre of the particle. It is assumed that when an activated biomass is formed on the surface of the particle, this activated biomass is immediately removed. Figure 2.16 depicts the movement of the surface and the temperature profile of the biomass particle. The particle is continuously heated to a temperature where it decomposes. The movement of the reaction front continues until the particle is totally consumed or the particle is ejected from the reactor.

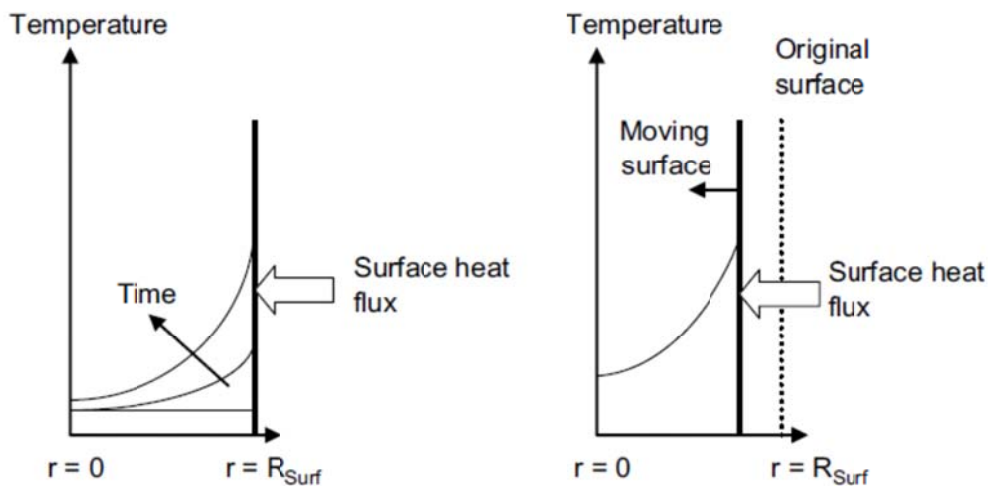


Figure 2.16: Outline of solid material undergoing surface decomposition at time  $t$  (left) and  $t + \Delta t$ <sup>7</sup>

By using available kinetic constants from the literature (see Table 2.10 and Table 2.11), the model obtains a good prediction of the yield of organic, char and gas including water from PCR pine wood pyrolysis (see Figure 2.17). An increase of the gas yield and a decrease of the char yield are observed when the temperature increases from 450 to 625°C. The predicted organic oil yield obtains a maximum at a temperature in the range of 525 – 575°C. The predicted organic oil yields at the optimal temperature were about 4 – 10 wt% higher than that of experiments. The difference is considered due to a poor mass balance obtained in the PCR experiments (average losses of  $7.6 \pm 2.2\%$ wt).<sup>7</sup>

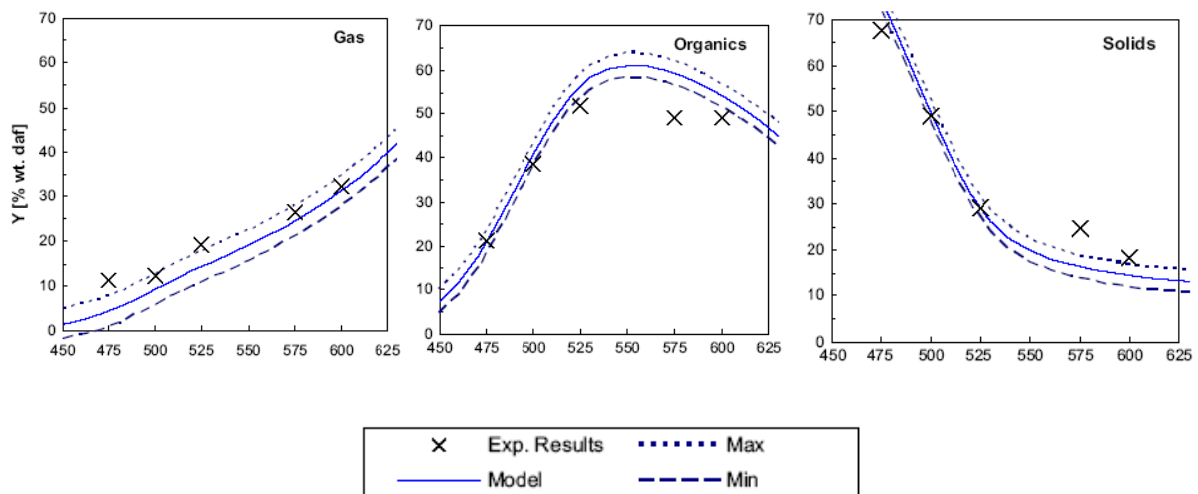


Figure 2.17: Experimental yields (symbols) and model predictions with reaction temperature (°C) for pine wood.<sup>7</sup>

## 2.5 Applications and prospects of bio-oil

### 2.5.1 Fast pyrolysis as a pretreatment technology for energy carriers

Biomass is considered an alternative fuel that can replace fossil fuel and thereby reduce CO<sub>2</sub> emission. However, biomass has a low bulk density which can be as low as 150 – 200 kg/m<sup>3</sup> and this leads to high transportation costs. Bio-oil produced from biomass by fast pyrolysis has a density of 1100 – 1200 kg/m<sup>3</sup>,<sup>1,20</sup> nearly five to eight times higher than the bulk density of crop and agricultural residues. On the other hand the energy recovery of the oil compared to raw biomass is in the range of 55 – 78%.<sup>12</sup> As a result, the transportation costs of bio-oil are reduced by 87% compared to raw biomass.<sup>20</sup> Bio-oil is used as a fuel for boilers, diesel engines and gas turbine.<sup>20</sup> The possibilities for applications of bio-oil are summarized in Figure 2.18.

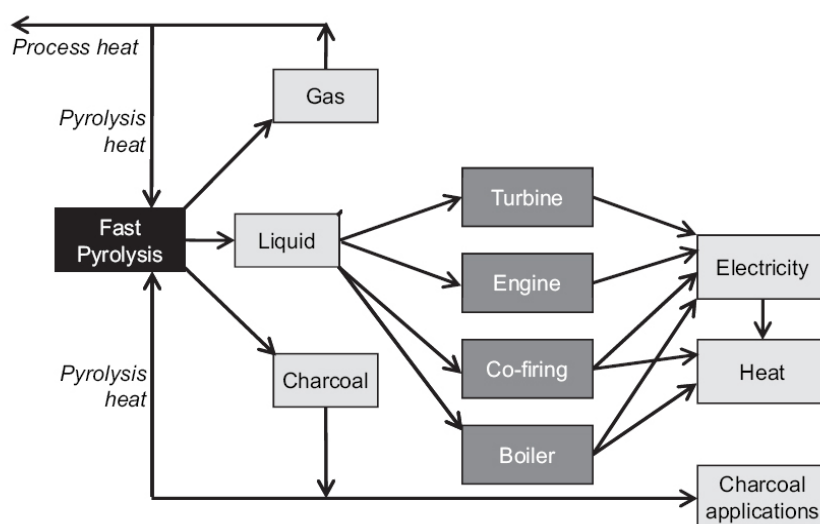


Figure 2.18: Applications for fast pyrolysis products<sup>20</sup>

Bio-oil is close to being a commercial fuel for combustion, and it can partially replace conventional fuel demand of a power station.<sup>20</sup> Although bio-oil has poor combustion properties,<sup>19</sup> e.g., poor ignition (cetane index below 10), high viscosity (20 – 1000 cP), low energy content (HHV below 18 MJ/kg), low thermal stability, low pH value (pH of 2 – 4), and high emission levels, the flame characteristics of bio-oil combustion are relatively similar to those of light fuel oil.<sup>19</sup> This was demonstrated by combusting bio-oil without changes of boiler operation and emission levels.<sup>19</sup> Bio-oil has been used commercially co-fired with coal in a utility boiler for power generation at Manitowoc public utilities in Wisconsin (USA). Bio-oil has also been used as a fuel for natural gas co-firing tests in which a quantity of 15 tons of bio-oil with a throughput of 1.6 m<sup>3</sup>/h (an equivalent

of 8 MWth) was used in a 350 MWe natural-gas fired power station in the Netherlands (2002).<sup>48</sup> Bio-oil has also been approved as a fuel for boilers at a Swedish district heating plant.<sup>19</sup>

Bio-oil has been tested in diesel engines by manufacturers such as Ormrod Diesels and Wärtsilä Diesel and research institutes such as Aston University, VTT, MIT, and the University of Rostock.<sup>19</sup> The results obtained indicate that the use of bio-oil causes some serious problems. Diesel engines are designed to operate on fossil fuels (acid free fuel) and therefore severe wear and erosion were observed at the injection nozzles, due to the fuel's acidity and the presence of fine char particles.<sup>2</sup> High oil viscosity and less thermal stability resulted in damage to nozzles and injection systems and formation of carbon deposits in the combustion chamber and in the exhaust valves.<sup>19</sup> Wärtsilä<sup>2,13</sup> tested bio-oil combustion in a 1.5 MWe medium speed diesel power plant modified for bio-oil which lead to some conclusions and suggestions for bio-oil diesel engine tests<sup>2,13</sup>: no standard engine component gaskets could tolerate the low pH of the bio-oil, the bio-oil had to be heated to less than 90 °C for viscosity reduction and the oil feed tank had to be equipped with a mixer and temperature control to avoid segregation of bio-oil. However, Wärtsilä discontinued the project due to the poor quality of the bio-oil (especially the high solid content) for the diesel engine. Ormrod<sup>14</sup> tested the use of bio-oil in a Blackstone ER6 230 kW diesel engine. Serious erosion and corrosion problems were reported when using standard materials and deposit formation of lacquer on the injector nozzle and fuel pump plunger causing the latter to stop were also observed. Bio-oil used in diesel engine gives low NO<sub>x</sub> and SO<sub>x</sub> emissions, 10 times higher CO emission and almost the same CO<sub>2</sub> when compared to diesel oil.<sup>2,19</sup> The thermal efficiency of the bio-oil (32.4%) is almost equal to that of diesel oil (34.3%).<sup>2,26d</sup> Using emulsions of bio-oil in diesel oil seems to be a promising method of applying bio-oil in a diesel engine. Bio-oil is not miscible with hydrocarbon fuels, but by adding surfactants it can be emulsified in diesel fuel. CANMET Energy Technology Center (CETC)<sup>2</sup> has produced stable emulsions with 30 wt% bio-oil in diesel fuel and has found that the physical properties of these emulsions were more similar to those of the diesel fuel than to those of bio-oil. Bertoli et al.<sup>2</sup> tested successfully CETC's emulsions with 30% wood pyrolysis oil in No. 2 diesel fuel in an unmodified diesel engine. The results show no traces of corrosion in the fuel injection system. Consequently, the production of a stable bio-oil emulsion in diesel oil is believed to be a promising method for the application of bio-oil in unmodified diesel engines.

Although bio-oil is believed to be a potential fuel for gas turbines, experience with bio-oil combustion in gas turbines is limited. Orenda aerospace (Canada) is a pioneer when it comes to using bio-oil in gas turbines. Bio-oil was tested in a 2.5 MWe industrial gas turbine (GT2500) from



Orenda aerospace that uses diesel oil and/or kerosene.<sup>15</sup> The preliminary bio-oil tests identified some problems with the operation of the emergency systems, the metering valve performance and the diesel system hot gas back flow. Several modifications of the GT 2500 were reported necessary, such as modifications of nozzles to allow larger fuel flows and dual fuel operation, a complete low-pressure bio-oil supply system and improvements of vanes and blades, stainless steel parts and polymeric components. Although the GT 2500 was successfully tested with bio-oil from idle to full load,<sup>15</sup> Orenda carried out only limited test runs with the GT 2500 due to limited availability of quality bio-oil for gas turbine application. A 75 kW gas turbine (T216 GT) at the University of Rostock (Germany) was tested in dual fuel set-up.<sup>2,16</sup> The combustion chamber was modified to enable dual fuel operation with diesel and bio-oil. Under dual fuel operation with a fuel blend of 40% bio-oil and 60% diesel they were able to achieve 73% of the full output power that would have been obtained from diesel alone. Compared to straight diesel operation, CO and hydrocarbon emissions were higher while the NOx was lower.<sup>2,16</sup>

### **2.5.2 Bio-refinery**

In the bio-refinery concept, fast pyrolysis is considered a possible component for densification of volumetric biomass and the production of bio-oil. For industrial application bio-oil shows undesirable properties such as low heat value, high acid component content, and increase of viscosity and phase separation during storage time.<sup>52</sup> As a result, bio-oil from fast pyrolysis is not a realistic liquid transport fuel substitution. Upgrading technologies are the next step for liquid transport fuel production or chemical production from biomass. The technologies at centralized facilities include hydrotreating, gasification and catalytic cracking processes. So far the upgrading technologies of biomass/bio-oil are in the early stages of demonstration projects and the upgraded oil properties seem promising for transport fuel productions. The leading companies such as Anellotech, Envergent, KiOR, GTI, RTI, KIT, Choren, BTG, TEII and RELL have developed upgrading bio-oil technologies where fast pyrolysis is combined with other processes (see Table 2.12).<sup>24</sup> In order to produce a conventional transport fuel such as diesel, gasoline, kerosene, methane and LPG the upgraded of bio-oil is considered a part of refining the feedstock and the product is processed further in conventional refining process units. Some possible combinations are shown in Figure 2.19. The connection of upgraded the bio-oil to a refinery stream takes advantage of the economies of scale and experience of a conventional refinery.

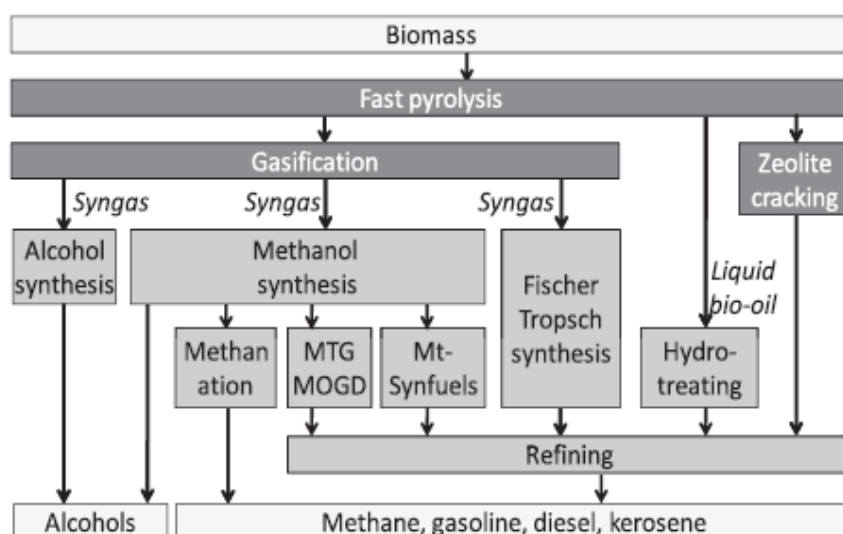


Figure 2.19: Upgrading of bio-oil to biofuels and chemicals<sup>20</sup>

Table 2.12: Integrated processes for upgrading bio-oil<sup>24</sup>

Company	Process	Development
Anellotech	CP	Reported to be developing a 2 t/d plant (planned completion of construction in 2014)
Envergent	FP+HP	Demonstration 1 t/d hydrotreating plant in Kapolei, Hawaii (USA), expected commissioning in 2014
KiOR	CP (FCC)	1 t/d pilot plant in Texas (USA). Funding of five plants in Mississippi (USA)
GTI	IH <sup>2</sup>	Proof of principle on lab scale. Recipient funded by Department of Energy (DoE) (USA)
RTI	VU	Lab scale entrained flow pyrolysis reactor for catalytic vapor upgrading
KIT	FP+G+S	12 t/d FP plant constructed G+S unit expected to be constructed by 2012
Choren	IP+G+S	45 MWth demonstration facility – intermediate pyrolysis + gasification + synthesis
BTG/Gronigen/Twente	FP+U	Bio-oil gasification trial completed on Choren gasifier. Development of hydroprocessing catalysts
RELL	CP+SR	Development of 25 t/d pilot plant (Toledo, Ohio, USA) for advanced pyrolysis and stream reforming for diesel and gasoline

CP=catalytic pyrolysis, FP= fast pyrolysis, HP= hydroprocessing, FCC=fluid catalytic cracking, IH<sup>2</sup>= catalytic hydro-pyrolysis and vapor hydrodeoxygenation, VU=vapor upgrading, G=gasification, S=synthesis, IP=intermediate pyrolysis, U=upgrading, SR=stream reforming

## Gasification of bio-oils/bioslurry

The integration of de-centralized fast pyrolysis and centralized gasification to produce syngas for methanol or for Fischer-Tropsch processes is a promising concept where fast pyrolysis could be used as a pre-treatment process and for densification of biomass. It offers cheaper transport and handling of biomass feedstocks from origin to the site of gasification. Many of the advantages of bio-oil gasification compared to solid gasification in terms of capital cost, performance and product cost can be seen from Table 2.13.<sup>20</sup> Bioslurry is a mixture of bio-oil and char and has been investigated as a feed for the gasification process.<sup>51,62</sup> Char has a yield of 15 – 25 wt% db<sup>1,20,24</sup> and an excellent grindability.<sup>17</sup> Char containing 15 – 28% of the energy content of the original biomass<sup>13</sup> is totally utilized. Bioslurry has an energy density of 21 – 23 GJ/m<sup>3</sup>,<sup>17</sup> which is 4 – 10 times higher than that of biomass, and this means that bioslurry not only retains 85 – 94% of the energy of the feedstock, but leads to a significant reduction of transport cost<sup>17,18,61</sup> and increased efficiency of the gasification process. The overall cost of delivering biomass for a distance of 100 km from the pyrolysis plant to the bioenergy plant (including costs of biomass production, harvest, farm haulage and road transport) is estimated to be 9.44 Australian dollar/GJ (\$A/GJ), which exceeds the 3.14 \$A/GJ for delivering bioslurry with 20 wt% char loading (including biomass production, harvest, farm haulage, road transport and bioslurry road transport, plant capital and operating costs<sup>61</sup>). The lower costs are mainly caused by lower transport costs (6.14 \$A/GJ for the biomass scenario compared with 3.55 \$A/GJ for the bioslurry scenario). Recently pressurized gasification (10 – 80 bar) has been developed for conversion of biomass to highly concentrated H<sub>2</sub> and CO (50% CO and 30% H<sub>2</sub>), high carbon conversion (>99%) and a tar free syngas.<sup>18,62</sup> Feeding bioslurry and bio-oil into a pressurized gasifier is known to be a simple and possible process<sup>18,62</sup> and probably easier and cheaper than feeding biomass because the bioslurry can be fed using pumps instead of a complicated pneumatic transport method.

The gasification of bio-oil/bioslurry has been studied by several organizations.<sup>18,24,63</sup> A 500 kWth entrained flow gasifier has been used for research and development of bio-oil gasification by BTG, but results are not yet reported in literature.<sup>24</sup> The bioslurry concept is being studied by Dynamotive (bio-oil plus project)<sup>24</sup> and by KIT (a bioliq project) for use in a pressurized gasifier. KIT has developed a 5 MW pilot gasifier that can operate at a maximum of 80 bar and 1200 °C producing synthetic biofuels from bioslurry<sup>18</sup> and plans to finish construction of a demonstration bioslurry gasification, gas cleaning and synthesis plants in 2012.<sup>24,63</sup>

Table 2.13: Comparison of solid biomass gasification and bio-oil gasification<sup>20</sup>

Impact from using liquid bio-oil	Capital cost	Performance	Product cost
Transport costs	Lower	Higher	Lower
Very low alkali metals	Lower	Higher	Lower
Handling and transporting costs	Lower	None	Lower
Liquid feeding to a gasifier particularly pressurised	Lower	Higher	Lower
Lower gas cleaning requirements	Lower	Higher	Lower
Higher costs for fast pyrolysis	Higher	Lower	Higher
Lower efficiency from additional processing step	Higher	Lower	Higher

### Catalytic fast pyrolysis of biomass

The catalyst fast pyrolysis process is known to produce a low oxygen bio-oil,<sup>64</sup> it performs at atmospheric pressure and does not use hydrogen. Zeolite is often used as a suitable catalyst in the catalytic fast pyrolysis.<sup>20</sup> There are two main possible integrations of zeolite cracking into fast pyrolysis (see Figure 2.20): 1) zeolite cracking can be directly integrated with a fast pyrolysis process (one step process) or 2) the zeolite cracking can operate on fast pyrolysis vapors in a separated catalytic reactor (two step process).

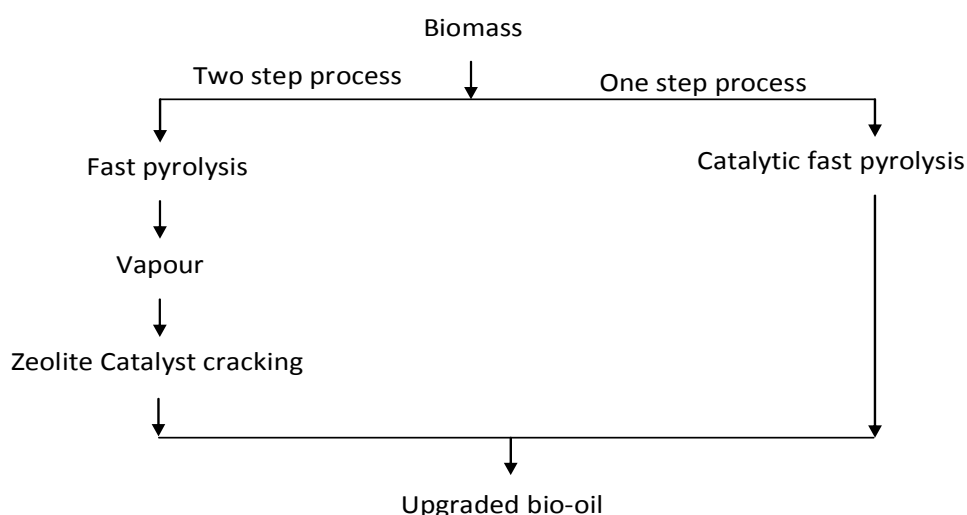


Figure 2.20: Methods of upgrading fast pyrolysis products with zeolite cracking catalyst<sup>20</sup>

The one step process of catalytic fast pyrolysis has been studied by many organizations for various zeolite types such as ZSM-5, H-Y zeolites, H-ZSM-5, Na/Y zeolites, FCC, clinoptilolite (see Table 2.14). Huber et al.<sup>65,66</sup> developed a catalytic fast pyrolysis process that uses ZSM-5 to produce a bio-oil having gasoline, diesel fuel, heating oil fractions and BTX (benzene, toluene and xylenes) in a one step process. The process requires high heating rates and high ratios of zeolite and biomass to ensure that the vapors enter the catalyst pores to avoid thermal decompositions. The Huber research group at the University of Massachusetts has developed a catalytic fast pyrolysis pilot plant for 15 barrels/day bio-oil.<sup>67</sup> Torren et al.<sup>68</sup> used ZSM-5 at 600 °C in a catalytic fast pyrolysis reactor. The result obtained is promising with an aromatic yield of 14% and olefin yield of 5.4% based on carbon. The aromatics mostly contain BTX (see Table 2.15). The one step process has also been investigated by Anellotech, BioEcon, Virginia Polytechnic Institute and State University<sup>20</sup> to produce gasoline and BTX. Because the zeolite catalyst fast pyrolysis operates at a single temperature and high catalyst/biomass ratios, the operation of the reactor is less flexible. Coke formation and catalyst deactivation are recognized problems.<sup>20</sup>

Table 2.14: An overview of zeolite catalysts and organizations studying catalytic fast pyrolysis<sup>20</sup>

Organization	Catalyst
<b>One step process</b>	
Anadolu University (TUR)	Clinoptilolite  (natural zeolite, NZ), ZSM-5, H-Y
Aston U. (GBR) BioECon Netherlands, and Kior (USA)	ZSM-5 nk
CPERI, (GRE)	MCM-41
East China U. Science and Technology, Shanghai, (CHN)	HZSM-5
Exelus (USA)	nk
Georgia Institute of Technology, (USA)	H-Y zeolites
Michigan State U. (USA)	nk
Sichuan U. (CHN)	Na/Y zeolite
Southeast U. Nanjing, (CHN)	FCC
U. Leeds, (GBR)	ZSM-5
U. Massachusetts (USA)	ZSM-5
Virginia Tech (USA)	H-ZSM-5 Zr based superacids

Two step process	
Aston U. (GBR)	ZSM-5
East China University of Science and Technology (CHN)	HZSM-5
Instituto Superior Técnico, (PRT) + Kior + Petrobras	FCC and FCC + ZSM-5
Norwegian U. Science and Technology (NOR) + CPERI (GRE) + SINTEF (NOR)	Al-MCM-41, FCC, SBA-15
U. Science and Technology of China, Anhui, (CHN)	HZSM-5, HY, ZrO <sub>2</sub> &TiO <sub>2</sub> , SBA-15, Al/SBA-15.
University of Seoul, Kongju National University, Kangwon National University, (KOR)	Spent HZSM-5

The two step process of catalytic fast pyrolysis often consists of a catalyst bed reactor downstream from a primary fast pyrolysis reactor. The bio-oil oxygen is largely converted into H<sub>2</sub>O, CO and CO<sub>2</sub> in the catalytic reactor.<sup>69</sup> The primary pyrolysis vapors from the fast pyrolysis of biomass have been found to be very reactive with the zeolite catalyst to produce aromatics.<sup>69,70</sup> The aromatics from the zeolite catalytic vapor reactor are high octane number components that can be used for gasoline blending and have typical yields of 20 wt%.<sup>69</sup> Due to operation in two reactors (a fast pyrolysis reactor and a catalytic vapor reactor), the two step catalytic fast pyrolysis has flexible operational temperatures and vapor/catalyst ratio. Even though char is separated from the primary fast pyrolysis reactor which minimizes the contact between the zeolite and metal components in the char, catalyst deactivation and coke formation are however still recognized problems.<sup>20</sup> Some organizations use ZSM-5, HZSM-5, FCC, SBA-15, Al/ SBA-15, HY and ZrO<sub>2</sub>-TiO<sub>2</sub> to investigate the two step catalytic fast pyrolysis process (see Table 2.14).

Table 2.15: Detailed carbon yield distribution and product selectivity.<sup>68</sup>

	WHSV/h <sup>-1</sup>			
	0.1	0.2	0.8	1.7
Overall yields				
Aromatics	14.0	11.0	12.1	9.5
Olefins	5.4	8.2	8.6	6.1
Methane	2.8	4.5	8.8	8.0
Carbon monoxide	26.2	26.3	23.1	29.9
Carbon dioxide	9.4	8.1	4.9	5.6
Coke	36.8	30.2	26.1	19.9
Aromatic selectivity				
Benzene	24.8	23.1	29.1	33.4
Toluene	34.1	30	21.9	17.2
Ethylbenzene	0.6	1.2	0.5	0.2
<i>m</i> -Xylene and <i>p</i> -xylene	12.9	12	5	2.6
<i>o</i> -Xylene	2.5	1.9	0.8	0.3
Styrene	3.3	4.4	5.9	5.2
Phenol	1.1	4	8.1	5.1
Indene	1.4	7.1	8.9	8.4
Benzofuran	4.3	1.6	2.1	1.4
Naphthalene	14.9	14.7	17.7	26.1
Light hydrocarbon selectivity				
Methane	34.2	35.4	50.6	57
Ethylene	59.8	41	41.3	37
Propylene	5.4	16.6	6.1	4.3
Butene	0.2	1.9	0.4	0.3
Butadiene	0.4	5	1.7	1.5

WHSV: Weight hourly space velocity (WHSV = Mass Flow/Catalyst Mass)

### Hydrogen upgrading of biomass/bio-oils

Hydrotreating is a process that uses hydrogen and a catalyst to reduce the oxygen content of bio-oil and improve the quality of the product. To minimize hydrogen consumption in hydrotreating, the process must involve hydrodeoxygenation (HDO) and the saturation of aromatic rings carries less emphasis.<sup>71</sup> The reactions taking place during the HDO process which involves 1) water separation; 2) dehydration reaction due to polymer reactions; 3) decarboxylation reaction in which oxygen is removed in the form of water; 4) hydrogenation reaction that involves saturation of unsaturated components and 5) hydrogenolysis reaction that breaks down high molecular components.<sup>71</sup> Because bio-oil contains high oxygenates and aromatics, a 2-stage operation (with CoMo or NiMo catalyst) is often required for conversion of bio-oil. The first stage is often performed at temperatures below 300°C and pressure of 21 MPa to remove significant oxygen components and produce a stabilized oil product.<sup>71</sup> The second stage is performed at more severe conditions (temperatures around 350 °C and a pressure of 21 MPa) to remove oxygen of phenols and furans that have low HDO reactivities.<sup>71</sup>

Table 2.16: Catalytic upgrading of pyrolysis by hydrotreating<sup>24</sup>

Organisation	Catalyst
Dynamotive, Canada	nk
East China U. Science and Technology, Shanghai, China	CoMo–P sulfided
East China U. Science and Technology, Shanghai, China	Pd on ZrO <sub>2</sub> with SBA1 <sub>5</sub>
Guangzhou Institute of Energy Conversion, China	NiMo on Al <sub>2</sub> O <sub>3</sub>
Groningen University, Netherlands	Ru and homogeneous Ru
IRCELYON CNRS Université Lyon 1,	CoMo/Al <sub>2</sub> O <sub>3</sub>
Mississippi State U., USA	NiMo/ $\gamma$ Al <sub>2</sub> O <sub>3</sub>
	CoMo/ $\gamma$ Al <sub>2</sub> O <sub>3</sub>
	HZSM-5, SUZ-4
	Precious metal
Pacific Northwest Laboratory (PNNL), USA	Pd, Ru
REHydrogen, UK	nk
State U. Iowa, USA	nk
Technical U. of Munich, Germany	Pd on C
U. Jyväskylä, Finland/VTT, Finland	Ru on C
U. Kentucky, USA	Pt
U. Maine, USA	nk
U. Oklahoma, USA	Pd on carbon nanotubes
U. Twente, Netherlands	Precious metal
UOP, USA	Precious metal

Industrial hydrodesulfurization (HDS) catalysts, such as CoMo/Al<sub>2</sub>O<sub>3</sub>, NiMo/Al<sub>2</sub>O<sub>3</sub> used for hydrotreating in refining processes, are often used for the HDO process.<sup>71</sup> However, the catalyst support (Al<sub>2</sub>O<sub>3</sub>) is found to be unstable in the high water bio-oil and the sulfur level in the catalyst that is used for catalyst activation is not stable.<sup>71</sup> Recently some transition metal catalysts such as Pt/C, Pt/C and Ru/C have been investigated for HDO processes. The results show that both the yield and the deoxygenation levels for the transition catalysts, especially Ru/C, were higher than those of CoMo/Al<sub>2</sub>O<sub>3</sub> or NiMo/Al<sub>2</sub>O<sub>3</sub>. An overview of catalyst types and organizations studying HDO is presented in Table 2.16. PNNL, Dynamotive, State University of Iowa, Twente University, UOP, Groningen University and VVT have major research activities in this area. PNNL carried out a design study of HDO processes on 2000 dry t/d for gasoline and diesel productions<sup>72</sup>

## 2.6 Conclusion

The fast pyrolysis technologies are close to commercialization with the reactor types bubbling fluidized bed, circulating fluidized bed, rotary cone, auger and ablative; however, none of the reactor types demonstrates significant superiority to the others in terms of market attractiveness and technology strength. A wide range of biomass feedstock from wood, agriculture, industrial by-products, waste products and algae are investigated for use in the fast pyrolysis process. The reported results show that the ash content (especially the potassium content) and lignin content



cause a reduction in the bio-oil yield. The pyrolysis conditions (temperature, heating rate and reactor gas residence time) are found to have a strong influence on the product distribution. The temperature range of 450 – 550 °C and reactor gas residence time of less than 2 s are believed to be optimal conditions for maximizing bio-oil yield. The bio-oil has been considered a potential fuel for boilers, gas turbines and engine turbines. However, the aging (phase separation and increase of viscosity) is a challenge in the context of storage and application of the bio-oil. In the bio-refinery concepts producing transportation fuel from biomass, fast pyrolysis is considered a main component for densification biomass and production of bio-oil. Possible bio-oil upgrading technologies for the production of transport fuel involve hydrotreating, gasification and fluid catalytic cracking. These technologies are in the early stages of demonstration with upgrading oil properties showing promising prospects for transport fuel production.

## 2.7 References

1. Mohan D, Pittman C U, Jr, Steele P H. *Energ Fuels* **2006**, 20, 848.
2. Chiaramonti D, Oasmaa A, Solantausta Y. *Renew Sust Energ Rev* **2007**, 11, 1056 –1086
3. Lede J, Panagopoulos J, Li HZ, Villermaux J. *Fuel* **1985**, 64, 1514.
4. Miller RS, Bellan J. *Combust Sci Technol* **1997**, 126, 97–137.
5. Morf P, Hasler P, Nussbaumer T. *Fuel* **2002**, 81, 843–853.
6. Di Blasi C. *Biomass Bioenerg* **1994**,7, 87–98.
7. Bech N, Larsen M. B, Jensen P. A, Dam-Johansen K. *Biomass Bioenergy* **2009**, 33, 999-1011.
8. Bruchmüller J, van Wachem B. G. M, Gu S. Luo K. H. Brown R. C. A. *AIChE Journal* 2012, 58, 3030 - 3042
9. Di Blasi C. *Prog Energ Combust* **2008**, 34, 47–90.
10. Di Blasi, C. *Chemi Eng Sci* **1996**, 51, 1121–1132.
11. Diebold J, Power A. Engineering aspects of the vortex pyrolysis reactor to produce primary pyrolysis oil vapors for use in resins and adhesives, In: Bridgwater AV, editor. *Research in thermochemical biomass conversion*. London, UL: Elsevier; **1988**. p. 609-28
12. Trinh, T. N; Jensen, A. P.; Dam-Johansen. K.; Knudsen.N. O.; Sørensen, H. R.; Hvilsted. S. A. *Engery Fuel*  
**DOI:** 10.1021/ef301927y.
13. Gros S. Pyrolysis liquid as diesel fuel. Wärtsilä Diesel International. In: Seminar on power production from biomass II, 27–28 March 1995, Espoo, Finland.
14. Bridgwater A V, Toft A J, Brammer J G. *Renew Sustain Energy Rev* **2002**, 6, 181–246.
15. Bridgwater AV. *Developmenets in thermochemical biomass conversion*, Volume 1, First edition. Kluwer academic publishers 1997.

16. Strenziok R, Hansen U, Künster H. Combustion of Bio-oil in a Gas Turbine. Progress in Thermochemical Biomass Conversion. Oxford: Blackwell Science, **2001**, 1452-1458.
17. Abdullah H, Mourant D, Li C, Wu H. *Energ Fuels* **2010**, 24, 5669–5676.
18. Dahmen N, Henrich E, Dinjus E, Weirich F. *Energy, Sustainability and Society* **2012**, 1-44
19. Venderbosch R.H, Prins W. *Bioprod. Bioref* **2010**, 4, 178-208.
20. Bridgwater A.V. *Biomass bioengery* **2012**, 38 6 8 – 9 4
21. Oasmaa A, Solantausta Y, Arpiainen V, Kuoppala E, and Sipila K. *Energ Fuels* **2010**, 24, 1380–1388
22. Garcia-Perez M, Chaala A, Pakdel H, Kretschmer D, Rodrigue D, and Roy C. *Energ Fuels* **2006**, 20, 364-375
23. Oasmaa A, Kuoppala E. *Energ Fuels* **2003**, 17, 1075-1084
24. Butler E, Devlina G, Meierb D, McDonnell K. *Renew Sust Energ Rev* **2011**, 15, 4171–4186
25. Lede J, Panagopoulos J, Li HZ, Villermaux J. *Fuel* **1985**, 64, 1514.
- 26 (a). Ensyn. Ensyn Technologies Inc. and Tolko Industries LTD. Announce formation of partnership to build world's largest commercial fast pyrolysis plant. Available from: <http://www.ensyn.com/news/Ensyn-Press%20Release-HighNorth.pdf>; 2010.
  - (b). Task 34 - Pyrolysis, [http://www.pyne.co.uk/?\\_id=69](http://www.pyne.co.uk/?_id=69). Cited March 2013
  - (c). Janse, A. M. C.; Westerhout, R. W. J.; Prins, W. *Chem. Eng. Process* **2000**, 39, 239-252.
  - (d) Czernik S, Bridgwater A. *Energy Fuels* 2004;18:590–598
27. Brown R.C, Holmgren J. Fast pyrolysis and biooil upgrading. National program 207: bioenergy and energy alternatives – distributed biomass to diesel workshop. Richland, WA, USA; 2006.
28. de Wild, P. J, Huijgen, W. J. J, Heeres, H. J. *J Anal Appl Pyrol* **2012**, 93, 95-103.
29. Nowakowski D. J, Bridgwater A. V, Elliott D. C, Meier D, de Wild, P. *J Anal Appl Pyrol* **2010**, 88, 53-72.
30. Fahmi R, Bridgwater A.V, Donnison I, Yates N, Jones J.M. *Fuel* **2008**, 87, 1230–1240.
31. Azeez A M, Meier D, Odermatt J, and Willner T. *Energ Fuels* **2010**, 24, 2078–2085.
32. Fonts I, Juan A, Gea G, Murillo MB, Sánchez JL. *Ind Eng Chem Res* **2008**, 47, 5376.
33. Piskorz J, Scott DS, Westerberg IB. *Ind Eng Chem Process Des Dev* **1986**, 25, 265–270.
34. Shen L, Zhang D-K. *Fuel* **2003**, 82, 465.
35. Pokorna E, Postelmans N, Jenicek P, Schreurs S, Carleer R, Yperman J. *Fuel* **2009**, 88, 1344–1350.
36. Kang B-S, Lee KH, Park HJ, Park Y-K, Kim J-S. *J Anal Appl Pyrol* **2006**, 76, 32.
37. Park HJ, Park Y-K, Dong J-I, Kim J-S, Jeon J-K, Kim S-S, et al. *Fuel Process Technol* **2009**, 90, 186–195.
38. Garcia-Perez M, Wang XS, Shen J, Rhodes MJ, Tian F, Lee W-J, et al. *Ind Eng Chem Res* **2008**, 47, 1846–1854.
39. Boroson M.L, Howard J.B, Longwell J.P, Peters W.A. *AIChE Journal* **1989**, 35, 120-128.
40. Scott D. S, Plskorz J, Radleln D. *Ind.Eng.Chem.Process Des.Dev* **1985**, 24, 581-588.
41. Ibrahim, N. B.; Jensen, P. A.; Dam-Johansen K.; Helge, E. Characterization of Flash Pyrolysis Products of Wheat Straw, Rice Husk and Pine Wood, Biomass and Bioenergy, Submitted 2012

42. Jensen A, Dam-Johansen K, Wojtowicz M. A, Serio M. A. *Energ Fuels* **1998**, 12, 929-938.
43. Johansen J. M, Jakobsen J. G, Frandsen F. J, Glarborg P. *Energ Fuels* **2011**, 25, 4961-4971.
44. Bae Y. J, Ryu C, Jeon J. K, Park J, Suh D. J, Suh Y. W, Chang D, Park Y. K. *Bioresource Technol* **2011**, 102, 3512 -3520.
45. Nikolaisen, L.; Jensen, P. D.; Bech, K. S.; Dahl, J.; Busk, J.; Brødsgaard, T.; Rasmussen, M.O.; Bruhn, A.; Bjerre A. A.; Nielsen, H. B.; Albert, K. R.; Ambus, P.; Kadar, Z.; Heiske, S.; Sander, B.; Schmidt, E. R.; Energy Production from Marine Biomass (ulva lactuca) PSO Project No. 2008-1-0050, **2011**, Danish Technological Institute, Denmark
46. Toft AJ. PhD Thesis, Aston University; 1998.
47. Elliot D.C. Analysis and comparison of biomass pyrolysis/gasification condensates – final report, No. PNL-5943, Pacific Northwest Laboratory, Richland, WA, 1986.
48. Wagenaar BM, Venderbosch RH, Prins W and Penninks FWM, Bio-oil as a coal substitute in a 600 MWe power station, 12th European Conference and Technology Exhibition on Biomass for Energy, Industry and Climate Protection. June 17-21, Amsterdam, the Netherlands (2002)
49. Scott D.S. *J. Anal. Appl. Pyrolysis* **1999**, 51, 23-37.
50. Pollarda A.S, Roverc J.M, Brown R.C. *J Anal Appl Pyrol* **2012**, 93, 129–138
51. Scholze B, Hanser C, Meier D. *J Anal Appl Pyrol* **2001**, 58–59:387.
52. AV Bridgwater. Fast Pyrolysis of Biomass: A Handbook Volume 2.
53. Trung NT, Hvilsted S, Jensen PA, Sørensen H. R., Dam-Johansen K. FLASH PYROLYSIS PROPERTIES OF ALGAE AND LIGNIN RESIDUE. European biomass 20<sup>th</sup> conference, Milan June 2012
54. Scholze B, Hanser C, Meier D. *J Anal Appl Pyrol* **2001**, 58, 387-400.
55. Ba T, Chaala A, Garcia-Perez M, Rodrigue D, Roy C. *Energ Fuels* **2004**, 18, 704-712.
56. Mullen A C, Boateng A A. *J Anal Appl Pyrol* **2011**, 90, 197–203.
57. Norazana Binti Ibrahim. Bio-oil from Flash Pyrolysis of Agricultural Residues. Ph.D. Thesis 2012. DTU Chemical Engineering.
58. Bradbury A. O. W, Sakai Y, Shafizadeh F. J. *Appl. Polym. Sci.* **1979**, 23, 327.
59. Fagbemi L, Khezami L, Capart R. *Appl Energ* **2001**, 69, 293–306.
60. Antal MJ. *Ind Eng Prod Res Dev* **1983**, 22, 366–375.
61. Wu H, Yu Y, Yip K. *Energ Fuels* **2010**, 24, 5652–5659
62. Henrich E, Weirich F. *Environ Eng Sci* **2004**, 21, 53-64
63. Dahmen N. Fast pyrolysis in the bioliq process. *PyNe Newsletter* **2010**;27:8–10.
64. George W. H, Avelino C. *Angew. Chem. Int. Ed.* **2007**, 46, 7184 – 7201.
65. Huber G W, Bale B. *Sci Am* **2009**; 50, 299.
66. Williams P T, Nugranad N. *Energy* **2000**; 25(6):493e513.
67. KiOR. State of Mississippi pledges financial support for five KiOR biofuel facilities. Available from <http://www.kior.com/content/article.php?Atricle=1&s=2&s2=35&p=35&t=News-and-Events>; 2010 (cited 26.11.10).

68. Carlson T R, Cheng Y, Jae J, Huber G W. *Energy Environ Sci* **2011**, 4, 145–161.
69. Ju P H, Jong-In D, Jong-Ki J, Kyung-Seun Y, Jin-Heong Y, Jung M S. Conversion of the pyrolytic vapor of radiata pine over zeolites. *J Ind Eng Chem* **2007**, 13, 182 - 189.
70. Diebold J P, Beckman D, Bridgwater AV, Elliott D C, Solantausta Y. IEA technoeconomic analysis of the thermochemical conversion of biomass to gasoline by the NREL process. In: Bridgwater AV, editor. *Advances in thermochemical biomass conversion*. Blackie; **1994**. p. 1325e42.
71. Bu Q, Lei H, Zacher AH, Wang L, Ren S, Liang J, Wei Y, Liu Y, Tang J, Zhang Q, Ruan R. *Bioresour Technol.* **2012** 124, 470-477
72. Jones S B, Holladay J E, Valkenburg C, Stevens D J, Walton C W, Kinchin C. Production of gasoline and diesel from biomass via fast pyrolysis, hydrotreating and hydrocracking: a design case. Richland, Washington 99352: Pacific Northwest National Laboratory; **2009**. PNNL-18284.

February, 2014, DTU

**Appendix A2**

**Journal paper: Comparison of Lignin, Macroalgae,  
Wood, and Straw Fast Pyrolysis**

**Energinet.dk project no. 010077**

**Treatment of Lignin and waste residues by flash pyrolysis**

**Trung Ngoc Trinh, Peter Arendt Jensen, Kim Dam-Johansen, Niels Ole Knudsen,  
Hanne Risbjerg Sørensen, and Søren Hvilsted**

*Department of Chemical and Biochemical Engineering*

Technical University of Denmark

Søltofts Plads, Building 229, DK-2800 Lyngby, Denmark

**CHEC no. R1401**

# Comparison of Lignin, Macroalgae, Wood, and Straw Fast Pyrolysis

Trung Ngoc Trinh,<sup>†</sup> Peter Arendt Jensen,<sup>\*,†</sup> Kim Dam-Johansen,<sup>†</sup> Niels Ole Knudsen,<sup>‡</sup> Hanne Risbjerg Sørensen,<sup>‡</sup> and Søren Hvilsted<sup>†</sup>

<sup>†</sup>Department of Chemical and Biochemical Engineering, Denmark Technical University, Søtofts Plads Bygning 229, Kgs. Lyngby 2800, Denmark

<sup>‡</sup>DONG Energy, Kraftsværksvej 53, DK-7000, Fredericia, Denmark

## Supporting Information

**ABSTRACT:** A fast pyrolysis study on lignin and macroalgae (nonconventional biomass) and wood and straw (conventional biomass) were carried out in a pyrolysis centrifugal reactor at pyrolysis temperature of 550 °C. The product distributions and energy recoveries were measured and compared among these biomasses. The fast pyrolysis of macroalgae showed a promising result with a bio-oil yield of 65 wt % dry ash free basis (daf) and 76% energy recovery in the bio-oil while the lignin fast pyrolysis provides a bio-oil yield of 47 wt % daf and energy recovery in bio-oil of 45%. The physiochemical properties of the bio-oils were characterized with respect to higher heating value (HHV), molecular mass distribution, viscosity, pH, density, thermal behaviors, elemental concentrations, phase separation, and aging. The lignin and macroalgae oil properties were different compared to those of the wood and straw oils with respect to carbon and oxygen contents, HHV, thermal behaviors, and mean molecular weight. The HHV of wood, straw, lignin, and algae oils were 24.0, 23.7, 29.7, and 25.7 MJ/kg db, respectively. The distributions of metals, Cl and S in char and bio-oil were investigated for the biomasses. Almost all the metals (Al, Ca, Fe, K, Mg, Na, P, and Si) were contained in the chars at the pyrolysis temperature of 550 °C. The char properties were characterized, and their potential applications are discussed.

## INTRODUCTION

Bio-oil obtained from pyrolysis of biomass is considered to be an alternative fuel. Bio-oil is reasonable easily transported and can be used directly as a fuel in boilers, or it can be used as a feedstock to produce chemicals or transportation fuels.<sup>1,2</sup> Wood is often found to be an optimal feedstock for fast pyrolysis with a bio-oil yield of 70–75 wt %.<sup>1,2</sup> However, other biomass feedstock may be applicable. Among the forms of nonconventional biomass: macroalgae and lignin (industrial residue) may be attractive materials for fast pyrolysis due to their low price and noncompetitiveness with food crops.

Macroalgae may be cultivated in coastal areas. The species *Ulva lactuca* is considered as a potential macroalgae for production of biofuel.<sup>3</sup> It can produce up to 45 tons dry/ha/year and has a content of carbohydrates of up to 60% of dry matter.<sup>3</sup> The production rate of the macroalgae is estimated to be 2–6.5 times higher than that of terrestrial biomass per unit surface area.<sup>3,4</sup> Macroalgae often have a high ash content (10–40 wt %)<sup>3,5,6</sup> and contain large amounts of alkali metals and chlorides.<sup>3,5</sup> This will probably cause slagging, fouling, and aerosol formation related problems if the algae is used directly in combustion and gasification plants.<sup>7</sup> However, fast pyrolysis is performed at a lower temperature compared to combustion or gasification, and it is believed that the process may not be significantly disturbed by the ash. Most metal elements probably be concentrated in the char product.<sup>8,9</sup> Although macroalgae has been recognized as a promising feedstock for fast pyrolysis processes, according to our knowledge, no study on macroalgae fast pyrolysis has been performed to evaluate this potential. So far, only studies of macroalgae pyrolysis carried out in fixed bed reactors have been reported.<sup>10–12</sup> These

studies showed bio-oil yields of 15–52 wt % daf (13–47 wt % on as received basis) obtained from various macroalgae species. Fixed bed reactors have a lower biomass heating rate than that of fast pyrolysis reactors and this probably lead to a low bio-oil yield when macroalgae is pyrolyzed in a fixed bed reactor.

Lignin is the second most abundant biomass component (in wood and straw) and is a complex, amorphous cross-linked, and three-dimensional, highly branched polymer.<sup>13</sup> Lignin is mainly produced by the pulp and paper industry, and in the near future, it will also appear as a byproduct from the second generation bioethanol industry. The potential of lignin produced as a residue in the paper industry is more than 50 million tons/year.<sup>14</sup> However, only about 2% of the lignin residue is used as commercial products for producing lignosulphonates and kraft lignins.<sup>14</sup> Most of the available lignin is combusted to generate energy for the pulp mills. Since the fast pyrolysis process has been developed for bio-oil production from biomass, lignin may be used as a feedstock for this process to produce a higher value product such as a bio-oil that provide liquid fuels, petrochemical phenols, adhesives, or resins. Some studies have been conducted on lignin fast pyrolysis.<sup>15,16</sup> However, the obtained bio-oil yield from the lignin pyrolysis has been found to be much lower than that of typical biomasses.<sup>1,2,15,16</sup> In addition, the work of an international collaboration<sup>16</sup> on the lignin fast pyrolysis process figured out that highly concentrated lignin material is difficult to

Received: November 26, 2012

Revised: January 18, 2013

Published: January 21, 2013

process in a fluidized bed reactor because of plugging and agglomeration at a screw feeder, reactor, and condenser.

Different fast pyrolysis reactors such as bubbling fluidized bed reactors, circulating fluidized bed reactors, rotary cone reactors, auger reactors, and ablative reactors have been developed for the fast pyrolysis process and are close to commercialization.<sup>1</sup> The main difference among these reactors is that different heat transfer methods are used to obtain a high heating rate. The pyrolysis centrifugal reactor (PCR), a type of ablative reactor, has been developed at the CHEC center at DTU Department of Chemical Engineering. By a high centrifugal force, biomass particles can gain a high heating rate of 200–2000 K/s.<sup>17</sup> The main advantages of this concept compared to fluid bed reactors are a compact design that uses a low flow rate of carrier gas and can treat relatively large biomass particles. Studies of pyrolysis conditions on the PCR of wood, straw, lignin, and sewage sludge<sup>9,17,18</sup> have figured out that temperatures around 525–575 °C and gas residence time around 0.8 s should be used to obtain maximum bio-oil yield.

There is a paucity of lignin and macroalgae fast pyrolysis information for bio-oil production and bio-oil properties in the literature.<sup>10,15,16</sup> Previous investigations were concerned on the pyrolysis conditions needed to obtain a maximum bio-oil production. Thus, an overall comparative investigation of fast pyrolysis of lignin, macroalgae, wood, and straw are reported in this study. Furthermore, since the wood, straw, lignin, and macroalgae show a variety of biomass compositions especially with respect to ash and lignin contents, the results of this paper can also contribute with knowledge on the influence of the biomass compositions on pyrolysis and bio-oil properties.

## EXPERIMENTAL SECTION

**1. Experimental Apparatus.** The pyrolysis centrifugal reactor (PCR) was developed at the CHEC center (DTU Chemical Engineering) and is described in detail elsewhere.<sup>17</sup> A sketch of the PCR is presented in Figure 1. The pyrolysis of biomass takes place

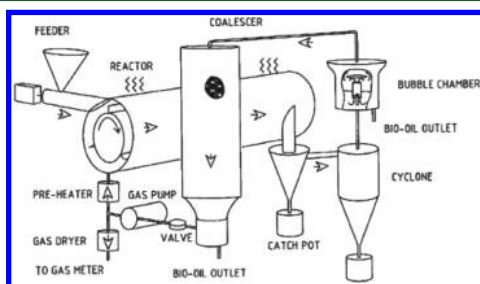


Figure 1. Sketch of the pyrolysis centrifugal reactor (PCR).

inside the reactor, whereby char, bio-oil, and gas are produced. The char particles are collected by cyclones. The bio-oil is condensed in a bubble chamber filled with isopropanol as a condensing solvent. The temperature in the bubble chamber is controlled to be 30–40 °C by means of a cooling water system. The light oil fraction and aerosols are further condensed by a coalescer filled with Rockwool. A recycled gas product is pumped back to maintain a desired gas residence time of 0.5–2 s in the reactor. Before entering the reactor, the gas is heated to around 550 °C. The gas products are dried by a water condenser and a gas filter to totally remove liquid before entering a gas meter.

The liquid fraction collected from the bubble chamber, coalescer, and water condenser is filtered through a Whatman filter paper (pore size of 5 μm). The char left on the filter is washed thoroughly by ethanol and then dried in an oven at 100 °C. The bio-oil yield is determined from the liquid that passed through the filter paper. The char yield is determined from the chars collected in the cyclones and

the char left on the filter paper. The gas measured from the gas meter is used to calculate the gas yield by the ideal gas equations.

The pyrolysis of the wood, straw, lignin, and algae were performed on the PCR with constant operation conditions: an rotor speed of 8870 rpm, a gas residence time of 0.8 s, a total experimental time of 60–90 min, feed consumption of 350–750 g biomass for each run, and a feeding rate of 340–990 g/h. The experiments were performed twice with each biomass to ensure reproducible pyrolysis products determinations. The operations of the PCR reactor using wood, straw, and algae were smooth and the experiments were carried out within 90 min. While the operation of the PCR using lignin was difficult, blocking of the nozzle connecting the cyclone, and the bubble chamber took place after 60 min operation. The obtained mass balance closures were in the range 96–99 wt % for the wood, straw, and algae PCR pyrolysis and 93–96 wt % for the lignin PCR pyrolysis tests.

**2. Characterization of the Biomasses and the Chars.** The applied lignin sample was a solid residual from a straw ethanol plant and provided by Inbicon A/S, DONG Energy, Denmark. The macroalgae (*Ulva lactuca*) was cultivated from May to September 2008 in a land-based facility at the Danish Shellfish Center, Nykøbing Mors, and provided by the Danish Technological Institute, Denmark. The wheat straw and beech wood were from Danish fields and woods. All biomasses were milled to a particle size of less than 1 mm.

The biomass samples and their char products were analyzed by the following methods: the moisture content by ASTM D2216, the ash content by ASTM D1102-84, the volatile content by ASTM D3175-02, the fixed carbon content by ASTM D3172-07a, higher heating value by a bomb calorimeter (IKA C-200). The size distribution of the char samples were measured by sieve analysis with sieve sizes 45–1000 μm.

The element contents of the wood, straw, lignin, and algae samples were analyzed by flash combustion (Thermo Finnigan, Flash EA1112) for CHN, by ICP-OES axial for Cl and S, and by ICP-OES radial for Al, Fe, P, Si, Ca, Mg, K, Na. The oxygen content was calculated by difference.

Thermogravimetric analysis (TGA) of the biomasses are carried out in the temperature range 100–1000 °C and at a constant heating rate of 10 °C/min in a N<sub>2</sub> flow using a TGA instrument (Netzsch STA 449 F1).

The biomass components were analyzed following the NREL protocols: a determination of extractives by NREL/TP-510-42619<sup>19</sup> and a determination of the structural carbohydrates and Klason lignin by NREL/TP-510-42618.<sup>20</sup> The biomasses were extracted in water and ethanol for determination of extractives. The biomasses were diluted in a strong acid for determination of structural carbohydrates and lignin. The Klason lignin content was determined as the residue left after acid digestion while soluble aliquot was used to analyze sugars such as glucan, xylan, galactan, mannan, arabinan, and rhamnan by a high pressure liquid chromatography (HPLC) (Shimadzu Prominence, HPLC, Shimadzu Corporation, Kyoto, Japan, the refractive index detector (RID-10A)) with an Aminex HPX-87H Ion Exclusion column (Bio-Rad Laboratories, U.S.A.) (eluent 12 mM H<sub>2</sub>SO<sub>4</sub>, flow 0.6 mL/min, column temp 63 °C) used for the straw, lignin, and algae and an Aminex HPX-87P (Bio-Rad Laboratories, U.S.A.) (eluent water, flow 0.5 mL/min column temp 80 °C) used for the wood.

**3. Characterization of the Bio-oils.** The isopropanol solvent was removed from the liquid samples collected from the PCR by a rotary vacuum evaporator at 30 °C to obtain the bio-oil samples. About 10–16 wt % water content and small amounts of volatiles of bio-oil samples were probably lost during the solvent removal. An amount of distilled water was added to these bio-oils to finalized a water content of 26–27 wt % in which bio-oil are found to obtain a homogeneous phase.<sup>21</sup> Thus, pH and TGA properties of the bio-oils are slightly influenced by the solvent removal (see the Supporting Information for further data).

The water content was determined by a Karl Fischer titration (Metrohm-701KT titrino). The HHV was measured by a bomb calorimeter (IKA C-200). The viscosity was determined by rotational viscosimeter (PAAR AMV 200). The density was measured by density meter (Anton paar, DMA 4100). The pH was determined by pH

meter (PHM 92, Lab pH meter). The phase separation was observed by a microscope (Nikon, Model Eclipse ME600L, Japan).

The element concentrations were analyzed by the following methods: C, H, N by flash combustion (Thermo Finnigan, Flash EA1112), Cl and S by ICP-OES axial, and Al, Fe, P, Si, Ca, Mg, K, Na by ICP-OES radial and the oxygen content was calculated by difference.

The molecular weight distribution was analyzed by size-exclusion chromatography (SEC) using the following instrument: Viscotek GPCmax VE-2001 equipped with Viscotek TriSEC Model 302 triple detector using two PLgel mixed-D columns from Polymer Laboratories. The samples were run in THF at 30 °C (1 mL·min<sup>-1</sup>). The molar-mass characteristics were calculated using polystyrene standards. In order to take a representative sample for SEC analysis the bio-oils were diluted with ethanol to make it homogeneous and then passed through a 0.2 μm filter.

Thermal behaviors of the bio-oils were analyzed by the TGA (STA, Netzsch STA 449 F1). The 8–10 mg samples were heated up from room temperature to 1000 °C at a constant heating rate of 10 °C/min under a N<sub>2</sub> flow.

## RESULTS AND DISCUSSION

**1. Characterization of the Biomasses.** The results of the proximate analysis, ultimate analysis, and elemental analyses of the biomasses are presented in Table 1. The volatile yield is in the range 84–76 wt % dry basis (db) for the wood and the straw, whereas a relative yield of 67–61 wt % db for the algae and lignin are determined. The ash contents are in the low range of 3–6 wt % db for the wood and straw and in the high range of 12–29 wt % db for the lignin and algae. The alkali metals (especially potassium) act as catalyst of biomass pyrolysis,<sup>22–24</sup> and they promote gas and char formations, leading to a reduced bio-oil yield and increased gas and char yields.<sup>1,22–24</sup> The lignin shows the highest carbon and the lowest oxygen content, resulting in the lowest O/C ratio when compared to the other biomasses. A low O/C value probably gives a relative high HHV of biomass.<sup>22,25</sup> The wood, straw, and algae have contents of carbon, oxygen, and O/C ratios in the ranges 47–53 wt % daf, 40–44 wt % daf, and 0.78–1.2 wt % daf, respectively.

Among the biomasses algae was observed to have higher nitrogen, sulfur, chloride, and alkali contents than that of the other feedstocks. The lignin was collected from a straw ethanol plant; thus, it was treated and washed several times; consequently, although the lignin has a high ash content, it contains relatively low amount of chlorine and alkali.

The results of the analysis of the biomasses' organic compositions are summarized in Table 2. Lignin is a complex, heavily cross-linked, and highly branched polymer.<sup>13</sup> The decomposition of lignin takes place at a higher pyrolysis temperatures than those of cellulose and hemicellulose components. A lignin rich material has been found to produce a relatively low bio-oil yield and a high char yield by the fast pyrolysis.<sup>15,16</sup> The wood and straw samples have Klason lignin contents of 25 and 18 wt % daf, respectively. While the lowest lignin content of 14 wt % daf was observed for the algae sample, the highest lignin content of 79 wt % daf appeared for the lignin sample. The sugars such as glucan, xylan, galactan, mannan, arabinan, and rhamnan are contained in the cellulose and hemicellulose components. Total contents of cellulose and hemicelluloses are of 62–66 wt % daf for the wood and straw and around 12–26 wt % daf for the lignin and algae. The algae shows a large extractive content (41 wt % daf) that consist of 21 wt % daf of protein (using a correlation of 4.43 × nitrogen for plant protein<sup>26</sup>) and probably a majority of starch.<sup>3,11,27</sup> The

**Table 1. Proximate Analyses of the Investigated Biomasses**

	wood	straw	lignin	algae
proximate analysis (% wt)				
moisture (% wt)	9.1	7.9	4.7	8.9
volatile (% wt db)	84.3	75.8	61.2	67.1 <sup>a</sup>
fixed carbon (% wt db)	13	18.5	26.7	6.5 <sup>a</sup>
ash (% wt db)	2.7	5.8	12.1	29.1
calorimetric analysis				
HHV (MJ/kg on db)	19.0	18.4	22.8	12.9
HHV (MJ/kg on daf)	19.5	19.4	25.9	18.2
ultimate analysis (% wt db)				
C	51.3	45.7	57.8	33.6
H	5.7	6.0	5.7	5.1
O	40.5	40.9	23.6	28.2
N	0.21	1.4	1.2	3.3
O/C	0.79	0.89	0.41	0.84
ultimate analysis (% wt daf)				
C	52.7	48.6	65.8	47.4
H	5.90	6.4	6.50	7.2
O	41.0	43.5	26.8	39.8
N	0.22	1.5	1.40	4.7
O/C	0.78	0.90	0.41	1.2
element analyses (% wt db)				
Al	0.05	0.03	0.07	0.29
Fe	0.05	0.04	0.30	0.31
P	0.01	0.13	0.06	0.34
Si	0.84	1.29	4.18	4.10
Mg	0.04	0.06	0.02	2.52
Ca	0.32	0.23	0.43	2.74
K	0.14	1.51	0.13	2.45
Na	0.02	0.07	0.28	0.23
Cl	<0.01	0.74	0.02	1.1
S	0.03	0.16	0.14	3.4

<sup>a</sup>The volatiles were determined by ASTM D3175-02 a method for coal and coke in which the sample is heated up 950 °C in nitrogen gas. Fixed carbon was calculated by a difference. The algae sample has a high content of S, Cl, N, K that have a significant release at 950 °C. Thus the result of organic volatile release is probably lower for the algae sample.

protein content of *Ulva lactuca* is found to varies greatly with seasons, and it is reported to have a protein content of 9–33 wt % db.<sup>27</sup>

The ash (especially the potassium) and lignin contents strongly influence the product yields and bio-oil properties. Among the biomasses, there is considerable variation of the ash and lignin contents. It is seen that the algae has the lowest lignin content of 14 wt % daf and the highest ash content of 29 wt % db. The lignin sample has an ash content of 12 wt % db, and the highest lignin content of 79 wt % daf. The straw sample has an ash content of 6 wt % and a low lignin content of 18 wt % daf. The wood is considered as probably the best feedstock for fast pyrolysis with an ash content of 3 wt % db (and a K content of 0.14%wt db) and a lignin content of 25 wt % daf.

Thermal analysis (TGA and DTG) of the biomasses was carried out at a heating rate of 10 °C/min, up to 1000 °C under N<sub>2</sub> flow. The TGA conversion of the biomasses are shown in Figure 2. The wood and straw experience a major initial mass loss between 200–500 °C, with DTG peak temperatures of 360 °C for wood and 340 °C for straw. The lignin experiences pyrolysis conversion in a broad temperature range from 120 to 550 °C, and its DTG peak temperature is 350 °C. The thermal



Table 2. Biomass Compositions

component	% wt db				% wt daf			
	wood	straw	lignin	algae	wood	straw	lignin	algae
ash	2.7	5.8	12.1	29.1	—	—	—	—
extractives	1.0	6.6	trace	28.7	1.0	7.0	trace	40.5
Klason lignin	23.8	17.0	69.3	9.8	24.5	18.0	78.8	13.8
cellulose	39.0	38.4	7.3	6.0	40.1	40.8	8.3	8.5
glucan	39.0	38.4	7.3	6.0	40.1	40.8	8.3	8.5
hemicellulose	21.3	24.2	3.2	12.2	21.8	25.7	3.6	17.2
xylan	17.1	20.7	2.4	4.7	17.6	21.9	2.7	6.7
galactan	1.6	1.0	0.6	trace	1.6	1.1	0.7	trace
mannan	1.6	trace	trace	trace	1.6	trace	trace	trace
arabinan	1.0	2.5	0.2	trace	1.0	2.7	0.2	trace
rhamnan	trace	trace	trace	7.5	trace	trace	trace	10.5
others	12.2	8.0	8.1	14.2	12.6	8.4	9.3	20.0

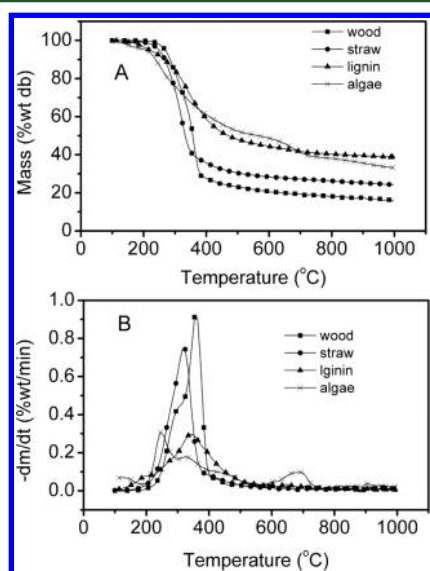


Figure 2. TGA (A) and DTG (B) for pyrolysis of the investigated biomasses.

decompositions of wood, straw, and lignin are consistent with lignocellulosic biomass pyrolysis data seen in the literature.<sup>28,29</sup> The thermal degradation of the algae is distinctly different from that of the lignocellulosic biomasses. The main DTG peaks of algae appear at a temperature of 250 °C and two overlapping peaks at 340 and 460 °C, and a small peak at 700 °C. The TGA pyrolysis peaks of cellulose and hemicelluloses are in the temperature range 180–320 °C while the peaks of protein, starch, and lignin probably overlap in the temperature range from 250 to 460 °C. These results are consistent with the decomposition temperatures of hemicelluloses,<sup>11,28</sup> cellulose,<sup>11,28</sup> protein and starch,<sup>10,28</sup> and lignin.<sup>11,28</sup> Algae has large contents of K (2.5 wt % db), Cl (1.1 wt % db), N (3.3 wt % db), and S (3.4 wt % db). The volatilization of these elements are found to be dominant at a temperature higher than 600 °C;<sup>30,31</sup> thus, the peak at a temperature of 700 °C is believed to correspond to a release of inorganic compounds, especially compounds of K, S, N, and Cl.

The Table 3 shows the TGA char yields obtained at temperature of 550 and 950 °C for the biomasses. The TGA char yields are 19, 24, 34, and 11 wt % daf at 550 °C and reduce to 13, 19, 27, and 7 wt % daf at 950 °C for wood, straw, lignin, and algae, respectively. It seems to be feedstocks with a high

Table 3. TGA Char at 550 °C

TGA char	wood	straw	lignin	algae
char at 550 °C (wt % daf)	19	24	34	21
fixed carbon (TGA char at 950 °C) (wt % daf)	13	19	27	7

lignin content or a high potassium content that cause in a high TGA char yield. A large fraction of S, Cl, and K have been found to be released at 950 °C,<sup>30,31</sup> and the algae sample has contents of K (2.5 wt % db), Cl (1.1 wt % db), N (4.5 wt % db), and S (3.4 wt % db). Thus, using the fixed carbon ASTM D3172-07a method developed for coal and coke is not suitable for the algae sample. The obtained fixed carbon of 7 wt % daf is probably uncertain.

**2. Fast Pyrolysis Product Distributions.** The pyrolysis experiments on the PCR of the biomasses were carried out with a gas residence time of 0.8 s, a reaction temperature of 550 °C, and feeding rates of 340–990 g/h. The temperature is believed to be sufficient to obtain full decomposition of the biomasses (see Figure 2B), and using a gas residence time of 0.8 s, considerable secondary reactions of tar will probably be avoided. The pyrolysis conditions used on the PCR have previously provided a maximum bio-oil yield from straw, wood, lignin, and sewage sludge.<sup>9,17,18</sup>

Table 4 summarized bio-oil and char yields data from different studies<sup>10,15,16,22,24,32–34</sup> together with data on carbohydrate compositions, ash content, and potassium content. Both carbohydrate composition and the ash influence pyrolysis products distribution of biomasses. However, the roles of the individual ash components on the pyrolysis process are not well understood. Alkali metals (especially potassium) have been found to catalyze the pyrolysis<sup>22–24</sup> and a high alkali content cause a decreased bio-oil yield,<sup>22–24</sup> an increased reaction water yield<sup>22,25</sup> and an increased gas and char yield,<sup>22–24</sup> whereas silicate seems to be inactive to pyrolysis of biomass. For wood and straw, the alkali content seems often to be proportional to the ash content;<sup>22</sup> thus, the effects of alkali metals are considered to be proportional to the ash content. The relative portions of cellulose, hemicelluloses, and lignin in biomass have a major influence on the product distribution and quality of the bio-oil.<sup>22,23</sup> The cellulose component mainly contributes to the pyrolysis bio-oil production,<sup>35</sup> while the hemicellulose component produces a lower bio-oil yield and higher gas and char yields.<sup>35</sup> The lignin component is also found difficult to pyrolyze and produces the lowest bio-oil yield and the highest char yield.<sup>15,16</sup> The

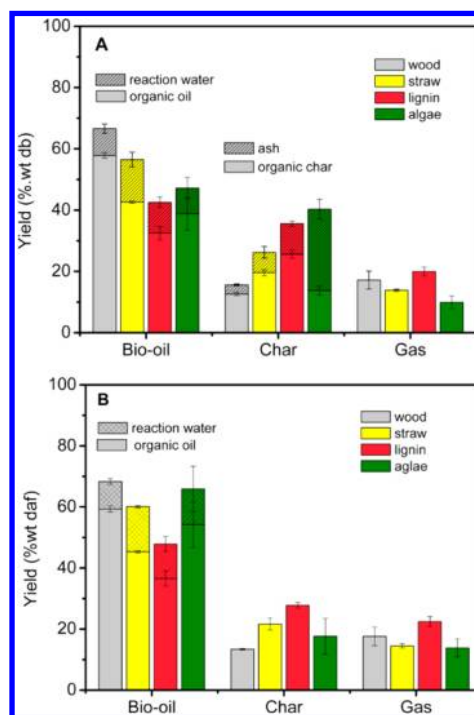
**Table 4.** Relation of the Carbohydrate Contents, Ash Content, and Potassium Content of Biomasses and the Bio-oil and Char Yields

sample	content (wt % daf) <sup>a</sup>			ash content (wt % db)	K content (wt% db)	yield (wt % daf) <sup>b</sup>		tech <sup>c</sup> –temp	ref
	cel	hem	lig			bio-oil	char		
wood									
beech	40	22	24	2.7	0.14	68	12	PCR, 550 °C	this study
beech	46	30	22	0.7	0.12	67	10	FBR, 470 °C	33
spruce	47	21	29	0.4	0.04	67	10	FBR, 470 °C	33
poplar aspen	42	31	16	0.4	–	77	14	FBR, 500 °C	32
willow	–	–	20	1.3	0.20	70	20	FBR, 507 °C	22
straw									
wheat straw	41	26	18	5.8	1.51	60	20	PCR, 550 °C	this study
wheat straw	42	24	21	6.0	1.50	61	23	PCR, 550 °C	34
rice straw	44	30	27	8.9	0.92	72	41	FBR, 491 °C	24
wheat straw	–	–	8	6.3	0.96	54	34	FBR, 509 °C	22
wheat straw	43	42	17	4.6	–	56	26	FBR, 550 °C	32
lignin									
straw lignin	8	4	79	12	0.13	47	27	PCR, 550 °C	this study
ETEK Lignin	~50	–	~50	0.2–0.6	0.02	58	27	FBR, 530 °C	16
ALM lignin	<0.2	<2	94	1.1–1.3	0.04	31	49	FBR, 530 °C	16
alcell lignin	0	0.1	96	0	–	39	43	FBR, 500 °C	15
granit lignin	–	–	90	<2	–	48	39	FBR, 500 °C	15
macroalgae									
<i>Ulva lactuca</i> <sup>d</sup>	9	17	14	29	2.45	65	20	PCR, 550 °C	this study
undaria	–	–	–	29	0.57	46	20	PTR, 500 °C	10
laminaria	–	–	–	31.2	10.25	46	17	PTR, 500 °C	10
pophyra	–	–	–	11.6	3.87	50	31	PTR, 500 °C	10
<i>Cladophora</i> sp.	–	–	–	13.3	–	19	26	FIR, 600 °C	11
<i>Lynghya</i> sp.	–	–	–	25.7	–	15	17	FIR, 600 °C	11
<i>Cladophora fracta</i>	–	–	–	6.3	–	51	–	TB, 600 °C	12
<i>Lemma minor</i>	–	–	–	9.5	–	40	39	QTR, 500 °C	47

<sup>a</sup>Cel: Cellulose. Hem: Hemicellulose. Lig: Lignin. <sup>b</sup>The bio-oil yield on daf was calculated from available data. <sup>c</sup>FBR: Fluidized bed reactor. TBR: transport bed reactor. PCR: pyrolysis centrifugal reactor. PTR: packed tube reactor. FIR: fix bed reactor. TB: tubular reactor. QTR: quartz tube reactor. <sup>d</sup>*Ulva lactuca* has a extractive content of 41 wt % daf.

extractives of biomass that contain a majority of protein and starch are known to enhance a bio-oil yield.<sup>36</sup> Based on literature results (see Table 4), it can be stated that the fast pyrolysis of wood as beech, spruce, poplar aspen, and willow (having low ash contents of 0.5–3 wt % db and lignin contents of 16–29 wt % db) often provide high bio-oil yield of 67–77 wt % daf,<sup>22,32,33</sup> while the fast pyrolysis of wheat straw (having ash contents of 4.5–6.5 wt % db that are rich in potassium and lignin contents of 8–21 wt % daf) obtain bio-oil yields of 54–61 wt % daf. The pyrolysis of lignin samples (having ash contents of 0–2 wt % db and lignin contents of 50–96 wt % db) show the lowest bio-oil yields of 31–58 wt % daf.<sup>15,16</sup> Results of macroalgae fast pyrolysis have not been found in literature. However, macroalgae have a low lignin content but a high potassium content and a high extractive content that is much higher than that of lignocellulosic biomass (less than 7 wt % daf). This results in macroalga fast pyrolysis properties are probably different from that of lignocellulosic rich biomasses.

Due to a considerable variation of the ash content in the biomasses used in this study, there are large differences between the product yields based on the dry feedstock and the dry ash free feedstock basis. The pyrolysis product yields on both bases are shown in Figure 3. The wood has the lowest ash content and produces a high bio-oil yield of 68 wt % daf. The straw with 5.8 wt % ash content obtained a bio-oil yield of 60 wt % daf. The results are consistent with a linear relationship observed between the bio-oil yield and an ash content in the range 1–7

**Figure 3.** Product distributions of biomass pyrolysis on PCR: (A) on dry feedstock basis. (B) on dry ash free feedstock basis.

wt % of wood and straw presented in the literature.<sup>22,37</sup> Samples with a high lignin content have also been shown to obtain a low bio-oil yields.<sup>15,16</sup> With a lignin content of 79 wt % daf, the lignin sample provided a bio-oil yield of 47 wt % daf. The algae sample has the lowest lignin content of 14 wt % daf and the highest ash content of 29 wt % db with a K content of 2.45 wt % db, and especially a high extractive content of 41 wt % daf. The obtained bio-oil yield of the algae sample was 65 wt % daf. It is slightly lower than that of the wood with about 3 wt % daf and higher than that of the straw with 5 wt % daf. The pyrolysis of various species macroalgae have been investigated in various fixed bed reactors.<sup>10</sup> The bio-oil yields obtained were in the range 46–50 wt % daf. In this study, the bio-oil yield obtained from the PCR is higher than that of the algae pyrolysis study on fixed bed reactors.<sup>10</sup>

Reaction water is formed by the decomposition of biomass cellulose, hemicelluloses, lignin, and protein. The reaction water yield was in the range 8–11 wt % daf for wood, lignin, and algae pyrolysis, while the highest yield of reaction water of 16 wt % daf was observed for the straw pyrolysis. It seems that the alkali, mainly potassium, catalyze the formation of reaction water,<sup>38</sup> and also, the high proportion of cellulose probably caused a high straw reaction water yield. Reaction water yields of 12–16 wt % db are reported for straw pyrolysis.<sup>25,34</sup> The obtained gas yields varied from 15 to 22 wt % daf for the biomasses (see Figure 3). The highest char yield of 27 wt % daf was obtained by the lignin sample, while the lowest char yield of 13 wt % daf appeared from the wood sample. The char yields were around 18 and 22 wt % daf for the algae and straw feedstocks, respectively. The char yields obtained on the PCR are 18–55% lower than the TGA char yields obtained at 550 °C (see Table 3) and almost similar to the values of the fixed carbon contents (except the algae case figured out the uncertain result of the fixed carbon content). This indicates that the biomasses PCR pyrolysis probably obtained a good conversion.

The oil and the char energy recovery were calculated based on the product yields of bio-oil and char and their heating values. The gas energy recovery was calculated by difference. The results are shown in Figure 4. With a high organic oil yield

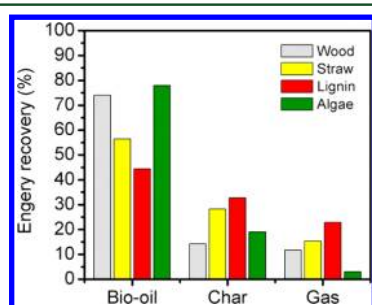


Figure 4. Energy recovery of gas, bio-oil, and char.

of 59 wt % daf, wood oil gained a 74% energy recovery whereas the straw and lignin oils contained 56% and 45%, respective of the feedstock energy content. An interesting result was found regarding the algae sample, the organic oil yield was 54 wt % daf, but the algae oil recovers 76% of the feedstock energy content. Some key issues when biomass is used as fuel are low energy density, poor grindability, and high transport costs;<sup>39</sup> this leads to a barrier for industrial applications of biomasses. Volumetric energy density of bio-oil enhances 4 folds in comparison to wood,<sup>40</sup> resulting in significant transportation

cost reduction and bio-oil is thereby easily stored and transported. Furthermore, it can be directly used as fuel in combustion and gasification plants. Thus, with 76% of the feedstock energy content recovered in the bio-oil, the fast pyrolysis of algae may be a promising way to provide a liquid fuel. Lignin is a solid residue from paper and bioethanol plants. By pyrolysis of lignin to produce bio-oil, 45% of lignin energy content is recovered in the bio-oil.

**3. Characterization of the Bio-oil Properties.** The HHV, pH, density, and elemental contents of the investigated bio-oils are presented in Table 5. The pyrolysis of biomasses

Table 5. Bio-oil Properties

	wood oil	straw oil	lignin oil	algae oil
water content (% wt)	27.3	25.7	27.4	26.6
HHV (MJ/kg) on wet basis	17.4	17.6	21.5	18.9
HHV (MJ/kg) on dry basis	24.0	23.7	29.7	25.7
pH	3.2	3.8	3.9	4.3
density @40 °C (g/mL)	1.12	1.15	1.09	0.98
element content (wt % dry basis)				
C (wt % dry basis)	57.0	58.8	65.6	59.5
H (wt % dry basis)	7.2	7.6	8.0	7.2
N (wt % dry basis)	0.5	1.62	1.7	4.0
O (wt % dry basis)	35.3	31.9	24.5	28.5
O/C	0.62	0.54	0.37	0.48
Al (mg/kg dry basis)	<5	22	<5	20
Ca (mg/kg dry basis)	33	124	<5	60
Fe (mg/kg dry basis)	30	55	25	277
K (mg/kg dry basis)	101	2870	161	732
Mg (mg/kg dry basis)	11	59	<8	2732
Na (mg/kg dry basis)	66	187	389	332
P (mg/kg dry basis)	<10	64	<10	113
Si (mg/kg dry basis)	<100	105	<100	<100
Cl (mg/kg dry basis)	<100	1045	300	6400
S (mg/kg dry basis)	400	1427	1800	7700
ash (wt % db) <sup>a</sup>	0.14	0.73	0.46	2.23
alkali content (mg/kg dry basis)	200	3180	550	1124
kg alkali/GJ oil	0.009	0.134	0.019	0.044

<sup>a</sup>Ash content is calculated from oxides of Al, Ca, Fe, K, Mg, Na, P, Si, and S.

produce organic acids,<sup>8,33</sup> causing the bio-oils to have pH values of about 2 to 4.<sup>33,37</sup> The pHs of the investigated bio-oils vary from 3.2 to 4.3. However, the acetic acid was found to be partially lost (37% acetic acid evaporated and condensed in distillate for the wood oil, see the Supporting Information for further data) during the solvent removal. Thus, the real pH values of bio-oils could be lower than the values shown in Table 5. Highly acidic oils may cause corrosion of steel. Thus, storage of the oils should be in acid-proof materials such as stainless steel or polyolefins. The density of the investigated oils was 0.98–1.15 g/mL. The density of algae oil shows a lower value than those of lignocellulosic oils. It is probably caused by the high proteins, lipids, and starches content in the algae.

The lignin oil and the algae oil have carbon contents of 60–66 wt % db and oxygen contents of 25–29 wt % db. In contrast, the wood oil and straw oil have lower carbon contents of 57–59 wt % and higher oxygen contents of 32–35 wt %. The differences in the carbon and oxygen contents of the oils are

Table 6. Summarization of Elemental Contents and Oil's HHV from Various Bio-oils

bio-oil	element content (wt % db) <sup>a</sup>					O/C	HHV (MJ/kg db)	tech <sup>b</sup>	ref
	C	H	O	N	S				
wood oil									
oak	60.9	2.6	36.5	0.2	0.02	0.60	24.1	AR	41
oak bark	58.3	4.6	37.4	0.4	0.3	0.64	24.4	AR	41
wood chip	53.9	7.2	38.9	0.1		0.72	22.3	Fix	11
rice husk	54.2	7.3	38.5	0.6		0.71	22.5	Fix	11
beech	57.0	7.2	35.2	0.5	0.04	0.62	24.0	PCR	this work
white oak	55.3	5.7	39.0	2.5		0.71	22.7	FBR	43
pine sawdust	55.1	6.2	38.8	0.0		0.70	22.5	FBR	25
straw oil									
barley straw	54.1	6.8	39.1	1.8		0.72	22.7	FBR	25
wheat straw	58.8	7.6	31.9	1.6	0.14	0.54	23.7	PCR	this work
macroalgae oil									
<i>Lyngbya</i>	50.6	7.9	41.5	5.8		0.82	21.6	Fix	11
<i>Cladophora</i>	45.3	7.1	47.6	3.1		1.05	18.5	Fix	11
<i>Ulva lactuca</i>	59.5	7.2	28.0	4.0	0.77	0.48	25.6	PCR	this work
microalgae oil									
<i>Chlorella protothecoides</i>	62.1	8.8	19.4	9.7		0.31	30.0	FBR	42
<i>Microcystis aeruginosa</i>	61.0	8.2	21.0	9.8		0.34	29.0	FBR	42
lignin oil									
straw lignin	65.6	8.0	24.5	1.7	0.18	0.37	29.7	PCR	this work

<sup>a</sup>The element content on dry basis was calculated from available data. <sup>b</sup>AR: Auger reactor. FBR: Fluidized bed reactor. PCR: pyrolysis centrifugal reactor. Fix: Fixed bed reactor.

Table 7. Relative Element Distribution in Bio-oil and Char (%)

		Al	Ca	Fe	K	Mg	Na	P	Si	Cl	S
wood	char	97.5	93.6	96.7	95.0	96.0	nd <sup>a</sup>	98.2	99.2	nd	nd
	bio-oil	nd	0.5	3.1	3.9	1.7	nd	nd	nd	nd	nd
straw	char	97.2	97.6	95.2	90.1	95.1	98.8	96.9	98.4	66.5	52.9
	bio-oil	3.0	2.3	5.8	8.1	4.4	7.5	2.0	0.3	6.1	38.2
lignin	char	99.9	92.2	92.4	93.5	96.1	95.1	94.1	93.2	54.3	25.0
	bio-oil	nd	nd	0.3	4.0	nd	4.7	nd	nd	nd	43.8
algae	char	93.9	97.1	90.6	97.9	96.1	94.3	95.2	93.2	40.0	75.3
	bio-oil	0.2	0.1	2.6	0.9	3.2	4.1	1.0	nd	25.0	15.8

<sup>a</sup>nd: not detected in the samples.

probably related to the cellulose content of the feedstocks. Cellulose degradation at pyrolysis condition produces a majority of monosugars and levoglucosans<sup>33</sup> that have a high oxygen content. Thus, a high cellulose content of the wood and straw probably causes the high oxygen contents in the bio-oils.

A summary of the elemental contents, ratios of O/C and the oil's HHV obtained from various studies are presented in Table 6.<sup>11,25,41–43</sup> The carbon and oxygen contents and O/C ratio of the wood and straw oils obtained in this study are consistent with literature data and are in the ranges of 54–61 wt % db, 32–39 wt % db, 0.54–0.72, respectively, while algae oil from different algae species (macroalgae and microalgae) show these values in a boarder range. The oil HHV seems to be proportional to the O/C ratio (see Table 6). With a lower O/C ratios the HHV of the algae oil and the lignin oil show higher values of 26 and 30 MJ/kg, respectively. The HHV of the wood oil and straw oil had similar values of around 24 MJ/kg db.

The wood and lignin oil were found to contain very low contents of ash forming elements, while the algae oil and straw oil contain some of these elements such as Ca (60–124 mg/kg db), Fe (55–277 mg/kg db), K (732–2870 mg/kg db), Mg (59–2732 mg/kg db). The ash forming elements especially

alkali have an impact on slagging, fouling, and aerosol formation related problems in case the oils are used as fuel for combustion and gasification.<sup>44</sup> The amount of alkali in a fuel per unit of energy may be used to estimate the fouling potential of the ash. Jenkins et al.<sup>7</sup> suggested that a value of 0.17 kg alkali/GJ is the threshold for probable fouling and a value of 0.34 kg alkali/GJ leads to certain fouling. These values for the bio-oils are much lower than the threshold. Thus, the use of the bio-oils as the feedstock for combustion application in boiler avoids a high risk of fouling.

In this study, the algae oil was found to have a high nitrogen content (4.0 wt % db), a sulfur content of 0.77 wt % db, and a chloride content of 0.64 wt % db. If the oil is used for combustion, the sulfur and chlorine may cause increased corrosion of boilers and the gas cleaning will be needed to prevent relatively high emissions of NO<sub>x</sub>, SO<sub>2</sub>, and HCl.

Table 7 shows the relative distribution of ash forming elements, Cl and S, in oil and char. Due to the low pyrolysis temperature of 550 °C compared to combustion or gasification, the fast pyrolysis reactor operation is not disturbed by the biomass ash content even with an ash rich biomass as the algae (29 wt %). The ash forming elements are mostly retained in the chars. The metal element distributions were 90.1–99.9% in the

chars and 0.1–8.1% in the bio-oils. The distribution of Cl and S in the char and oil products shows a broad range, and it seems to depend on the type of biomass. Cl and S appeared with a fraction of 6–25 and 16–44% in the bio-oils, respectively. The total recovery of Cl and S in the bio-oils and chars are 54–73% and 79–91%, respectively, and this indicates that some Cl and S are probably released to the gas phase.

The results of TGA and DTG measurements of the bio-oils are shown in Figure 5. The water contents were also analyzed

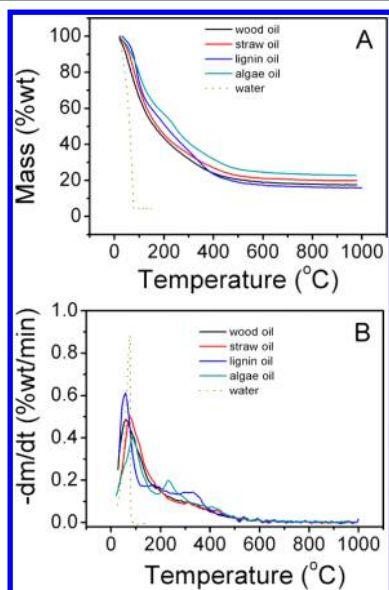


Figure 5. (A) TGA and (B) DTG of the pyrolysis oils.

to confirm the evaporation temperature of water at the TGA analysis conditions, and water was seen to evaporate at temperatures from 40 to 90 °C. The DTG curves of the bio-oils show two major mass loss peaks identified at 40–200 °C and 200–550 °C. The first peak of the bio-oils is believed to be the evaporation of the water (26–27 wt %) and light volatile components. The second peaks are probably the evaporations, cracking, and polymerization of high molecular fractions that could contain monolignols, moderate volatile polar compounds, monosugars and polysugars, extractive-derived compounds (majority of fatty and resin acids, paraffins, and phenanthrenes), and lignin derivatives.<sup>45</sup>

The bio-oils were classified by the TGA into four fractions that are shown in Table 8: a light fraction, a medium fraction, a heavy fraction, and a residual fraction. The light fraction of the wood, straw, and lignin oils corresponding to the first peak of

Table 8. Bio-oil Components Distribution

pyrolysis temp. (°C)	dry basis			
	wood oil	straw oil	lignin oil	algae oil
light fraction (wt %) <sup>a</sup>	40.9	38.8	35.2	21.9
medium fraction (wt %) <sup>b</sup>	30.9	30.8	39.4	42.0
heavy fraction (wt %) <sup>c</sup>	4.1	3.8	3.4	5.2
residual (wt %) <sup>d</sup> (char)	24.1	26.6	21.9	30.9

<sup>a</sup>Determined as the mass loss appearing from room temperature to 200 °C of the TGA curve and substrated the water content.

<sup>b</sup>Determined as the mass loss from 200 to 500 °C on TGA curve.

<sup>c</sup>Determined as the mass loss from 500 to 950 °C on TGA curve.

<sup>d</sup>The residual char after heating to 950 °C.

the DTG curves were 35–41 wt % db (26–30 wt % wet basis), whereas the algae oil fraction was 22 wt % db (16 wt % wet basis). With the high protein content (20 wt % daf) and rhamnan content (11 wt % daf) and the low xylan content (7 wt % daf) (see Table 2), the algae pyrolysis probably produces a oil with a lower amount of the light fraction compared to the lignocellulosic oils. Bio-oil cannot be totally distilled and thereby differ from conventional petroleum oils. If bio-oil is heated to 219 °C (under a vacuum pressure) to collect distillation fractions, it reacts and eventually forms a solid vacuum residue of around 50 wt % wet basis.<sup>2,37</sup> Therefore, only the light fractions (43–57 wt % wet basis including water) in this study may be distilled. The medium fractions of the bio-oils are in a range of 31–42 wt % db. It is believed that cracking and polymerization takes place when this fraction is raised to temperatures from 200 to 500 °C. The wood and straw oil show a lower content of this fraction than that of the lignin and algae oil. The minor heavy fractions (3.4–5.2 wt % db) are probably a gas release taking place during further cracking at 500–950 °C while the residue level of 22–31 wt % db are caused by the residual char formation.

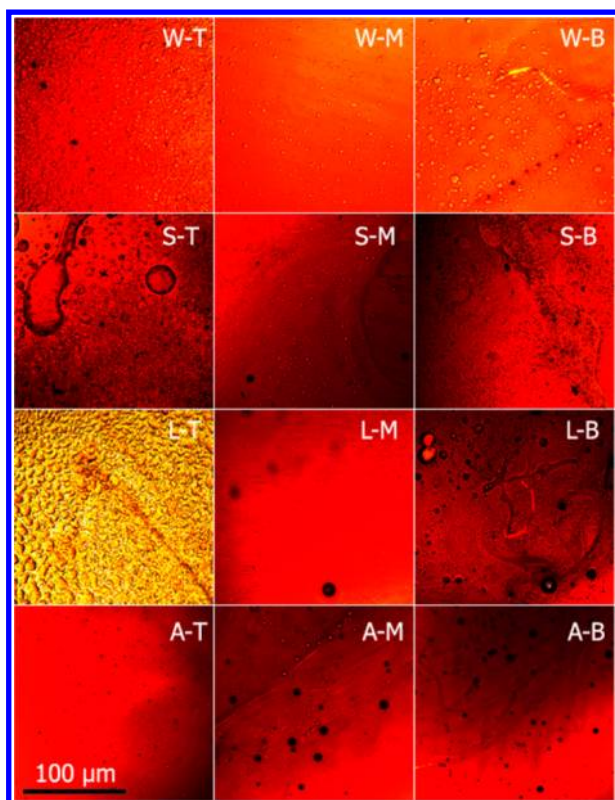
Phase separation during storage is caused by the instability of the bio-oil. Changes of the molecular structure and an increase of the oil viscosity may also take place during storage. The phase separation may be a hurdle for the oil utilization. In this study, the oil phase separation was determined by storing the oil samples in a tube at room temperature for a week. A one-third volume of the oil in the tube from the top, middle, and bottom parts were then taken, the water content was determined, and microscopic images of all the bio-oil samples were collected. The water content at the three positions varied less than 8% when compared with the water content of the whole bio-oil for the wood oil, straw oil, and algae oil (see Table 9). As can be seen in Figure 6, the images shown small

Table 9. Water Content (wt %) at Three Different Positions

	whole oil	top	middle	bottom
wood oil	27.3	27.1	25.6	29.0
straw oil	25.7	27.1	27.7	24.6
lignin oil	27.4	58.3	13.9	15.3
algae oil	26.6	24.7	27.5	27.8

aqueous droplets and fine char particles can be distinguished in all oil samples of straw, wood, and algae of the oils. It can be concluded that no severe phase separation was observed for the wood, straw, and algae oil samples at a water content of 26–27 wt %. In contrast, a clear phase separation was observed for the lignin oil. The water content of 58 wt % of the lignin oil top sample was an increase of about 2 times higher than that of the whole lignin oil and about 4 times higher than that of the middle and bottom samples (see Table 9). The top sample of the lignin oil was fluid and with a light color. It seems to be a mixture of water and light oil components (see Figure 6) whereas the middle and bottom phase were brown and more viscous. Phase separation occurs in bio-oil due to different polarities. The polarity of the compounds is related to their capacity to dissolve water.

A TG analysis of the bottom phase of the lignin oil was performed and a comparison with respect to TGA fractions between the bottom lignin oil samples and the whole lignin oil sample are presented in Table 10. The bottom oil sample has a large medium fraction (60 wt % db) (volatilization temperature



**Figure 6.** Microscope image of three different positions of the bio-oils (W: wood. S: straw. L: lignin. A: algae. T: top. M: middle. B: bottom).

**Table 10. Bio-oil Components Distribution**

pyrolysis temp. (°C)	dry basis	
	lignin oil	lignin bottom oil
light fraction (wt %) <sup>a</sup>	35.2	9.1
medium fraction (wt %) <sup>b</sup>	39.4	59.5
heavy fraction (wt %) <sup>c</sup>	3.4	4.8
residual (wt %) <sup>d</sup> (char)	21.9	26.6

<sup>a</sup>Determined as the mass loss appearing from room temperature to 200 °C of the TGA curve and substrated the water content.

<sup>b</sup>Determined as the mass loss from 200 to 500 °C on TGA curve.

<sup>c</sup>Determined as the mass loss from 500 to 950 °C on TGA curve.

<sup>d</sup>The residual char after heating to 950 °C.

of 200–500 °C) and a small amount of the light fraction (9 wt % db) (volatilization from room temperature to 200 °C). The result indicates that a majority of the light fraction remains in the top phase while the medium fraction mainly remains in the bottom phase after the phase separation of the lignin oil.

Bio-oil is known to contain some phenolics that are still reactive and may polymerize to form oligomers with molecular weights as high as 1000 or more.<sup>46</sup> The polymerization process during aging may take months or years. The most typical method to measure the aging of bio-oils is to use an accelerated aging procedure. In the present study, the bio-oils were placed in a tightly closed container and heated in an oven for 24 h at 80 °C.<sup>25,46</sup> The aged bio-oil samples are relevant to that of oil stored for a year at room temperature.<sup>25</sup> Figure 7 shows the molecular weight distributions of original and aged oils of wood, straw, lignin, and algae. The molecular mass distribution of the original bio-oils shows two main peaks at around 165 and 398 g/mol for the bio-oils of wood, straw, and lignin. While the algae oil has another third shoulder at around 1260 g/mol

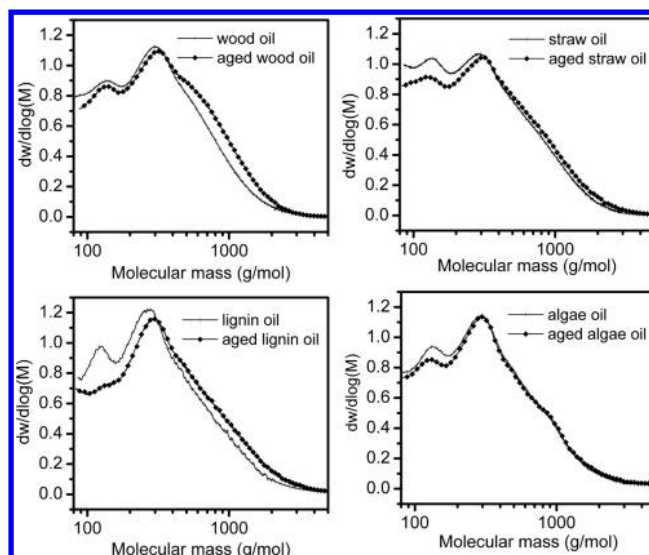


**Figure 7.** Molecular mass distribution of original and aged bio-oils.

together with two main peaks at 165 and 320 g/mol. The bio-oils produced on the PCR have mean molecular weights in the range of 404–455 g/mol (see Table 11) and that is consistent

**Table 11. Mean Molecular Weight of the Original Oils and Aged Oils**

	wood oil	straw oil	lignin oil	algae oil
mean molecular mass, $M_w$ (g/mol)	404	405	451	455
mean aged molecular mass, $M_w$ (g/mol)	462	453	574	482
$\Delta = M_w \text{ aged oil} - M_w \text{ fresh oil}$ (g/mol)	58	48	123	27
viscosity@ 40 °C (mPa·s)	16.1	25.0	9.4 <sup>a</sup> 102.1 <sup>b</sup>	100.9

<sup>a</sup>The viscosity of top sample. <sup>b</sup>The viscosity of bottom sample.

with other studies.<sup>22,41</sup> The mean average molecular weights of the lignin and algae oil are 46–50 g/mol higher than that of the wood and straw oil. The high lignin content (79 wt % daf) of the lignin sample and the high protein content (21 wt % daf) of the algae sample probably cause high lignin derivatives content in the lignin oil and high protein derivatives content in the algae oil, which probably result in the difference in molecular mass distribution and mean molecular mass of the lignin and algae oils when compared with the wood and straw oils.

The viscosity of the wood oil, straw oil, and algae oil were 16, 25, and 101 mPa·s, respectively (see Table 11). Due to phase separation, the viscosity measurement of the lignin oil presented some difficulties. To understand the viscosity of the lignin oil, the sample was turbulently mixed and then kept immobile for two hours. The top and bottom phases were then used for the viscosity measurements. As a result, the viscosities of the top and the bottom samples are 9.4 and 102 mPa·s, respectively.

As can be seen in Figure 7, the aged oils have reasonably similar molecular weight patterns as the original oils. A decreased proportion of the low molecular mass fraction with molecular weight less than 320 g/mol and an increased proportion of higher than 320 g/mol fraction were clearly observed of the aged oils. These results are consistent to those of Chaala et al.<sup>46</sup> who studied the aging of softwood bark oil.

They found that the aged oil had a considerable change of the faction with molecular mass higher than 1000 g/mol and the faction with molecular mass lower than 300 g/mol. The mean molecular weight of the aged bio-oil enhances from 48–123 g/mol for the lignocellulosic oils and 27 g/mol for the algae oil (see table 11). So this indicates that algae oil is least probe to aging.

**4. Characterization of Char Properties.** The elemental compositions and particle sizes of the chars obtained from the biomass pyrolysis experiments are shown in Table 12. The

**Table 12. Ultimate, Elemental, and Particle Size Analyses of Chars**

	wood char	straw char	lignin char	algae char
element composition (% wt db)				
C	57.0	52.8	55.6	20.7
H	3.3	3.5	3.3	1.5
N	0.4	1.1	1.2	2.3
O <sup>a</sup>	20.3	21.2	12.1	9.7
Al	0.34	0.12	0.17	0.64
Ca	1.95	0.92	0.98	6.25
Fe	0.33	0.16	0.69	0.65
K	0.85	5.46	0.31	5.63
Mg	0.22	0.22	0.05	5.69
Na	0.13	0.24	0.66	0.52
P	0.09	0.52	0.15	0.76
Si	5.20	5.09	9.70	8.97
Cl	<0.03	1.96	<0.03	0.98
S	0.05	0.34	0.09	6.21
element composition (% wt daf)				
C	69.7	67.2	77.0	60.5
H	4.0	4.5	4.6	4.4
N	0.5	1.4	1.7	6.7
O <sup>a</sup>	25.7	27.0	16.6	28.4
ash content (wt % db)	19.0	21.1	28.0	65.8
HHV (MJ/kg on dry basis)	19.0	21.1	20.6	6.0
HHV (MJ/kg on dry ash free basis)	23.5	26.8	28.7	17.6
particle size ( $\mu\text{m}$ )				
d <sub>50</sub>	60	–	68	67
d <sub>80</sub>	195	–	190	137
d <sub>90</sub>	324	–	463	210
d <sub>mean</sub>	61	–	53	67

<sup>a</sup>Calculated by difference.

chars from the lignocellulosic biomasses contain 69–77 wt % daf of carbon, 4.0–4.7 wt % daf of hydrogen, 17–27 wt % daf of oxygen and 0.5–1.7 wt % daf of nitrogen. In contrast the char of the algae contains lower contents of carbon (61 wt % daf) and higher nitrogen contents (6.7 wt % daf). The hydrogen and oxygen content have reasonably similar to those of the lignocellulosic biomasses. The ash contents of the lignocellulosic biomass are in the range 19–28 wt % db, while the highest ash content of 66 wt % db is obtained for the algae char.

The feedstock experiences high mechanical stress in the PCR, and consequently, the obtained char d<sub>50</sub>, d<sub>80</sub> and d<sub>mean</sub> are 60, 195, and 61  $\mu\text{m}$  for the wood char and 68, 190, and 53  $\mu\text{m}$  for the lignin char, respectively. The mean particle size is reduced around 3 times for both the PCR pyrolysis of the wood and lignin (data not show here). The particle chars have suitable particle sizes for being used in suspension fired boilers. Furthermore, the wood char and lignin char have HHV of 19–

21 MJ/kg db, are almost free of chloride and sulfur, and have reasonably low alkali contents. This makes the wood char and lignin char possible feedstocks for combustion in dust fired boilers. The straw and algae chars have relatively high alkali and chloride contents. Especially, the algae char has a low HHV of 6 MJ/kg db. A use of straw and algae chars for an energy recovery purpose seems not to be feasible and will probably lead to ash related problems for boilers. However, the straw and algae chars contain the high amounts of macronutrients such as N, P, K, N, S, and Ca, especially K. Therefore, the chars can serve as a high value fertilizer, and they can be used as a biochar on the fields.

## CONCLUSIONS

In this work, fast pyrolysis PCR experiments were conducted with wood, straw, algae, and lignin to produce bio-oils. The PCR pyrolysis process can be used to produce an energy rich bio-oil from high-ash biomasses, which are difficult to process effectively in combustion or gasification reactors. The pyrolysis of macroalgae showed promising results with a bio-oil yield of 65 wt % daf (organic oil yield of 54 wt % daf) and an energy recovery in the bio-oil of 76%. These results are similar to that of wood pyrolysis. The pyrolysis of lignin shows a much lower bio-oil yield of 47 wt % daf and an energy recovery in the bio-oil of 45%.

The obtained oils and chars were carefully characterized with respect to pH, density, elemental contents, HHV, thermal behaviors, phase separation and aging, elemental contents, HHV, and particle size distribution. The HHV of wood, straw, lignin, and algae oils was 24.0, 23.7, 29.7, and 25.7 MJ/kg db, respectively. The lignin and macroalgae oil properties were relatively different to those of the straw and wood bio-oil with respect to carbon content, oxygen content, HHV, mean molecular weight, viscosity, and thermal behavior. The main differences observed in the product yields and the bio-oil properties can be partially explained by differences of the biomass compositions especially differences with respect to ash, lignin, and extractive contents of the biomasses.

The bio-oils produced on the PCR obtain low metal concentrations. High-ash biomasses do not disturb the PCR process. Almost all the metals are contained in the chars at a pyrolysis temperature of 550 °C. Therefore, when the bio-oils are used in boilers or gasifiers slagging, fouling, and aerosol formation problems will be minimized.

With a high proportion of small size particles, a HHV of 19–21 MJ/kg db and being almost free of chloride and sulfur, the wood char and lignin char are considered also as promising fuels for gasification or combustion, whereas the straw and algae chars contained high amounts of macronutrients such as N, P, K, N, S, and Ca, and especially the high K content could makes the chars most valuable as raw materials for fertilizer production or to be used as biochars that can be spread on fields.

## ASSOCIATED CONTENT

### Supporting Information

Additional tables and comments regarding the use of isopropanol for condensation of the bio-oil from the pyrolysis gas. This material is available free of charge via the Internet at <http://pubs.acs.org>.

## AUTHOR INFORMATION

### Corresponding Author

\* E-mail: PAJ@kt.dtu.dk.

## Notes

The authors declare no competing financial interest.

## ACKNOWLEDGMENTS

Financial support of this PhD study by DONG energy A/S, Energinet.dk and DTU is gratefully acknowledged. The authors are very grateful to Tran Thuong Dang, Kim Chi Szabo, and Ingelis Larsen from Chemical and Biochemical Engineering Department, Technical University of Denmark, who have performed some of the analyses reported in this paper.

## REFERENCES

- (1) Butler, E.; Devlin, G.; Meier, D.; McDonnell, K. *Renewable Sustainable Energy Rev.* **2011**, *15*, 4171–4186.
- (2) Bridgwater, A. V. *Biomass Bioenergy* **2012**, *38*, 68–94.
- (3) Nikolaisen, L.; Jensen, P. D.; Bech, K. S.; Dahl, J.; Busk, J.; Brødsgaard, T.; Rasmussen, M. O.; Bruhn, A.; Bjerre, A. A.; Nielsen, H. B.; Albert, K. R.; Ambus, P.; Kadar, Z.; Heiske, S.; Sander, B.; Schmidt, E. R. *Energy Production from Marine Biomass (Ulva lactuca)*, PSO Project No. 2008-1-0050; Danish Technological Institute: Denmark, 2011.
- (4) Gao, K.; McKinley, K. R. *J. Appl. Phycol.* **1994**, *6*, 45–60.
- (5) Ross, A. B.; Jones, J. M.; Kubacki, M. L.; Bridgeman, T. *Bioresour. Technol.* **2008**, *99*, 6494–6504.
- (6) Li, D.; Chen, L.; Zhang, X.; Ye, N.; Xing, F. *Biomass Bioenergy* **2011**, *35*, 1765–1772.
- (7) Jenkins, B. M.; Baxter, L. L.; Miles, J.; Miles, T. R. *Fuel Process. Technol.* **1998**, *54*, 17–46.
- (8) DeSisto, W. J.; Hill, N.; Beis, S. H.; Mukkamala, S.; Joseph, J.; Baker, C.; Ong, T. H.; Stemmler, E. A.; Wheeler, M. C.; Frederick, B. G.; van Heiningen, A. *Energy Fuels* **2010**, *24*, 2642–2651.
- (9) Trung, N. T.; Jensen, P. A.; Dam-Johansen, K., The influence of pyrolysis temperature on sewage sludge pyrolysis products distribution, bio-oil and char properties. *Energy Fuels* **2013**, submitted.
- (10) Bae, Y. J.; Ryu, C.; Jeon, J. K.; Park, J.; Suh, D. J.; Suh, Y. W.; Chang, D.; Park, Y. K. *Bioresour. Technol.* **2011**, *102*, 3512–3520.
- (11) Maddi, B.; Viamaajala, S.; Varanasi, S. *Bioresour. Technol.* **2011**, *102*, 11018–11026.
- (12) Demirbas, A. *Energy Sources Part A.* **2006**, *28*, 933–940.
- (13) Buranov, A. U.; Mazza, G. *Ind. Crops Prod.* **2009**, *28*, 237–259.
- (14) Gosselink, R. J. A.; de Jong, E.; Guran, B.; Abacherli, A. *Ind. Crops Prod.* **2004**, *20*, 121–129.
- (15) de Wild, P. J.; Huijgen, W. J. J.; Heeres, H. J. *J. Anal. Appl. Pyrolysis* **2012**, *93*, 95–103.
- (16) Nowakowski, D. J.; Bridgwater, A. V.; Elliott, D. C.; Meier, D.; de Wild, P. J. *J. Anal. Appl. Pyrolysis* **2010**, *88*, 53–72.
- (17) Bech, N.; Larsen, M. B.; Jensen, P. A.; Dam-Johansen, K. *Biomass Bioenergy* **2009**, *33*, 999–1011.
- (18) Bech, N. In situ flash pyrolysis of straw. PhD thesis, Department of Chemical Engineering, DTU, Kgs. Lyngby, Denmark, 2008.
- (19) Sluiter, R.; Ruiz, C.; Scarlata, J.; Sluiter, J.; and Templeton, D. *Determination of Extractives in Biomass*, Technical Report NREL/TP-510-42619; NREL: Golden, CO, July 17, 2005.
- (20) Sluiter, A.; Hames, B.; Ruiz, R.; Scarlata, C.; Sluiter, J.; Templeton, D.; Crocker, D. *Carbohydrates and Lignin in Biomass Laboratory Analytical Procedure (LAP)*, Technical Report NREL/TP-510-42618; NREL: Golden, CO, April 2008.
- (21) Bridgwater A. V. *Fast Pyrolysis of Biomass: A Handbook*; IEA Bioenergy; PyNe: Paris, 2005; Vol. 3, pp 28–29.
- (22) Fahmi, R.; Bridgwater, A. V.; Donnison, I.; Yates, N.; Jones, J. M. *Fuel* **2008**, *87*, 1230–1240.
- (23) Abdullah, N.; Gerhauser, H. *Fuel* **2008**, *87*, 2606–2613.
- (24) Jensen, A.; Dam-Johansen, K.; Wojtowicz, M. A.; Serio, M. A. *Energy Fuels* **1998**, *12*, 929–938.
- (25) Oasmaa, A.; Solantausta, Y.; Arpiainen, V.; Kuoppala, E.; Sipila, K. *Energy Fuels* **2009**, *24*, 1380–1388.
- (26) Yoeh, H. H.; Wee, Y. C. *Food Chem.* **1994**, *49*, 245–250.
- (27) Harnedy, P. A.; Fitzgerald, R. J. *J. Phycol.* **2011**, *47*, 218–232.
- (28) Sanchez-Silva, L.; Lopez-Gonzalez, D.; Villasenor, J.; Sanchez, P.; Valverde, J. L. *Bioresour. Technol.* **2012**, *109*, 163–172.
- (29) Greenhalf, C. E.; Nowakowski, D. J.; Bridgwater, A. V.; Titiloye, J.; Yates, N.; Riche, A.; Shield, I. *Ind. Crops Prod.* **2012**, *36*, 449–459.
- (30) Yuan, S.; Chen, X.; Li, W.; Liu, H.; Wang, F. *Bioresour. Technol.* **2011**, *102*, 10124–10130.
- (31) Johansen, J. M.; Jakobsen, J. G.; Frandsen, F. J.; Glarborg, P. *Energy Fuels* **2011**, *25*, 4961–4971.
- (32) Scott, D. S.; Plskorz, J.; Radleln, D. *Ind. Eng. Chem. Process Des. Dev.* **1985**, *24*, 581–588.
- (33) Azeez, A. M.; Meier, D.; Odermatt, J. è.; Willner, T. *Energy Fuels* **2010**, *24*, 2078–2085.
- (34) Ibrahim, N. B. Bio-oil from flash pyrolysis of agricultural residues. PhD thesis, Department of Chemical Engineering, DTU, Kgs. Lyngby, Denmark, 2012.
- (35) Shen, D. K.; Gu, S.; Bridgwater, A. V. *Carbohydr. Polym.* **2010**, *82*, 39–45.
- (36) Wang, Y.; Wu, L.; Wang, C.; Yu, J.; Yang, Z. *Bioresour. Technol.* **2011**, *102*, 7190–7195.
- (37) Venderbosch, R. H.; Prins, W. *Biofuels, Bioproducts, Biorefining* **2010**, *4*, 178–208.
- (38) Coulson, M. Pyrolysis of perennial grasses from southern Europe. *Thermalnet Newsletter* **2006**, *2*, 6–6.
- (39) Wu, H.; Yu, Y.; Yip, K. *Energy Fuels* **2010**, *24*, 5652–5659.
- (40) Abdullah, H.; Mourant, D.; Li, C. Z.; Wu, H. *Energy Fuels* **2010**, *24*, 5669–5676.
- (41) Ingram, L.; Mohan, D.; Bricka, M.; Steele, P.; Strobel, D.; Crocker, D.; Mitchell, B.; Mohammad, J.; Cantrell, K.; Pittman, C. U. *Energy Fuels* **2007**, *22*, 614–625.
- (42) Miao, X.; Wu, Q.; Yang, C. *J. Anal. Appl. Pyrolysis* **2004**, *71*, 855–863.
- (43) Park, H. J.; Park, Y. K.; Dong, J. I.; Kim, J. S.; Jeon, J. K.; Kim, S. S.; Kim, J.; Song, B.; Park, J.; Lee, K. J. *Fuel Process. Technol.* **2009**, *90*, 186–195.
- (44) Matjie, R. H.; French, D.; Ward, C. R.; Pistorius, P. C.; Li, Z. *Fuel Process. Technol.* **2011**, *92*, 1426–1433.
- (45) Garcia-Perez, M.; Chaala, A.; Pakdel, H.; Kretschmer, D.; Roy, C. *Biomass Bioenergy* **2007**, *31*, 222–242.
- (46) Chaala, A.; Ba, T.; Garcia-Perez, M.; Roy, C. *Energy Fuels* **2004**, *18*, 1535–1542.
- (47) Muradov, N.; Fidalgo, B.; Gujar, A. C.; Raissi, A. *Bioresour. Technol.* **2010**, *101*, 8424–8428.



February, 2014, DTU

## **Appendix A3**

# **Journal paper: Influence of the Pyrolysis Temperature on Sewage Sludge Product Distribution, Bio-Oil, and Char Properties**

**Energinet.dk project no. 010077**

**Treatment of Lignin and waste residues by flash pyrolysis**

**Trung Ngoc Trinh, Peter Arendt Jensen, Kim Dam-Johansen, Niels Ole Knudsen,**

**And Hanne Risbjerg Sørensen**

*Department of Chemical and Biochemical Engineering*

Technical University of Denmark

Søltofts Plads, Building 229, DK-2800 Lyngby, Denmark

**CHEC no. R1401**

# Influence of the Pyrolysis Temperature on Sewage Sludge Product Distribution, Bio-Oil, and Char Properties

Trung Ngoc Trinh,<sup>†</sup> Peter Arendt Jensen,<sup>\*,†</sup> Kim Dam-Johansen,<sup>†</sup> Niels Ole Knudsen,<sup>‡</sup> and Hanne Risbjerg Sørensen<sup>‡</sup>

<sup>†</sup>Department of Chemical and Biochemical Engineering, Denmark Technical University (DTU), Søtofts Plads Bygning 229, DK-2800 Kongens Lyngby, Denmark

<sup>‡</sup>DONG Energy, Kraftsværksvej 53, DK-7000 Fredericia, Denmark

## S Supporting Information

**ABSTRACT:** Fast pyrolysis may be used for sewage sludge treatment with the advantages of a significant reduction of solid waste volume and production of a bio-oil that can be used as fuel. A study of the influence of the reaction temperature on sewage sludge pyrolysis has been carried out using a pyrolysis centrifugal reactor (PCR) at 475, 525, 575, and 625 °C. Maxima of both organic oil yield of 41 wt % on a dry ash free feedstock basis (daf) and a sludge oil energy recovery of 50% were obtained at 575 °C. The water-insoluble fraction, molecular-weight distribution, higher heating value (HHV), and thermal behaviors of sludge oils were found to be considerably influenced by the applied pyrolysis temperatures. The sludge oil properties obtained at the optimal temperature of 575 °C were a HHV of 25.5 MJ/kg, a water-insoluble fraction of 18.7 wt %, a viscosity of 43.6 mPa s at 40 °C, a mean molecular weight of 392 g/mol, and metal concentrations lower than 0.14 wt % on a dry basis (db). Less optimal oil properties with respect to industrial applications were observed for oil samples obtained at 475 and 625 °C. Char properties of the 575 °C sample were an ash content of 81 wt % and a HHV of 6.1 MJ/kg db. A total of 95% of the sewage sludge phosphorus content was recovered in the char. The solid waste amount (char compared to sludge) was reduced to 52% on a bulk volume basis at the pyrolysis temperature of 575 °C.

## INTRODUCTION

Sewage sludge produced from a wastewater treatment plant consists of a mixture of undigested organics (plant residue, paper, oils, food, and fecal material), microorganisms, and inorganic material. Traditionally, the most common ways to manage sewage sludge disposal are landfilling and agricultural reuse. However, some heavy metals are toxic to plants and may also be transferred to humans through their presence in crops. Therefore, the legislation of the European Union (EU, Directive 86/278/CEE)<sup>1</sup> was issued to qualify sewage sludge used in agriculture, and the threshold values show in Table 1 must be fulfilled regarding the accumulation of sewage sludge

**Table 1. Limit Values for the Amount of Heavy Metals That May Be Added Annually to Agricultural Land Based on a 10 Year Average (kg ha<sup>-1</sup> year<sup>-1</sup>)<sup>1</sup>**

parameters	limit values (kg ha <sup>-1</sup> year <sup>-1</sup> ) <sup>a</sup>
cadmium	0.15
copper	12
nickel	3
lead	15
zinc	30
mercury	0.1
chromium <sup>b</sup>	

<sup>a</sup>The threshold values were issued in 1986. <sup>b</sup>It is not possible at this stage to fix limit values for chromium. The EU council will fix these values on the basis of proposals to be submitted by the commission within 1 year following notification of this directive.

on land. Several European countries have even stricter regulations. As a result, the disposal of sewage sludge is becoming of increasing concern in the EU, where sewage sludge disposal<sup>2</sup> was estimated to be 40% for landfilling and 37% for farmland applications in 2008. However, because environmental standards may become stricter in the future, the sewage sludge proportion used on farmland will probably be reduced. Consequently, the treatment cost of sludge disposal will increase.

In European countries, annual sewage sludge production exceeds 10 million tons/year (2010).<sup>2,3</sup> Sewage sludge has volatile contents of 40–88 wt % on a dry basis (db) and higher heating values (HHVs) of 11–26 MJ/kg db.<sup>2</sup> Thus, the sewage sludge is a potential important feedstock for thermal conversions, such as gasification, fast pyrolysis, and incineration processes that can reduce the sewage sludge volume and use the sludge energy content. In recent years, the treatment of sewage sludge by fast pyrolysis has been demonstrated to be a promising alternative to farmland and landfilling applications.<sup>4–9</sup> Fast pyrolysis using a high heating rate has been considered as a process not only for treating sewage sludge that can considerably reduce the volume of solid waste but also can produce a bio-oil, which can be used as fuel for boilers and also may be upgraded to a transport fuel. Many pyrolysis reactor types, such as bubbling and circulating fluidized-bed reactors, ablative reactors, auger reactors, and rotating cone reactors,

Received: November 30, 2012

Revised: February 22, 2013

Published: February 22, 2013

have been developed to obtain a high oil yield.<sup>10,11</sup> The fast pyrolysis reactors typically achieve heating rates of 700–1500 K/s.<sup>12,13</sup> The pyrolysis centrifuge reactor, developed in the CHEC center at the DTU Chemical Engineering, uses a high centrifugal force to gain a high feedstock heating rate.<sup>12</sup> The main advantages of this concept compared to fluid-bed reactors are a compact design that uses a low flow rate of carrier gas. The effects of the applied operational conditions of sewage sludge fast pyrolysis have been studied by several authors.<sup>5,9–11</sup> It is pointed out that the applied pyrolysis temperature is a main parameter that directly influences the properties of the pyrolysis products and the product distributions. The temperature influences the pyrolysis reactions, secondary cracking reactions, char formation, and polymerization reactions.

Similar to wood and straw pyrolysis oils, sewage sludge pyrolysis oil has a high viscosity and relatively low stability (phase separation)<sup>10,14,15</sup> when compared to a heating oil no. 2; this may lead to limited industrial applications. Besides, sewage sludge oil is known to have a lower oxygen content, HHV, and higher nitrogen and sulfur contents compared to the wood and straw oils.<sup>8,9,15,16</sup> Although, the sludge oil has high nitrogen and sulfur contents that cause an increase of NO<sub>x</sub> and SO<sub>x</sub> emissions if the sludge oil is combusted in boilers, the sludge oil has gained attention because of a high heating value (27–33 MJ/kg db)<sup>8,9,15,16</sup> and the fact that the oil is produced from a waste material. Upgrading of the sludge oil by a hydrotreating process is a possible next step to reduce the nitrogen and sulfur contents and also increase the heating value of the sludge oil, which thereby could be used as a feedstock for conventional refineries.

Some studies investigated the influence of the sewage sludge fast pyrolysis temperature on product yields (gas, bio-oil, and char)<sup>5,9–11</sup> and chemical components that have been analyzed by gas chromatography–mass spectrometry (GC–MS).<sup>17,18</sup> The sludge oil is comprised of components soluble in water or solvents, derivatives of sewage sludge constituents that are partially pyrolyzed during fast pyrolysis, and oligomers/polymers formed by condensation of vapors.<sup>19,20</sup> A complete chemical analysis of sewage sludge bio-oil is difficult to obtain. Only a fraction of about 32–44% of lignocellulosic oil<sup>21</sup> (and probably a similar proportion for sewage sludge oil) can be detected by GC.

Little is presently known about the influence of the pyrolysis temperature on properties of the sludge oils, which are important with respect to industrial applications. The objectives of this work were to study the effect of the pyrolysis temperature in the range of 475–625 °C on the product distributions (gas, reaction water, organic oil, and char yields) as well as bio-oil properties (HHV, water-insoluble fraction, molecular mass distribution, ash content, viscosity, density, thermal behavior, and elemental distributions) and char properties (ash content, HHV, particle-size distributions, and morphology) of sewage sludge pyrolyzed at a high heating rate.

## EXPERIMENTAL SECTION

**Experimental Apparatus.** The pyrolysis centrifuge reactor (PCR) shown in Figure 1 is described in detail elsewhere.<sup>22</sup> The centrifugal reactor is made of stainless steel and has an inner diameter of 85 mm. It is electrically heated by four independent heating zones along the reactor length. The pyrolysis of sludge takes place inside the reactor, whereby char, bio-oil, and gas are produced. Large char particles are removed by a change-in-flow separator, whereas fine char particles are collected by a cyclone. The change-in-flow separator and cyclone were heated to 420 °C to avoid tar condensation and blocking of the tubes.

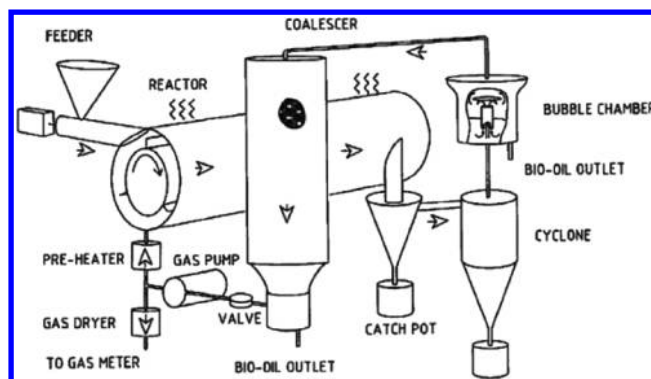


Figure 1. Sketch of the PCR.

The vapor products are condensed in a bubble chamber filled with isopropanol as a condensing solvent. The temperature in the bubble chamber is controlled to be 30–40 °C by means of a cooling water system. Possible ester formation reactions between isopropanol and carboxylic acids are believed to be negligible at the low temperature and in the absence of strong acid or base catalysts. The isopropanol was also used as a condensing solvent in fast pyrolysis experiments by Fonts et al.<sup>8,9</sup> The light oil fraction and aerosols are further condensed by a coalescer filled with Rockwool. A recycled gas flow maintains a desired gas residence time in the reactor. The gas is pumped back to a preheater and heated to around 400 °C before being fed back to the reactor. The gas products are dried by a water condenser and a gas filter to remove liquid before coming to a gas meter.

The liquid fraction collected from the bubble chamber, coalescer, and water condenser is filtered through a Whatman filter paper (pore size of 20–25 μm). The char left on the filter is washed thoroughly by ethanol and acetone and then dried under an infrared light bulb within 10 min. The char yield is determined from the chars collected in the char separator, the cyclone, and the char left on the filter paper. The bio-oil yield is determined from the liquid that passed through the filter paper. The gas volume was measured using a gas flow meter. An average molecular mass of sewage sludge pyrolysis gas produced at reactor temperatures of 475–600 °C was found to be from 26 to 32 g/mol.<sup>7,9</sup> The average molecular mass of the gas in the present study was assumed to be 29 g/mol, and this value was used to calculate the gas mass yield in this study. Thus, the inaccuracy of the gas yield relative to the feedstock is probably ±1.5 wt % on a dry ash free feedstock basis (daf).

In this study, the PCR was operated with constant operation conditions: a rotor speed of 14800 rpm, a gas reactor residence time of 0.8 s, a feeding rate of 1.3 kg/h, a total experimental time of 20 min, and a feed consumption of around 430 g sludge for each run. Before a pyrolysis experiment, the sewage sludge was purged with nitrogen to remove air and the sludge was then introduced into the reactor by the screw feeder.

With respect to practical implications, it was observed that, during the sewage sludge PCR pyrolysis experiments conducted at a low temperature (475 °C), a blockage of the nozzle connecting the cyclone and the bubble chamber appeared when experiments were performed for longer times than 20 min. The phenomenon does not appear when using wood or straw feedstocks for the PCR pyrolysis experiments. This indicates that the sewage sludge oils produced at the low temperature may contain some sludge derivatives and fine char particles, which probably agglomerate to form solid particles because of insufficient heat transfer at the low temperature of the nozzle. The deposit of these particles probably caused the blockage.

**Characterization of the Sewage Sludge and Sludge Char.** Proximate, ultimate, and element analyses were carried out on the sewage sludge feedstock, which had a particle size of 45–830 μm. The sludge char samples were analyzed by the following methods: the moisture content by ASTM D2216, the ash content by ASTM D1102-84, the particle size by sieve analysis with sieve sizes of 45–1000 μm, HHV by a bomb calorimeter (IKA C-200), total CHN by a flash

combustion (Thermo Finnigan, Flash EA1112), Cl and S by inductively coupled plasma–optical emission spectroscopy (ICP–OES) axial, and Al, Ca, Fe, K, Mg, Na, P, Ti, Si, Cr, Zn, and Cd by ICP–OES radial. The oxygen content was calculated by difference.

The raw non-digested sewage sludge was collected from a Danish wastewater treatment plant in the town of Store Heddinge. The sludge was dried before pyrolyzing in the PCR. The results of proximate, ultimate, and element analyses of the feedstock sewage sludge are presented in Table 2. The sludge contains a high ash content of 47 wt

**Table 2. Characteristics of Sewage Sludge**

proximate analysis	
moisture (wt %)	7.3
volatile matter (wt %) (determined at 950 °C)	38.0
fixed carbon (wt %)	7.9
ash (wt %) (determined at 550 °C)	46.8
ultimate analysis	
C (wt % db <sup>a</sup> )	28.0
H (wt % db)	3.4
O (wt % db) <sup>b</sup>	10.3
S (wt % db)	0.9
N (wt % db)	4.0
HHV (MJ/kg db)	10.9
element analysis	
Cl (wt % db)	0.05
P (wt % db)	3.41
Al (wt % db)	1.77
Fe (wt % db)	8.07
Si (wt % db)	8.25
Ti (wt % db)	0.23
Ca (wt % db)	3.71
K (wt % db)	0.67
Mg (wt % db)	0.43
Na (wt % db)	0.26
Cd (mg/kg db)	0.84
Cr (mg/kg db)	69.8
Zn (mg/kg db)	1035

<sup>a</sup>db = dry feed basis. <sup>b</sup>O% = 100% – ash% – C% – H% – N% – S%.

% (as received). The total alkali and earth alkali metal content (Ca, K, Na, and Mg) was found to be 5.03 wt % db. These alkali metals are known to act as catalysts for the pyrolysis reactions<sup>23–25</sup> and have a large effect on the pyrolysis yield and product compositions.<sup>23</sup> Fahmi et al.<sup>23</sup> showed that the organic oil yield increased 11 wt % when *Festuca arundinacea* was washed to reduce the content of alkali and earth alkali metals (Na, K, Ca, and Mg) from 3.56 to 0.84 wt % db.

Thermogravimetric analysis (TGA) of sewage sludge was carried out at a temperature range of 110–1000 °C and at a constant heating rate of 10 °C/min in a N<sub>2</sub> flow using a TGA instrument (Netzsch STA 449 F1).

The morphologies and dominant element distributions of chars were investigated by means of a scanning electron microscope (SEM, INSPECT) equipped with an energy-dispersive X-ray (EDX) detector.

**Characterization of the Bio-Oil Product.** To obtain bio-oil samples without solvents, the isopropanol solvent was removed from the bio-oils by a rotary vacuum evaporator at a temperature of 37 °C. This method was also used to remove isopropanol solvent by Fonts et al.<sup>8,9</sup> About 15–22 wt % of water and small amounts of light organic species (less than 3 wt %) of the bio-oil samples were lost during the solvent removal (for further information, see the Supporting Information). The loss of some light organic species may have a minor influence on the viscosity of the sludge oil samples.

The properties of the bio-oil were measured by the following methods: the water content by a Karl Fischer titration (Metrohm-701KT titrino), the ash content by ASTM D1102-84, the HHV by a

bomb calorimeter (IKA C-200), the viscosity by a rotational viscometer (PAAR AMV 200), the density by a density meter (Anton paar, DMA 4100), the total CHN content by a flash combustion (Thermo Finnigan, Flash EA1112), Cl and S by ICP–OES axial, and Al, Ca, Fe, K, Mg, Na, P, Ti, Si, Cr, Zn, and Cd by ICP–OES radial.

The molecular-weight distribution was analyzed by size-exclusion chromatography (SEC) using the following instrument: Viscotek GPCmax VE-2001 equipped with Viscotek TriSEC model 302 triple detector using two PLgel mixed-D columns from Polymer Laboratories. The samples were run in tetrahydrofuran (THF) at 30 °C (1 mL min<sup>-1</sup>). The molar-mass characteristics were calculated using polystyrene standards (162–371 000 g/mol). To take a representative sample for SEC analysis, the bio-oils were diluted with ethanol to make it homogeneous and then passed through a 0.2 μm filter.

The water-insoluble fraction of the oil samples were measured according to Ba et al.<sup>19</sup> A total of 5 g of bio-oil was slowly dropped into 500 mL of chilled water under strong stirring for 2 h to precipitate all components of the water-insoluble fraction. The mixture was filtered and then washed in deionized water under strong stirring for 14 h. Subsequently, the mixture was filtered by filter paper with a pore size of 0.2 μm. The filtered sample was dried at vacuum at a temperature of 60 °C.

Thermal behaviors of the bio-oils were analyzed by the TGA (STA, Netzsch STA 449 F1). A total of 8–10 mg samples were heated from room temperature to 1000 °C at a constant heating rate of 10 °C/min under N<sub>2</sub> flow.

## RESULTS AND DISCUSSION

**Product Distributions of the Sewage Sludge PCR Pyrolysis.** TGA has been used to characterize sewage sludge.<sup>18,26,28</sup> TGA and differential thermogravimetry (DTG) pyrolysis analysis results of the feedstock sewage sludge with a heating rate of 10 °C/min are shown in Figure 2. The major

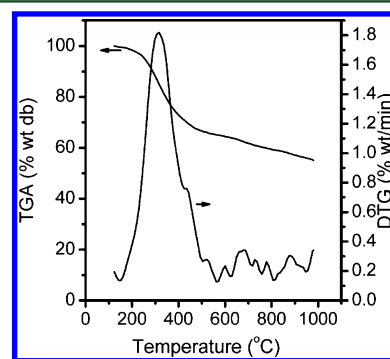


**Figure 2.** TGA and DTG for pyrolysis of the dried sewage sludge. The sludge sample was heated at 10 °C/min to 1000 °C in nitrogen.

mass loss of the sewage sludge takes place in a temperature range of 150–575 °C. The peak mass loss at temperatures of 155–400 and 400–575 °C are probably the decomposition of less complex organic structures (probably mainly cellulose from paper, cardboard, wood garden waste, and kitchen waste) and decomposition of more complex organic structures, respectively. The TGA char yields at 400 and 575 °C are 72 and 65 wt % db and correspond to char fractions of 53 and 16 wt % daf, respectively. These results imply that the sewage sludge probably has a higher proportion of simple organic structures than that of complex organic structures. The sewage sludge contains high amounts of volatile inorganic elements, such as S (0.9 wt % db), Na (0.26 wt % db), K (0.67 wt % db), and Cl (0.05 wt % db) (see Table 2). Thus, the small peaks observed

at temperatures higher than 575 °C seen on the DTG curve may be caused by the release of some inorganic compounds.<sup>27,28</sup>

The sewage sludge PCR pyrolysis experiments were performed at four different temperatures of 475, 525, 575, and 625 °C. The temperature range is believed to cover the full decomposition temperatures of sewage sludge.<sup>18,26,28</sup> The experiments were performed twice at each pyrolysis temperature to ensure reproducible pyrolysis product determinations. The obtained mass balance closures were in a range of 92–99%. The average product yields of two experiments and standard deviations ( $\pm 2$ ) are shown in Figure 3. The char yield

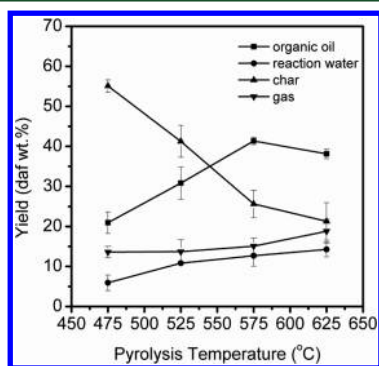


Figure 3. Pyrolytic product yields of sewage sludge (daf).

decreases from approximately 55 to less than 21 wt % daf, whereas the gas yield slightly increases from 14 to 19 wt % daf when the temperature increases from 475 to 625 °C. The increase in the organic oil yield is accompanied by a decrease in the char yield when increasing the temperature from 475 to 575 °C. The organic oil yield reaches a maximum of 41 wt % daf (bio-oil yield of 54 wt % daf) at 575 °C. An increase of the gas yield together with a slight decrease of the organic oil yield (38 wt % daf) is obtained at 625 °C. This is probably caused by secondary reactions of bio-oil decomposition. Thus, the optimal temperature to obtain a maximal organic oil yield is found to be around 575 °C in this study. The trends of the product yields and the optimal temperature found in this work are consistent with other pyrolysis sewage sludge studies, where the sewage sludge samples obtained a maximum bio-oil yield of 31–52 wt % daf at 525–575 °C in fluidized-bed reactors.<sup>5,9</sup> The PCR char yield of 25 wt % daf obtained at the reactor temperature of 575 °C, and this is 6 wt % daf lower than the TGA char yield (31 wt % daf or 65 wt % db) (see Figure 2) obtained at 575 °C. Different evolution trends of reaction water yield are found in the literature.<sup>6,29</sup> An increased trend of the reaction water yield from 2 to 20 wt % daf was observed by Piskorz et al.<sup>6</sup> when the reaction temperature was increased from 350 to 700 °C, while a decreased trend of the reaction water yield from 16 to 13 wt % db with an increasing temperature from 400 to 550 °C was obtained by Shen et al.<sup>29</sup> for sewage sludge pyrolysis. The different evolution trends with respect to the pyrolysis temperature are probably caused by differences of pyrolysis conditions, reactor types, and feedstock. In this study, the reaction water yields vary from 6 wt % daf at 475 °C to 14 wt % daf at a pyrolysis temperature at 625 °C, as seen in Figure 3.

The heating rate has a large influence on the pyrolysis product distributions. A modeling of the PCR process has indicated that a typical particle initial heating rate of 200–1000 K/s is obtained,<sup>12</sup> which is much higher than that of fixed-bed

reactors having a heating rate of less than 100 K/min.<sup>25,30</sup> Bio-oil yields obtained from these low heating rate reactors were 22–42 wt % daf<sup>26,31</sup> and are 1.3–1.6 times lower than that of the PCR.

The recovered energy contents in bio-oil and char were calculated by the product yields and their heating values. Figure 4 shows the energy distributions in the bio-oil and char. The

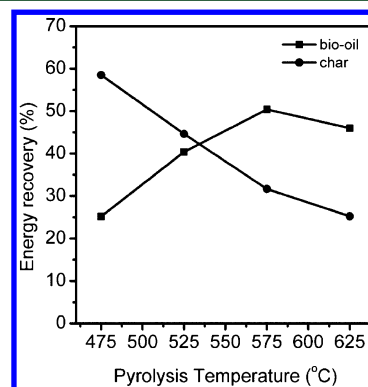


Figure 4. Energy recovered in bio-oil and char compared to the feedstock sewage sludge.

char energy recovery decreased from about 59 to 32%, whereas the oil energy recovery increased from 25 to 50% when the temperature was increased from 475 to 575 °C. Thus, most of the energy content was transferred from the char into the bio-oil. At the temperature of 625 °C, the oil energy recovery slightly decreased because of secondary reactions of the sludge oil. Thus, in this study, the maximal bio-oil energy recovery of 50% is obtained at a pyrolysis temperature of 575 °C. The optimal temperature to obtain a maximum bio-oil energy recovery is similar to the optimal temperature for obtaining a maximum organic oil yield.

**Characterization of the Bio-Oil.** Table 3 summarized some of the results from the analysis of the sewage sludge bio-oil samples. In this work, the water-insoluble fractions were 16–19 wt % of the 525 and 575 °C oil samples, which is lower than the level found in the 475 and 625 °C samples. A typical water-insoluble fraction contains oligomeric materials, polycyclic aromatic hydrocarbons (PAHs), and extractives and has a mean molecular weight in a broad range of 650–6900 g/mol (for lignocellulosic bio-oil).<sup>19,32</sup> It probably causes instability of the bio-oil (phase separation and viscosity increase during storage). The HHV on a dry basis of sludge oils obtained at the pyrolysis temperature of 525–575 °C is 1.7 times higher than that of the 475 °C sludge oil. The trend of HHV evolution in this work is consistent with those reported by Park et al.,<sup>18</sup> who also investigated sewage sludge pyrolysis. The fraction of cellulose derivatives containing a high oxygen content probably decreases with an increasing pyrolysis temperature, leading to a decreased oxygen content of sludge oils produced at a higher pyrolysis temperature.

SEC was used to investigate the molecular-weight distribution of the bio-oil samples. As seen in Figure 5, the three oil samples obtained from pyrolysis temperatures of 525, 575, and 625 °C had two main peaks of 90–340 and 340–3500 g/mol, whereas the 475 °C sample had a broader peak of 90–3500 g/mol. When the temperature increased from 525 to 625 °C, the magnitude of the first peak decreased along with an increase of the second peak. The condensation of aromatic compounds

Table 3. Bio-Oil Properties

sludge oil sample	457 °C	525 °C	575 °C	625 °C
water content (wt %)	27.8 ± 1.8	30.3 ± 1.2	30.2 ± 0.8	28.5 ± 1.1
water-soluble content (wt %) <sup>a</sup>	41.1	54	51.1	49.5
water-insoluble fraction (wt %)	31.1	15.7	18.7	21.8
ash content (wt %)	0.8	0.2	0.4	0.2
HHV (MJ/kg db)	15.5 ± 1.1	24.8 ± 0.2	25.5 ± 0.1	23.1 ± 0.5
density (g/mL)	1.08 ± 0.02	1.04 ± 0.01	1.03 ± 0.02	1.07 ± 0.02
viscosity at 40 °C (mPa s)	81.1 ± 0.8	36.9 ± 0.6	43.6 ± 1.3	137.7 ± 3.1
mean molecular weight, $M_w$ (g/mol)	430	386	392	481

<sup>a</sup>Water-soluble fraction = 100 – water-insoluble fraction – water content.

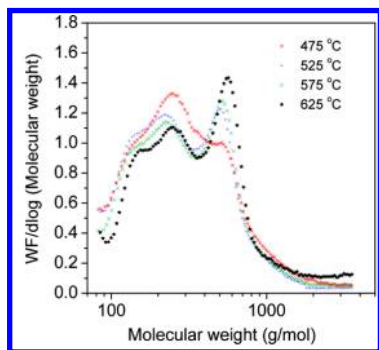


Figure 5. Size-exclusion chromatography (SEC) determined molecular-weight distribution of sludge oils.

during biomass pyrolysis was studied by Elliot.<sup>20</sup> When the pyrolysis temperature is higher than 600 °C, alkyl groups are cleaved from phenolics, resulting in cyclization reactions,<sup>20</sup> and eventually, PAHs are formed at 700 °C. The findings in this study suggest that a recombination of volatiles to form the high molecular compounds (molecular mass of 450–700 g/mol) perhaps take place in the 625 °C samples (see Figure 5), resulting in an increase of the mean molecular mass (see Table 3). The mean molecule mass ( $M_w$ ) values of the 475 and 625 °C samples were 430 and 481 g/mol, which are higher than those of the 525 and 575 °C samples. These results are consistent with the water-insoluble fractions of the oil samples (see Table 3), which are supposed to consist of condensed aromatic compounds and sewage sludge derivatives, which are supposed to have a molecular mass of 700–3500 g/mol.<sup>33</sup> This indicates that a higher content of these derivatives is observed in the 475 °C sludge oil sample and also a higher condensed aromatic content is presented in the 625 °C sludge oil sample.

Oil viscosities have been found to be related to average molecular weight.<sup>34</sup> In this work, the measured oil viscosity values are around 40 mPa s for the 525 and 575 °C samples and 81 and 137 mPa s for the 475 and 625 °C oil samples, respectively (see Table 3). A lowering of the oil viscosities from 157 to 115 cSt with an increasing pyrolysis temperature from 400 to 550 °C was also observed by Shen and Zhang,<sup>29</sup> who pyrolyzed a mixture of sewage sludge and putrescible garbage.

TGA can be used to characterize the evaporation, thermal degradation, and combustion behavior of bio-oil. The TGA and DTG experimental data of the sludge oil samples made using a heating rate of 10 °C/min up to a temperature of 1000 °C in a nitrogen gas flow are shown in Figure 6. On the basis of the DTG curves, the same pattern with two main mass loss peaks at 40–200 and 200–500 °C are observed for the four sludge oil samples. The first peak (at temperatures of 40–200 °C) of the sludge oil samples is probably evaporation of water (28–30 wt

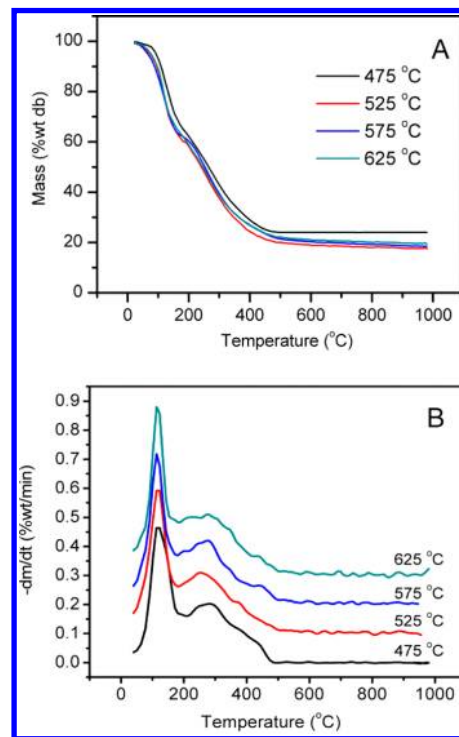


Figure 6. (A) TGA and (B) DTG of sewage sludge oil produced at 475, 525, 575, and 625 °C in a  $N_2$  flow.

% content of the bio-oil samples) and light volatile components. The second peak (at temperatures of 200–500 °C) is probably the evaporation, cracking, and polymerization of high molecular fractions that could contain monolignols, moderate volatile polar compounds, mono- and polysugars, extractive-derived compounds (fatty and resin acids, paraffins, and phenanthrenes),<sup>33</sup> and sewage sludge derivatives.

On the basis of the mass loss TGA profiles (see Figure 6A), water contents determined by Karl Fischer titration, and ash contents determined by ASTM D1102-84, the bio-oil compounds are classified into three fractions: light organics, medium organics, and pyrolytic chars, as shown in Table 4. The oils produced at the different temperatures were reasonably similar; only the 475 °C oil sample deviated. The light organic fraction of the 475 °C sample (11.6 wt % daf) was lower than that of the other samples (15.5–17.6 wt % daf). It is believed that a pyrolysis temperature higher than 475 °C increases the cracking of volatiles to form more gas (see Figure 3) and also increases the light organic oil fraction. This indicates that the light organic fraction of the sludge oils of 12–18 wt % daf can be distilled. The medium organic fractions that correspond to the second peak are on a level of 52–55 wt % daf for all of the

Table 4. Bio-Oil Component Distribution

	on a wet basis				on a dry and ash-free basis			
pyrolysis temperature (°C)	457	525	575	625	457	525	575	625
water (wt %) <sup>a</sup>	27.8	30.3	30.2	28.6				
light organic fraction (wt %) <sup>b</sup>	8.4	11.5	10.8	12.6	11.6	16.5	15.5	17.6
medium organic fraction (wt %) <sup>c</sup>	39.7	38.2	37.6	36.8	55.0	54.8	53.9	51.5
pyrolytic char fraction (wt %) <sup>d</sup>	23.4	19.8	20.0	22.0	32.4	28.4	28.6	30.8
ash (wt %) <sup>e</sup>	0.8	0.2	0.4	0.2				

<sup>a</sup>Determined by Karl Fischer titration. <sup>b</sup>Determined from room temperature to 200 °C and subtraction of the water content. <sup>c</sup>Determined from the 200–500 °C section of the TGA curve. <sup>d</sup>Determined as the weight at 500 °C on the TGA curve and subtraction of the ash content. <sup>e</sup>Determined by ASTM D1102-84.

Table 5. HHV Value and Elemental Compositions of Bio-Oil from Various Materials (db)<sup>a</sup>

bio-oil	C (wt %)	H (wt %)	O (wt %)	N (wt %)	S (wt %)	HHV (MJ/kg)	bio-oil yield (wt % daf)	technology <sup>b</sup>	reference
pine sawdust	53.4	4.9	41.7	nd <sup>c</sup>	0.01	22	73	FBR	35
brown forest residue	56.5	4.4	38.2	0.41	0.04	23	66	FBR	35
green forest residue	55.3	5.2	39.0	0.40	0.03	22	59	FBR	35
eucalyptus	53.3	5.2	41.3	0.13	0.03	21	71	FBR	35
barley straw	54.2	3.3	40.7	1.84	nd	23	55	FBR	35
Timothy hay	52.9	4.1	42.0	0.99	nd	22	62	FBR	35
reed canarygrass	54.1	4.7	40.4	0.83	nd	22	76	FBR	35
pine wood	62.7	5.8	31.3	0.01	0.02	26		AR	36
oak wood	60.9	2.0	36.8	0.03	0.03	24		AR	36
pine bark	67.3	4.8	27.3	0.04	0.04	23		AR	36
oak park	58.3	3.6	37.3	0.36	0.36	24		AR	36
sewage sludge <sup>d</sup>	53.7	7.4	27.6	9.6	1.8	25	54	PCR	this work
sewage sludge	58.4	8.4	22.3	9.8	0.9	30	49	FBR	15
sewage sludge						27–33		FBR	8
sewage sludge						31–32	48–52	FBR	9
sewage sludge						23–28	39–58	FBR	16

<sup>a</sup>Calculated from available data. <sup>b</sup>AR, auger reactor; FBR, fluidized-bed reactor; and PCR, pyrolysis centrifugal reactor. <sup>c</sup>nd = not detected. <sup>d</sup>Oil produced at the pyrolysis temperature of 575 °C.

oil samples. Elliot et al.<sup>20</sup> distilled several different bio-oils by vacuum distillation, and distillation data were converted to atmospheric pressure using a petroleum hydrocarbon vapor pressure chart. The distillation residues were obtained to be of a wide range level of 47–78 wt % db at a final temperature of 390 °C. Coke formation was observed at around 205–210 °C, and bio-oil decompositions were initiated at around 280 °C. It was noted that bio-oil cannot be distilled at a temperature higher than 210 °C. Thus, the majority of the medium organic fraction when heated above 210 °C will decompose to generate pyrolytic char and lower molecular weight species. The pyrolytic char fraction of the 475 °C sample is higher than that of the other oil samples. The obtained char fractions (see Table 4) show the same tendencies as that of the water-insoluble fractions (see Table 3). Tuya et al.,<sup>19</sup> who analyzed softwood bark pyrolytic oil, showed that an oil sample with a higher water-insoluble fraction will form a higher pyrolytic char fraction when the oil is heated.

The elemental compositions, heating values, and bio-oil yields of different pyrolysis oils are shown in Table 5. Sewage sludge pyrolysis obtains a lower bio-oil yield than that of wood probably because of the high ash content (especially alkali content). However, sewage sludge has a lower oxygen content (22–28 wt % db), probably leading to a higher sewage pyrolysis oil HHV when compared to wood oils.

The analysis of the element distributions in sludge oil and char were carried out on the 575 °C samples, and the results are shown in Table 6. The contents of carbon, hydrogen, and

Table 6. Element Analyses and Element Recoveries of the 575 °C Bio-Oil and Char (db)

element	char	bio-oil	element recovery <sup>a</sup> (%)		
			char	bio-oil	total (char + bio-oil)
C (wt %)	14.6	53.7	32	38	70
H (wt %)	1.0	7.4	18	71	89
O (wt %) <sup>b</sup>	2.1	27.6	10	74	84
S (wt %)	0.5	1.8	36	39	75
N (wt %)	1.8	9.6	27	48	75
ash (wt %)	80.3	0.57	97	0.3	97
Cl (wt %)	0.04	0.12	49	48.0	97
Al (wt %)	2.68	0.006	92	0.1	92
Fe (wt %)	12.45	0.14	94	0.6	95
P (wt %)	5.29	0.01	95	0.4	95
Si (wt %)	12.85	0.02	95	1.5	96
Ti (wt %)	0.33	0.00	87	0.8	88
Ca (wt %)	5.49	0.09	90	1.8	92
K (wt %)	1.03	0.04	94	0.1	94
Mg (wt %)	0.64	0.01	91	0.0	91
Na (wt %)	0.41	0.02	96	0.0	96
Cd (mg/kg)	1.16	0.10	84	3.0	87
Cr (mg/kg)	111.5	0.51	97	0.2	98
Zn (mg/kg)	1495	97.80	88	2.3	90

<sup>a</sup>Calculated on the basis of a dry feedstock basis. <sup>b</sup>O% = 100% – ash% – C% – H% – N% – S%.

oxygen are 53.7, 7.4, and 27.6 wt % db in the bio-oil, respectively. The nitrogen and sulfur contents in the bio-oil were 9.6 and 1.8 wt %, respectively, and much higher than those of lignocellulosic oils, with typical levels of 0.03–1.8 wt % db nitrogen and 0.0–0.36 wt % db sulfur (see Table 5). The sewage sludge nitrogen and sulfur were transferred 39 and 48% to the bio-oil and 36 and 27% to the char, respectively. The recoveries of nitrogen and sulfur in the total bio-oil and char are 75%, and this indicates that some nitrogen and sulfur are probably released to the gas phase. Because the nitrogen and sulfur contents in sludge oil are so high, it may cause corrosion of equipment and environmental problems related to NO<sub>x</sub> and SO<sub>2</sub> emissions when the oil is combusted.

The contents of some ash-forming elements and heavy metals (Cl, Al, Fe, P, Si, Ti, Ca, K, Mg, Na, Cd, Cr, and Zn) in the char and bio-oil as well as recovered fractions are shown in Table 6. During the sludge pyrolysis at 575 °C, most of the metallic elements remain in the char (element recoveries of 84–97%); thus, the bio-oil has low levels of metals (0.0–0.14 wt %), with the most abundant elements being Fe (0.14 wt % db), Cl (0.12 wt % db), and Ca (0.09 wt % db). The lower levels of metal contents in the oils can probably be obtained if the PCR char separation system is improved. The incomplete recovery of metallic elements in the char and oil (88–98%) is believed mainly to be caused by the limited mass balance of 94% obtained for the 575 °C samples rather than metals contained in the pyrolysis gas product (with the exception being Cl and S that may also be present in the gas). The low concentration of K (0.04 wt %) and Cl (0.12 wt %) in the sludge oil should make it possible to avoid slagging, fouling, and aerosol formation problems when the oil is used for combustion or gasification.<sup>37</sup>

**Characterization of the Biochar.** Table 7 shows the ash content, organic content, and heating values of the generated

**Table 7. Sludge Char Properties**

pyrolysis temperature (°C)	457	525	575	625
ash content (wt % db)	71.3	73.8	80.5	82.3
organic content (wt % db)	28.7	26.2	19.5	17.7
HHV (MJ/kg db)	8.8	7.9	6.1	5.1

chars. The ash content of the chars rises from 71 to 82 wt % along with a decrease from 29 to 18 wt % of the organic char content when the pyrolysis temperature is increased from 475 to 625 °C. The sewage sludge and the char particle-size distributions are shown in Figure 7. The feedstock experiences

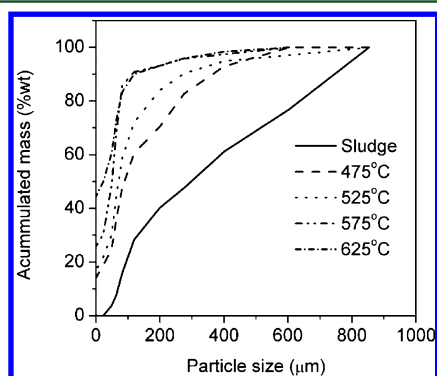


**Figure 7.** Particle-size distribution of char.

high mechanical stress in the PCR, and char exposed to higher temperatures is often more fragile. As a result, the fraction of the char particles less than 90 µm increases from 52 to 88 wt % when the pyrolysis temperature is increased from 475 to 625 °C.

When the inorganic element analysis of the 575 °C sample is taken into account (see Table 6), most metal elements in the sewage sludge are concentrated in the char product. SEM images of the 475 and 625 °C char samples are presented in Figure 8, and they confirm the results of the char particle-size

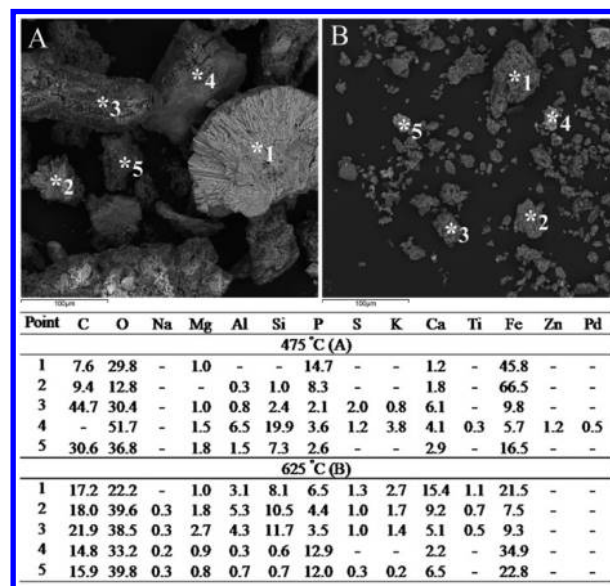


**Figure 8.** SEM-EDX of chars of sewage sludge (A at 475 °C and B at 675 °C).

distribution measurements. Obviously, the char obtained at 475 °C has a larger particle size than the 625 °C char, and both char samples exhibit diverse particle shapes. EDX was used to identify the predominant elements at some selected points. As seen in panels A and B of Figure 8, elements such as Fe, P, Al, Ca, Mg, Si, Na, and K obtain a considerable non-uniform distribution in the char particles at both low and high reaction temperatures. A similar phenomenon was reported by Ábrego et al. on sewage sludge char.<sup>38</sup>

In principle, the sludge chars may be managed by incineration or disposal on farmland or landfilling. With the high ash contents of 71–83 wt % and the low HHVs of 5.1–8.8 MJ/kg, the sludge chars are unattractive for combusting to use the energy content. However, the high contents of N, P, K, Ca, Mg, and S that are all important macronutrients of fertilizer could make the sludge char valuable as a fertilizer, especially phosphorus, which is a scarce element. With 95 wt % of phosphorus recovered in the char (see Table 6), fast pyrolysis is a promising method to recycle phosphorus into soil. The leaching of diffuent phosphorus from pyrolysis char and the phosphorus nutrient availability in soil were studied by Bridle et al.<sup>39</sup> and Liu et al.<sup>40</sup> The results from these studies show that it is possible to use pyrolysis char on soil to provide phosphorus. A significant release of heavy metals with low boiling points (e.g., As, Hg, Cd, and Se) from sewage sludge was observed during carbonization above 550 °C,<sup>41</sup> whereas heavy metals with high boiling points (e.g., Pb, Co, Ni, Cu, Zn, and Sr) remained in a sludge char. Thus, if the sludge char is used on farmland, the heavy metal contents of the char (see Tables 1



and 6) limited by Directive 86/278/CEE<sup>1</sup> must be adequately taken into account. Landfilling is also a practical method to manage the sludge char disposal. In terms of sewage sludge treatment, the solid waste amount (from sludge to ash-rich char) is reduced to about 44 wt % on a mass basis and 52% on a bulk volume basis.

## CONCLUSION

The product distributions of fast sewage sludge pyrolysis with respect to organic oil, gas, char, and reaction water were determined using reactor temperatures in the range of 475–625 °C, and the char and bio-oil properties were investigated. Similar to conventional biomass pyrolysis, an increasing gas yield and a decreasing char yield were observed with an increased temperature. A maximal organic oil yield of 41 wt % daf and a maximal bio-oil energy recovery of 50% were obtained at the optimal reactor pyrolysis temperature of 575 °C.

Measurements of the molecular-weight distributions of the sludge oil indicate that the condensed aromatic content increases when the pyrolysis temperature is increased from 525 to 625 °C, while higher contents of the sewage sludge derivatives were observed in the low-temperature bio-oil of 475 °C in this study. This can partially explain the observed differences of HHV, viscosity, and thermal behaviors of the sludge oils. A sludge oil was obtained at the optimal reactor temperature of 575 °C with a HHV of 25.1 MJ/kg, a water-insoluble fraction of 18.7 wt %, a viscosity of 43.6 mPa s at 40 °C, an average molecular weight of 392 g/mol, and metallic concentrations lower than 0.14 wt %, while less optimal oil properties with respect to industrial applications were found for the 475 and 625 °C oil samples. High sulfur and nitrogen contents of the sludge oil compared to conventional bio-oil from biomass may limit the further industrial applications of the sludge oil. The char properties of the 575 °C char sample were an ash content of 81 wt % db and a HHV of 6.1 MJ/kg db, where 95 wt % of the sewage sludge phosphorus content was recovered in the char. The solid waste bulk volume (the char compared to the sludge) was reduced 52% by pyrolysis at 575 °C. It is seen that the fast pyrolysis process provides a promising method to reduce the cost for landfilling and produce a bio-oil that can be used as a fuel.

## ASSOCIATED CONTENT

### Supporting Information

Calculation of water and light fraction loss during solvent removal. This material is available free of charge via the Internet at <http://pubs.acs.org>.

## AUTHOR INFORMATION

### Corresponding Author

\*E-mail: [paj@kt.dtu.dk](mailto:paj@kt.dtu.dk).

### Notes

The authors declare no competing financial interest.

## ACKNOWLEDGMENTS

Financial support of this study by DONG Energy A/S, Energinet.dk, and DTU is gratefully acknowledged. The authors are very grateful to Tran Thuong Dang and Kim Chi Szabo from the Department of Chemical and Biochemical Engineering, DTU, who have performed some of the analyses reported in this paper.

## REFERENCES

- (1) European Commission (EC). *European Commission Council Directive 1986/278/EEC of June 12, 1986, on the Protection of the Environment, and in Particular of the Soil, When Sewage Sludge Is Used in Agriculture*; EC: Brussels, Belgium, 1986.
- (2) Fytili, D.; Zabaniotou, A. *Renewable Sustainable Energy Rev.* **2008**, *12*, 116–140.
- (3) Milieu, Ltd. *Environmental, Economic and Social Impacts of the Use of Sewage Sludge on Land. Final Report. Part III: Project Interim Reports*; Milieu, Ltd.: Brussels, Belgium, 2010; [http://ec.europa.eu/environment/waste/sludge/pdf/part\\_iii\\_report.pdf](http://ec.europa.eu/environment/waste/sludge/pdf/part_iii_report.pdf).
- (4) Manara, P.; Zabaniotou, A. *Renewable Sustainable Energy Rev.* **2012**, *16*, 2566–2582.
- (5) Fonts, I.; Juan, A.; Gea, G.; Murillo, M. B.; Sánchez, J. L. *Ind. Eng. Chem. Res.* **2008**, *47*, 5376–5385.
- (6) Piskorz, J.; Scott, D. S.; Westerberg, I. B. *Ind. Eng. Chem. Proc. Des. Dev.* **1986**, *25*, 265–270.
- (7) Shen, L.; Zhang, D. K. *Fuel* **2003**, *82*, 465–472.
- (8) Fonts, I.; Juan, A.; Gea, G.; Murillo, M. B.; Arauzo, J. *Ind. Eng. Chem. Res.* **2008**, *48*, 2179–2187.
- (9) Fonts, I.; Azuara, M.; Gea, G.; Murillo, M. B. *J. Anal. Appl. Pyrolysis* **2009**, *85*, 184–191.
- (10) Butler, E.; Devlin, G.; Meier, D.; McDonnell, K. *Renewable Sustainable Energy Rev.* **2011**, *15*, 4171–4186.
- (11) Fonts, I.; Gea, G.; Azuara, M.; Ábrego, J.; Arauzo, J. s. *Renewable Sustainable Energy Rev.* **2012**, *16*, 2781–2805.
- (12) Bech, N.; Larsen, M. B.; Jensen, P. A.; Dam-Johansen, K. *Biomass Bioenergy* **2009**, *33*, 999–1011.
- (13) Janse, A. M. C.; Westerhout, R. W. J.; Prins, W. *Chem. Eng. Process.* **2000**, *39*, 239–252.
- (14) Oasmaa, A.; Solantausta, Y.; Arpiainen, V.; Kuoppala, E.; Sipila, K. *Energy Fuels* **2010**, *24*, 1380–1388.
- (15) Fonts, I.; Kuoppala, E.; Oasmaa, A. *Energy Fuels* **2009**, *23*, 4121–4128.
- (16) Pokorna, E.; Postelmans, N.; Jenicek, P.; Schreurs, S.; Carleer, R.; Yperman, J. *Fuel* **2009**, *88*, 1344–1350.
- (17) Fonts, I.; Azuara, M.; Lázaro, L.; Gea, G.; Murillo, M. B. *Ind. Eng. Chem. Res.* **2009**, *48*, 5907–5915.
- (18) Park, E. S.; Kang, B. S.; Kim, J. S. *Energy Fuels* **2008**, *22*, 1335–1340.
- (19) Ba, T.; Chaala, A.; Garcia-Perez, M.; Rodrigue, D.; Roy, C. *Energy Fuels* **2004**, *18*, 704–712.
- (20) Elliot, D. C. *Analysis and Comparison of Biomass Pyrolysis/Gasification Condensates, Final Report*; Pacific Northwest Laboratory: Richland, WA, 1986; PNL-5943.
- (21) Azeez, A. M.; Meier, D.; Odermatt, J.; Willner, T. *Energy Fuels* **2010**, *24*, 2078–2085.
- (22) Trinh, T. N.; Jensen, P. A.; Dam-Johansen, K.; Knudsen, N. O.; Sorensen, H. R.; Hvilsted, S. *Energy Fuels* **2013**, DOI: 10.1021/ef301927y.
- (23) Fahmi, R.; Bridgwater, A. V.; Donnison, I.; Yates, N.; Jones, J. M. *Fuel* **2008**, *87*, 1230–1240.
- (24) Jensen, A.; Dam-Johansen, K.; Wojtowicz, M. A.; Serio, M. A. *Energy Fuels* **1998**, *12*, 929–938.
- (25) Mohan, D.; Charles, U.; Steele, P. H. *Energy Fuels* **2006**, *20*, 848–889.
- (26) Karayildirim, T.; Yanik, J.; Yuksel, M.; Bockhorn, H. *Fuel* **2006**, *85*, 1498–1508.
- (27) Johansen, J. M.; Jakobsen, J. G.; Frandsen, F. J.; Glarborg, P. *Energy Fuels* **2011**, *25*, 4961–4971.
- (28) Urban, D. L.; Antal, M. J. *Fuel* **1982**, *61*, 799–806.
- (29) Shen, L.; Zhang, D. K. *Fuel* **2005**, *84*, 809–815.
- (30) Inguanzo, M.; Domínguez, A.; Menéndez, J. A.; Blanco, C. G.; Pis, J. J. *J. Anal. Appl. Pyrolysis* **2002**, *63*, 209–222.
- (31) Sánchez, M. E.; Menéndez, J. A.; Domínguez, A.; Pis, J. J.; Martínez, O.; Calvo, L. F.; Bernad, P. L. *Biomass Bioenergy* **2009**, *33*, 933–940.
- (32) Scholze, B.; Hanser, C.; Meier, D. *J. Anal. Appl. Pyrolysis* **2001**, *58*, 387–400.

- (33) Garcia-Perez, M.; Chaala, A.; Pakdel, H.; Kretschmer, D.; Roy, C. *Biomass Bioenergy* **2007**, *31*, 222–242.
- (34) Oasmaa, A.; Kuoppala, E. *Energy Fuels* **2003**, *17*, 1075–1084.
- (35) Oasmaa, A.; Solantausta, Y.; Arpiainen, V.; Kuoppala, E.; Sipila, K. *Energy Fuels* **2009**, *24*, 1380–1388.
- (36) Ingram, L.; Mohan, D.; Bricka, M.; Steele, P.; Strobel, D.; Crocker, D.; Mitchell, B.; Mohammad, J.; Cantrell, K.; Pittman, C. U. *Energy Fuels* **2007**, *22*, 614–625.
- (37) Matjie, R. H.; French, D.; Ward, C. R.; Pistorius, P. C.; Li, Z. *Fuel Process. Technol.* **2011**, *92*, 1426–1433.
- (38) Ábrego, J.; Arauzo, J. S.; Sánchez, J. L.; Gonzalo, A.; Cordero, T. S.; Rodríguez-Mirasol, J. *Ind. Eng. Chem. Res.* **2009**, *48*, 3211–3221.
- (39) Bridle, T. R.; Pritchard, D. *Water Sci. Technol.* **2004**, *50*, 169–175.
- (40) Liu, W.; Zeng, F.; Jiang, H.; Yu, H. J. *Bioresour. Technol.* **2011**, *102*, 3471–3479.
- (41) Yoshida, T.; Antal, M. J. *Energy Fuels* **2009**, *23*, 5454–5459.

February, 2014, DTU

## **Appendix A4**

# **Journal paper: Fast Pyrolysis of Lignin Using a Pyrolysis Centrifuge Reactor**

**Energinet.dk project no. 010077**

**Treatment of Lignin and waste residues by flash pyrolysis**

**Trung Ngoc Trinh, Peter Arendt Jensen, Zsuzsa Sárossy, Kim Dam-Johansen, Niels Ole Knudsen, Hanne Risbjerg Sørensen and Helge Egsgaard**

*Department of Chemical and Biochemical Engineering*

Technical University of Denmark

Søltofts Plads, Building 229, DK-2800 Lyngby, Denmark

CHEC no. R1401

# Fast Pyrolysis of Lignin Using a Pyrolysis Centrifuge Reactor

Trung Ngoc Trinh,<sup>†</sup> Peter Arendt Jensen,<sup>\*,†</sup> Zsuzsa Sárosy,<sup>†</sup> Kim Dam-Johansen,<sup>†</sup> Niels Ole Knudsen,<sup>‡</sup> Hanne Risbjerg Sørensen,<sup>‡</sup> and Helge Egsgaard<sup>†</sup>

<sup>†</sup>Department of Chemical and Biochemical Engineering, Denmark Technical University, Søtofts Plads Bygning 229, Kgs. Lyngby 2800, Denmark

<sup>‡</sup>DONG Energy, Kraftsværksvej 53, DK-7000, Fredericia, Denmark

**ABSTRACT:** Fast pyrolysis of lignin from an ethanol plant was investigated on a lab scale pyrolysis centrifuge reactor (PCR) with respect to pyrolysis temperature, reactor gas residence time, and feed rate. A maximal organic oil yield of 34 wt % dry basis (db) (bio-oil yield of 43 wt % db) is obtained at temperatures of 500–550 °C, reactor gas residence time of 0.8 s, and feed rate of 5.6 g/min. Gas chromatography mass spectrometry and size-exclusion chromatography were used to characterize the chemical properties of the lignin oils. Acetic acid, levoglucosan, guaiacol, syringols, and p-vinylguaiacol are found to be major chemical components in the lignin oil. The maximal yields of 0.62, 0.67, and 0.38 wt % db were obtained for syringol, p-vinylguaiacol, and guaiacol, respectively. The reactor temperature effect was investigated in a range of 450–600 °C and has a considerable effect on the observed chemical components and molecular mass distribution of the lignin oils. The obtained lignin oil has a very different components composition when compared to a beech wood oil.

## 1. INTRODUCTION

Lignin, with a typical biomass weight fraction of 15–33 wt %, is the second most abundant component in biomass<sup>1</sup> and may account for up to 40% of the biomass energy content. Lignin has a complex, amorphous cross-linked and highly branched structure,<sup>2</sup> and it is biosynthesized by nonspecific radical reactions using only a few aromatic building blocks such as p-coumaryl, coniferyl, and sinapyl alcohols derivatives.<sup>1,2</sup> Today lignin is mainly produced by the pulp and paper industry. In the near future it is expected also to appear as a byproduct in the second generation bioethanol industry based on lignocelluloses. The potential of lignin produced as a residue in the paper industry is more than 50 million tons/year, but only about 2% of the lignin residue is used as commercial products for producing lignosulfonates (1,000,000 tons/year) and kraft lignins (less than 100,000 tons/year).<sup>3</sup> Most of the lignin is used as a low-value fuel for pulping boilers. Thus lignin may be a potential source for bio-oil production by fast pyrolysis.

The research on fast pyrolysis of lignin shows some initial promising results for lignin utilization.<sup>4–6</sup> However plugging/agglomeration in the fuel feeder system of a fluidized bed reactor and condenser have been observed and is probably due to low melting point of lignin and high molecular mass of lignin oil.<sup>5,6</sup> Also a low bio-oil yield of lignin fast pyrolysis (20–58 wt % db)<sup>5–7</sup> has been obtained compared to that of wood fast pyrolysis.<sup>8–10</sup> New strategies of fast pyrolysis of lignin that could enhance the lignin value have been suggested: 1) Catalyst fast pyrolysis using some kind of catalysts such as a zeolite<sup>7,11</sup> could produce a higher fraction of high value aromatics. 2) Formate-assisted fast pyrolysis<sup>12</sup> using calcium formate/formic acid as a hydrogen production source for the chemical transformation in situ could produce a bio-oil almost free of oxygen (O/C of 0.067 on dry basis).<sup>12</sup> However catalyst deactivation, decrease of bio-oil yield, and cost of formic acid are some possible barriers of these strategies. Thus efforts on reactor modifications or new reactor designs for conventional fast pyrolysis (without catalyst) are

conducted to overcome these barriers and enhance the bio-oil yield.

Bubbling fluidized bed reactors, circulating fluidized bed reactors, rotary cone reactors, auger reactors, and ablative reactors are close to commercialization for the use for fast biomass pyrolysis.<sup>13</sup> The main difference among these reactors is the applied heat transfer method, and heating rates of 700–1500 K/s<sup>14,15</sup> are often obtained. The ablative pyrolysis reactor was developed by Diebold et al.<sup>16</sup> In their approach, the centrifugal forces are used to press the biomass on to a hot surface, and a high biomass heating rate can be obtained by this technology. The pyrolysis centrifuge reactor (PCR), a type of ablative reactor, has been developed at the CHEC center at DTU Chemical engineering.<sup>15</sup> By a high centrifugal force, biomass particles can gain a heating rate of 200–2000 K/s.<sup>15</sup> The main advantage of this concept compared to fluid bed reactors is a compact design that uses a low flow rate of carrier gas, and the biomass pyrolysis is obtained without a heat carrier. Also, the PCR can treat relatively large biomass particles.

Lignin fast pyrolysis is found to be a promising method to produce monomeric phenols.<sup>6,17</sup> Guaiacols, syringols, alkyl phenols, and catechols<sup>5,6,17</sup> are known as major phenols to be present in lignin oil. These phenols are known to have economic potential in the use for petrochemical products and transportation fuels. Yields of 1.5–3, 0.8–2.6, 0.3–1.2, and 0.4–1.2 wt % (on dry basis) from lignin pyrolysis have been obtained for guaiacols, syringols, alkylphenols, and catechols, respectively,<sup>5,11,17</sup> and a total monomeric phenols yield of 5–7 wt % db<sup>5,17</sup> is also reported when pyrolyzing lignin in bubbling fluidized bed reactors.

The PCR uses centrifugal forces for obtaining a high heat transfer rate. Also the PCR reactor rotor continuously moves the lignin that is fed into the reactor by the feeder. Thus the PCR may

Received: March 26, 2013

Revised: May 31, 2013

Published: June 5, 2013

provide less problems with plugging/agglomeration in the feeder compared to fluidized bed reactors. Only little information of the effects of lignin fast pyrolysis conditions with respect to temperature, gas residence time, and feed rate on product yields, monomeric phenols yields, and molecular weight distribution of bio-oil is provided by the available literature.<sup>5,6</sup> Thus the objectives of this work were to provide detailed knowledge on the lignin fast pyrolysis process and the properties of the obtained lignin bio-oil. Also, a comparison between the lignin pyrolysis and beech wood fast pyrolysis is conducted. Wood is an appropriate benchmark fuel, because there is often obtained high bio-oil yields with wood.

## 2. EXPERIMENTAL SECTION

**2.1. Experimental Apparatus.** The pyrolysis centrifuge reactor was developed at the CHEC center (Technical University of Denmark) and is described in detail elsewhere.<sup>15</sup> A sketch of the PCR is presented in Figure 1, and pictures of the reactor are shown in Figure 2. The

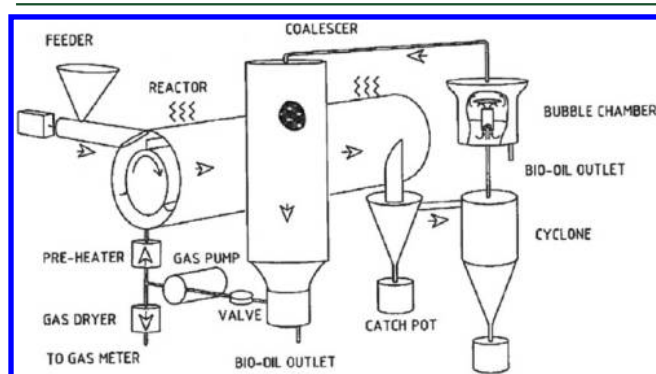


Figure 1. Sketch of the pyrolysis centrifuge reactor (PCR).

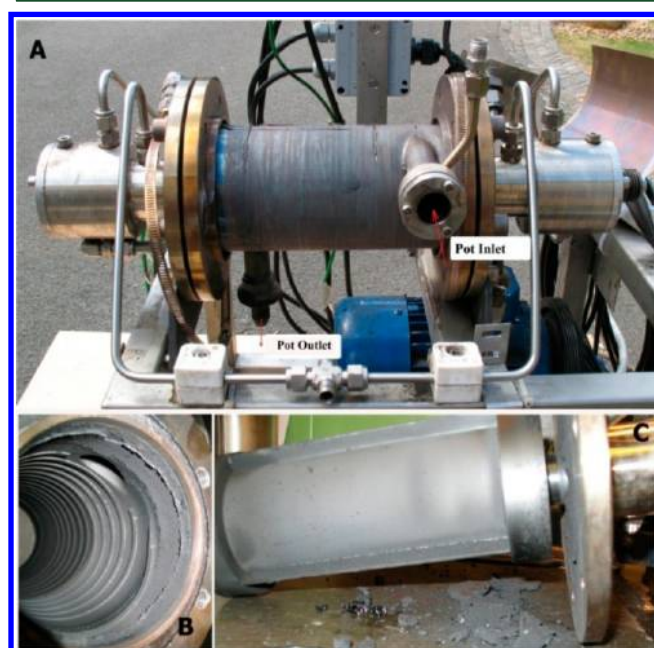


Figure 2. The reactor (A) is shown with insulation and electrical heating elements removed, reactor wall (B) and rotor (C) after few hours run with lignin pyrolysis.

centrifuge reactor is made of stainless steel and has an inner diameter of 85 mm. It is electrically heated by four independent heating zones along the reactor length. The lignin is introduced into the reactor by a screw

feeder. Pyrolysis of lignin takes place inside the reactor, whereby char, bio-oil, and gas are produced. The char particles are collected by cyclones heated to 500 °C. The bio-oil is condensed in a bubble chamber filled with isopropyl alcohol as a condensing solvent. The temperature in the bubble chamber is controlled to be 30–50 °C by means of a water cooling system. Possible ester formation reactions between isopropyl alcohol and carboxylic acids are believed to be negligible at the low temperature and in the absence of strong acid or base catalysts. The isopropyl alcohol was also used as a condensing solvent in fast pyrolysis experiments by Fonts et al.<sup>18</sup> and Trinh et al.<sup>19,20</sup> The light oil fraction and aerosols are further condensed by a coalescer filled with Rockwool. A recycled gas product is pumped back to maintain a desired reactor gas residence time (0.5–5 s). Before entering the reactor, the gas is heated to 500–550 °C. The gas products are dried by a water condenser and a gas filter to totally remove liquid before entering a gas meter.

The lignin PCR pyrolysis experiments were performed with the following operation conditions: a rotor speed of 18000 rpm, a reactor gas residence time of 0.8 s (and 4.2 s for investigation of the influence of reactor gas residence time), a total fuel feeding time of 50–62 min, a feed consumption of 204–481 g lignin for each run, and feeder rates of 4.1–10.4 g/min. The obtained mass balance closures were in the range of 93–96%.

The liquid fraction collected from the bubble chamber, coalescer, and water condenser is filtered through a Whatman filter paper (pore size of 5 μm). The char left on the filter is washed thoroughly by ethanol and then dried in an oven at 100 °C. The bio-oil yield is determined from the liquid that passed through the filter paper. The organic oil yield (db) is the bio-oil yield (db) subtracted the reaction water yield. The char yield is determined from the chars collected in the cyclones and the char left on the filter paper. The gas yield is calculated based on a gas volume determined from a gas meter and gas components compositions obtained from Gas Chromatography (GC) analyze.

**2.2. Characterization of Lignin, Bio-Oil, and Gas Products.** The applied lignin sample provided by Inbicon A/S, DONG Energy, Denmark was a dried sample of distillation residual remaining from hydrolyzed, fermented wheat straw. The wheat straw was pretreated to a severity of  $\log(R_0) = 3.70$ . The severity factor is typically expressed as a log value such that  $\log(R_0) = t \times \exp(T - T_{ref}) / 14.75$ , where  $R_0$  is the severity factor,  $t$  is the residence time in minutes,  $T$  is the temperature, and  $T_{ref}$  is the reference temperature, typically 100 °C.<sup>21</sup> The lignin has particle sizes of less than 840 μm. The properties of the lignin were measured by the following methods: the moisture content by ASTM D2216, the ash content by ASTM D1102-84, and higher heating value by a bomb calorimeter (IKA C-200). The element contents of the lignin sample were analyzed by flash combustion (Thermo Finnigan, Flash EA1112) for CHN, by ICP-OES axial for Cl and S, and by ICP-OES radial for Al, Fe, P, Si, Ca, Mg, K, and Na. The oxygen content was calculated by difference.

The biomass components of the lignin sample were analyzed following the NREL/TP-510-42618 protocol.<sup>22</sup> The biomasses were diluted in a strong acid for determination of the structural carbohydrates. The soluble aliquot was used to analyze sugars that are formed from decomposition of cellulose (glucan) and hemicelluloses (xylose, galactose, mannaose, arabinanose, and rhamnase) by a HPLC (Shimadzu Prominence - HPLC, Shimadzu Corporation, Kyoto, Japan, the refractive index detector (RID-10A)) with an Aminex HPX-87H Ion Exclusion column (Bio-Rad Laboratories, USA) (eluent 12 mM H<sub>2</sub>SO<sub>4</sub>, flow 0.6 mL/min, column temperature of 63 °C). The Klason lignin content was determined as the residue left after acid digestion.

Thermogravimetric analysis (TGA) of the lignin was carried out in the temperature range of 25–1000 °C at a constant heating rate of 10 °C/min in a N<sub>2</sub> flow using a TGA instrument (Netzsch STA 449 F1).

Noncondensable gas components (H<sub>2</sub>, CO, CO<sub>2</sub>, CH<sub>4</sub>, C<sub>2</sub>, C<sub>3</sub>) were analyzed by a GC (Agilent Technologies, 6890N, USA, 10 ft Porapak N and 14 ft 13 × Molsieve columns) using FID and TCD detection systems and He carrier gas. The gas product collected from the PCR was sent to gas chromatography to analyze within 15 min in order to minimize the hydrogen loss.

Higher heating value (HHV) of bio-oil and char were measured by a bomb calorimeter (IKA C-200), while the HHV of the gas product is calculated based on HHV of individual gas components.

The chemical components of the bio-oils were analyzed by Gas Chromatography Mass Spectrometry (GC-MS) using a Hewlett-Packard HP 6890 Gas Chromatograph interfaced to a HP5973 Mass Selective Detector (Agilent, Denmark). Samples (1  $\mu\text{L}$ ) were injected in split mode (1:20) using an HP 7683 autosampler (Agilent, Denmark). The source and rod temperatures were 230 and 150  $^{\circ}\text{C}$ , respectively. The products were separated using a 0.32 mm i.d.  $\times$  30 m WCOT fused silica column coated with VF-23 ms at a thickness of 0.25  $\mu\text{m}$  (Analytical, Denmark). The carrier gas was He at a flow rate of 1.2 mL/min. Separation of a wide range of products was achieved using a temperature program from 70 to 250  $^{\circ}\text{C}$  at 10  $^{\circ}\text{C}/\text{min}$ . The applied ionization energy was 70 eV. Full mass spectra were recorded every 0.3 s (mass range  $m/z$  40– $m/z$  450). Products were identified using NIST search engine version 2.0 f. (Agilent, Denmark). In order to identify components in the bio-oil samples, 100  $\mu\text{L}$  of bio-oil added to the 600  $\mu\text{L}$  of deuterated phenol solution then was analyzed on GC-MS. In order to quantify some of the identified components in the bio-oils, standard solutions were added to each sample, with known amounts of the compounds of interest. Standard solutions of glacial acetic acid, o-guaiacol, syringol, and p-vinylguaiacol were prepared in isopropyl alcohol. 100  $\mu\text{L}$  of bio-oils was taken, and 600  $\mu\text{L}$  of the standard solutions was mixed in. Blank samples were prepared using bio-oil and deuterated phenol solutions. Besides the compound identification, calculations were carried out to estimate the amount of organic compounds in the bio-oils, separated by GC-MS. The total peak area for all eluted compounds was calculated for each lignin sample, and the area of the added deuterated standard was subtracted (sum of peak areas). The known amount of deuterated phenol solution was responsible for the relevant deuterated phenol area, and it was compared with the sum of peaks areas. Hence an estimate could be made for the weight of the eluted organic compounds.

The molecular weight distribution of the bio-oils was analyzed by size-exclusion chromatography (SEC) using the following instrument: Viscotek GPCmax VE-2001 equipped with Viscotek TriSEC Model 302 triple detector using two PLgel mixed-D columns from Polymer Laboratories. The samples were run in THF at 30  $^{\circ}\text{C}$  (1 mL/min). The molar-mass characteristics were calculated using polystyrene standards. In order to take a representative sample for the analysis the bio-oils were diluted with ethanol to make it homogeneous and then passed through a 0.2  $\mu\text{m}$  filter.

### 3. RESULTS AND DISCUSSION

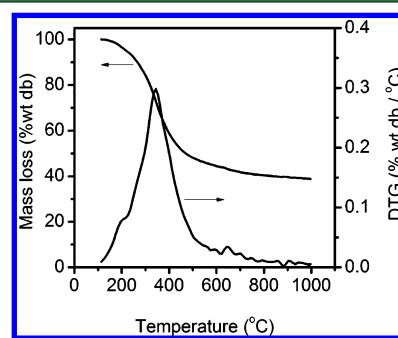
The properties of lignin were measured and can be seen in Table 1. The lignin has a volatile content of 61.2 wt % on dry basis (db) (determined at 950  $^{\circ}\text{C}$ ) and an ash content of 12.1 wt % db and a relatively low potassium content of 0.13 wt % db. The potassium content is important as it is found to influence the pyrolysis process through catalysis that increases the char formation and decreases the production of bio-oil.<sup>7,23,24</sup> The lignin was collected from a wheat straw ethanol plant, and it was thus treated and washed several times; consequently although the lignin has a high ash content, it contains a relatively low potassium content when compared to virgin wheat straw.<sup>24</sup> The lignin sample has a Klason lignin content of 78.8 wt % dry ash free basis (daf) and a higher heating value (HHV) of 22.4 MJ/kg db.

Figure 3 shows the TGA and DTG profiles of the lignin sample. The thermal decomposition appears in a temperature range of 150–550  $^{\circ}\text{C}$ . A main temperature peak at 350  $^{\circ}\text{C}$  and a shoulder at 220  $^{\circ}\text{C}$  were observed in the DTG curve. The peak and the shoulder are believed to correspond to decompositions of lignin having a content of 79 wt % daf<sup>5,6</sup> and hemicellulosic components,<sup>25</sup> respectively. The TGA and DTG of lignin results are consistent with data in the literature.<sup>5,6</sup> The TGA char yield at 550  $^{\circ}\text{C}$  is 46 wt % db.

**Table 1. Lignin Properties**

parameter	value
moisture (wt %)	4.7
volatile (wt % db)	61.2
fixed carbon (wt % db)	26.7
ash (wt % db)	12.1
HHV (MJ/kg on db)	22.4
elemental content (wt % db)	
C	57.8
H	5.7
O <sup>a</sup>	23.6
N	1.2
Cl	0.02
S	0.14
Al	0.07
Fe	0.30
P	0.06
Si	4.18
Mg	0.02
Ca	0.43
K	0.13
Na	0.28
biomass components (wt % daf)	
Klason lignin <sup>b</sup>	78.8 $\pm$ 0.23
cellulose	8.3
glucan	8.3
hemicellulose	3.6
xylose	2.7
galactose	0.7
mannose	trace
arabinose	0.2
rhamnose	trace

<sup>a</sup>By difference. <sup>b</sup>The Klason lignin content was determined as the residue left after acid digestion.



**Figure 3.** TGA and DTG profiles of lignin.

Compare with wood, lignin is generally found to be more difficult to use in a fast pyrolysis reactor.<sup>6</sup> Pluggings/agglomerations in the feeder of fluidized bed reactors are reported when pyrolyzing a pure lignin material.<sup>5,6</sup> The PCR lignin fast pyrolysis experiments were also observed to be more difficult than that of wood, straw, or algae<sup>19</sup> because of plug formation in the tubes between the reactor outlet and the condenser. A plug at the pot outlet (char pot) was observed within 10 min of the PCR operation at a pyrolysis temperature of 400  $^{\circ}\text{C}$  and a feed rate of 10.4 g/min (see the char block in Figure 4). Melting of the



Figure 4. The block at outlet pot.



Figure 5. The block at nozzle (A: bio-oil condensing system, B: nozzle in front view, C: nozzle in top view).

unconverted lignin at low temperature and consequently its agglomeration at the pot outlet probably cause the plugging. The phenomenon disappears when the reactor temperature is higher than 450 °C.

However a plugging of the nozzle connecting the cyclone and the condenser on the laboratory PCR (see Figure 5) appeared after 60–70 min operation at the runs conducted at temperatures higher than 450 °C. The deposits probably contain heavy tar and fine lignin char particles (particles with a size smaller than 10 μm that cannot be separated efficiently in the cyclones). The nozzle has a low temperature, and this may cause the plugging. Furthermore, the nozzle diameter of 4.8 mm may be too small to avoid the plug for a long PCR test. The limitations can probably be solved for longer tests of lignin pyrolysis with modifications of the nozzle and adding a hot gas filter that may remove the fine char particles.

The results of the effect of changed pyrolysis conditions with respect to temperature, reactor gas residence time, and feed rate on product yields distribution are presented in Figures 6–8. The effect of temperature on lignin pyrolysis product yields is

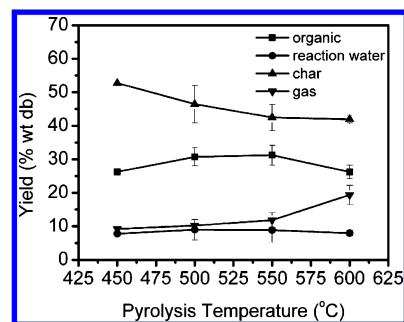


Figure 6. The effect of pyrolysis temperature at a reactor gas residence time of  $0.8 \pm 0.07$  s and a feed rate of 10.4 g/min.

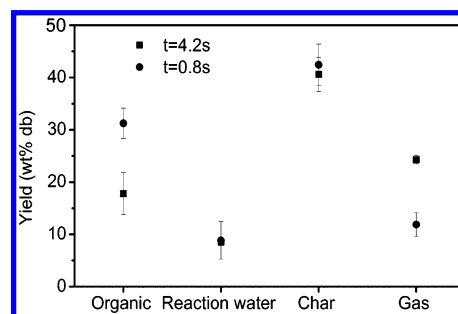


Figure 7. The effect of reactor gas residence time at temperature of 550 °C and feed rate of 10.4 g/min.

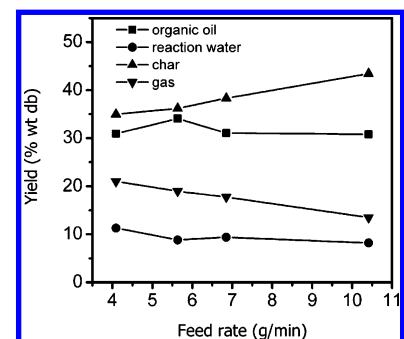


Figure 8. The effect of feed rate at reactor gas residence time of 0.8 s and temperature of 550 °C.

observed to be similar to that of wood pyrolysis.<sup>26</sup> A maximal organic oil yield of 30–31 wt % db is obtained at temperatures of 500–550 °C (see Figure 6). A decrease of the organic oil yield from 31 to 25 wt % db is observed when the temperature is increased from 550 to 600 °C. The decrease of the organic oil yield together with a large increase of the gas yield indicate that secondary reactions are important at temperatures higher than 550 °C, and the phenomena is consistent with other biomass fast pyrolysis studies.<sup>27,28</sup> A decrease of the char yield from 53 to 43 wt % db and an increase of the gas yield from 9 to 20 wt % db were obtained when increasing the temperature from 450 to 600 °C. In contrast the water reaction yield of 8 wt % db seems not to be significantly influenced by the pyrolysis temperature.

The reactor gas residence time has a large influence on the organic oil yield and gas yield (see Figure 7). The organic oil yield decreases from 31.2 to 17.8 wt % db, and the gas yield increases from 11.8 to 24.3 wt % db when the reactor gas residence time increases from 0.8 to 4.2 s. Cracking of organic vapors (secondary reactions) to generate noncondensable gases increase with a longer gas residence time,<sup>27,28</sup> and this explains the results.

**Table 2. Proximate Analysis of the Char Sample Produced at Temperature of 550 °C, Reactor Gas Residence Time of 0.8 s, and Feed Rate of 10.4 g/min**

parameter	value
volatile (wt % db) <sup>a</sup>	26.2
fixed carbon (wt % db)	46.4
ash (wt % db)	27.4

<sup>a</sup>Determined at 950 °C.

The char obtained at the temperature of 550 °C, with a reactor gas residence time of 0.8 s and a feed rate of 10.4 g/min, has a volatile content of 26.2 wt % and an ash content of 27.4 wt % (see Table 2). Because of the high char volatile content it may be possible to enhance the organic oil yield if the PCR pyrolysis conditions are optimized.

Bio-oil yield depends on feed rate, gas residence time and pyrolysis temperature.<sup>29</sup> The feed rate is often investigated to determine a maximal capacity of a reactor for bio-oil production obtaining a high yield. An increase of the feed rate at a constant temperature is known to slightly increase bio-oil yield<sup>29–31</sup> in fluidized bed reactors. An initial increase of the feed rate possibly increases the amount of gas produced at temperatures of 450–550 °C, and probably minimizes secondary reactions. However, a further increase of the feed rate will reduce the heating rate of the biomass particles, leading to a decreased bio-oil yield. In this study the feed rate is investigated in a range of 4.1–10.4 g/min. The organic oil yield obtains a maximum of 34 wt % db at a feed rate of 5.6 g/min (see Figure 8) and slightly decreases from 34 to 31 wt % db with an increasing feed rate from 5.6 to 10.4 g/min, while the gas yield decreases from 21 to 13 wt % db and the char yield increases from 35 to 43 wt % db with an increasing feed rate from 4.1 to 10.4 g/min.

At the maximal organic oil yield of 34 wt % db, a PCR char yield of 36 wt % db was obtained at a temperature of 550 °C, a reactor gas residence time of 0.8 s, and a feed rate of 5.6 g/min. The char yield is 10 wt % lower than the TGA char yield at 550 °C (46 wt % db) and 3 wt % lower than the TGA char yield at 950 °C (39 wt % db) (see Figure 3). This indicates that the lignin PCR fast pyrolysis probably obtained optimal conditions for a maximal organic oil yield.

The feedstock ash influences the pyrolysis products distribution of biomasses.<sup>8,23,32</sup> However the roles of the individual ash

components on the pyrolysis process are not well understood. Potassium has been found to considerably catalyze the pyrolysis<sup>8,23,24</sup> by decreasing the bio-oil yield and increasing the gas and char yield,<sup>8,32</sup> whereas silicate seems to be inactive to pyrolysis of biomass. The feedstock lignin content has a major influence on the product distribution.<sup>8,32</sup> The lignin component produces a low bio-oil yield and a high char yield compared to cellulose.<sup>5,6</sup> Table 3 summarizes data on feedstock ash, potassium and lignin contents, with pyrolysis product yields of wood and lignin. With a low potassium content (less than 0.12 wt % db) and a lignin content of 16–29 wt % daf, wood fast pyrolysis often provides a high bio-oil yield of 67–76 wt % daf.<sup>8–10</sup> Thus wood is considered as the best material for producing bio-oil. Lignin samples from ethanol plants and pulp and paper mills have a negligible potassium content (less than 0.13 wt % db)<sup>5,6</sup>

**Table 4. Higher Heating Value (HHV) of the Lignin Pyrolytic Products and Energetic Distribution at the Reactor Pyrolysis Temperature of 550 °C, Reactor Gas Residence Time of 0.8 s, and Feed Rate of 10.4 g/min**

pyrolysis products	HHV (MJ/kg) on dry feedstock basis	product yields (wt % dry feedstock basis)	energetic yield (%)
gas	10.6	13.1	6.3
bio-oil <sup>a</sup>	24.8	40.3	44.6
char	20.6	42.7	39.2
total	-	96.1	90.1

<sup>a</sup>A water content of 20 wt % that is reaction water.

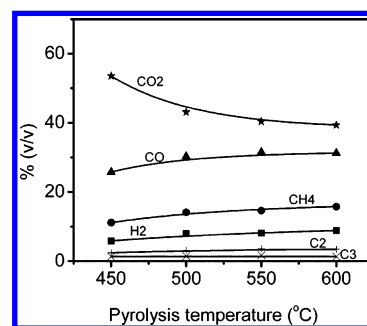


**Figure 9.** The effect of pyrolysis temperature on gas components at reactor gas residence time of 0.8 s and feed rate of 10.4 g/min.

**Table 3. Relation of the Lignin, Ash Content, and Potassium Content of Biomasses and the Pyrolytic Product Yields**

sample	lignin content (wt % daf)	ash content (wt % db)	K content (wt % db)	yield (wt % daf) <sup>a</sup>			tech <sup>b</sup> -temp	ref
				bio-oil	char	gas		
Wood								
beech	24	2.7	0.14	68	12	19	PCR, 550 °C	this study
beech	22	0.7	0.12	67	10	23	FBR, 470 °C	10
spruce	29	0.4	0.04	67	10	23	FBR, 470 °C	10
poplar aspen	16	0.4	-	76	14	11	FBR, 500 °C	9
willow	20	1.3	0.20	70	21	9	FBR, 507 °C	8
Lignin								
straw lignin	79	12	0.13	47	27	19	PCR, 550 °C	this study
alcell lignin	96	0	-	39	43	21	FBR, 500 °C	5
granit lignin	90	<2	-	48	39	15	FBR, 500 °C	5
organosolv lignin	96	0.0	-	55	36	15	FBR, 500 °C	5
organosolv lignin	95	0.1	-	52	31	17	FBR, 500 °C	5
ALM lignin <sup>c</sup>	94	1.1–1.3	0.04	31	48	6	FBR, 530 °C	6

<sup>a</sup>The bio-oil yield on daf was calculated from available data. <sup>b</sup>FBR: fluidized bed reactor, PCR: pyrolysis centrifuge reactor. <sup>c</sup>The ALM lignin manufactured by Asian Lignin Manufacturing India Pvt. Ltd. was a coproduct in the manufacture of pulp for printing and writing papers.



Table 5. GC-MS Results on % Peak Area of Bio-Oils

component <sup>a</sup>	% peak area					
	lignin oil <sup>b</sup>					wood oil
	450 °C, 0.8 s <sup>c</sup>	500 °C, 0.8 s	550 °C, 0.8 s	600 °C, 0.8 s	550 °C, 4.2 s	550 °C, 0.8 s
acids	6.76	6.02	6.15	8.33	8.55	25.88
acetic acid	6.76	6.02	6.15	8.33	8.55	25.88
nonaromatic ketones	3.01	2.66	2.55	3.42	3.74	13.3
hydroxyacetone	3.01	2.66	2.55	3.42	3.04	7.16
1,2-ethanediol, monoacetate	- <sup>d</sup>	-	-	-	-	3.93
1-(acetyloxy)-2-propanone	-	-	-	-	-	0.73
2,3-butanedione	-	-	-	-	0.70	-
2-hydroxy-3-methyl-2-cyclopenten-1-one	-	-	-	-	-	0.69
2-methyl-cyclopentanone	-	-	-	-	-	0.79
furans	4.13	5.09	1.01	0.6	1.3	8.61
furfural	1.02	1.20	0.51	-	0.74	5.16
5-methyl-furfural	2.56	2.79	-	-	-	-
furfuryl alcohol	0.55	0.50	0.50	0.60	0.56	1.35
5-hydroxymethylfurfural	-	0.60	-	-	-	0.84
γ-crotonolactone	-	-	-	-	-	1.26
glycerol	2.48	2.12	2.91	3.36	2.38	-
levoglucosan	5.60	8.04	2.55	2.49	3.76	7.10
lignin-derived phenols	1.89	1.94	2.89	7.85	3.23	0.48
phenol	1.11	0.92	1.52	2.79	1.59	0.48
2,4-dimethylphenol	-	-	-	0.70	-	-
4-methylphenol	-	-	-	3.09	-	-
p-ethylphenol	-	-	0.73	1.27	0.78	-
2,4,6-trihydroxyphenyl-2-pentanone	0.78	1.02	0.64	-	0.86	-
guaiacols	24.35	20.94	27.4	18.26	23.56	11.4
o-guaiacol	5.50	4.65	6.18	5.40	5.78	1.85
p-methylguaiacol	2.73	2.27	3.21	2.29	2.69	1.27
p-ethylguaiacol	2.07	1.77	2.95	-	2.41	0.75
p-vinylguaiacol	8.31	7.37	9.35	7.32	7.14	2.12
isoeugenol	2.08	2.05	2.29	1.47	1.85	2.48
acetoguaiacon	0.65	0.77	0.80	-	0.83	-
coniferyl alcohol	3.01	2.06	2.62	1.78	2.86	2.93
syringols	17.16	17.03	18.3	13.12	18.34	10.3
syringol	7.39	6.88	9.03	8.77	7.79	3.08
methoxyeugenol	3.77	3.83	3.57	1.19	2.89	2.50
3',5'-dimethoxyacetophenone	3.41	2.94	3.37	2.10	3.01	2.09
syringaldehyde	0.97	0.91	0.72	-	0.73	0.74
acetosyringone	1.62	2.47	1.61	1.06	3.92	1.89
methoxy benzenes	3.99	3.81	4.43	2.08	4.53	3.05
trimethoxybenzene	1.93	1.75	1.95	1.13	1.70	1.29
1,2,3-trimethoxy-5-methyl-benzene	0.56	0.78	0.80	-	0.67	-
benzenemethanol, 2,5-dimethoxy-, acetate	1.50	1.28	1.68	0.95	2.16	1.76
sterols <sup>e</sup>	6.02	5.04	6.46	4.22	5.49	0.59
stigmasterol	2.06	1.47	2.84	1.78	2.53	-
sitosterol	2.79	2.01	3.62	2.44	2.96	0.59
isofucosterol	1.17	1.56	-	-	-	-
stigmastan-3,5-diene	-	0.59	0.69	-	0.91	-

<sup>a</sup>Identified components having peak area less than 0.5% are not listed in this table. <sup>b</sup>The max molecular weight observed in this study is 400–450 g/mol (in the case of sterols). <sup>c</sup>Temperature and reactor gas residence time. <sup>d</sup>Peak <0.5%. <sup>e</sup>Sterols replied on the computer's suggestion for identification.

and high lignin contents of 79–96 wt % daf, resulting in relatively low bio-oil yields of 31–55 wt % daf for fast pyrolysis. It is seen that the lignin content has a considerable effect on the bio-oil yield.

The HHV of the pyrolysis products and the energetic distribution at the reactor pyrolysis temperature of 550 °C, reactor gas residence time of 0.8 s, and feed rate of 10.4 g/min are presented in Table 4. The HHV of the lignin oil is 24.8 MJ/kg on

wet basis (a water content of 20 wt %) or 30.7 MJ/kg db. The HHV of the lignin oil seems to be higher than that of wood oil (typical value of 22–23 MJ/kg db).<sup>8,26,32</sup> This is probably related to the low oxygen content in the lignin feedstock (24 wt % db oxygen in the lignin) when compared to wood (43–47 wt % db).<sup>8,31,32</sup> By pyrolysis of lignin, 45% of the energy content is recovered in the organic oil, 6% in the gas, and 39% in the char. A poor energy recovery of the pyrolysis products (90%) is believed

to be caused of inaccuracies in analyses (e.g., water content, heating value) and a loss of pyrolysis products (4 wt %) that is probably mainly bio-oil. About 5–10% of the feedstock energy in the form of char is often combusted to provide energy for fast pyrolysis process. Alternatively the gases can be used to supply the energy need for the process.

The effect of pyrolysis reactor temperature on gas composition is presented in Figure 9. A decrease of the CO<sub>2</sub> concentration from 54 to 39 v/v % and increase of CO from 25 to 31 v/v % is observed in the temperature range of 450–600 °C. An increasing trend of CO and a decreasing trend of CO<sub>2</sub> with increasing pyrolysis temperature are found.<sup>33</sup> H<sub>2</sub> and hydrocarbon gases are produced by cracking and dehydrogenation reactions on which the temperature has a considerable influence whereby the concentrations of H<sub>2</sub> and hydrocarbon gases increase at higher temperature. The evolution trends of gas components are consistent to other literature data.<sup>27,33</sup> The concentrations of H<sub>2</sub>, CH<sub>4</sub>, and C<sub>2</sub><sup>+</sup> of 8, 14, and 5 v/v%, respectively, at a temperature of 500–550 °C are similar to gas concentrations obtained by wood, coconut shell, and straw pyrolysis.<sup>27</sup>

The components of lignin oils produced at different pyrolysis temperatures and reactor gas residence times were analyzed by GC-MS. PCR wood oil produced at 550 °C and a reactor gas residence time of 0.8 s was also analyzed. The wood oil is considered as a reference source to compare with the lignin oils. An overall comparison of bio-oil properties from lignin, wood, straw, and macroalgae PCR pyrolysis with respect to HHV, molecular mass distribution, viscosity, pH, density, thermal behaviors, elemental concentrations, phase separation, and aging was published in another work.<sup>18</sup> The identified components of the lignin oils and wood oil are listed in Table 5. The main chemical groups of the lignin oils and wood oil are acids, nonaromatic ketones, furans, glycerol, levoglucosan, lignin-derived phenols, guaiacols, syringols, methoxy benzenes, and sterols (see Figure 10). Major peaks of acetic acid, levoglucosan,

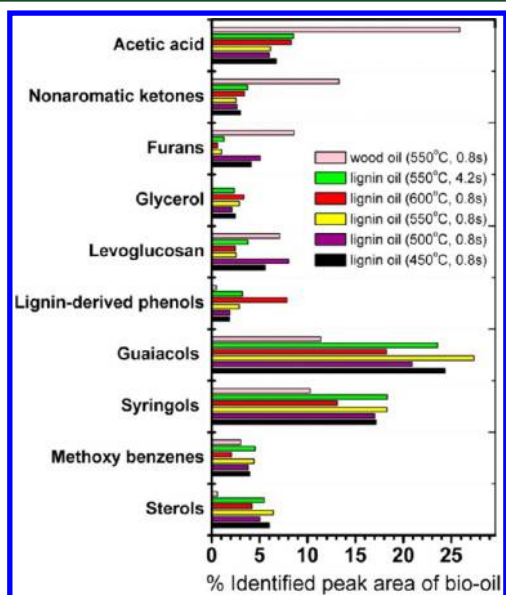


**Figure 10.** A comparison of chemical groups in the lignin oils and wood oil.

o-guaiacol, syringol and p-vinylguaiacol which have proportions of 32–40% (identified peak area) are observed in the bio-oils (see Table 5). The identified GC-MS components are estimated to account for approximately 29–38 wt % db of the bio-oil.

Levoglucosan is product of cellulose degradation,<sup>34</sup> while furans and acetic acid are found to be formed by further degradation of levoglucosan.<sup>34</sup> Phenols (guaiacols, syringols, lignin-derived phenols) are mainly believed to be formed by lignin degradations due to a difference of the lignin and cellulose contents between the wood sample (cellulose content of 40 wt % daf and lignin content of 25 wt % daf) and the lignin sample (cellulose content of 8 wt % daf and lignin content of 79 wt % daf). This may cause the large difference in the relative amount of chemical groups of the wood and lignin oils. The levoglucosan, furans, and acetic acid peak proportions obtained in the lignin oil produced at a temperature of 550 °C and a reactor gas residence time of 0.8 s are 2.6, 1.0, and 6.2%, respectively, and that are 3–10 times lower than that of the wood oil at the same pyrolysis conditions. In contrast the total amount of phenols (sum of lignin-derived phenols, guaiacols, and syringols) of the lignin oil is 48.6%, and this is 2.2 times higher than that of the wood oil. This shows that lignin fast pyrolysis is a promising method to produce phenols. The pyrolysis temperature is found to influence the produced amount of the different chemical groups (see Figure 10). The further degradation of levoglucosan probably leads to a decrease of the levoglucosan proportion and an increase of the acetic acid concentration when the temperature increases from 500 to 600 °C. Cyclization reactions and polymer polycyclic aromatic hydrocarbon formation to form larger molecular masses were found at a pyrolysis temperature range of 600–700 °C by Elliot.<sup>35</sup> These cyclization reactions probably cause a decreased proportion of methoxy benzenes, syringols, guaiacols, and furans for the 600 °C lignin oil samples when compared with the others. The effect of a reactor gas residence time change from 0.8 to 4.2 s is found to be negligible with respect to the chemical groups concentrations (except for the guaiacols group).

Four key chemical components (acetic acid, syringol, p-vinylguaiacol, and o-guaiacol) having a total peak area of 25–32% were quantified to evaluate the effect of pyrolysis temperature on the PCR lignin pyrolysis. The quantified mass yields are presented in Figure 11. The syringol, p-vinylguaiacol, and

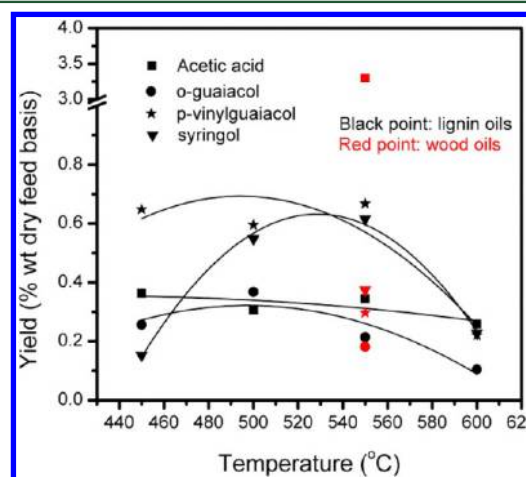


**Figure 11.** The effect of temperature on the yields of selected compounds.

o-guaiacol obtain maximal yields of 0.64, 0.76, and 0.37 wt % db, respectively, at temperatures of 500–550 °C. The acetic acid yield shows a gradual decrease from 0.42 to 0.26 wt % db when the temperature increases from 450 to 600 °C. Figure 11 also presents the acetic acid, syringol, p-vinylguaiacol, and o-guaiacol

yields of the PCR beech wood pyrolysis. As mentioned the lignin and cellulose contents have a considerable influence on phenols and acetic acid yields. Therefore, the PCR lignin pyrolysis obtains 1.7–2.5 times higher yields of the syringol, p-vinylguaiacol, and o-guaiacol and 10 times lower yield of acetic acid than those of the PCR wood pyrolysis.

The molecular weight distribution of the lignin oil samples is presented in Figure 12. The four oil samples obtained at the

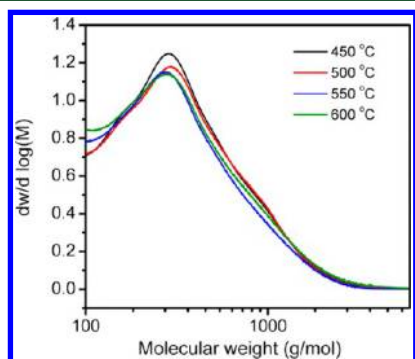


**Figure 12.** The effect of temperature on molecular weight distribution.

different pyrolysis temperatures have nearly similar molar weight profiles. The species of the lignin oils have molecular masses in the range of 100–3000 g/mol. The amount of species with low molecular weight (100–250 g/mol) increases, and the amount of the species with high molecular weight (250–3000 g/mol) decreases with an increase in the temperature from 450 to 550 °C. This indicates that derivatives of lignin which could be oligomers with molecular mass of 250–3000 g/mol appear at higher concentration at a lower pyrolysis temperature. However when the temperature raises from 550 to 600 °C the amount of high molecular weight (250–3000 g/mol) increases again. This result is consistent with the observed decrease of phenols concentration at 600 °C due to cyclization reactions and polymer polycyclic aromatic hydrocarbon reactions (600–700 °C) by Elliot.<sup>35</sup> This probably causes an increase of the high molecular fraction. As can see in Table 6, the mean molecule mass values

**Table 6.** Mean Molecular Mass of Bio-Oils at the Reactor Gas Residence Time of  $0.8 \pm 0.07$  s and Feed Rate of 10.4 g/min

parameter	variable			
temperature (°C)	450	500	550	600
mean molecular mass (g/mol)	428	420	370	429

(420–429 g/mol) of the 450, 500, and 600 °C oil samples are higher than that of the 550 °C sample (370 g/mol). These results indicate that a higher content of the lignin derivatives is observed at the lower temperatures (450–500 °C), and a higher amount of polymers/oligomers is formed at 600 °C.

#### 4. CONCLUSIONS

A residual lignin sample from an ethanol plant with a lignin content of 79 wt % daf was successfully pyrolyzed on a pyrolysis centrifuge reactor (PCR) without plugging of feeder. However, after an hour of operation plugging at the cooling nozzle was observed. The effects of pyrolysis conditions as temperature (450–600 °C), reactor gas residence time (0.9 and 4.2 s), and feed rate (4.1–10.4 g/min) on trends of product yields were similar to those of wood fast pyrolysis. The optimal pyrolysis

conditions of the lignin PCR to obtain a maximal organic oil yield is a temperature of 550 °C, a short reactor gas residence time (0.8 s), and a feed rate of 5.6 g/min. The maximal organic oil yield of 34 wt % db (bio-oil yield of 43 wt % db) is, however, much lower than that of wood fast pyrolysis.

GC-MS analysis of the lignin oil was conducted. Yields of syringol, p-vinylguaiacol, and o-guaiacol obtained maximal values of 0.62, 0.67, and 0.38 wt % db, at a pyrolysis temperature of 500–550 °C. Molecular mass distributions indicate that a higher content of the lignin derivatives is formed in the lower temperature range (450–500 °C) and formation of oligomer/polymer species takes place above 600 °C.

#### AUTHOR INFORMATION

##### Corresponding Author

\*E-mail: PAJ@kt.dtu.dk.

##### Notes

The authors declare no competing financial interest.

#### ACKNOWLEDGMENTS

Financial support of this PhD study by DONG energy A/S, Energinet.dk, and DTU is gratefully acknowledged. The authors are very grateful to Kim Chi Szabo and Ingelis Larsen from the Chemical and Biochemical Engineering Department, Technical University of Denmark who have performed some of the analyses reported in this paper.

#### REFERENCES

- (1) Mohan, D.; Pittman, J.; Mohan, D.; Steele, P. H. *Energy Fuels* **2006**, *20*, 848–889.
- (2) McCarthy, J.; Islam, A. Lignin chemistry, technology, and utilization: a brief history. In *Lignin: Historical, Biological and Materials Perspectives*; Glasser, W. G., Northey, R. A., Schultz, T. P., Eds.; ACS Symposium Series 742; American Chemical Society: Washington, DC, 2000; pp 2–100.
- (3) Gosselink, R. J. A.; de Jong, E.; Guran, B.; Abacherli, A. *Ind. Crops Prod.* **2004**, *20*, 121–129.
- (4) Baumlin, S.; Broust, F.; Bazer-Bachi, F.; Bourdeaux, T.; Herbinet, O.; Toutie Ndiaye, F.; Ferrer, M.; Lédé, J. *Int. J. Hydrogen Energy* **2006**, *31*, 2179–2192.
- (5) de Wild, P. J.; Huijgen, W. J. J.; Heeres, H. J. *J. Anal. Appl. Pyrolysis* **2012**, *93*, 95–103.
- (6) Nowakowski, D. J.; Bridgwater, A. V.; Elliott, D. C.; Meier, D.; de Wild, P. *J. Anal. Appl. Pyrolysis* **2010**, *88*, 53–72.
- (7) Li, X.; Su, L.; Wang, Y.; Yu, Y.; Wang, C.; Li, X.; Wang, Z. *Front. Environ. Sci. Eng.* **2012**, *6*, 295–303.
- (8) Fahmi, R.; Bridgwater, A. V.; Donnison, I.; Yates, N.; Jones, J. M. *Fuel* **2008**, *87*, 1230–1240.
- (9) Scott, D. S.; Plskorz, J.; Radleln, D. *Ind. Eng. Chem. Process Des. Dev.* **1985**, *24*, 581–588.
- (10) Azeez, A. M.; Meier, D.; Odermatt, J.; Willner, T. *Energy Fuels* **2010**, *24*, 2078–2085.
- (11) Hicks, C. J. *J. Phys. Chem. Lett.* **2011**, *2*, 2280–2287.
- (12) Mukkamala, S.; Wheeler, M. C.; van Heiningen, A. R. P.; DeSisto, W. *J. Energy Fuels* **2012**, *26*, 1380–1384.
- (13) Butler, E.; Devlin, G.; Meier, D.; McDonnell, K. *Renewable Sustainable Energy Rev.* **2011**, *15*, 4171–4186.
- (14) Janse, A. M. C.; Westerhout, R. W. J.; Prins, W. *Chem. Eng. Process.* **2000**, *39*, 239–252.
- (15) Bech, N.; Larsen, M. B.; Jensen, P. A.; Dam-Johansen, K. *Biomass Bioenergy* **2009**, *33*, 999–1011.
- (16) Diebold, J. P.; Scahill, J. W. Improvements in the Vortex Reactor Design. In *Developments in Thermochemical Biomass Conversion*; Bridgwater, A. V., Boocock, D. G. B., Ed.; Blackie Academic & Professional: London, 1997; p 242.

- (17) de Wild, P.; Van der Laan, R.; Kloekhorst, A.; Heeres, E. *Environ. Prog. Sustainable Energy* **2009**, *28*, 461–469.
- (18) Fonts, I.; Azuara, M.; Gea, G.; Murillo, M. B. *J. Anal. Appl. Pyrolysis* **2009**, *85*, 184–191.
- (19) Trinh, N. T.; Jensen, A. P.; Dam-Johansen, K.; Knudsen, N. O.; Sørensen, H. R.; Hvilsted, S. A. *Energy Fuels* **2013**, *27*, 1399–1409.
- (20) Trinh, N. T.; Jensen, A. P.; Dam-Johansen, K.; Knudsen, N. O.; Sørensen, H. R. *Energy Fuels* **2013**, *27*, 1419–1427.
- (21) Overend, R. P.; Chornet, E. *Philos. Trans. R. Soc., A* **1987**, *321*, 523–536.
- (22) Sluiter, A.; Hames, B.; Ruiz, R.; Scarlata, C.; Sluiter, J.; Templeton, D.; Crocker, D. *Carbohydrates and Lignin in Biomass Laboratory Analytical Procedure (LAP)*; Technical Report NREL/TP-510-42618; Issue Date: April 2008.
- (23) Abdullah, N.; Gerhauser, H. *Fuel* **2008**, *87*, 2606–2613.
- (24) Jensen, A.; Dam-Johansen, K.; Wojtowicz, M. A.; Serio, M. A. *Energy Fuels* **1998**, *12*, 929–938.
- (25) Sanchez-Silva, L.; Lopez-Gonzalez, D.; Villasenor, J.; Sanchez, P.; Valverde, J. L. *Bioresour. Technol.* **2012**, *109*, 163–172.
- (26) Bridgwater, A. V. *Biomass Bioenergy* **2012**, *38*, 68–94.
- (27) Fagbemi, L.; Khezami, L.; Capart, R. *Appl. Energy* **2001**, *69*, 293–306.
- (28) Boroson, L. M.; Howard, B. J.; Longwell, P. J.; Peters, A. W. *AIChE J.* **1989**, *35*, 120–128.
- (29) Mante, O. D.; Agblevor, F. A. *Biomass Bioenergy* **2011**, *35*, 4417–4425.
- (30) Choi, H. S.; Choi, Y. S.; Park, H. C. *Renewable Energy* **2012**, *42*, 131–135.
- (31) Park, H. J.; Park, Y. K.; Dong, J. I.; Kim, J. S.; Jeon, J. K.; Kim, S. S.; Kim, J.; Song, B.; Park, J.; Lee, K. J. *Fuel Process. Technol.* **2009**, *90*, 186–195.
- (32) Oasmaa, A.; Solantausta, Y.; Arpiainen, V.; Kuoppala, E.; Sipila, K. *Energy Fuels* **2009**, *24*, 1380–1388.
- (33) Jung, S. H.; Kang, B. S.; Kim, J. S. *J. Anal. Appl. Pyrolysis* **2008**, *82*, 240–247.
- (34) Aho, A.; Kumar, N.; Eranen, K.; Holmbom, B.; Hupa, M.; Salmi, T.; Murzin, D. Y. *Int. J. Mol. Sci.* **2008**, *9*, 1665–1675.
- (35) Elliot, D. C. *Analysis and comparison of biomass pyrolysis/gasification condensates – final report*; No. PNL-5943; Pacific Northwest Laboratory: Richland, WA, 1986.

**Appendix A5**

**Journal paper: Properties of slurries made of fast pyrolysis  
oil and char or beech wood**

**Energinet.dk project no. 010077**

**Treatment of Lignin and waste residues by flash pyrolysis**

**Trung Ngoc Trinh, Peter Arendt Jensen, Kim Dam-Johansen,  
Niels Ole Knudsen, Hanne Risbjerg Sørensen, Peter Szabo**

*Department of Chemical and Biochemical Engineering*

Technical University of Denmark

Søltofts Plads, Building 229, DK-2800 Lyngby, Denmark

**CHEC no. R1401**



ELSEVIER

Available online at [www.sciencedirect.com](http://www.sciencedirect.com)

ScienceDirect

<http://www.elsevier.com/locate/biombioe>

# Properties of slurries made of fast pyrolysis oil and char or beech wood



Trung Ngoc Trinh<sup>a,\*</sup>, Peter Arendt Jensen<sup>a</sup>, Kim Dam-Johansen<sup>a</sup>,  
Niels Ole Knudsen<sup>b</sup>, Hanne Risbjerg Sørensen<sup>b</sup>, Peter Szabo<sup>a</sup>

<sup>a</sup>Department of Chemical and Biochemical Engineering, Denmark Technical University, Søtofts Plads Bygning 229, Kgs. Lyngby 2800, Denmark

<sup>b</sup>DONG Energy, Kraftsværksvej 53, DK-7000 Fredericia, Denmark

## ARTICLE INFO

### Article history:

Received 15 April 2013

Received in revised form

28 October 2013

Accepted 20 December 2013

Available online 16 January 2014

### Keywords:

Bioslurry

Pressurized gasification

Biomass fast pyrolysis

Slurry pumping

Biomass energy densification

## ABSTRACT

The properties of slurries made of pyrolysis oil mixed with wood, char or ground char were investigated with respect to phase transitions, rheological properties, elemental compositions, and energy density. Also the pumping properties of the slurries were investigated at temperatures of 25, 40 and 60 °C and solid loadings from 0 to 20 wt%. The phase transitions of the wood slurry samples were observed at lower solid loadings compared to the char slurry samples. The apparent viscosity of the slurry samples was found to be considerably impacted by solid loading (0–20 wt%) and temperature (25–60 °C), especially in the phase transition region. The slurry viscosities with 20 wt% char loading, 20 wt% ground char loading and 15 wt% wood loading (at a shear rate of 100 s<sup>-1</sup>) are 0.7, 1.0 and 1.7 Pa.s, respectively at 60 °C and these values increases 1.2–1.4 times at 40 °C and 3–4 times at 25 °C. The wood, char and ground char slurry samples with 5–20 wt% solid loading obtain a volumetric energy density of 21–23 GJ/m<sup>3</sup>. The slurry sample with 20 wt% ground char having a  $d_{80}$  of 118 μm was pumped successfully into a pressurized chamber (0–6 bar) while plugging appeared when the slurry samples with 15 wt% char having a  $d_{80}$  of 276 μm was pumped into the pressurized chamber.

© 2013 Elsevier Ltd. All rights reserved.

## 1. Introduction

Using biomass as a feedstock for boilers and gasifiers is a considerable challenge since biomass has a low bulk density and a low energy density [1,2] that causes high transportation cost [3] and high processing cost. Besides, the energy consumption needed to grind the biomass to a suitable size for suspension boilers or entrained flow gasifiers is relatively high [4,5].

Entrained flow pressurized gasification has the capability for converting biomass to a tar free syngas with a high concentration of H<sub>2</sub> and CO (50% CO and 30% H<sub>2</sub>) [6,7], and a high fuel carbon conversion (>99%) can be obtained. However, using a

high amount of auxiliary gases in the hopper system when feeding solid fuels into a pressurized gasifier cause a reduced efficiency, high complexities, and high cost [4,7,8]. In contrast pumping of viscous slurries such as fly ash-water mixtures [9], or bio-oil-char mixtures (bioslurry) [5,6] into a high pressure reactor is known to be a simple, reliable and do not cause a large use of auxiliary gases. The use of a slurry as feedstock for a pressurized gasifier probably reduce operating costs and operating problems [4] compared to that of raw solid biomass.

Fast pyrolysis of biomass often provides bio-oil yields of 55–75 wt%, char yields of 10–20 wt% and gas yields of 10–20% wt [10]. The produced gas that contains about 10% of the biomass energy content is often proposed to be used as heat

\* Corresponding author. Tel.: +45 52687953.

E-mail addresses: [tnt@kt.dtu.dk](mailto:tnt@kt.dtu.dk), [trinhntrung@gmail.com](mailto:trinhntrung@gmail.com) (T.N. Trinh).  
0961-9534/\$ – see front matter © 2013 Elsevier Ltd. All rights reserved.  
<http://dx.doi.org/10.1016/j.biombioe.2013.12.018>

source for the fast pyrolysis process. The char and bio-oil may contain approximately 90% of the biomass heating value [5]. A bioslurry with 20% char content has a density of around  $1250 \text{ kg/m}^3$  and an energy density of about  $23 \text{ GJ/m}^3$  [11]. This is 3 times the bulk density and 4 times the energy density of that of biomass [11]. Fast pyrolysis can be considered as a densification step to supply a slurry for gasification and thereby reduce the costs of gasifier operation, as well as reducing cost for transportation and milling of the biomass. Power consumption for milling of biomass to a final average sizes from 0.2 to 0.6 mm is higher in a range of from 3 to 5 times than that of milling pyrolytic char [4]. Recently considerable efforts to make a commercial bioslurry have gained attention by several organizations [5,10]. Dynamotive has built a fast pyrolysis 200 tpd plant in Guelph (2007) for producing bioslurry (BioOil Plus) [12] as fuel for boilers, gasifiers and kiln furnaces. Karlsruhe Institute of Technology (Germany) (KIT) has installed a two-MWth fast pyrolysis plant and a five-MWth gasifier (2011) [5], for which the slurry is used as a feedstock for gasification to produce gasoline.

Some information on bioslurry properties (mixture of bio-oil and char) is provided by Abdullah et al [11] and Dahmen et al. [5]. Abdullah et al [11]. characterized slurry properties (from mallee bio-oil and its pyrolytic char) with respect to rheological properties, elemental content, static stability, and volumetric energy density with char loading from 8 to 20 wt% at 25 and 50 °C. The results demonstrated that the slurry has a non-Newtonian characteristic with pseudo-plastic behavior that has a good pumpability. The slurry properties are considerably influenced by the char loadings and the temperature. A maximum slurry viscosity of 0.5 Pa.s for a slurry with 20 wt% char loading (having  $d_{90}$  of 74  $\mu\text{m}$ ) was obtained at a temperature of 25 °C.

Although bioslurry is a promising feedstock for pressurized gasification [5,6], an overall investigation of bioslurry properties as a pressurized gasification feedstock has not been performed. Furthermore, using same wood to produce the bioslurry is also an interesting concept that could ensure that a maximum amount of slurry is made based on the amount of bio-oil that is produced. The fine char is mixed with the bio-oil and if possible residual oil is mixed with wood. However, to date, no data on bioslurry with wood is mentioned in the literature. Thus the objectives of this work are to study the behavior of bioslurry as a feedstock for pressurized gasification with respect to visually observed phase transition, elemental compositions, energy densification, rheological properties, and possibilities to pump the slurry at pressurized conditions. Slurries made by mixing pyrolysis oil with beech wood, char (from the fast pyrolysis process) and ground char were investigated and the feasibility of the feedstocks was evaluated. Furthermore, the data also provide important properties of bioslurries that also can be used as a feedstock for boilers and atmospheric gasifiers.

## 2. Experimental section

### 2.1. Materials and method

Bio-oil and char were produced from pyrolysis of Danish beech wood on a pyrolysis centrifugal reactor (PCR) at 550 °C

[13]. The yields of 69 wt% (as received) for bio-oil, 14 wt% (as received) for char and 16 wt% “as received” for gas were obtained at the applied temperature [13]. If all the char and bio-oil products were used to produce a bioslurry, the slurry would have a char concentration of 17 wt% and contain 88% energy contents of the beech wood (information on the energy recovery is presented in reference 13). The bio-oil has a water content of 25 wt% and a higher heating value (HHV) of 18.3 MJ/kg “as received”. Ground char was produced by milling of the pyrolysis char. Bioslurry samples with the wood (moisture content of 9 wt%), the char (moisture content less than 0.5 wt%) and ground char (moisture content less than 0.5 wt%) were prepared by mixing the bio-oil with the wood, char and ground char, respectively. No additional additives were used. Physical and chemical properties of the wood and chars were measured by the following methods: the ash content by ASTM D1102 – 84, the higher heating value (HHV) by a bomb calorimeter (IKA C-200), the elemental contents by flash combustion (Thermo Finnigan, Flash EA1112) for CHN, by an inductively coupled plasma–optical emission spectroscopy, (ICP-OES) axial for Cl and S, and by ICP-OES radial for Al, Fe, P, Si, Ca, Mg, K, and Na, and the oxygen content was calculated by difference. The size distribution was determined by sieve analysis using a sieve with sizes of 45–1000  $\mu\text{m}$ . Pore size distribution was measured by mercury porosimeter (mercury porosimeter pascal 140 and 440, Porotec). The macropores were measured by the pascal 140 equipment (at pressure up to 400 kPa), and mesopores and micropores were measured by the pascal 440 equipment (at pressure up to 200 MPa). Bulk density of the wood and chars were calculated by measuring the mass of solid in a certain volume. The wood, char and ground char samples were continuously poured and tapped on a 250 ml graduated cylinder until obtaining a constant volume. The samples were repeated 3 times to determine a standard deviation. The grinding of char is believed to cause no changes to the physical and chemical properties of the char (except the particle size distribution and bulk density). Thus the properties of the ground char were assumed to be similar to the char.

Physical and chemical properties of the bio-oil were measured by the following methods: water content by a Karl Fischer titration (Metrohm-701 KT titrino), the ash content by ASTM D1102 – 84, HHV by a bomb calorimeter (IKA C-200), density by density meter (Anton paar – DMA 4100), the elemental contents by flash combustion (Thermo Finnigan, Flash EA1112) for CHN, by ICP-OES axial for Cl and S, and by ICP-OES radial for Al, Fe, P, Si, Ca, Mg, K, and Na, and the oxygen content was calculated by difference.

The values of the slurry samples with respect to HHV and elemental contents were calculated based on the chars/wood and bio-oil data with relevant proportions. Bulk density of the slurry samples was calculated by measuring a mass of slurry in a certain volume. The slurry samples prepared with given solid loadings were poured into a 50 ml volumetric flask and kept immobile for an hour for sufficient soaking of bio-oil into the solid particles. The rheological properties of slurries were performed on a rheometer (TA Instruments, Advanced rheometer AR 2000 with a 6 cm parallel plate geometry) at shear rates of 5–300  $\text{s}^{-1}$  and temperatures of 25, 40 and 60 °C.

## 2.2. Experimental setup for pumping test

Pumping tests were conducted using some of the bioslurry samples. A peristaltic pump (Watson-Marlow 520S IP31) with an internal tube diameter of 9.6 mm was used. A schematic diagram of the pump test is presented in Fig. 1. The bioslurry was prepared in a slurry bottle using a given char loading. The slurries were stirred and heated to a given temperature to obtain a homogenous temperature and to keep the char particles well dispersed. A 500 ml tank was pressurized by nitrogen gas before starting the pump. Due to a limitation of the maximum pump pressure, the pressure of the tank was set at 0–6 bar. A relief valve was installed on the top of the pressurized tank to keep a constant pressure during pumping. The slurry bottle, tube and pressurized tank were heated to the investigated temperatures (25–60 °C) by electric trace heating. The bioslurry samples were pumped into the tank by the peristaltic pump within 20–25 min. A pump speed of 5 rpm was used in the tests of slurry samples with various char and ground char loadings, pressures and temperatures.

## 3. Results and discussion

### 3.1. Characterization of wood, char and ground char

Entrained flow pressurized gasification reactors are often designed for a relatively short fuel residence time in the reactor. For the bioslurry sample composed of bio-oil and solid (biomass or chars), the bio-oil easily formed tiny droplets that can obtain a high conversion when injected into the gasifier, while the solid particles are required to be of small size to obtain a good conversion [4,5]. Utilization of coal with a particle size of 50–100  $\mu\text{m}$  is required for most gasifiers [11] to obtain a good conversion. However, biomass has been found to be more reactive than coal [14–16]. Fig. 2 and Table 1 show the particle size distributions of the wood, char and ground

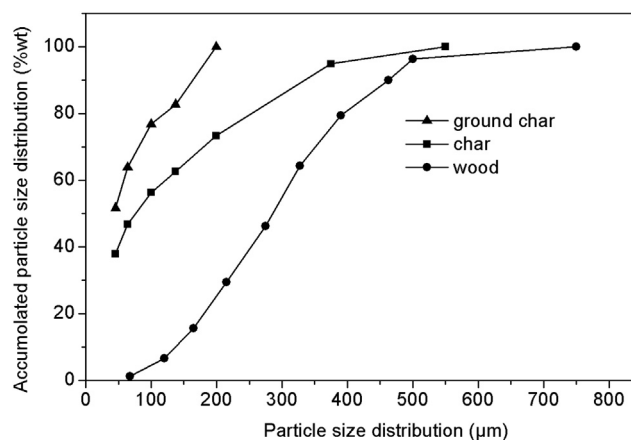


Fig. 2 – Wood and char particle size distributions.

char samples. The wood had a  $d_{50}$  of 300  $\mu\text{m}$  and  $d_{80}$  of 392  $\mu\text{m}$  which is believed to be a suitable size for entrained flow gasification [15,16] and probably also for pressurized gasification with a low pressure fluidized-bed gasifiers. The size reduction of wood to less than 400  $\mu\text{m}$  requires a significant power consumption for milling when compared to that of pyrolysis process [4]. Thus the use of wood particles with a size of less than 400  $\mu\text{m}$  is probably not feasible [4]. The wood sample with  $d_{80}$  of 392  $\mu\text{m}$  ( $d_{50}$  of 300  $\mu\text{m}$ ) (see Table 1) was used for the experiment. The char and ground char have a  $d_{80}$  of 276  $\mu\text{m}$  ( $d_{50}$  of 90  $\mu\text{m}$ ) and  $d_{80}$  of 118  $\mu\text{m}$  ( $d_{50}$  of 45  $\mu\text{m}$ ), respectively. The size of the char and the ground char are believed to be a suitable feedstock for entrained flow pressurized gasifiers using pressures up to 20–50 bar.

The pore size distributions of wood and char samples are presented in Fig. 3, both samples have a majority of macropores (pore size larger than 0.5  $\mu\text{m}$ ) and a minor amount of mesopores (pore size of 0.08–0.5  $\mu\text{m}$ ) and micropores (1.8–80 nm). The wood pores mainly appear in two ranges of

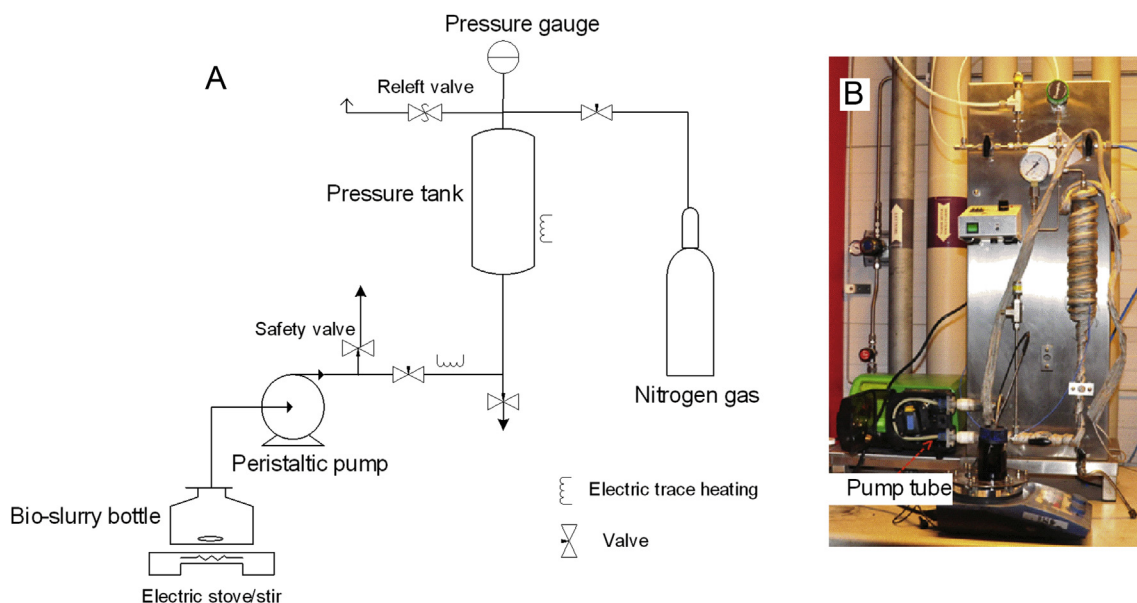


Fig. 1 – Pressurized pump setup (A: PI-diagram, B: picture).



**Table 1 – The morphological properties of the wood, char and ground char samples.**

	Wood	Char	Ground char
$d_{50}$ ( $\mu\text{m}$ )	300	90	45
$d_{80}$ ( $\mu\text{m}$ )	392	276	118
Bulk density ( $\text{kg}/\text{m}^3$ )	$267 \pm 60$	$362 \pm 38$	$342 \pm 13$

0.1–20 and 20–100  $\mu\text{m}$  while the char mainly had pore sizes in a range of 3–50  $\mu\text{m}$ . The difference was probably influenced to bio-oil absorption of the char samples and the wood sample.

### 3.2. Phase transition and rheological properties of the slurries

The bioslurry samples are stirred to obtain a homogeneous phase for the phase transition studies. Table 2 shows the phase transitions of the bioslurry samples with solid loadings in a range of 0–25 wt% that were evaluated based on visual observations. The slurry samples with char and ground char transformed from liquid to a paste phase (liquid-paste form) at the solid loadings of 15–20 wt% and become totally solid phase when the solid concentration was 25 wt% (see Fig. 4). While the wood slurry samples have the phase transition at lower solid loadings (10–15 wt% for the liquid to paste change and 15–20 wt% for the paste to solid change). The solid forms are difficult or even impossible to pump into a pressurized reactor. Thus the solid loading of 20 wt% for the char and ground char slurries and 15 wt% for the wood slurry samples were used for the rheological and pump properties investigations.

As can be seen in Fig. 5, the apparent viscosity of the slurry samples with solid loadings higher than 10 wt% for char and ground char, and 5 wt% for the wood were observed to have a non-Newtonian pseudo-plastic behavior (with a good pumpability) in the investigated shear rate range at temperatures of 25, 40 and 60 °C. The investigation of fluid behavior as function of shear rate is important with respect to pumping properties. The phase transition from liquid to paste form takes place rapidly by adding solid from 15 to 20 wt% for the char and ground char slurry samples and from 10 to 15 wt% for the wood slurry sample. The paste phase considerably enhanced the apparent viscosity at all investigated temperatures of 25, 40 and 60 °C.

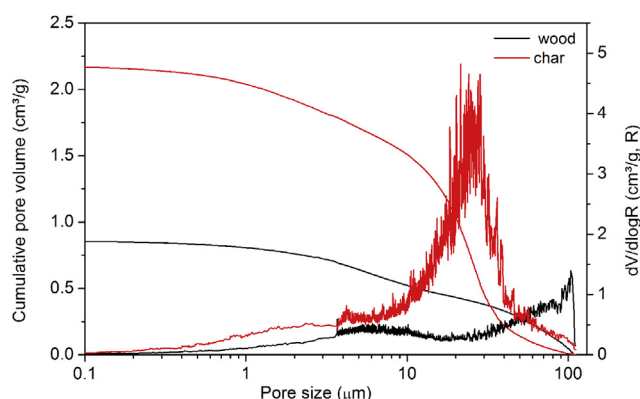
**Fig. 3 – Pore size distribution of the wood and char.**

Fig. 6 presents the effect of the temperature and solid loading of slurries on apparent viscosity at the shear rate of  $100 \text{ s}^{-1}$ . At the phase transition region (from liquid to paste form), the slurry viscosities were observed to increase 5–7 times of that of the char and ground char slurries and 10–17 times for the wood slurry. The slurry viscosities of the transition region (the slurry solid just before phase transition to a paste) at temperatures of 25, 40 and 60 °C are 2.4, 0.8 and 0.7 Pa.s for 20 wt% char loading, 3.9, 1.5 and 1.0 Pa.s for 20 wt% ground char loading, and 5.3, 2.2 and 1.7 Pa.s for 15 wt% wood loading, respectively. Increasing slurry viscosity with a decreasing temperature from 60 to 25 °C or increasing solid loading is also seen at lower solid loading levels. The rheological properties with respect to effect of char loading, temperature and apparent viscosity are consistent to those of bioslurry samples from bio-oil and pyrolysis char found by Abdullah et al. [11].

The high degree of oil absorption to the wood compared to the chars caused a rapid increase of the slurry viscosity and made the phase transition occur at a lower solid loading (15 wt% for the paste phase transition and 20 wt% for the solid phase transition). Wood was found to have more hydrophilic properties [17] and the pyrolysis char to be more hydrophobic [18], Bio-oil that is miscible to ethanol and immiscible in petroleum oil has hydrophilic properties, which probably caused the bio-oil absorption in the char to be more difficult than in the wood. Furthermore, the char has a higher amount of small pores (less than 31  $\mu\text{m}$ ) but a smaller amount of large pores (more than 31  $\mu\text{m}$ ) compared to the wood (see Fig. 3). Thus those could explain the different phase transition of the wood slurry compared to the char slurry samples. The ground char slurry has a higher viscosity than the char slurry at the same solid concentration. The phenomenon was also found by He et al [17] who investigated rheological properties of biomass-water slurries. In order to operate a pump to inject slurry into a pressurized gasifier, the slurry viscosity is expected not to be higher than a few Pa.s [1]. Thus the bioslurry samples with a solid loading of 20 wt% for the char and ground char and 15 wt% for the wood can probably be pumped into a pressurized gasifier at a temperature of 60 °C.

### 3.3. The elemental content of the bioslurries

Pressurized gasifiers are often operated at temperatures of 1200–1800 °C, thus a refractory wall (SiC material) is used to protect the reactor wall against the harsh conditions such as high temperature, corrosion and erosion in the gasifier. The refractory wall is designed to operate with a thick slag layer generated by the gasifying process and the slag layer itself reduces the heat loss from the reactor and protect the walls against high temperature. The viscosity of the slag layer is often required to be about 8–15 Pa.s and not more than 25 Pa.s to maintain a continuous movement of the slag layer into the quench zone [5,19]. Due to the high gasifier temperature, the slag is found to be rich in Ca and Si [19] while other ash forming elements are released in the gas phase. In this study the total CaO plus SiO<sub>2</sub> were 2.7 and 0.33 wt% in the bioslurry (see Fig. 7) at 20 wt% char loading and 15 wt% wood loading, respectively. Thus, in the case of the wood slurry, the amount of slag forming ash provided to a gasifier seems not to be

**Table 2 – Visible observation of phase transitions.**

Solid load (wt %)	Char loading			Ground char loading			Wood loading		
	Liquid	Paste	Solid	Liquid	Paste	Solid	Liquid	Paste	Solid
0 <sup>a</sup>	X			X			X		
5	X			X			X		
7.5	X			X			X		
10	X			X			X		
12.5	X			X			X		
15	X			X				X	
20		X <sup>b</sup>			X <sup>b</sup>				X <sup>b</sup>
25			X <sup>b</sup>			X <sup>b</sup>			X <sup>b</sup>

<sup>a</sup> Bio-oil.  
<sup>b</sup> Investigated at 25, 40 and 60 °C.

adequate to protect the gasifier walls to obtain a long service life when gasifying the bioslurry. In order to obtain a safe operation with a low Ca and Si content feedstock, additives such as silica or clay should probably be added to obtain an adequate slag layer coverage.

The slurry samples produced by mixing of 80–85 wt% of bio-oil (having a water content of 25 wt%) and 15–20 wt% char or wood provided slurries that has carbon content of 43–45 wt %, hydrogen content of 6.8–7.4 wt% and oxygen content of 44–48 wt% (see Fig. 7). Thus the wood, char and ground char slurry samples had relatively similar C, H and O contents in comparison to those of beech wood, and have low N (<0.4 wt

%), S (<0.03 wt%) and Cl (<0.1wt%) contents. If all the char and bio-oil products from the wood PCR pyrolysis are used to produce a bioslurry, the slurry will have a char concentration of 17 wt% and it has a relatively similar elemental composition to that of beech wood.

### 3.4. Energy density of the slurries

Table 3 shows the mass energy density, bulk density and volumetric energy density. The grinding of char was considered not to change the mass energy density (HHV), the HHV of the ground char is thus assumed to be the same value as that

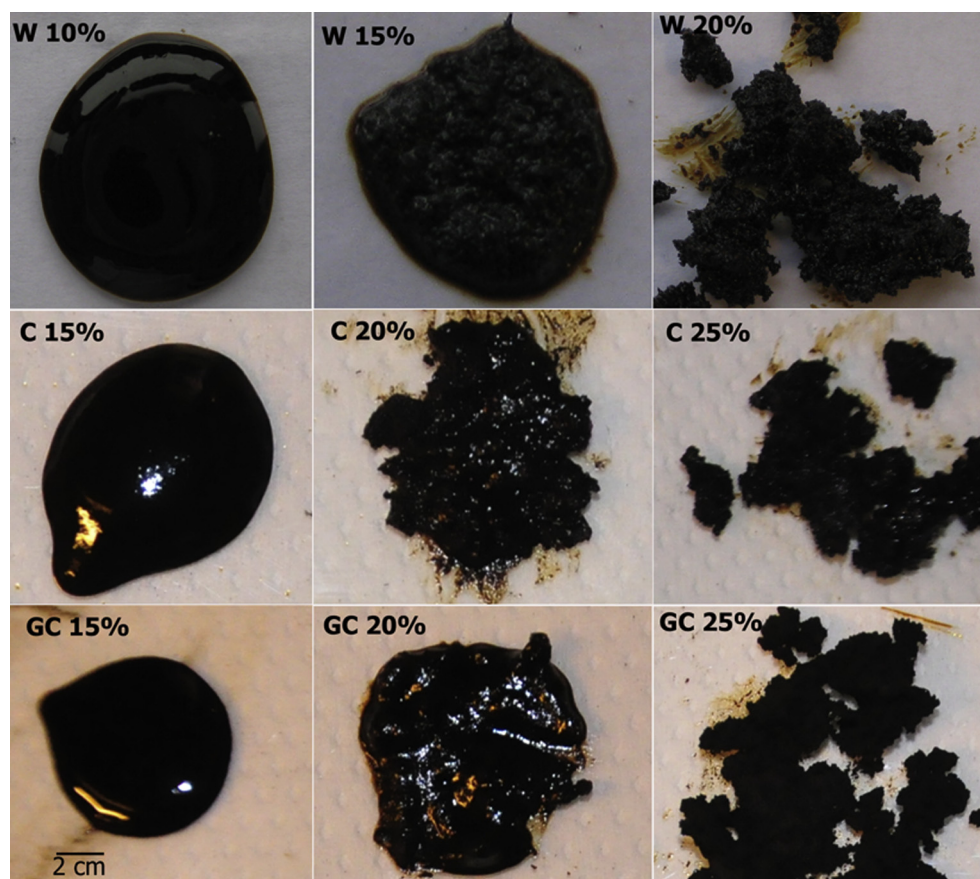


**Fig. 4 – Images of the slurries at 25 °C with different solid loading (W: wood slurry, C: char slurry, GC: ground char slurry).**

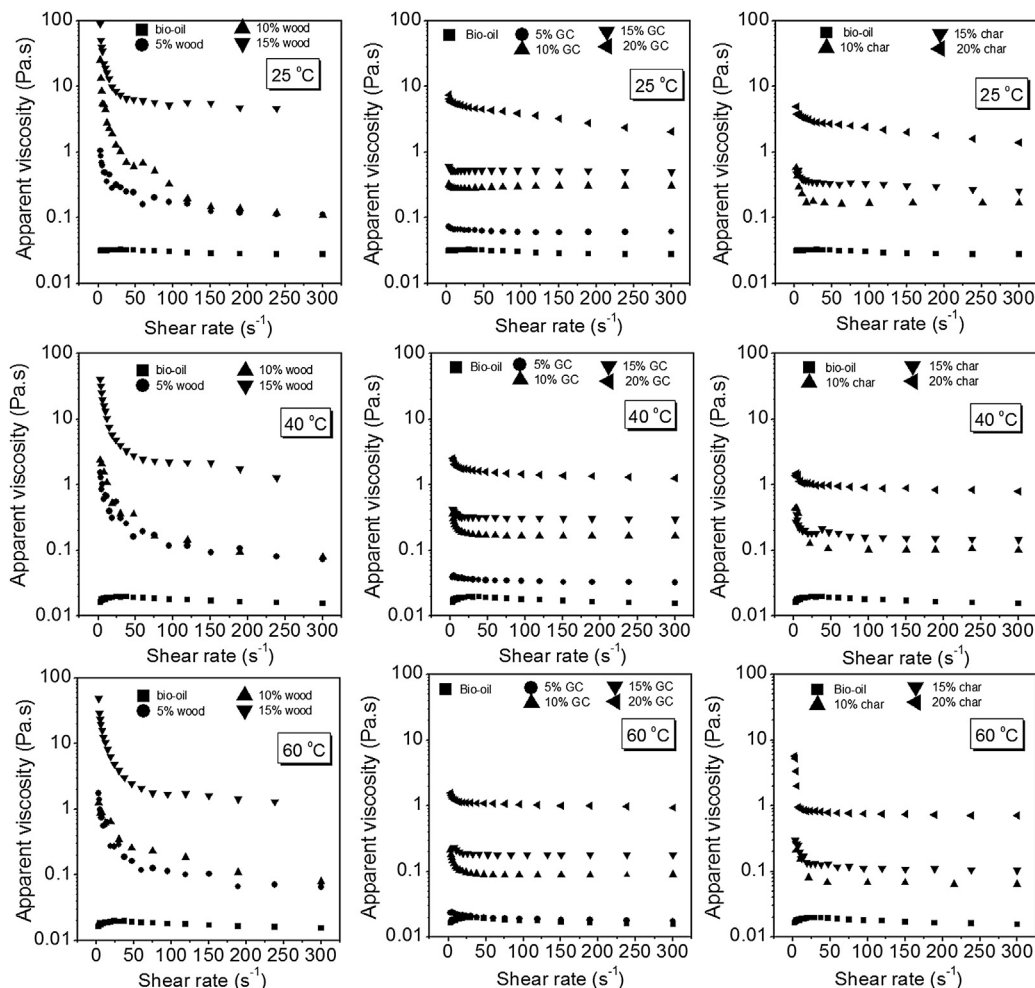


Fig. 5 – The apparent viscosity of bioslurries as a function of share rate at temperatures of 25, 40 and 60 °C (GC: ground char).

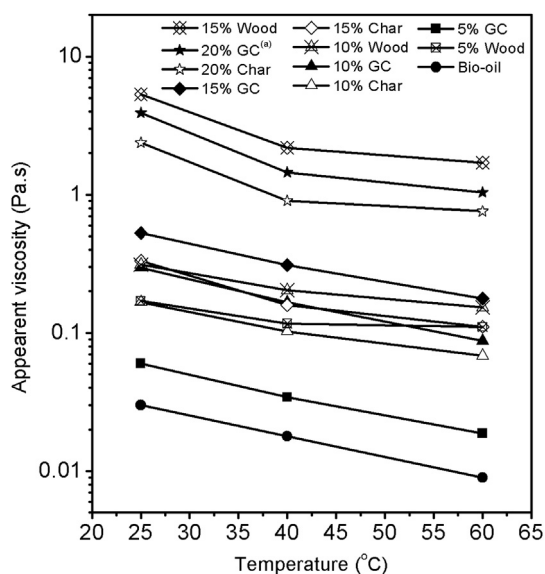


Fig. 6 – Effect of temperature and char loading on bioslurry viscosity at shear rate of  $100 \text{ s}^{-1}$  (aGround char).

of the char. The wood and chars slurry's HHVs vary in a limited range of 18.2–18.5 MJ/kg, while their bulk densities increased from 1125 to 1254  $\text{kg/m}^3$  when the solid concentrations increases from 0 to 20 wt%. The densities of the slurries increased by about 7–14% when compared to that of the bio-oil. The volumetric energy densities of the slurries with chars loading of 15–20 wt% are 21–23  $\text{GJ/m}^3$ . For a better illustration of the volumetric energy density of the slurries, the energy densification factors (EDF), were calculated as the ratios of the volumetric energy density of the slurries or chars relative to the wood and are presented in Fig. 8. Due to the low wood bulk density of 267  $\text{kg/m}^3$ , the wood has a low volumetric energy density of 4.6  $\text{GJ/m}^3$ . Consequently, the EDF of the char and wood slurries obtained a 4.5–5 fold increase. The results of the volumetric energy density and EDF of the char slurry are consistent to those reported by Abdullah et al. [11] who studied a bioslurry made from mallee pyrolysis. Biomass fast pyrolysis is, thus, a promising method to produce a high energy volume density fuel. Bioslurries have even a higher volumetric energy density than solid fuel provided by biomass torrefaction in combination with pelletizing (TOP) which produces fuels having volumetric energy densities of 11–19  $\text{GJ/m}^3$  [20].

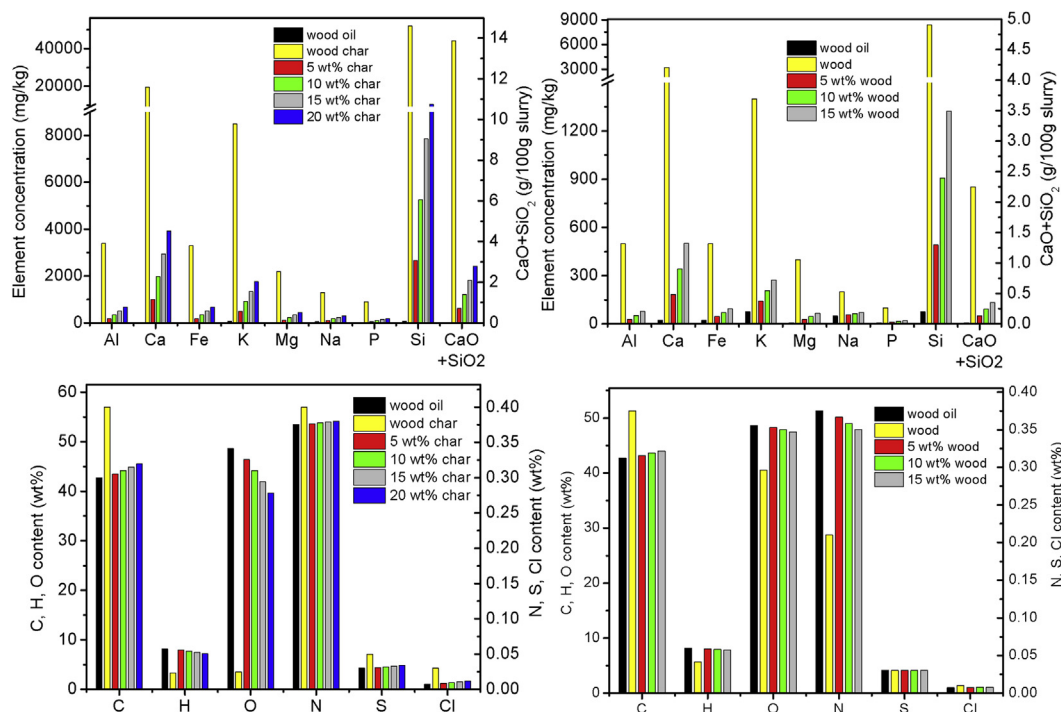


Fig. 7 – The elemental compositions of bio-oil, char, wood and bioslurry.

### 3.5. Pumping investigation of char and ground char slurries

Pumping of slurry is influenced by type and size of the applied pump. However, in this work, the slurries with char and ground char loadings from 0 to 20 wt% which corresponds to viscosity from 30 mPas to 6 Pas (at temperatures of 25–60 °C, see Fig. 6) were investigated using the peristaltic pump test rig at a speed of 5 rpm within pressure of 0–6 bar and temperatures of 25–60 °C. It may be a challenge to pump the slurries due to the high viscosity and large size of the solid particles. The results are presented in Fig. 9. The bio-oil pumping is observed not to be influenced much by the applied temperatures (25–60 °C) and pressure (0–6 bar), and flow rates of 10–11 ml/min are obtained. The pump tests of the slurry samples with 10, 15 and 20 wt% of ground char at 25 °C, and 15 wt% of ground char loading at 40 °C were conducted

successfully. The results showed that the flow rates of the slurry samples were not influenced by the char loadings from 0 to 20 wt%, the applied temperatures and pressure treatments as they demonstrated similar values as that of the bio-oil.

A pump test of the slurry sample with 10 wt% char loading at 25 °C was successful, however for a test of the slurry with a char loading of 15 wt% at temperatures of 25 and 40 °C, plugging appeared within 7 min. The plug was identified in a pump tube (having an internal tube diameter of 9.6 mm) (see Fig. 1). The viscosity of the slurry with 15 wt% char loading at 40 °C (0.16 Pa.s) is relatively similar to that of the slurry with 10 wt% ground char loading at 25 °C (0.17 Pa.s) and much lower than the slurry with a ground char loading of 15 wt% at 25 °C (0.52 Pa.s). Thus the block was probably caused by larger char particles that accumulated on the tube wall. This indicates that the char particle size is more important for the pumping

Table 3 – The mass energy density, volume energy density and bulk density of the wood, char and ground char slurry.

Solid loading (wt%)	HHV (MJ/kg “as received”)		Bulk density (kg/m <sup>3</sup> )			Volumetric energy density (GJ/m <sup>3</sup> )		
	Char/G.Char <sup>b</sup>	Wood	Char	G.Char	Wood	Char	G.Char	Wood
0 <sup>a</sup>	18.3	18.3	1125	1125	1125	20.6	20.6	20.6
5	18.4	18.3	1152	1144	1152	21.2	21.0	21.1
10	18.4	18.2	1204	1149	1201	22.2	21.1	21.9
15	18.5	18.2	1244	1160	1254	23.0	21.5	22.8
20	18.6	–	1258	1184	–	23.4	22.0	–
100%	19	17.3	362	342	267	6.9	6.5	4.6

<sup>a</sup> Bio-oil with 25 wt% water content.

<sup>b</sup> Ground char.

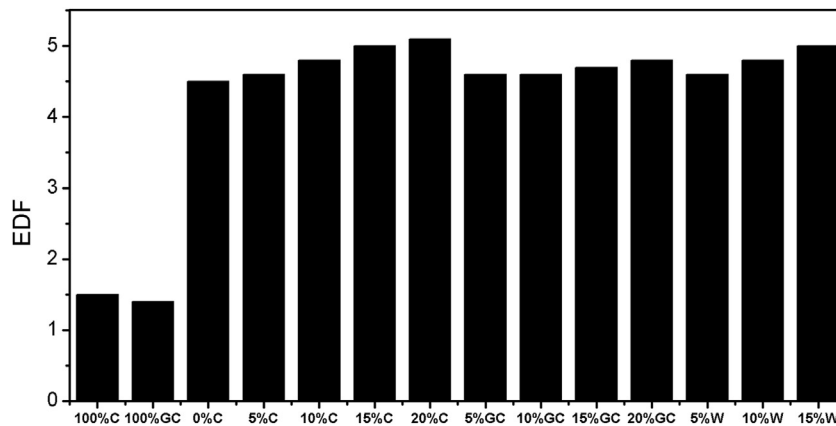


Fig. 8 – Energy densification factors of the bioslurries with various chars and wood loadings (C: char, GC: ground char, W: wood).

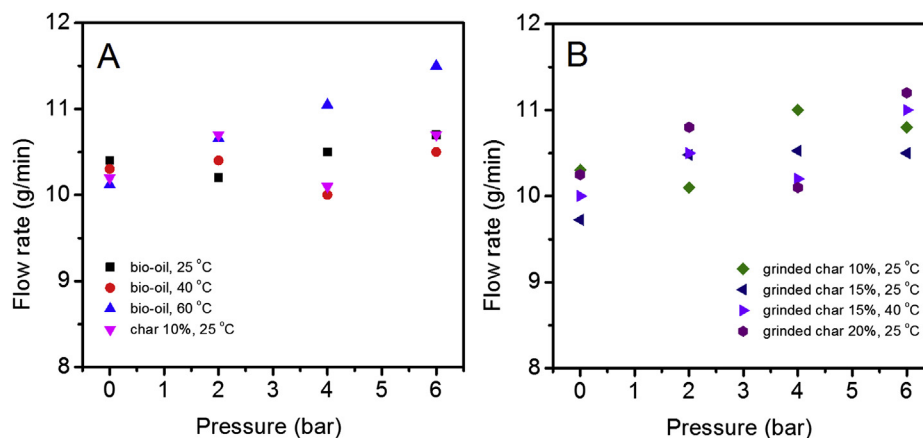


Fig. 9 – The effect of pressure of the pumping on slurry flow rate with bio-oil and char loading (A) and ground char loading (B).

properties than the slurry viscosity with char concentrations of 0–20 wt % and temperatures of 25–60 °C. Using a small particle size of less than 118  $\mu\text{m}$  ( $d_{80}$ ) is favorable with respect to pumping and this is probably also a suitable size for atomizer nozzles of gasifiers.

#### 4. Conclusions

The properties of bioslurry made of pyrolysis oil mixed with wood, char and ground char were investigated in this study. The slurries with wood, char and ground char with 5–20 wt% solid loadings obtained volumetric energy densities of 21–23  $\text{GJ}/\text{m}^3$ , consequently considerable volumetric energy densifications (4.5–5 times) were obtained when compared to beech wood. This significantly reduces transportation costs when bioslurry is transported from a biomass slurry production site to a central bioenergy plant as compared to transportation of biomass. The wood, char and ground char slurry samples had similar C, H and O contents to that of the beech

wood and had low N (<0.4 wt%), S (<0.03 wt%) and Cl (<0.1wt %) contents. The apparent viscosity of the slurry samples was found to be considerably impacted by solid loading level (0–20 wt%) and temperature (25–60 °C). A slurry sample with 20 wt% ground char loading (having a  $d_{80}$  of 118  $\mu\text{m}$ ) was pumped successfully into a pressurized chamber (0–6 bar) while plugging appeared when using a slurry sample with 15 wt% char loading (having a  $d_{80}$  of 276  $\mu\text{m}$ ). Thus, the ground char slurry might be considered as a promising feedstock for feeding by pumping into a pressurized gasifier.

#### Acknowledgment

Financial support of this PhD study by DONG energy A/S, Energinet.dk and DTU is gratefully acknowledged. The authors are very grateful to Rasmus Lundgaard Christensen and Søren Vestergaard Madsen from Chemical and Biochemical Engineering Department, Technical University of Denmark who built the pressurized pump setup.

## REFERENCES

- 
- [1] A review on biomass densification technologies for energy application. <http://www.inl.gov/technicalpublications/Documents/4886679.pdf> Cited April 2013.
- [2] Plötze M, Niemz P. Porosity and pore size distribution of different wood types as determined by mercury intrusion porosimetry. *Wood Prod* 2011;69:649–57.
- [3] Wu H, Yu Y, Yip K. Bioslurry as a fuel. 1. Viability of a bioslurry-based bioenergy Supply Chain for mallee biomass in Western Australia. *Energy Fuels* 2010;24:5652–9.
- [4] Svoboda K, Pohorely M, Hartman M, Martinec J. Pretreatment and feeding of biomass for pressurized entrained flow gasification. *Fuel Process Technol* 2009;90:629–35.
- [5] Dahmen N, Henrich E, Dinjus E, Weirich F. The bioliq bioslurry gasification process for the production of biosynfuels, organic chemicals, and energy. *Energy Sustain Soc* 2012;2:1–44.
- [6] Henrich E, Weirich F. Pressurized entrained flow gasifiers for biomass. *Environ Eng Sci* 2004;21:53–64.
- [7] Kitzler H, Pfeifer C, Hofbauer H. Pressurized gasification of woody biomass—variation of parameter. *Fuel Process Technol* 2011;92:908–14.
- [8] Wiinikka H, Carlsson P, Marklund M, Grönberg C, Pettersson E, Lidman M, et al. Experimental investigation of an industrial scale black liquor gasifier. Part 2: influence of quench operation on product gas composition. *Fuel* 2012;92:117–29.
- [9] Chandel S, Singh SN, Sehadi V. A comparative study on the performance characteristics of centrifugal and progressive cavity slurry pumps with high concentration fly ash slurries. *Part Sci Technol* 2011;29:378–96.
- [10] Bridgwater AV. Review of fast pyrolysis of biomass and product upgrading. *Biomass Bioenergy* 2012;38:68–94.
- [11] Abdullah H, Mourant D, Li C, Wu H. Bioslurry as a fuel. 3. Fuel and rheological properties of bioslurry prepared from the bio-oil and Biochar of mallee biomass fast pyrolysis. *Energy Fuels* 2010;24:5669–76.
- [12] <http://www.dynamotive.com/fuels/#industrialfuels>, Cited March 2013.
- [13] Trinh NT, Jensen PA, Dam-Johansen K, Knudsen NO, Sørensen HR, Hvilsted S. A comparison of lignin, macroalgae, wood and straw fast pyrolysis. *Energy Fuels* 2013;27:1399–409.
- [14] Gjernes E, Fjellerup J, Hansen LK, Rathmann O, Kirkegaard M, Bak J, et al. Theoretical and experimental investigation of coal and biomass combustion and gasification properties at high pressure and temperature. Final report. Roskilde, Denmark: Risø, National Laboratory; 1995. Risø-R-859 (EN).
- [15] Qin K, Jensen PA, Lin W, Jensen AD. Biomass gasification behavior in an entrained flow reactor: gas product distribution and soot formation. *Energy Fuels* 2012;26:5992–6002.
- [16] Qin K, Lin W, Jensen PA, Jensen AD. High-temperature entrained flow gasification of biomass. *Fuel* 2012;93:589–600.
- [17] He W, Park CS, Norbeck JM. Rheological study of Comingled biomass and coal slurries with hydrothermal pretreatment. *Energy Fuels* 2009;23:4763–7.
- [18] Liu Z, Zhang F, Wu J. Characterization and application of chars produced from pinewood pyrolysis and hydrothermal treatment. *Fuel* 2010;89:510–4.
- [19] Wang P, Massoudi M. Slag behavior in gasifiers Part I: influence of coal properties and gasification conditions. *Energies* 2013;6:784–806.
- [20] Maciejewska A, Veringa H, Sanders J, Peteves SD. Co-firing of biomass with coal: constraints and role of biomass pretreatment. Petten, The Netherlands: DG JRC's Institute for Energy; 2006.

**Appendix A6**

**MODEL OF LIGNIN PCR PYROLYSIS**

**Energinet.dk project no. 010077**

**Treatment of Lignin and waste residues by flash pyrolysis**

**Trung Ngoc Trinh, Peter Arendt Jensen, Kim Dam-Johansen.**

*Department of Chemical and Biochemical Engineering*

Technical University of Denmark

Søltofts Plads, Building 229, DK-2800 Lyngby, Denmark

CHEC no. R1401

## INTRODUCTION

Lignin is the second most abundant component in biomass with a typical biomass weight fraction of 15 – 33 wt%.<sup>1</sup> Lignin has a complex, amorphous cross-linked and highly branched structure and it is bio-synthesized by non-specific radical reactions using only a few aromatic building blocks such as p-Coumaryl, coniferyl, and sinapyl alcohols derivatives.<sup>2</sup> This leads to the lignin being found difficult to pyrolyse and produces a relatively low bio-oil yield (21 – 55 wt% daf)<sup>3,4</sup> compared with other biomass constituents (cellulose and hemicellulose). The product distribution of lignin fast pyrolysis depends on several factors: lignin type, ash content and pyrolysis conditions (e.g. pyrolysis temperature, heating rate, gas residence time, solid residence time).

Kinetics studies of lignin fast pyrolysis can improve our understanding of the lignin pyrolysis process and also provide information for design and reactor up scaling. The kinetic models for cellulose and wood have been studied extensively and there have been obtained a good agreement with experimental data.<sup>5-9</sup> In contrast little effort has been devoted to lignin fast pyrolysis kinetic. Most of lignin pyrolysis kinetic studies have been focused on a single step model and the kinetic parameters are fitted based on the experimental data of thermogravimetric analysis (TGA).<sup>10,11</sup> However a one step model cannot predict the bio-oil yield, the most important product of fast pyrolysis.

To establish a comprehensive model for biomass fast pyrolysis, the model shall accurately describe two main components: (1) a kinetics scheme including kinetic parameters and (2) a reactor configuration. The modified Broido-Shafizaded scheme and kinetic parameters reported by Miller and Bellan<sup>12</sup> obtain good predictions of organic oil, char and gas yields for cellulose, hemicellulose and lignin pyrolysis.<sup>5-9,12,13</sup> The biomass pyrolysis rate is considered to be the sum of the three biomass constituents.<sup>13</sup> However the influence of ash (especially alkaline acts catalyst for pyrolysis,<sup>17</sup> probably changing the kinetic parameters' values) is not adequately understood for fast pyrolysis. Therefore the simulated results for biomass with a high ash content do often obtained a poor prediction when using kinetic parameters of the pure biomass components.<sup>8</sup> The reactor configuration is extensively investigated in fluidized-bed reactor,<sup>14</sup> vortex pyrolysis reactor<sup>15</sup> and pyrolysis centrifuge reactor.<sup>8</sup> The results show that the heat transfer rate has a significant influence on the yield distribution.

Bech et al.<sup>8</sup> developed successfully a PCR model that includes the primary pyrolysis reaction, secondary reaction and particle shrinkage mechanism. With the Broido-Shafizaded scheme, parameters for cellulose represented a good fit for wood but is unsuccessful for straw due to a high ash content (6.4 wt%). The kinetic parameters probably change when there is high content of alkali metal present in the biomass. By modifying these parameters, the straw PCR model obtained an acceptable fit also for straw PCR pyrolysis.



The simulated data provided knowledge on how operation changes such as the level of centrifuge force, pyrolysis temperature, and particle temperature profile influence the yields of bio-oil, gas and char.

The objectives of this work are to investigate the use of lignin kinetic pyrolysis data in the established PCR model developed by Bech et al.<sup>8</sup> The simulated results show some of the limitations of the reactor. This provides valuable information for improving the pyrolysis centrifuge reactor.

### MODEL DESCRIPTION

A model of wood and straw PCR pyrolysis was developed by Bech et al.<sup>8</sup> to study the behavior of fast pyrolysis with respect to predicted product yields, solid particle temperature profile, and optimum of pyrolysis conditions. The model uses a Broido-Shafizadeh scheme (see Figure 7.1) and a particle shrinkage mechanism during biomass pyrolysis. The shrinking particle is converted to an activated biomass that is further degraded to gas, char and tar fractions. The degradation of biomass is assumed to be influenced only by the formation of activated biomass. The mathematical model is summarized below.

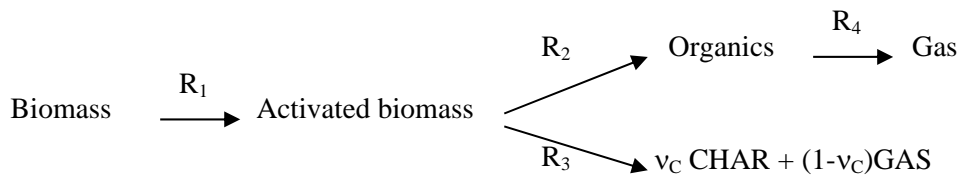


Figure 7.1: The Broido-Shafizadeh model for biomass pyrolysis<sup>5,8</sup>

The movement of the surface is expressed by the differential equation of the mass balance for a single particle:

$$\frac{d}{dr}(r^s v) + r^s r_{p,1} = 0 \quad (1)$$

Where

$v$ : the velocity of retracing surface

$r$ : the particle characteristic size

$r_{p,1}$ : the rate of reaction for the initial reaction.

By integrating the limitations of particle size and substituting the reaction rate with a Arrhenius first order reaction, the movement of the surface is given by

$$\frac{dR_{surf}(t)}{dt} = -\frac{1}{R_{surf}^s} \int_0^{R_{surf}} r^s A_1 \exp\left(\frac{-E_1}{R_g T(r)}\right) dr \quad (2)$$

Where

$R_{surf}$ : the initial characteristic size of the particle

$E_1$ : the activation energy

$A_1$ : the pre-exponential factor

$R_g$ : the gas constant

$T(r)$ : the temperature profile within the particle

The transient temperature profile of the particle is expressed with the partial differential equation

$$\rho \cdot c_p \frac{\delta T}{\delta t} = \frac{1}{r^s} \frac{\delta}{\delta r} \left( k \cdot r^s \frac{\delta T}{\delta r} \right) \quad (3)$$

Or

$$\frac{\delta T}{\delta t} = \alpha \frac{1}{r^s} \frac{\delta}{\delta r} \left( r^s \frac{\delta T}{\delta r} \right) \quad (4)$$

Where

$s$ : the shape factor

$\rho$ : the solid density

$c_p$ : the specific soil heat capacity

$k$ : thermal conductivity

$\alpha = k/\rho c_p$ : the thermal diffusivity

The initial and boundary conditions of equation (2) and (4) are:

Initial condition 1:

$$R_{surf}(t=0) = R_0$$

(5)

Initial condition 2:

$$T(t=0, r) = T_0 \quad (6)$$

Boundary condition 1:

$$k \frac{\delta T}{\delta r} \Big|_{r=R_{surf}} = h(T^\infty - T_{R_{surf}}) \quad (7)$$

Boundary condition 2:

$$\frac{\delta T}{\delta r} \Big|_{r=0} = 0 \quad (8)$$

The model was made dimensionless:

$$\frac{\delta \theta}{\delta \tau} \eta^2 = 2 \left( s + 1 + u\eta \frac{\delta \eta}{\delta \tau} \right) \frac{\delta \theta}{\delta u} + 4u \frac{\partial^2 \theta}{\partial u^2} \quad (9)$$

Initial and boundary conditions

$$\frac{\delta \theta}{\delta u} \Big|_{u=1} = \frac{1}{2} \frac{hR_{surf}}{k} (\theta^\infty - \theta|_{u=1}) = \frac{Bi(R_{surf})}{2} (\theta^\infty - \theta|_{u=1}) \quad (10)$$

Or

$$\frac{\delta \theta}{\delta u} \Big|_{u=1} = \frac{1}{2} \frac{hR_{surf}}{k} (\theta^\infty - \theta|_{u=1}) = \frac{Bi(R_o)}{2} \eta (\theta^\infty - \theta|_{u=1}) \quad (11)$$

$$\theta(t=0, r) = 0$$

(12)

Where dimensionless variables are:

$$\theta = \frac{T - T_o}{T_o^\infty - T_o} : \text{temperature.}$$

$$\tau = \frac{\alpha t}{R_o^2} : \text{time.}$$

$$x = \frac{r}{R_{surf}(t)} : \text{position within the particle, the moving surface is always located at 1 and the center of the particle is located 0}$$

$u = x^2$  : to satisfy the symmetry boundary condition at the center

$\eta = \frac{R_{surf}(t)}{R_o}$  : track the position of the surface in time

$\gamma_i = \frac{E_i}{R_g T_o}$  : activation energy

$Bi = \frac{hR_{surf}}{k}$  : Biot number

$T_o = 293$  K

$T_o^\infty$  : reactor temperature

The movement of the surface is expressed by:

$$\frac{\delta\eta}{\delta\tau} = -\frac{R_o^2 A_1}{2\alpha} \eta \int_0^1 u^{\frac{s-1}{2}} \exp\left(-\frac{\gamma_1}{\left(\frac{T_o^\infty}{T_o} - 1\right)\theta(u) + 1}\right) du \quad (13)$$

With the initial condition

$$\eta(\tau = 0) = 1$$

The heat transfer coefficient is depended on the characteristic length of the particle, centrifugal force and biomass geometry when biomass is pressed on the hot surface under a centrifugal force.<sup>8</sup> the heat transfer coefficient is expressed:

$$h = \frac{1}{59(s+1)} r\rho gG \quad (14)$$

All reactions in the Broido-Shafizadeh scheme (see Figure 7.1) are assumed to be irreversible first order with an Arrhenius type of rate expression. The gas, tar, char and biomass fractions are calculated by equations 15 - 19

$$\frac{dW_B}{dt} = -k_1 W_B$$

(15)

$$\frac{dW_A}{dt} = k_1 W_B - (k_2 + k_3) W_A$$

(16)

$$\frac{dW_O}{dt} = k_2 W_A - k_4 W_O$$

(17)

$$\frac{dW_G}{dt} = \gamma_g k_3 W_A + k_4 W_O$$

(18)

$$W_C = 1 - W_B - W_O - W_g$$

(19)

At a steady state condition, the activate biomass is assumed to be consumed immediately when formed.

Thus:

$$\frac{dW_A}{dt} = 0$$

Where

$W_O$ : organic fraction

$W_G$ : gas fraction including reaction water.

$W_B$ : biomass fraction

$W_A$ : activate biomass fraction.

$W_C$ : char fraction.

$\gamma_g$ : the gas/char selectivity of reaction 3 in Broido-Shafizadeh scheme.

$$k_i = A_i e^{\frac{-E_i}{RT}}$$

$k_i$ : reaction rate constants

$A_i$ : pre-exponential factor

$E_i$ : Activation energy

The equations from (15) to (19) are simplified and converted to be dimensionless for solving the equations. The rate of biomass consumption is also expressed based on the movement of the surface (equation 13). Thus the fractions of gas, tar, char and biomass are expressed by equations from 20 to 26:

$$\frac{\delta X_o}{\delta \tau} = -S_o \frac{\delta X_b}{\delta \tau} - B \frac{X_o}{X_o e_o^{-1} + X_g e_g^{-1}} \quad (20)$$

$$\frac{\delta X_g}{\delta \tau} = -(1 - S_o) \gamma_g \frac{\delta X_b}{\delta \tau} + B \frac{X_o}{X_o e_o^{-1} + X_g e_g^{-1}} \quad (21)$$

$$\frac{\delta X_b}{\delta \tau} = X_{b,0} (1 + s) \eta^s \frac{\delta \eta}{\delta \tau} \quad (22)$$

$$X_c = 1 - X_b - X_g - X_o \quad (23)$$

$$B = \frac{V \cdot r_{p,4} \cdot P \cdot M_b}{F \cdot R_g \cdot T \cdot \tau_\infty} \quad (24)$$

$$e_i = \frac{M_i}{M_b} \quad (25)$$

$$S_o = \frac{r_{p,2}}{r_{p,2} + r_{p,3}} \quad (26)$$

### Where

$X_o$ : organic fraction with dimensionless time  $\tau$

$X_g$ : gas fraction with dimensionless time  $\tau$

$X_b$ : biomass fraction with dimensionless time  $\tau$

$X_c$ : char fraction with dimensionless time  $\tau$

$\gamma_g$ : the gas/char selectivity of R3

$B$ : the dimensionless molar masses  $e_i$ 's and the organic selectivity  $S_o$

$r_{1-3}$ : reaction rate of Broido-Shafizadeh model.

$r_4$ : organic cracking rate.

$V$ : volume of reactor.

Mi: molar mass.

Orthogonal collocation and gauss integration were used to approximate the transient temperature profile inside particles and the surface movement while the mass fractions is performed by using a FORTRAN-based semi-implicit Runge-Kuta integration routine SIRUKE for this model. The used reactor parameters are presented in Table 7.1 and the lignin PCR code is presented in appendix 4.

Table 7.1: Reactor parameters

Parameter	Value
$V_r$ (gas volume of reactor, m <sup>3</sup> )	$5 \cdot 10^{-4}$
G (the dimensionless centrifuge reactor)	$1 \cdot 10^3$ to $30 \cdot 10^3$
$T_{p,\infty}$ (reactor temperature, °C)	450 to 650
$T_o$ (room temperature, °C)	20
t (solid residence time, s)	1.4 to 7.8
P (reactor pressure, Pa )	$10^5$

## RESULTS AND DISCUSSIONS

The lignin sample has a composition of 78.8 wt% daf for lignin, 8.3 wt% daf for cellulose, 3.6 wt% daf for hemicellulose and 9.3 wt% daf for others (see Table 7.2). Because the lignin sample has 9.3 wt% daf unidentified fraction and a small fraction of hemicellulose, the kinetic parameter of cellulose<sup>12</sup> was used to be representative for the 21 wt% daf of the lignin sample. Thus the lignin sample was represented by superposition of cellulose and lignin components with proportions of 21 and 79 wt% daf, respectively. The kinetic parameters of lignin and cellulose components for the primary reactions proposed by Miller and Bellan<sup>12</sup> and for the secondary reaction of tar proposed by Liden et al.<sup>16</sup> were used to simulate the lignin PCR pyrolysis (see Table 7.3). The simulated lignin PCR results with respect to effect of pyrolysis temperature are presented in Figure 7.2 (see set data 1). The organic oil yield obtain an acceptable fit with the experimental data. However the char and gas yields show a large deviations between modeling and experimental results. A higher gas yield and lower char yield of the simulated results are observed at the investigated temperature of 450 – 600 °C. Although this approach proved initially unsuccessfully, the simulated results suggest that the gas/char selectivity ( $\gamma_g$ ) of reaction 3 in the Broido-Shafizadeh scheme need to be modified to obtain an acceptable fit for the lignin PCR pyrolysis.

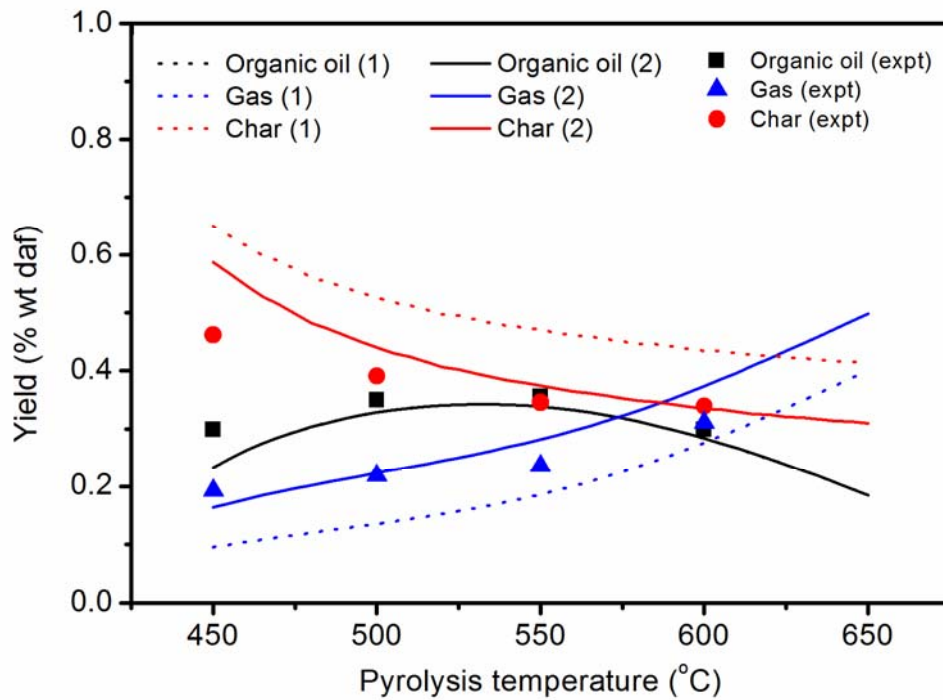


Figure 7.2: Simulated effect of temperature on the lignin PCR pyrolysis. Experimental yields (symbols) and predicted product yields (1: the yields superposed by using a compositions of 21% cellulose and 79 % lignin (using kinetic parameter shown in Table 7.3 ( $\gamma_g=0.75$ ), 2: the yields superposed by compositions of 21% cellulose and 79 % lignin (kinetic parameters in Table 7.3 with a modified  $\gamma_g$  of the lignin component ( $\gamma_g=0.55$ )).

Table 7.2: The biomass compositions

Component (wt % daf)	
Extractives	trace
Klason lignin	78.8
Cellulose	8.3
Hemicellulose	3.6
Others	9.3
Element analyses (%wt db)	
Ash	12.1
Al	0.07
Fe	0.30
P	0.06
Si	4.18
Mg	0.02
Ca	0.43
K	0.13
Na	0.28
Cl	0.02
S	0.14



By fitting  $\gamma_g$  of the lignin component (all other kinetic parameters in Table 7.3 are fixed), the yields of gas, char and organic obtained an acceptable fit with a  $\gamma_g$  change from 0.75 to the value of 0.55 (see Figure 7.2 – data set 2). Differences of less than 6 wt% daf of the product yields between simulated and experimental data (except the char yield at 450 °C) are observed at the temperature ranges of 450 – 600 °C. The differences are assumed due to loss of products (3 – 7 wt%) on the lignin PCR experiments, inaccuracies of analytic results on water content and gas components and an incomplete separation between char and organic. The much lower char yield of the experimental data at 450 °C compared to the simulated result is probably explained by a deposition of solid particle (pyrolytic char and unconverted lignin) at the cyclone and exit port of the reactor. The PCR set-up was often blocked by this deposit when experiments were carried out at low temperatures of 400 – 450 °C.

Table 7.3: Model parameters

Parameter	Value	Ref
<b>Lignin</b>		
S (particle shape 0: Slab; 1: Cylinder; 2: Sphere )	2	8
$l_{p,\infty}$ (length of the assumed path, m)	298	-
MMD (Particle mass mean diameter, m)	$361 \times 10^{-6}$	-
$\rho$ (kg/m <sup>3</sup> )	700	8
Cp (J/(kg.K))	2100	8
K (W/(mK))	0.21	8
$A_1$ (s <sup>-1</sup> )	$9.6 \times 10^8$	12
$E_1$ (kJ/mol)	107.6	12
$A_2$ (s <sup>-1</sup> )	$1.5 \times 10^9$	12
$E_2$ (kJ/mol)	143.8	12
$A_3$ (s <sup>-1</sup> )	$7.7 \times 10^6$	12
$E_3$ (kJ/mol)	111.4	12
$A_4$ (s <sup>-1</sup> )	$4.3 \times 10^6$	16
$E_4$ (kJ/mol)	108	16
$\gamma_g$	0.75	12
<b>Cellulose</b>		
S (particle shape 0: Slab; 1: Cylinder; 2: Sphere )	2	8
$l_{p,\infty}$ (length of the assumed path, m)	298	-
MMD (Particle mass mean diameter, m)	$361 \times 10^{-6}$	-
$\rho$ (kg/m <sup>3</sup> )	700	8
Cp (J/(kg.K))	2446	8
K (W/(mK))	0.13	8
$A_1$ (s <sup>-1</sup> )	$2.8 \times 10^{19}$	12
$E_1$ (kJ/mol)	242.4	12
$A_2$ (s <sup>-1</sup> )	$3.28 \times 10^{14}$	12
$E_2$ (kJ/mol)	196.5	12
$A_3$ (s <sup>-1</sup> )	$1.3 \times 10^{10}$	12
$E_3$ (kJ/mol)	150.5	12
$A_4$ (s <sup>-1</sup> )	$4.3 \times 10^6$	16
$E_4$ (kJ/mol)	108	16
$\gamma_g$	0.35	12

The ash content (especially potassium) is found to be a catalyst for pyrolysis and that promotes formation of char.<sup>17</sup> The applied lignin sample has an alkali (Na, K and Ca) content of 0.84 wt% db (see Table 7.2). This probably influences the char formation in the lignin PCR experiments. Besides, the lignin sample is a residue of a bio-ethanol plant. Its structure may differ from common lignin types (klason lignin, alcell lignin, organosolv lignins) produced from pulp and paper plants. Lignin from bio-ethanol plants shows a different pyrolysis behaviour from klason lignin, alcell lignin and organosolv lignins on the TGA at the same conditions.<sup>11</sup> Therefore, the modification of  $\gamma_g$  that is proposed for the used lignin<sup>12</sup> is probably adequate.

The established model was used to investigate the effect of centrifugal acceleration (G) on the product fractions. The simulated results are presented in Figure 7.3. An increasing G from  $2 \cdot 10^3$  to  $15 \cdot 10^3$  results in considerable changes in product fractions: a decrease of unconverted lignin fraction and increase of organic oil, pyrolytic char and gas fractions. However, the change is less important with a further increasing G. The optimal temperature for maximal organic oil fraction moves down with an increase of the G value. The organic fraction enhances from 4 to 33 wt% daf when G increases from  $2 \cdot 10^3$  to  $15 \cdot 10^3$  and obtain 39 wt% daf at the G of  $30 \cdot 10^3$ . The result suggests that a maximal organic oil yield at could be obtained to be approximately 39 wt% daf.

In order to obtain an organic oil yield above 30 wt% daf (an unconverted lignin fraction below 12 wt% daf at 550 °C) the lignin PCR pyrolysis has to operate with a G of above  $10 \cdot 10^3$ . It means that the rotor has to perform at least 14800 rpm to obtain such an organic oil yield. The heat transfer rate of the biomass is considerably influenced by the centrifugal force in the current reactor (see more detail of the reactor configuration in chapter 8), leading to the consequence that a high organic oil yield can only be obtained if a high rotor speed is used. Thereby the reactor probably has a problem which is related to a high rotor speed when it is scaled up. A new design reactor that could use both mechanical and centrifugal forces for increasing the heat transfer rate and this should be considered to obtain a high degree of organic oil yield with a low rotor speed.

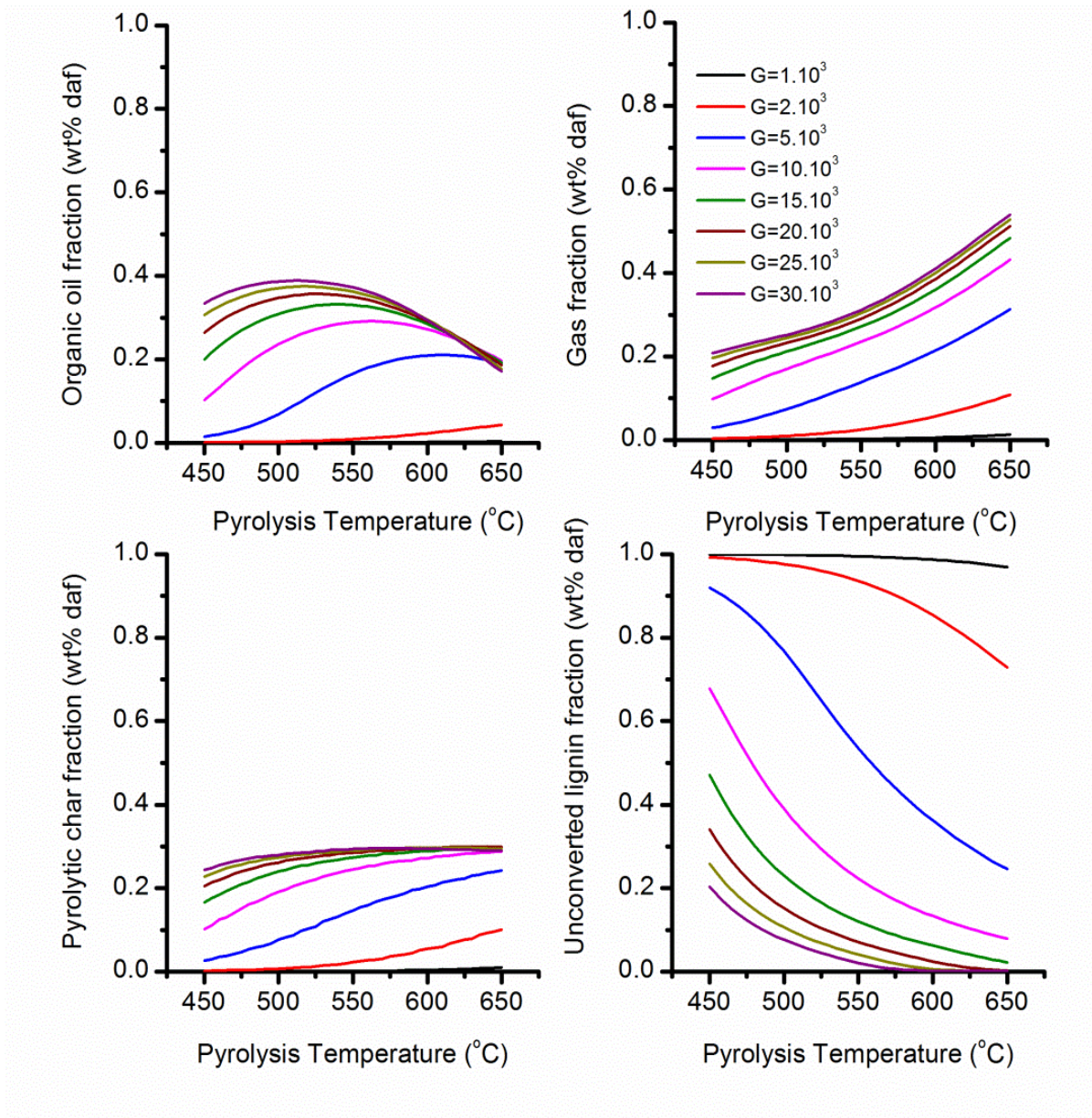


Figure 7.3: The predicted product fractions of lignin PCR pyrolysis with various centrifugal force values

## CONCLUSIONS

The Broido-Shafizadeh scheme and kinetic parameters of Miller and Bellan<sup>12</sup> are applied in a lignin PCR model developed by Bech et al.<sup>8</sup> An acceptable fit between simulated and experimental data is obtained by only modification of the ratio of gas and char selectivity ( $\gamma_g$  to be 0.55). The modification of the  $\gamma_g$  value is probably influenced by presence of alkali and by using lignin from a bio-ethanol plant. A maximum bio oil yield is obtained by using a rotational velocity and thereby a high G force.

For engineering purposes, the current reactor probably has a problem which is related to a high rotor speed when it is scaled up. Hence a new design reactor should be considered using both mechanical and centrifugal forces for increasing heat transfer rate to obtain a high degree of organic oil yield at a low rotor speed.

## 7.1 Reference

- (1) Mohan, D.; Pittman, J.; Mohan, D.; Steele, P. H. *Energy Fuels* 2006, 20, 848-889.
- (2) McCarthy, J.; Islam, A. Lignin chemistry, technology, and utilization: a brief history. In *Lignin: Historical, Biological and Materials Perspectives*; Glasser, W. G., Northey, R. A., Schultz, T. P., Eds.; ACS Symposium Series 742; American Chemical Society: Washington, DC, 2000; pp 2-100.
- (3) de Wild, P. J.; Huijgen, W. J. J.; Heeres, H. J. J. *Anal. Appl. Pyrolysis* 2012, 93, 95-103
- (4) Nowakowski, D. J.; Bridgwater, A. V.; Elliott, D. C.; Meier, D.; de Wild, P. J. *Anal. Appl. Pyrolysis* 2010, 88, 53-72
- (5) Bradbury, A. O. W.; Sakai, Y.; Shaflzadeh, F. J. *Appl. Polym. Sci.* 1979, 23, 327.
- (6) Miller RS, Bellan J. *Combust Sci Technol* 1997, 126, 97–137.
- (7) Di Blasi, C. *Chemical Engineering Science* 1996, 51, 1121–1132.
- (8) Bech, N.; Larsen, M. B.; Jensen, P. A.; Dam-Johansen, K. *Biomass and Bioenergy* 2009, 33, 999-1011.
- (9) Bruchmüller, J.; van Wachem, B. G. M.; Gu, S.; Luo, K. H.; Brown. R. C. *AIChE Journal* 2012, 58, 3030-3041
- (10) Ferdous. D.; dalai. A.K.; Bej, S.K.; Thring, R. W.; *Energy Fuel* 2002, 16, 1405-1412.
- (11) Jiang. G.; Nowakowski, D.; J.; Bridgwater. A. V. *Thermochimica Acta* 2010, 498, 61-66
- (12) Miller, R.S, Bellan J. *Combust Sci Technol* **1997**, 126, 97–137.
- (13) Di Blasi, C. *Progress in Energy and Combustion Science* **2008**, 34, 47–90.
- (14) Papadikis, K.; Gu, S.; Bridgwater, A.V. *Chemical engineering Journal* **2009**, 149, 417-427
- (15) Miller, R.S.; Bellan, J. *Engery Fuel* **1998**, 12, 25-40.
- (16) Liden. A. G.; Berruti, F.; Scott. D. S. *Chem Eng Comm* **1988**, 65, 207-221
- (17) Oasmaa A, Solantausta Y, Arpiainen V, Kuoppala E, and Sipila K. *Energy Fuels* **2010**, 24, 1380–1388

\*\*\* Appendix - Lignin PCR code \*\*\*

```

PROGRAM PCR
  IMPLICIT DOUBLE PRECISION (A-H,O-Z)
  EXTERNAL FUN,DFUN,OUT
  PARAMETER (MAX=100)
  DIMENSION DIF2(MAX),DIF3(MAX),VECA(MAX),VECB(MAX),Y(MAX),
&W(2*MAX**2+10*MAX+8),EA(4),RES(100,100)
  COMMON/VAR1/A(100,100),B(100,100),AO(4),DIF1(100),E(3),
&GAMMA(4),ROOT(100),VECINT(100),YOLD(100),NN,NS,BE,BETA,
&AK,H,G,GAMMAG,THERMDIF,YSURF,RO,RHO,TO,TINFO,TINF,XS0,
&YINF,ENDTIME,EMIS,BOLTZ,DELTA
  OPEN(11, FILE='aPART.DAT'); OPEN(21, FILE='aSIEVE.DAT')
  OPEN(31, FILE='aTEMP.DAT')

! REACTOR WALL TEMPERATURES TO INVESTIGATE
  TEMP1=450.D00          ! Min. temperature [C]
  TEMP2=650.D00          ! Max. temperature [C]
  IRUN=40                ! Step size [C]
  DTEMP=(TEMP2-TEMP1)/IRUN
! INITIATE aTEMP.DAT OUTPUT FILE
  WRITE(31,*)' FORCE  TEMP  ORG  GAS  CHAR
&STRAW'
! START TEMPERATURE LOOP
  DO JJ=0,IRUN
! REACTOR PARAMETERS
  G=17.D03                ! Nominal force on particle/gravity [-] (17004, 10071, 4927)

  TIME=1.D00*298.D00/(G*0.041*9.81D00)**0.5D00          ! Particle residence time [s](2.8, 3.3, 6.0)

  T0=20.D00+273.15D00    ! Feed initial temperature [K]
  TINFO=TEMP1+JJ*DTEMP+273.15D00    ! Reactor wall temperature [K]
  SLIT=2.5D-3            ! Average distance from rotor tip to wall [m]

  FS=12.5D00/1000/60     ! DAF Straw feed rate [kg/s]
  FG=19.D00/1000/60     ! Gas feed rate [kg/s]

  REAKT=TINFO            ! Gas temperature [K]
  REAKP=1.D5             ! Reactor pressure [Pa]

  REAKV=0.5D-3          ! Gas volume [m^3]
! PARTICLE SHAPE
  NS=2                  ! 0: Slab; 1: Cylinder; 2: Sphere
! SIEVE DATA: NUMBER OF SIEVES, MAX SIZE [M] AND WEIGHT FRACTION

  NSIEVE=16 !1

  RES(2,1)=0.D00; RES(3,1)=0.D00 !RES(2,1)=630.D-6; RES(3,1)=0.D00
  RES(2,2)=106.D-6; RES(3,2)=14.0D-2 !RES(2,2)=RES(2,1); RES(3,2)=100.D-2    ! STRUCTURE OF RES:

  RES(2,3)=125.D-6; RES(3,3)=10.0D-2    ! 1  2  3  4  5  6  7
  RES(2,4)=150.D-6; RES(3,4)=3.5D-2    !SIEVE#  MAX_SIZE  FRACTION  ORG_YIELD  GAS_YIELD  CHAR_YIELD
STRAW_YIELD
  RES(2,5)=180.D-6; RES(3,5)=0.1D-2    !1

```

```

RES(2,6)=212.D-6; RES(3,6)=8.3D-2    !2
RES(2,7)=250.D-6; RES(3,7)=10.8D-2  !3
RES(2,8)=300.D-6; RES(3,8)=7.3D-2   !..
RES(2,9)=355.D-6; RES(3,9)=3.7D-2   !NSIEVE+1
RES(2,10)=425.D-6; RES(3,10)=12.1D-2 !NSIEVE+2 RESULT FOR FEED ORG_YIELD GAS_YIELD CHAR_YIELD
STRAW_YIELD
RES(2,11)=500.D-6; RES(3,11)=0.1D-2
RES(2,12)=600.D-6; RES(3,12)=24.3D-2
RES(2,13)=710.D-6; RES(3,13)=0.1D-2
RES(2,14)=850.D-6; RES(3,14)=3.6D-2
RES(2,15)=1000.D-6; RES(3,15)=2.1D-2
RES(2,16)=1180.D-6; RES(3,16)=0.1D-2
RES(2,17)=1400.D-6; RES(3,17)=0.1D-2
! CHECK SIEVE INPUT
SUM=0.D00
DO I=1,NSIEVE+1
  RES(1,I)=I-1
  SUM=SUM+RES(3,I)
ENDDO
SUM=((SUM-1)**2)**0.5
IF (SUM.GT.1.D-2) THEN
  WRITE(*,*)' SIGTEANALYSE SUMMER IKKE TIL 100 !'
  GOTO 300
ENDIF
! INITIATE aSIEVE.DAT OUTPUT FILE
WRITE(21,*)
WRITE(21,5)G,T0-273.15,TINFO-273.15,TIME,FS*3600,FG*3600
5  FORMAT(F10.0,'G',F10.0,'C',F10.0,'C',F10.1,'S',F10.1,'Kg/h',
& F10.1,'Kg/h')
WRITE(21,*)'FRAC  DMIN  DMAX  DAV FRACTION  O
&RG  GAS  CHAR  STRAW'
! START FRACTION LOOP
DO II=2,NSIEVE+1
! COLLOCATION PARAMETER
  N=5                ! Number of interior collocation point
  NN=N
  IF(N+8.GT.MAX) THEN
    WRITE(*,*)' N STØRRE END MAX !'
    GOTO 300
  ENDIF
  ALFA=0.D00
  BETA=(REAL(NS)-1.D00)/2.D00
  N0=0
  N1=1

! KINETIC DATA: PRE EXPONENTIAL FACTORS [1/S] AND ACTIVATION ENERGIES [J/MOL]
  A0(1)=9.6D8; EA(1)=107.6D3    ! R1 Activation: Biomass(s) -> ILC(l)
  A0(2)=1.5D9; EA(2)=143.8D3    ! R2 Organics formation: ILC(l) -> Organics(g)
  A0(3)=7.7D6; EA(3)=111.4D3    ! R3 Char and gas formation: ILC(l) -> (1-GammaG)Char(s) +
(GammaG)Gas(g)
  A0(4)=4.3D6; EA(4)=108D3      ! R4 Organics Cracking: Organics(g) -> Gas(g)
  GAMMAG=0.25D00                ! Gas selectivity in R3 [-]

! CONVERT TO DIMENSIONLESS ACTIVATION ENERGIES
DO J=1,4

```

```

      GAMMA(J)=EA(J)/8.314D00/T0
      ENDDO
! INITIAL DISTANCE TO CENTER [M] AND DIMENSIONLESS SLIT [M]
      R0=(RES(2,II-1)+RES(2,II))/2.D00/2.D00
      DELTA=SLIT/R0
! PHYSICAL PARAMTERES FOR PARTICLE
      AK=0.21D00          ! Conductivity [W m-1 K-1]
      CP=2100.D00        ! Specific Heat Capacity [j/kg/K]
      RHO=700.D00        ! True Density [kg/m3]
      EMIS=0.0D00
      BOLTZ=5.76D-8      ! Boltzmann Constant [m2kg/s2/K]
      THERMDIF=AK/CP/RHO ! Thermal Diffusivity [m2/s]
      YSURF=100.DO      ! Initial surface temperature [K]
! MOLECULAR MASSES AND GAS CONSTANT
      R=8.314D00        ! Gas constant [J/K/mol]
      STRAW=5000.D-3    ! Straw molecular mass [kg/mol]
      TAR=530.D-3      ! Tar molecular mass [kg/mol]
      GAS=35.D-3       ! Gas molecular mass [kg/mol]
! DIMENSIONLESS MOLECULAR WEIGHTS AND DIMENSIONLESS RESIDENCE TIME
      E(1)=1.D00
      E(2)=TAR/STRAW
      E(3)=GAS/STRAW
      TAUM=THERMDIF*TIME/R0**2
! TAR CRACKING CONSTANT
      TCRR=A0(4)*DEXP(-EA(4)/R/REAKT)
      BE=REAKV*TCRR*REAKP*STRAW/(FS+FG)/TAUM/R/REAKT
! DETERMINATION OF ROOTS IN ORTHOGONAL POLYNOMIALS DISCRETIZATION
      CALL JCOBI(MAX,N,N0,N1,ALFA,BETA,DIF1,DIF2,DIF3,ROOT)
! PREPARATION OF DISCRETIZATION MATRICES
      DO J=1,N+1
        CALL DFOPR(MAX,N,N0,N1,J,1,DIF1,DIF2,DIF3,ROOT,VECA)
        CALL DFOPR(MAX,N,N0,N1,J,2,DIF1,DIF2,DIF3,ROOT,VECB)
        DO I=1,N+1
          A(J,I)=VECA(I)
          B(J,I)=VECB(I)
        ENDDO
      ENDDO
! GAUSS INTEGRATION WEIGHTS FOR RATE EXPRESSION
      CALL DFOPR(MAX,N,0,1,N,3,DIF1,DIF2,DIF3,ROOT,VECINT)
! INTEGRATION PARAMETERS FOR SIRUKE
      DO J=1,N+8
        W(J)=1.D00
      ENDDO
      W(N+1+8)=0.D00
      W(N+2+8)=TAUM      ! ENDTIME
      W(N+3+8)=1.D-20   ! INITIAL STEP
      W(N+4+8)=1.D-4    ! TOLERANCE
      W(N+5+8)=-(N+5+4) ! NUMBER OF ALGEBRAIC EQ
      NPR=-20          ! -(PRINT FREQUENCY)
!!INITIAL CONDITIONS
      DO J=1,N
        Y(J)=0.D00
      ENDDO
      Y(N+1)=1.D00      ! DIMENSIONLESS POSITION OF SURFACE - ETA
      Y(N+2)=0.D00     ! DIMENSIONLESS TIME - TAU

```





```

40  FORMAT(' -',3F10.0,5F10.4)
! WRITE COMBINED FEED RESULT TO aTEMP.DAT
  WRITE(31,50)G,TINFO-273.15,RES(4,NSIEVE+2),RES(5,NSIEVE+2),
  & RES(6,NSIEVE+2),RES(7,NSIEVE+2)
50  FORMAT(2F10.0,4F10.4)
  ENDDO
300 CLOSE(11)
    CLOSE(21)
    CLOSE(31)
  END

!*****  FUN  *****
! DIFFERENTIAL EQUATIONS          *
! Y(1), Y(2)..Y(NN) DIMENSIONLESS TEMPERATURE IN INTERIOR *
! Y(NN+1) DIMENSIONLESS POSITION OF SURFACE - ETA *
! Y(NN+2) DIMENSIONLESS TIME - TAU *
! Y(NN+3) DIMENSIONLESS TAR FRACTION *
! Y(NN+4) DIMENSIONLESS GAS FRACTION *
! ALGEBRAIC EQUATIONS            *
! Y(NN+5) BIOT NUMBER - BI *
! Y(NN+6) THIELE MODULUS - THIEL *
! Y(NN+7) SCALING FACTOR - SF *
! Y(NN+8) DIMENSIONLESS CHAR FRACTION *
!*****

  SUBROUTINE FUN(N,Y,F)
    IMPLICIT DOUBLE PRECISION (A-H,O-Z)
    COMMON/VAR1/A(100,100),B(100,100),AO(4),DIF1(100),E(3),
    &GAMMA(4),ROOT(100),VECINT(100),YOLD(100),NN,NS,BE,BETA,
    &AK,H,G,GAMMAG,THERMDIF,YSURF,RO,RHO,TO,TINFO,TINF,XS0,
    &YINF,ENDTIME,EMIS,BOLTZ,DELTA
    DIMENSION Y(*),F(*)

! CALCULATE NEW EFFECTIVE FORCE ON PARTICLE
  GEF=(Y(NN+1)/DELTA)**(1.D00/3.D00)*G
! CALCULATE NEW SOLID CONVECTIVE AND RADIATIVE HEAT TRANSFER COEFFICIENTS
  HCONV=1.D00*1.D00/(NS+1)*0.017D00*R0*Y(NN+1)*RHO*9.81D00*GEF
  HRAD=EMIS*BOLTZ*(TINFO**2.D00+(YSURF*(TINFO-T0)+T0)**2.D00)*
  &(TINFO+(YSURF*(TINFO-T0)+T0))
! OVERALL HEAT TRANSFER COEFFICIENT
  H=HCONV+HRAD
! CALCULATE NEW BIOT-NUMBER
  Y(NN+5)=H*R0*Y(NN+1)/AK
! CALCULATE NEW SURROUNDING TEMPERATURE
  YINF=1.D00
! SKIP PARTICLE TEMPERATURE AND SIZE CALCULATION IF PARTICLE HAS "DISSAPEARED"
  IF (R0*Y(NN+1).LT.5.D-6) THEN
    DO I=1,NN+1
      F(I)=0
    ENDDO

  ELSE

! (WITHIN ELSE STATEMENT)CHANGE IN DIMENSIONLESS POSITION OF SURFACE - GAUSS INTEGRATION
  SUM=0.D00
  DO I=1,NN

```

```

    REAC=DEXP(-GAMMA(1)/((TINFO/T0-1.D00)*Y(I)+1.D00))
    SUM=SUM+2.D00/(REAL(NS)+1.D00)*VECINT(I)*REAC
ENDDO
    REAC=DEXP(-GAMMA(1)/((TINFO/T0-1.D00)*YSURF+1.D00))
    SUM=SUM+2.D00/(REAL(NS)+1.D00)*VECINT(NN+1)*REAC ! DETTE LED GIVER IKKE NOGET DA VECINT(NN+1)=0
    F(NN+1)=-0.5D00*R0**2*Y(NN+1)*A0(1)/THERMDIF*SUM
! (WITHIN ELSE STATEMENT) DETERMINATION OF NEW SURFACE TEMPERATURE
    SUM1=0.D00
    DO I=1,NN
        SUM1=SUM1+A(NN+1,I)*Y(I)
    ENDDO
    YSURF=(YINF*Y(NN+5)/2.D00-SUM1)/(A(NN+1,NN+1)+Y(NN+5)/2.D00)
! (WITHIN ELSE STATEMENT) RIGHT-HAND SIDE OF DIFFERENTIAL EQUATIONS
    DO J=1,NN
        SUM1=0.D00
        SUM2=0.D00
        DO I=1,NN
            SUM1=SUM1+A(J,I)*Y(I)
            SUM2=SUM2+B(J,I)*Y(I)
        ENDDO
        F(J)=1.D00/(Y(NN+1))**2*((2.D00*(NS+1+ROOT(J))*Y(NN+1)*
        &F(NN+1))*SUM1+A(J,NN+1)*YSURF)+4.D00*ROOT(J)*(SUM2+
        &B(J,NN+1)*YSURF)
    ENDDO
! END OF ELSE STATEMENT
ENDIF

! DIFFERENTIAL EQs FOR TAR AND GAS FRACTION
    TSURF=YSURF*(TINFO-T0)+T0
    ST=A0(2)*DEXP(-GAMMA(2)*T0/TSURF)/(A0(2)*DEXP(-GAMMA(2)*
    &T0/TSURF)+A0(3)*DEXP(-GAMMA(3)*T0/TSURF))
    REAC=BE*Y(NN+3)/(Y(NN+3)/E(2)+Y(NN+4)/E(3))
    F(NN+3)=-ST*XSO*(NS+1)*Y(NN+1)**NS*F(NN+1)-REAC
    F(NN+4)=-1.D00-ST)*GAMMAG*XSO*(NS+1)*Y(NN+1)**NS*
    &F(NN+1)+REAC
! CHAR FRACTION
    Y(NN+8)=1.D00-Y(NN+3)-Y(NN+4)-XSO*Y(NN+1)**(NS+1)
! CALCULATION OF THIELE MODULUS
    Y(NN+6)=-F(NN+1)*Y(NN+1)
! CALCULATION OF SCALING FACTOR FOR OUTPUT FILE
    Y(NN+7)=Y(NN+1)/YOLD(NN+1)
! CHANGE IN DIMENSIONLESS TIME
    F(NN+2)=1.D00
! SAVE RESULTS TO COMPUTE DELTA VALUES
    DO J=1,NN+8
        YOLD(J)=Y(J)
    ENDDO
    RETURN
    END
!*****
!*** DFUN ***
!*****
    SUBROUTINE DFUN(N,Y,DF)
    IMPLICIT DOUBLE PRECISION (A-H,O-Z)
    COMMON/VAR1/A(100,100),B(100,100),A0(4),DIF1(100),E(3),

```

```

&GAMMA(4),ROOT(100),VECINT(100),YOLD(100),NN,NS,BE,BETA,
&AK,H,G,GAMMAG,THERMDIF,YSURF,RO,RHO,TO,TINFO,TINF,XSO,
&YINF,ENDTIME,EMIS,BOLTZ,DELTA
DIMENSION Y(*),DF(N,*)
RETURN
END
!*****
!*** OUT ***
!*****
SUBROUTINE OUT(N,X,Y)
IMPLICIT DOUBLE PRECISION (A-H,O-Z)
COMMON/VAR1/A(100,100),B(100,100),A0(4),DIF1(100),E(3),
&GAMMA(4),ROOT(100),VECINT(100),YOLD(100),NN,NS,BE,BETA,
&AK,H,G,GAMMAG,THERMDIF,YSURF,RO,RHO,TO,TINFO,TINF,XSO,
&YINF,ENDTIME,EMIS,BOLTZ,DELTA
DIMENSION Y(*),X(*)
! WRITE TO SCREEN FOR PROGRAM CONTROL
WRITE(*,1) 1000*RO**2*Y(NN+2)/THERMDIF,Y(NN+3),Y(NN+4),
&Y(NN+8),XSO*Y(NN+1)**(NS+1)
! WRITE TO FILE
WRITE(11,17) Y(NN+2),1000*RO**2*Y(NN+2)/THERMDIF,
&1000*RO*Y(NN+1),Y(NN+7),Y(NN+1),1.D00-Y(NN+1)**(NS+1),H,
&Y(NN+3),Y(NN+4),Y(NN+8),Y(NN+5),Y(NN+6),(Y(I),I=1,NN),YSURF
1  FORMAT(F10.0,10X,2F10.2,2F10.2)
17  FORMAT(F10.5,F10.0,4F10.4,F10.0,3F8.2,F13.4,F8.2,80F10.4)
RETURN
END

```

February, 2014, DTU

**Appendix A8**

**Construction of new Pyrolysis Centrifuge Reactor**

**Energinet.dk project no. 010077**

**Treatment of Lignin and waste residues by flash pyrolysis**

**Trung Ngoc Trinh, Peter Arendt Jensen, Kim Dam-Johansen, Rasmus Lundgaard Christensen.**

*Department of Chemical and Biochemical Engineering*

Technical University of Denmark

Søltofts Plads, Building 229, DK-2800 Lyngby, Denmark

CHEC no. R1401

## 1. Limitations of pyrolysis centrifuge reactor setup

The PCR concept was developed in an attempt to obtain some advantages when compared to fluid bed reactors or circulating fluid bed reactors<sup>1</sup>. The PCR can use relatively large particle sizes due to a high heating rate created by a strong centrifuge force, the PCR is a compact design, and it can use a low flow rate of carrier gas and still obtain a short gas residence times (less than 1 s). The compact design may also make it possible to construct a mobile pyrolysis unit that can operate in-situ on a farmers field. Thus a high power consumption for grinding biomass to a suitable size and pumping and heating of a large amount of carrier gas is probably reduced in this concept. A first version of the lab scale PCR set-up was developed by Neils et al.<sup>1</sup> The PCR set-up operation manual is presented in appendix 1 and the reactor, char separator, cyclone and bio-oil condenser structures are presented in Figure 1. Wood and straw PCR pyrolysis were investigated by Niels Bech<sup>1</sup> and Norazana Binti Ibrahim.<sup>2</sup> Also nonconventional biomasses (lignin, sewage sludge and macroalgae) PCR pyrolysis have been investigated in this work. However the PCR set-ups have some limitations

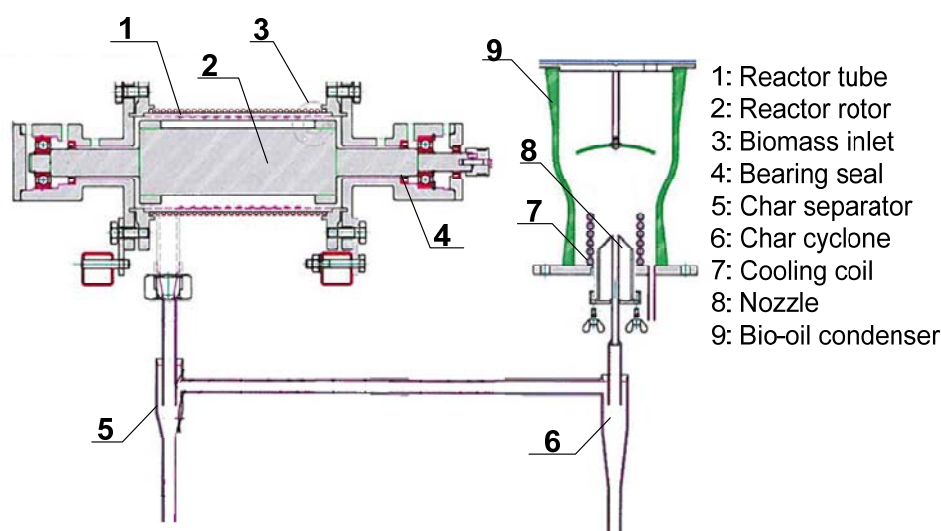


Figure 1: Sketch of the old PCR reactor, char separator, cyclone and bio-oil condenser.<sup>1</sup>

### a. High speed of rotor

A higher organic oil yield (e.g. 35 wt% daf for lignin pyrolysis) and a higher area-specific throughput could be obtained if the rotor speed has been increased to obtain a higher centrifugal force (RCF) and these values are found to significantly decreased at a centrifuge force of less than 10000 G because of a low biomass heating rate. The rotor construction is a cylindrical core that has attached three vertical blades that create a centrifugal force (see Figure 2). Lignin particles seem to obtain a relatively high heating rate at

the rotor speed of more than 14800 rpm. Thus, a PCR reactor scale-up to a reactor capacity with hundreds kg/h feeding probably have some risks due to the high rotor speed.

Solution:

A new rotor could be designed with arc shaped movable blades. Thus biomass particles are pressed on the hot reactor wall by both centrifugal and mechanical forces, leading to the biomass could obtain a high heating rate at a relatively low rotor speed.

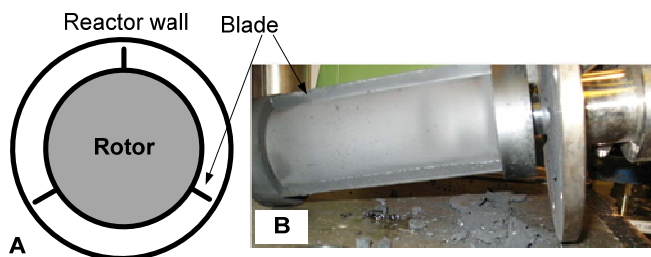


Figure 2: Sketch of PCR reactor (side view) (A) and picture of PCR rotor (B).

b. Block at nozzle:

A block at the nozzle at the inlet to the condenser appears in some cases when the PCR set-up is used even for short time experiments (down to 14 min with lignin). The block is probably formed by agglomeration of fine char particles and heavy organic species. In the first version of the PCR set-up, a cooling surface area of the bio-oil condenser was 180 cm<sup>2</sup>. The cooling surface area is found to be insufficient to keep a constant liquid temperature of less than 65 °C in the condenser, causing a quick evaporation of iso-propanol solvent (that is added to condense bio-oil at the beginning of an experiment), water and a light oil fraction with conditions as a high gas flow rate and temperature higher than 50 °C. The cooling of the bio-oil in the condenser is controlled by a cooling bath having a temperature of 2 °C. The condenser cannot remain at a temperature lower than 60 °C within 14 min, consequently, the oil viscosity in the condenser increases rapidly (within 10 – 14 min), probably causing the blocking. Signs of blocking at the nozzle appears often when the condenser temperature is higher than 65 °C. In order to understand the influence of the cooling surface area on the blocking process, we connected an external cooler with a surface area of 100 cm<sup>2</sup> to the existing internal cooling system of the condenser, and thereby the experimental time could be increased to 25 min. For some runs, we tried to get the bio-oil out of the condenser and added more condensing solvent (having a temperature of 12 °C). Then the PCR lignin experiments could be performed for 60 – 70 min. Besides, the blocking is probably also due to the nozzle size. The nozzle diameter of 4.8 mm may be too small to avoid the plugging for a long PCR test.

Solution:

- The cooling surface area of the condenser should be calculated and designed again to keep a constant temperature at a low level (less than 40 °C). This minimizes the evaporation of solvent, water and light oil fraction thus the oil viscosity in the condenser could be maintained at a low value during experiments.
- The diameter of the nozzle should be enlarged to minimize the blocking but it must be considered to maintain a gas velocity that ensures that the liquid does not drop down in the char cyclone (see Figure 1).
- The light oil fraction collected after the aerosol coalescer should be recycled to the condenser to reduce oil viscosity.

c. Sticking blades of gas pump

The gas pump is blocked after 70 - 80 min performing experiments. The problem is supposed to be caused by aerosol formed during pyrolysis that deposits accumulatively in the centrifugal gas pump and sticks to blades of the gas pump. The aerosol coalescer seems not to collect effectively the tiny aerosol particles (particle size of 10 nm to 500 nm).

Solution:

An aerosol coalescer should be replaced by an electrostatic precipitator that is known to more effectively aerosols.

d. Low pressure bearing seals

Two seals at the bearings of the PCR reactor have a operation pressure limitation of 0.5 bar. Thus, the PCR set-up cannot operate at a pressure higher than 0.5 bar. Biomass fast pyrolysis is often performed at an atmospheric pressure or very low pressure. However the seals are easily broken if the pressure increase because of a block in the system.

Solution:

- High pressure seals that could operate at a rotor speed of 5000 rpm should replace the current seals that made it difficult to conduct experiment and make larger modification impossible.

## 2. Development outline of the new pyrolysis centrifuge reactor setup

### 2.1. Development objectives of the new pyrolysis centrifuge reactor setup

Recent studies show that by adding hydrogen (at atmospheric pressure)<sup>3</sup> or using catalysts (e.g zeolite types at atmospheric pressure)<sup>4</sup> in a fast pyrolysis process a bio-oil with less oxygen content and a higher heating value may be produced. The bio-oil may then be used as a feedstock for conventional refinery processes. The objectives of the new PCR set-up are to obtain flexibility in operation. By small modifications of the set-up it shall be possible to conduct the following type of experiments:

- Conventional fast pyrolysis.
- Hydrogen fast pyrolysis.
- Catalyst fast pyrolysis.

Also the new PCR set-up was designed to overcome the limitations of the first PCR version. It is expected to work at a relatively low rotor speed (less than 2800 rpm) in a continuous mode and also to obtain a relatively high bio-oil yield, and use a relatively large biomass particle size (few millimeters).

### 2.2. Development outline of pyrolysis centrifuge reactor setup.

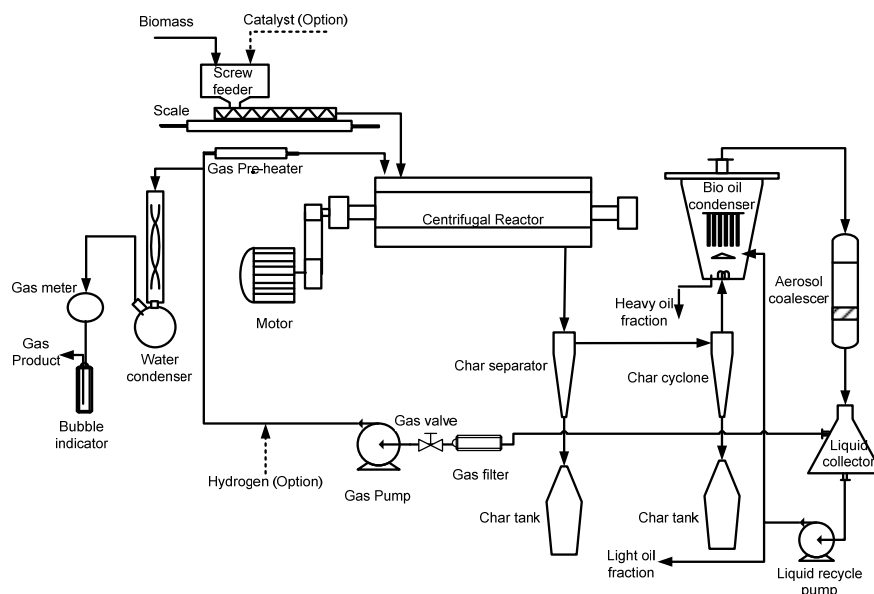


Figure 3: Simplified PI Diagram of new PCR set-up

#### 2.2.1. Operational principle.

The operational principle of the new PCR set-up is based on the old set-up.<sup>1</sup> The main modifications of new set-up are on the reactor and the bio-oil condensing system (see detail at parts 2.2.2 and 2.2.3). A



simplified PI-diagram of the new PCR set-up is presented in Figure 3 and a detailed PI-diagram is shown in appendix 2. The design capacity of the set-up with respect to the condenser cooling system and the reactor is 1 kg/h to 3 kg/h of biomass input. However, the maximal capacity with respect to bio-oil yield will be determined when the set-up is tested.

Biomass is introduced into the horizontally oriented reactor by a screw feeder. The rotation of the reactor rotor with arc-shape movable blades presses biomass particles on the hot surface of the reactor wall and drive the solid particles forward. The char is separated from the gas by both centrifugal and mechanical forces. The rotor speed is expected to be less than 2800 rpm. Heat is provided by three heating elements wrapped along the length of the reactor to maintain reactor wall temperatures of 400 – 600 °C. Char is separated by a char separator (change-in-flow separator) and a cyclone. The char separator and cyclone should keep at temperatures of 300 – 500 °C to avoid condensation of bio-oil, char blocking and further cracking of the bio-oil. Vapor is condensed in the bio-oil condenser where the temperature is about 30 – 40 °C to minimize evaporation of solvent (that is added to condense bio-oil at the start of an experiment), water and light oil fractions. Evaporation leads to an increase of oil viscosity in the bio-oil condenser. The cooling of the bio-oil condenser is controlled by a cooling bath having a cooling water temperature of 2 °C. The aerosol formed during fast pyrolysis and light oil fraction are further condensed by an aerosol coalescer and a gas filter. Some of the light oil fraction collected in the coalescer is recycled to the bio-oil condenser to reduce oil viscosity. Thus the heavy oil fraction is collected from the bio-oil condenser and the light oil fraction is collected from the coalescer. A part of the gas product is recycled to the reactor. Before entering the reactor, the gas is heated to 400 – 500 °C. The recycled gas flow rate related to gas residence time is controlled by a gas valve. The set-up can use gas residence times in the range of 0.5-5 s. The volume of produced gas product is measured by a gas meter. In case the set-up is used with the hydrogen injection option, the hydrogen is mixed with the recycled gas before entering the reactor. If it is wanted to use catalytic fast pyrolysis, biomass and catalyst may be mixed before being feed to the reactor.

### 2.2.2. The new PCR reactor.

The new reactor structure is shown in Figure 4 (a detail drawing of the reactor is presented in appendix 3) and pictures of the reactor are shown in Figure 5. With the arc-shape movable blades, the biomass particles are pressed on to the hot reactor walls not only by the centrifugal force but also by mechanical force. The clearance between the wall and the rotor is 5 mm and the tips of the blades rotate freely from the rotor to the reactor wall (see Figure 4D). This allows the reactor to possibly treat relatively large particle sizes (a maximum of 5 mm). With the given reactor structure, a high biomass heating rate is probably obtained at a

low rotor speed. However in an earlier test the rotor speed is found to be proportional with the PCR solid residence time.<sup>1</sup> The decrease of rotor speed may result in an increase of the solid residence time.

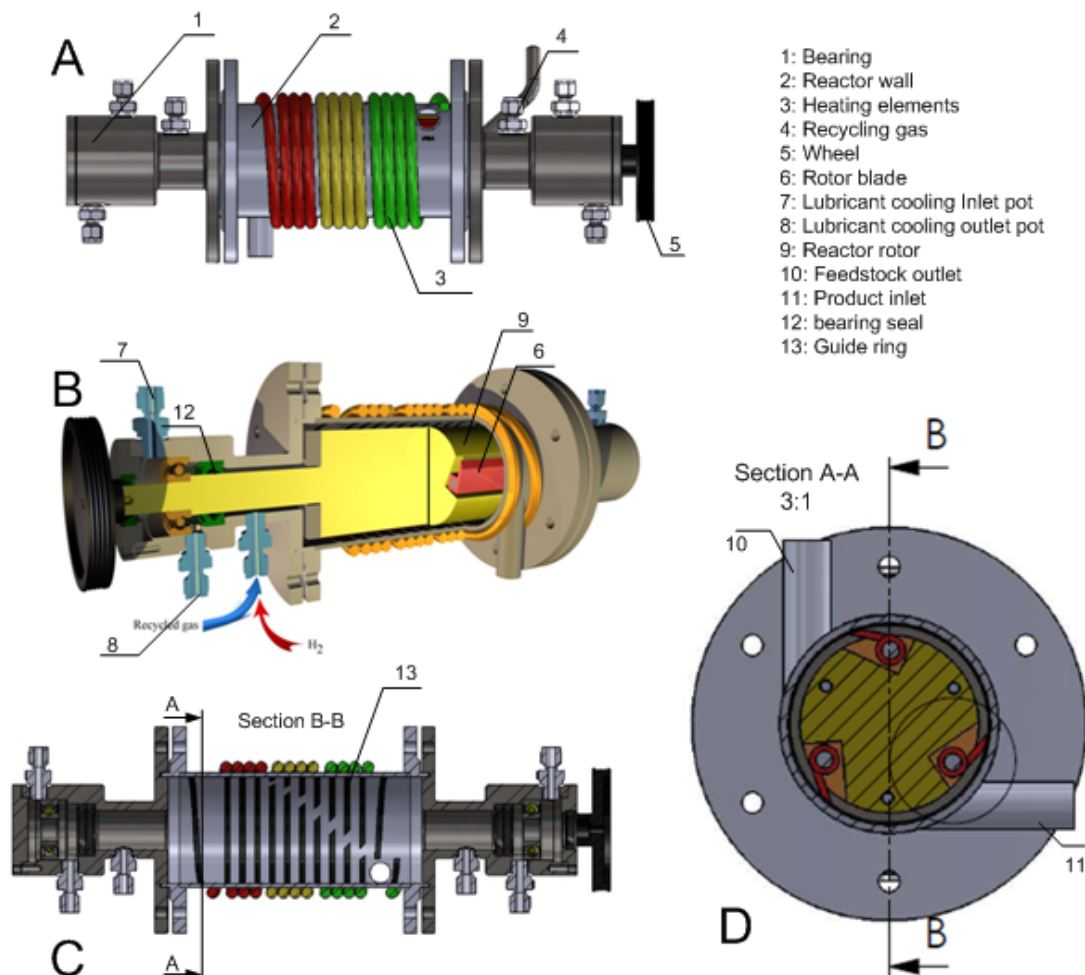


Figure 4: Modified pyrolysis centrifuge reactor removed insulation (A: overview of PCR reactor, B: cut-view of reactor, C: cut-view of reactor without rotor (front view), D: cut-view of reactor (side view))

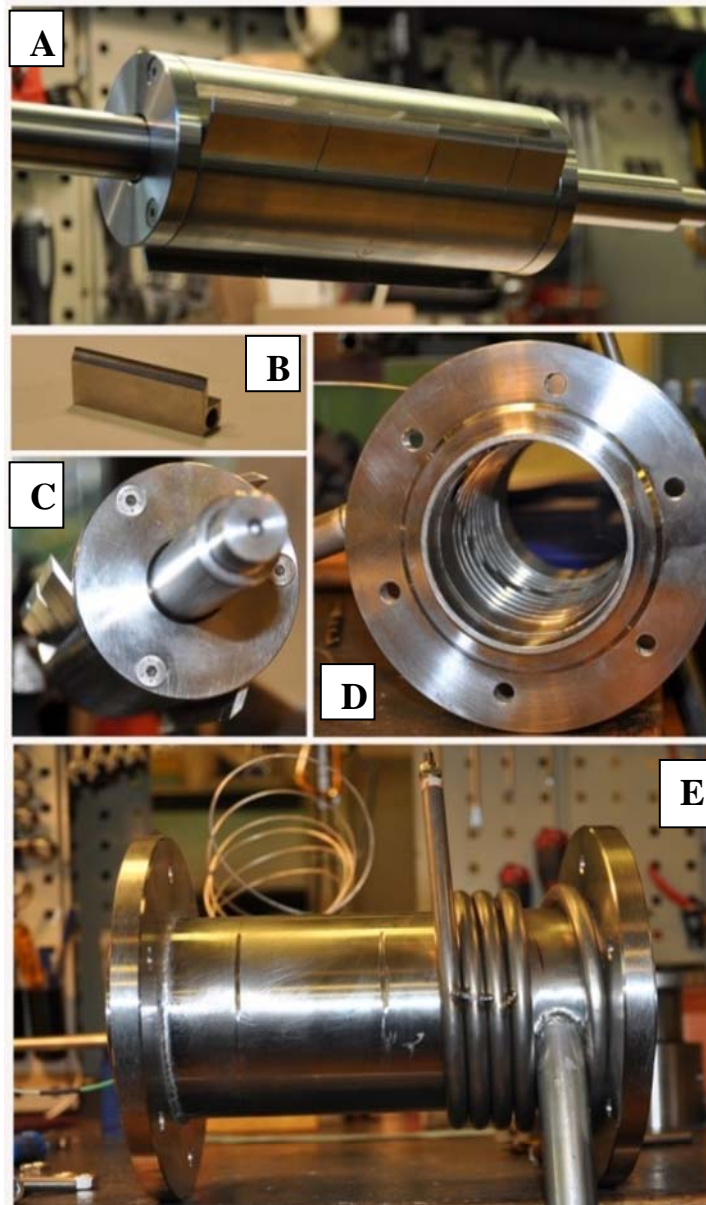


Figure 5: The new pyrolysis centrifuge reactor (A, C: reactor rotor, B: rotor blade, D: reactor wall with guide rings, E: reactor wall with heating elements)

Guide rings on the reactor wall are cut to control the movement of the particles in the reactor chamber (see Figure 4C). Helix rings at both ends of the reactor tube are added to guide the solid and vapor flows towards the exit. New bearing seals that have a operation pressure limitation of 10 bar are installed to increase the robustness of the reactor system.

### 2.2.3. Bio-oil condenser

The old bio-oil condenser has an insufficient cooling surface area for operating a long time. Based on the experimental data, the cooling surface area of the bio-oil condenser is calculated to be  $800 \text{ cm}^2$  for a feed rate of  $1 \text{ kg/h}$  of biomass. The calculation is presented in appendix 4. In order to avoid a plug of the nozzle, the diameter of nozzle is enlarged to  $10 \text{ mm}$  (see Figure 6). However a suitable diameter of the nozzle that prevent the plug and also prevent a fall down of liquid from the condenser to the cyclone should be examined in the trial tests.

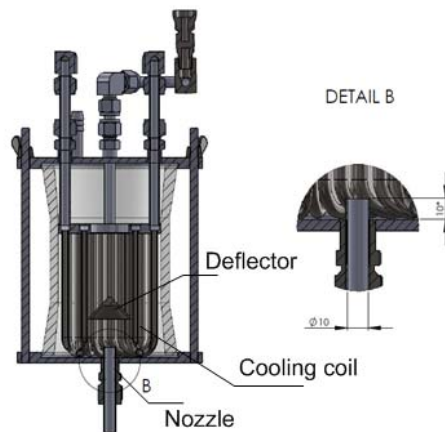


Figure 6: Bio-oil condenser

### 2.3. Final version of new pyrolysis centrifuge reactor setup

The main specifications of the new PCR set-up and old PCR set-up are summarized in Table 1 and the detail engineering construction drawings of the new set-up are shown in appendix 3.

Table 1: Specifications and main dimensions for the new experimental set-up and old experimental set-up

Specification	Value	
	New reactor	Old reactor
Reactor		
Reactor length (mm)	187	185
Reactor inner diameter (mm)	81.4	81.4
Reactor contacted surface area (m <sup>2</sup> )	0.051	0.051
Reactor wall-to-rotor clearance, max (mm)	5	2.2
Rotor speed of motor wheel, max (rpm)	2820	2820
Rotor speed of reactor wheel, max (rpm)	2820	20000
Motor, related power, max (W)	370	370
Reactor heating (Inconell 600, Ø 8.5 mm)		
Zone split over full reactor power (W)	1000:1000:1000	510:170:510:680
Heating temperature, max (°C)	980	900
Tracing at cyclone (HQS HORST)		
Tracing temperature , max (°C)	900	900
Power, max (W)	370	370
Length (m)	2.1	2.1
Tracing at nozzle (HQS HORST)		
Tracing temperature , max (°C)	900	900
Power, max (W)	170	170
Length (m)	1	1
Temperature sensors for all		
Type	K-type thermocouple	K-type thermocouple
Temperature range (°C)	-100 to 1100	-100 to 1100
Accuracy @ 500 °C	± 2	± 2
Gas preheater (AIR PROC)		

Temperature, max (°C)	540	540
Power (W)	750	750
Gas pump		
Flow rate, max (L/min)	58	58
Power, max (W)	120	120
Temperature, max (°C)	50	50
Bio-oil condenser		
Total volume (l)	1.5	1.5
Total cooling surface area (cm <sup>2</sup> )	800	150
Feeder		
Feeder rate range (L/h)	0.1 - 105	0.1 – 105
Agitation	Yes	Yes
Volume (L)	8	8
Gas meter		
Gas flow, max (Nm <sup>3</sup> /h)	5	5
Accuracy, %vol	± 0.5	± 0.5

### 3. Conclusions

The new lab scale PCR set-up has been constructed and is ready for trial tests. Considerable modifications of the reactor and condenser designs have been done to overcome the limitations of the old PCR set-up. It is expected that the new PCR can obtain a high bio-oil yield at a relatively low rotor speed (less than 2800 rpm). The new rotor design is protected by a submitted patent proposal.

### References

1. Neils Bech, In situ flash pyrolysis of straw. PhD thesis 2008, DTU chemical engineering
2. Norazana Binti Ibrahim, Bio-oil from Flash Pyrolysis of Agricultural Residues, PhD thesis 2012, DTU chemical engineering
3. Mukkamala, S.; Wheeler, M. C.; van Heiningen, A. R. P.; DeSisto, W. J. Energy Fuels 2012, 26, 1380-1384.
4. Bridgwater A.V. biomass and bioenergy 2012, 3 6 8 - 9 4

## Appendix 1

Operational manual for old pyrolysis centrifuge reactor set up

Version TNT - 19 Nov 2010

## Preparation

- Turn on the main power.
- Close flow rate meters (F1, F2 and F3), open the nitrogen gas source, adjust nitrogen pressure regulator (PG1) at 0.5 bar.
- Check the nozzle of bio oil condenser (C3) for sure that no block inside.
- Check the pipes of char separator (C9) and char cyclone (C10) for sure that no block inside by a drill.
- Close valve V6 and V7, open valve V2 and set flow rate meter (F1) at level of 20 mm to purge ethanol, pyrolysis products in the last run about 4 minutes and then close the F1.
- Adjust pressure in system (P1) to zero by valve V8. Check gas pump (C11) can turn freely and check for noise. Turn off after checking.
- Assemble bio oil condenser (C3) (remember a slight layer of vacuum silicone gel is coated between rubber seal and steal or glass).
- Weight empty char tanks (C9 and C10) and then connect them to char separator (C8) and char cyclone (C7) (a slight layer of vacuum silicone gel is coated between rubber seal and steal or glass).
- Weight Aerosol coalescer (C4) and then connect the rubber tube to bio oil condenser (C3).
- Weight empty bio oil collector (C5) and connect to both bio oil condenser (C3) and gas pump (C11).
- Check empty screw feeder (C1) and then weight feedstock and fill into screw feeder. Close the cap of feeder (there is a rubber seal between cap and feed tank).
- Prepare about 120ml i-propanol( or previous bio oil) for condensing bio oil product in bio oil condenser (C3).
- Prepare tissue in beaker and weight in order to clean bio oil after run in bio oil condenser (C3)

## Leak check and purge

- Close valve V3, V4, V5, F3, V10, V12, V13. Open valve V2, V6, V7, V8. Set pressure meter (P2) at 200mbar by adjusting F1 and then close valve V-2. Wait for 5 mins, if pressure indicated P2 is not decreased less than 150mbar. This means no leak in system, otherwise leak in somewhere.  
In case leak, using snoop check all connections in system and cap of feeder to find leak and fix them.
- After checking leak, the valve V4 and V2 are opened to purge air in feed tank (C1) about 10mins and then close V4, open V12.

## Setting parameters and run

- Turn on mini gas pump (C18) and set F3 of 10 mm
- Turn on electric control box and set the tracing values for S6 of 380 -420°C. Turn on and set oil circulation (S7=70°C) (check rotation of rotor at lubricant oil tank (C17)
- When the tracing and oil temperature have reached the SP, connect the power of motor and then start motor at 30Hz
- Turn on the thermal control box. Set the temperature at four zones in reactor and gas pre-heater (S5, S1, S2, S3, S4).
- When the temperature of reactor zones (S1, S2, S3, S4) and gas pre-heater (S5) have reached the set points. Adjust pressure in system (P2) to zero by valve V8, start gas pump (C11). And adjust from zero to set point by valve V-8 and pressure meter P1.
- Open sufficiently valve V9 for cooling water that is used to control S10 about 38 – 42°C and valve V1 for cooling air. Check water and air to vent.
- Weight empty syringe and then get approximately 120g i-propanol (or bio oil in syringe), open valve V5 to inject the i-propanol (or bio oil) into bio oil condenser (C3). Close valve V-5. Be careful that i-



propanol has a low boiling point of 82°C and thus avoid to inject i-propanol in C11 before run long time.

- Close the valve V-2.
- Set rotor speed to set point.
- Note all temperature reading
- Note gas meter reading.
- Set the agitation and feeder then start. Note time.
- Half-way through the run make a note of all readings and note time (time ½) in data sheet.
- Stop feeder when desired time has elapsed and note time.

### **Collecting products**

- Turn off tracing.
- Reduce rotor speed to 30hz
- Reduce gas pre-heater and all zones in reactor to 15°C.
- Note gas meter reading.
- Open valve V3 and crank up large flow rate meter (F2) shortly in order to purge product inside reactor. Close F2 and V3.
- Open valve V2 and adjust small flow rate meter (F1) at level 20 mm.
- Turn off gas pump (C11).
- Close valve V6, V7, then dissociate and weight char tanks (C9 and C10).
- Open V5, V10, use the syringe to collect bio oil from C3 and C12 and weight
- Weight bio oil from bio oil collector (C5)
- Collect bio oil from C3, C12, C5 and filter it by Whatman filter paper # 7, the filtered liquid is kept to analyze water content, HHV, pH, viscosity,... the solid remained on the filter paper is continuously washed by ethanol and acetone and is considered as char fraction, put the char on the disk and dry under inferred light about 20mins then weight
- Turn off cooling water (V9)
- Disconnect and weight aerosol coalser (C4).
- Disassemble bio oil condenser, wipe off bio oil remaining on bio oil condenser by the tissue and weight.

### **Cleaning and shutting down.**

- Open valve V8, inject 20ml ethanol to this way to clean reactor and close V8.
- When all zones temperature of reactor is below 180°C turn off motor.
- Close vale V2 and low flowrate meter (F1).
- When temperature is below 120°C, turn off oil circulation (C15).
- Open valve V6, V7, clean down pipes of char separator (C10) and char cyclone (C9) with drill.
- Open the feed tank (C1), withdraw the residual feedstock and weight.
- Adjust pressure in system (P2) to zero. Open valve V8, turn on gas pump to remove ethanol inside reactor. Turn off gas pump and close valve V8.
- Turn off the main power.
- Close the nitrogen gas source.

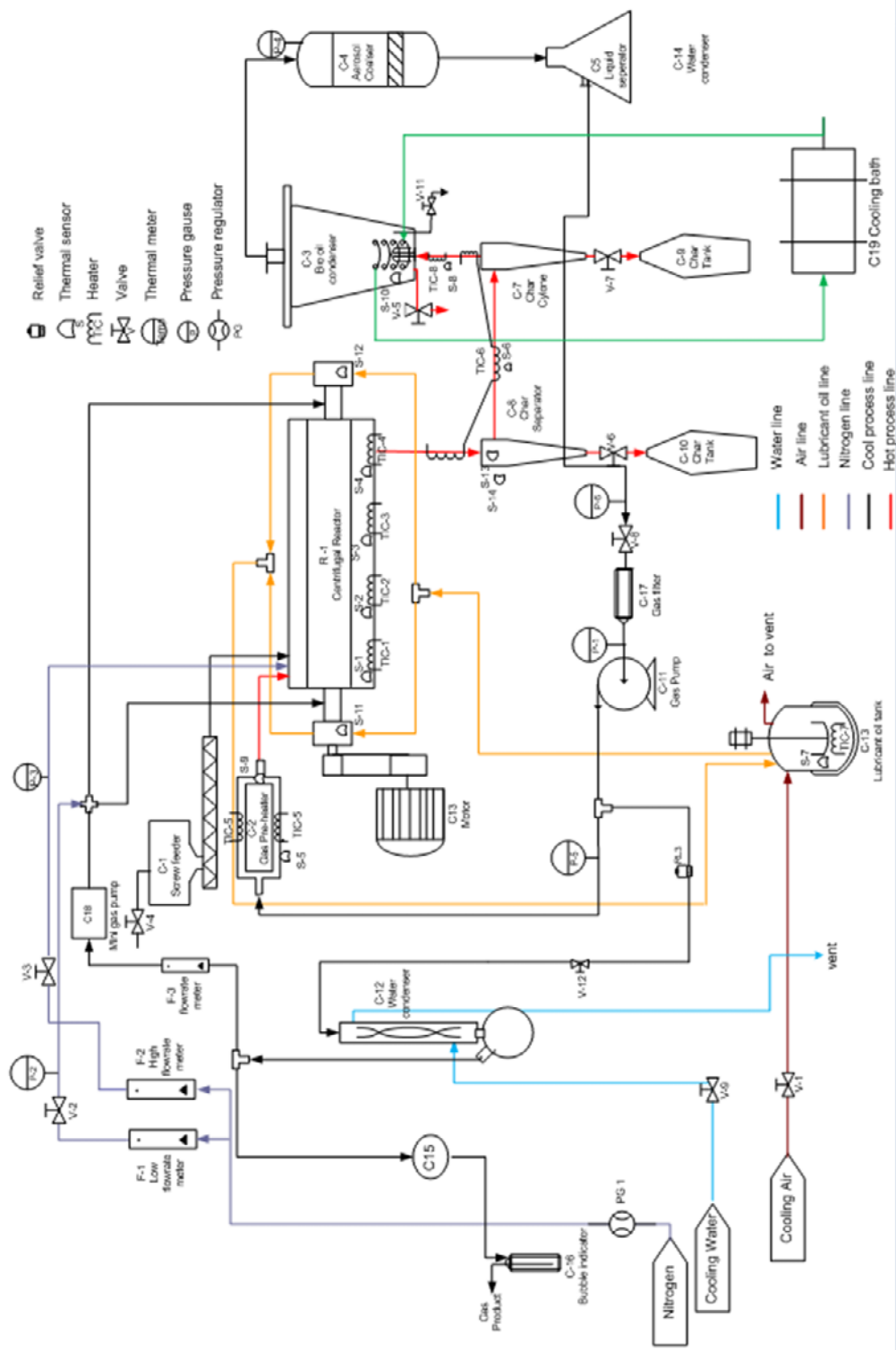


Figure 1: The PI diagram of old PCR set-up

## List of components

C-1: Screw feeder.

C-2: Gas preheater.

C-3: Bio-oil condenser.

C-4: Aerosol coalescer.

C-5: liquid separator.

M-13: Motor.

C-7: Char cyclone.

C-8: Char separator.

C-9: Char tank.

C-10: Char tank.

C-11: Gas pump.

C-12: Water condenser.

C-13: lubricant oil tank.

R -1: Centrifugal reactor.

C-15: Gas meter.

C-16: Bubble indicator.

C-17: Gas filter.

C-18: Mini gas pump.

TIC: Heating element.

S: Thermal sensor.

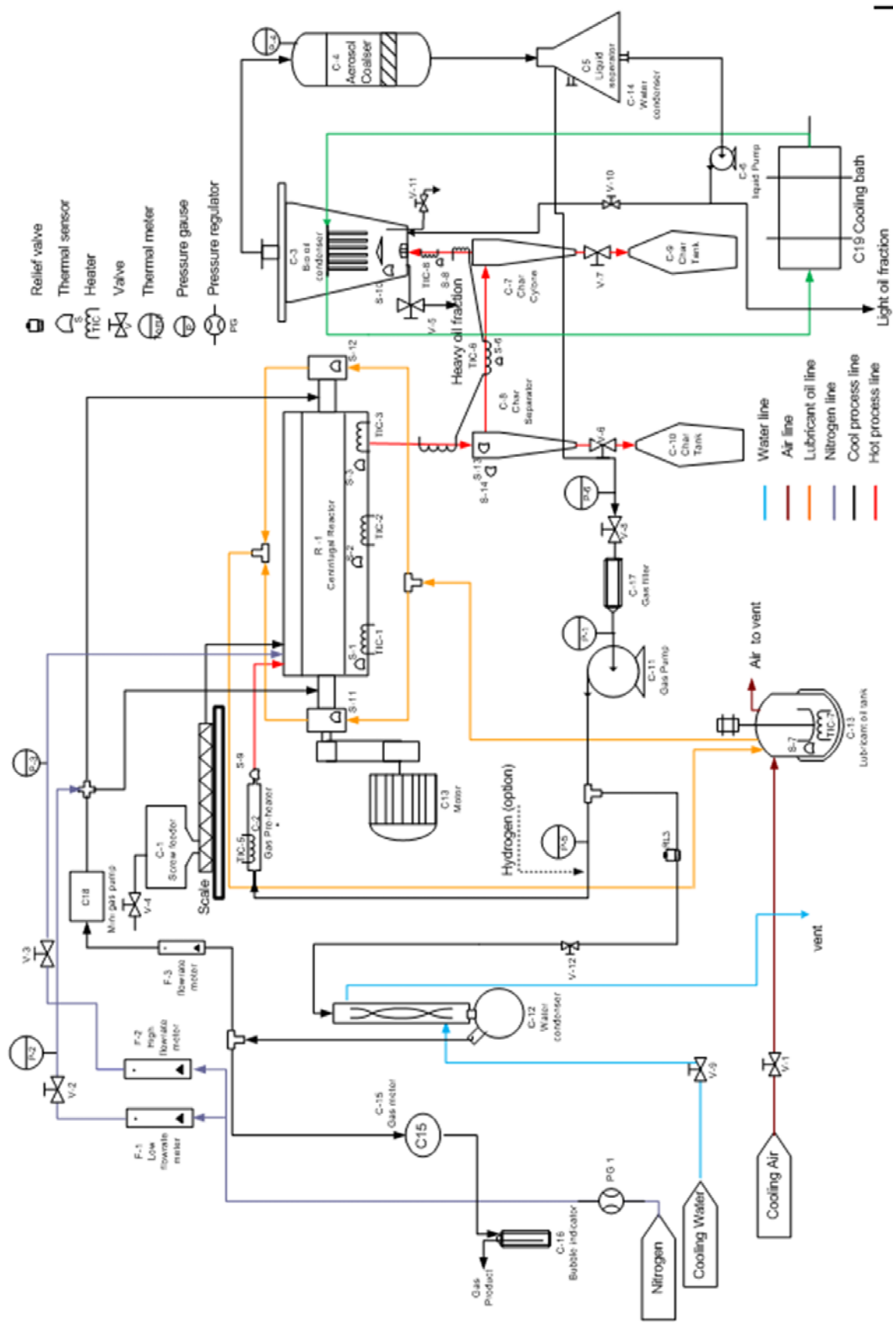
V: Valve.

P: Pressure meter.

F: Flow meter.

## Appendix 2

The PI – Diagram of new PCR set-up



## Appendix 3

The Pyrolyzer construction drawing

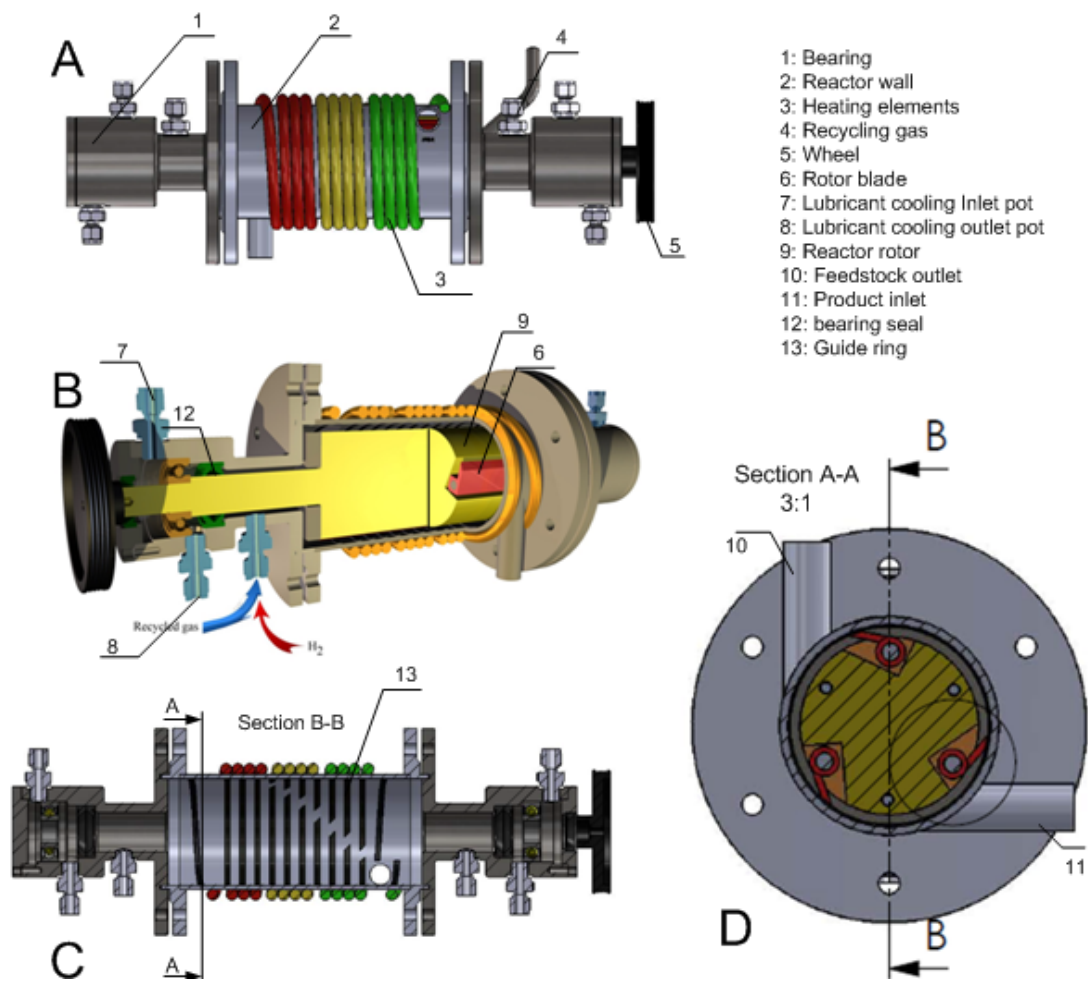


Figure 1: Figure 4: Modified pyrolysis centrifuge reactor drawing removed insulation (A: overview of PCR reactor, B: cut-view of reactor, C: cut-view of reactor without rotor (front view), D: cut-view of reactor (side view))





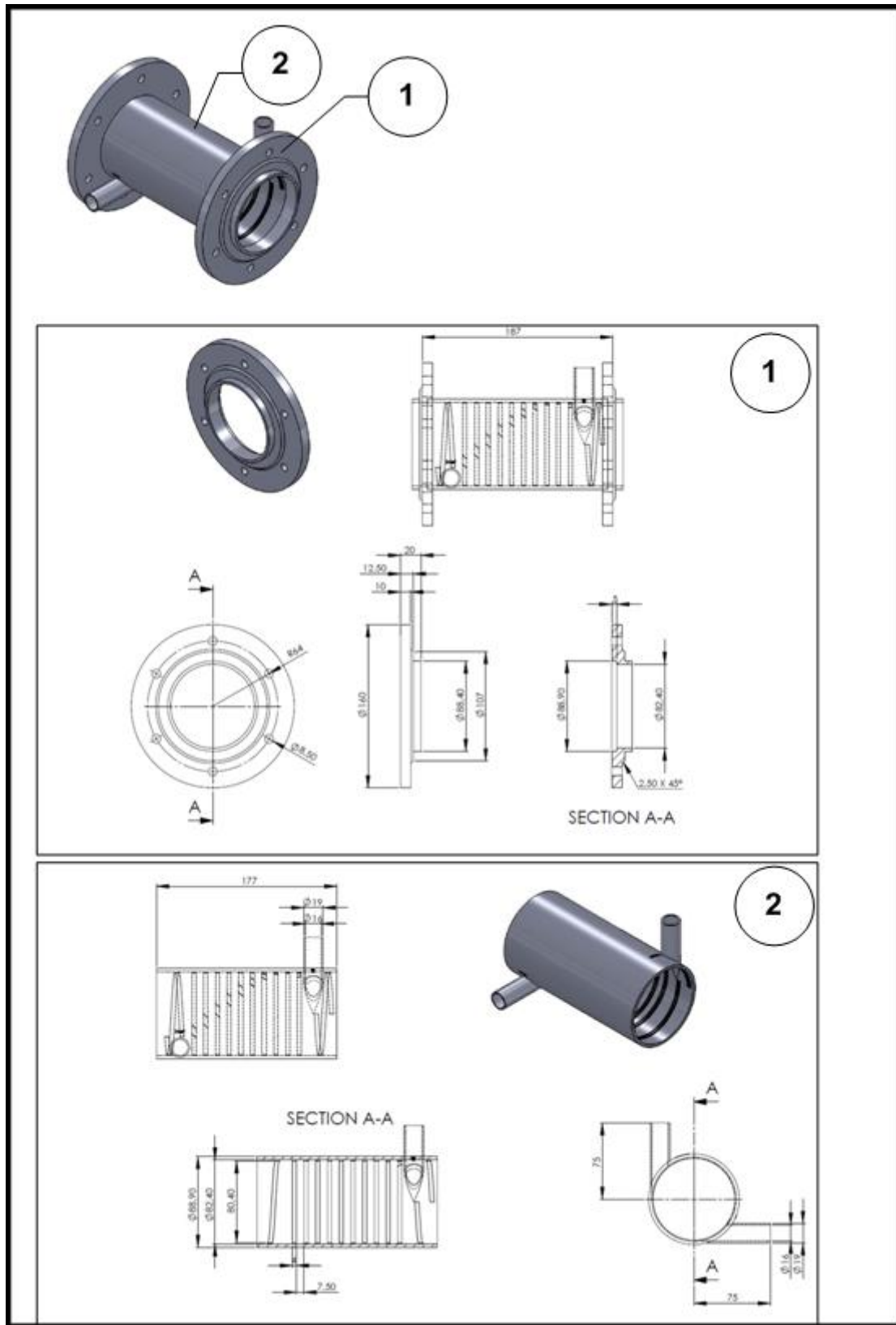


Figure 3: PCR reactor tube drawing.

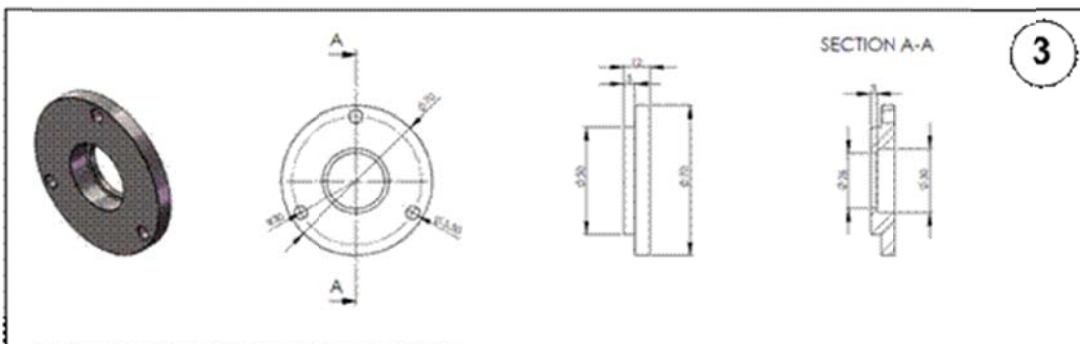
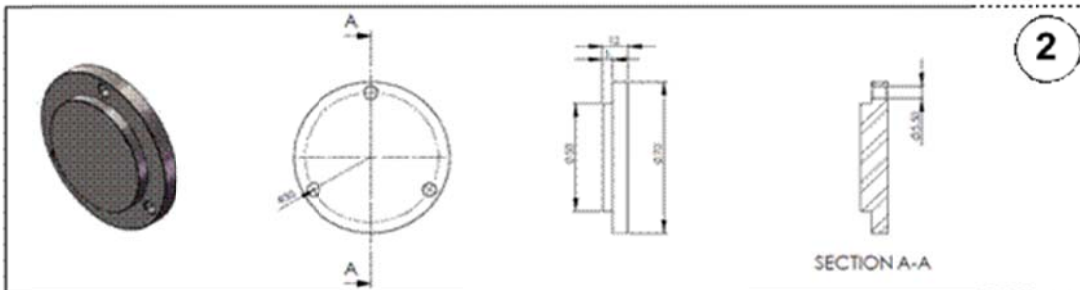
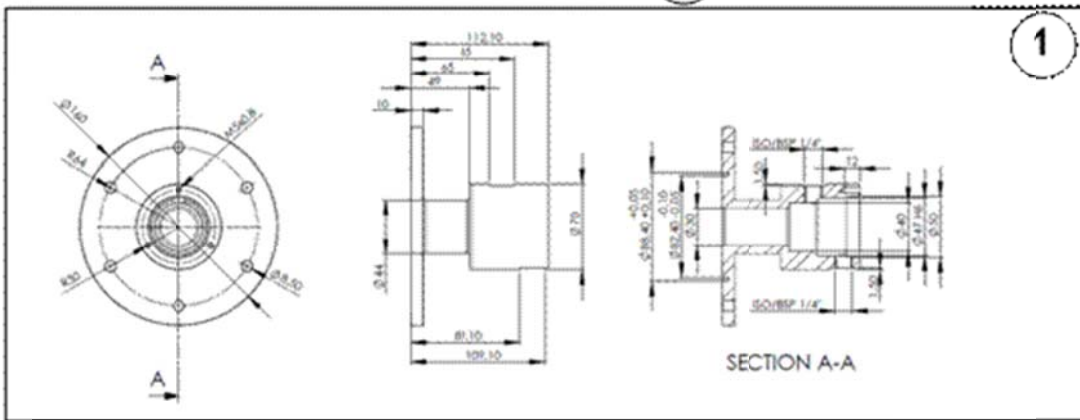
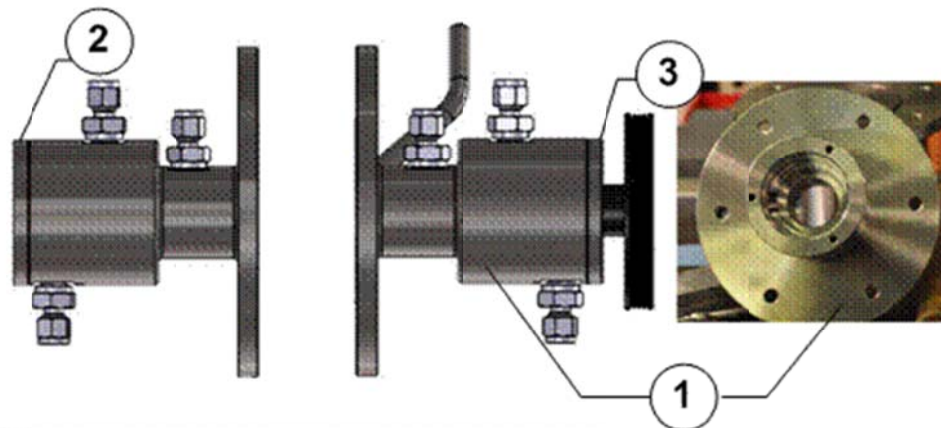


Figure 4: Bearings of reactor drawing.

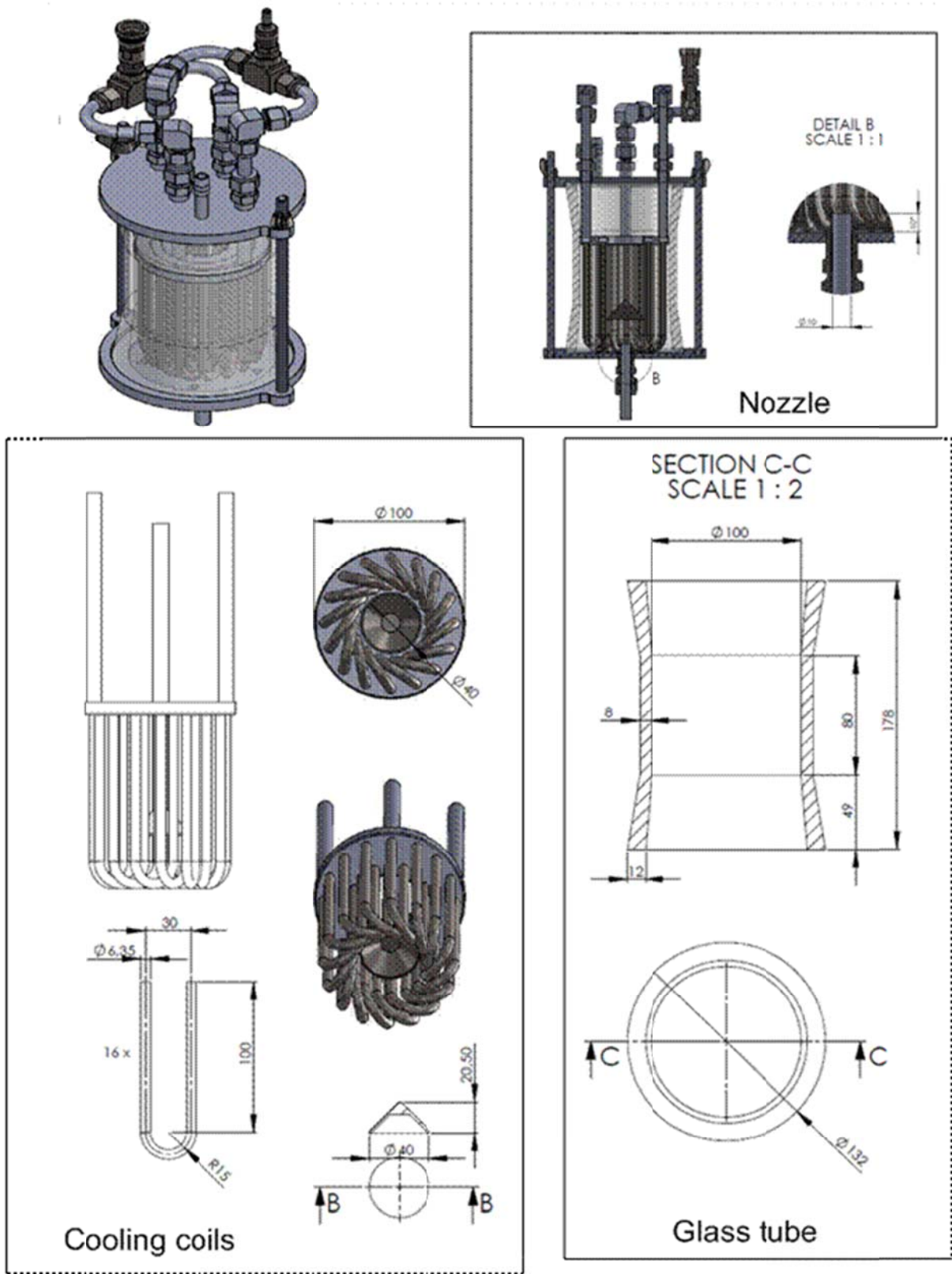


Figure 5: Bio-oil condenser drawing

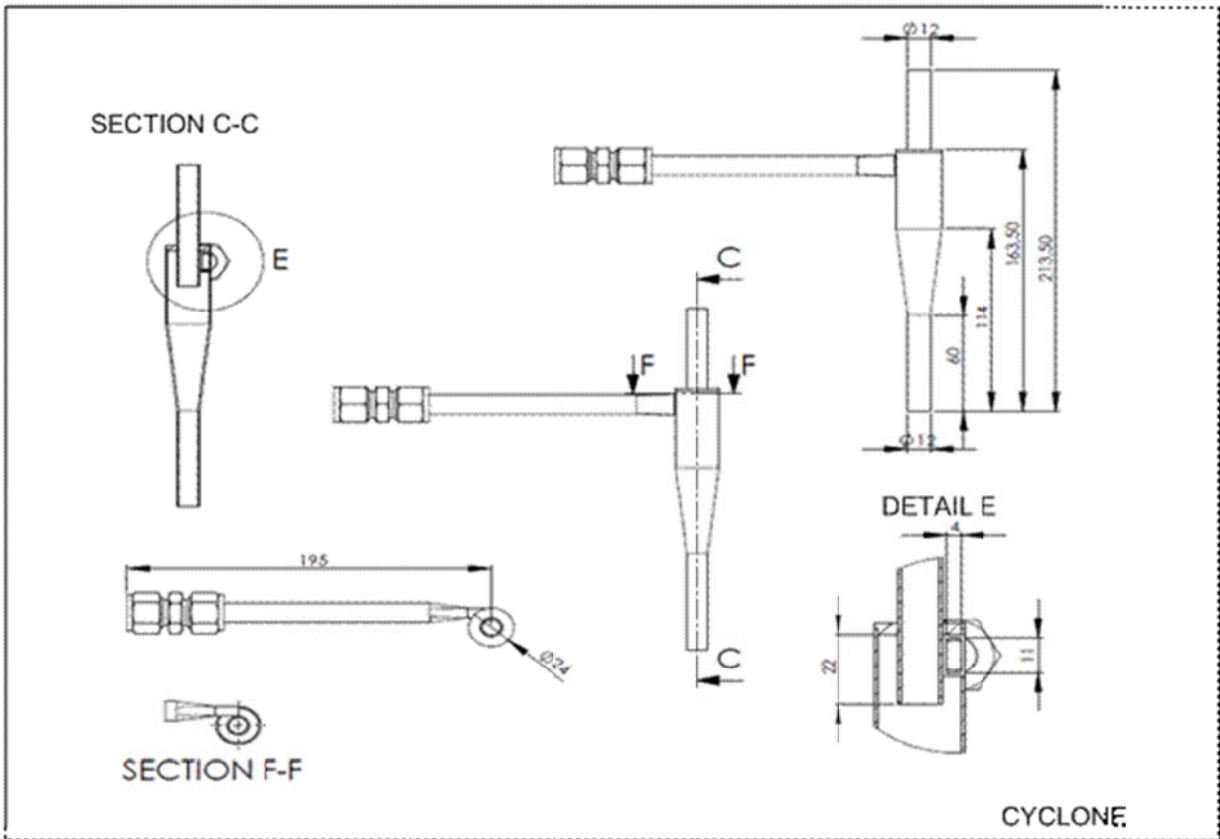
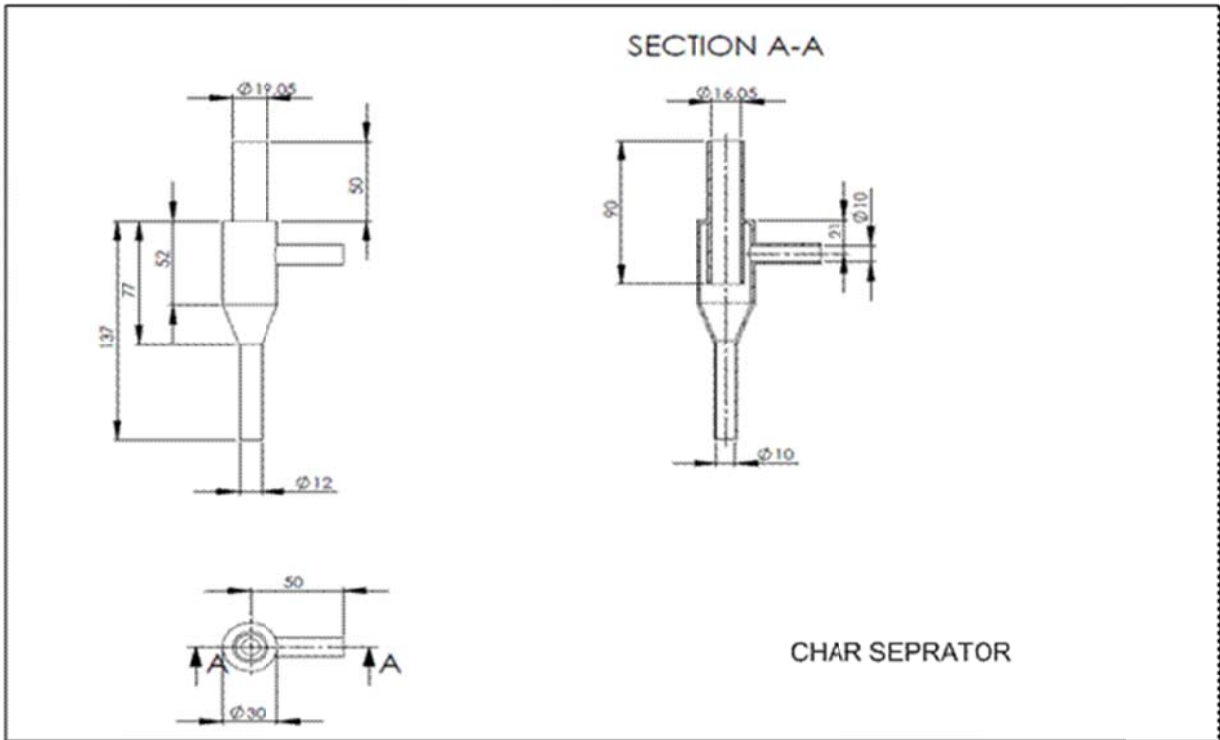


Figure 6: Char separator and cyclone drawings

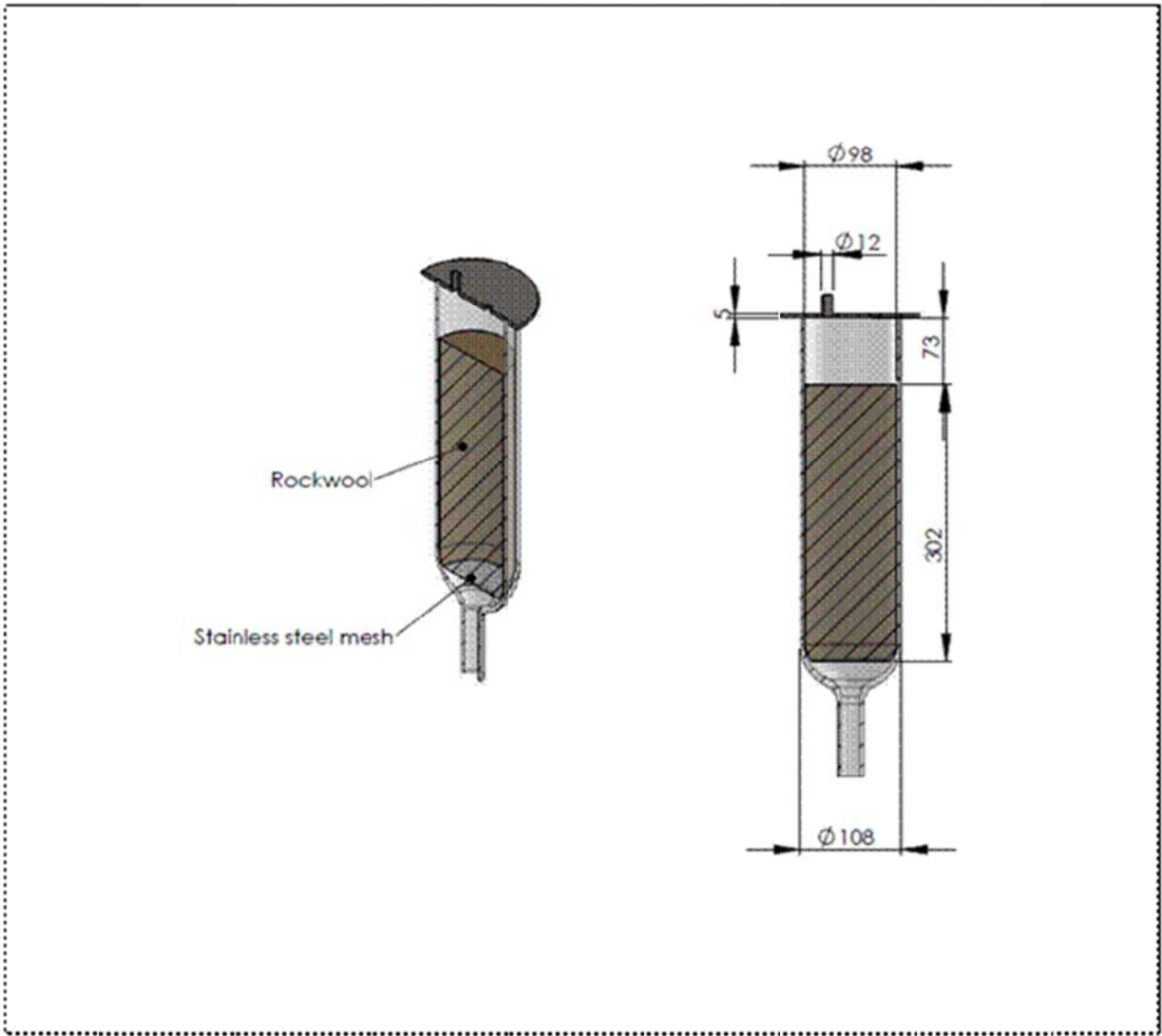


Figure 7: Aerosol coalescer drawing.

## Appendix 4

Calculation of surface area of bio-oil condenser

The cooling surface area of 180 cm<sup>2</sup> is found to be not enough for keeping a low constant temperature at the condenser. The surface area is calculated to design the new bio-oil condenser that can perform at a PCR reactor capacity of 1 kg/h. The surface area is calculated based on the equations from 1 to 11.

### Bio-oil heat release

$$Q_{oil} = Q_{oil1} + Q_{oil2} \quad (1)$$

$$Q_{oil1} = m_{oil} \times C_{P_{oil}} \times (T_{H1} - T_{H2}) \quad (2)$$

$$C_{P_{oil}} = 0.3 \times C_{P_{water}} + 0.7 \times C_{P_{organic}} \quad (3)$$

Assumed that bio-oil contain 30% water

$$Q_{oil2} = \delta_{oil} \times m_{oil} \quad (4)$$

$$\delta_{oil} = 0.3 \times \delta_{water} + 0.7 \times \delta_{porganic} \quad (5)$$

Assumed that bio-oil contain 30% water

### Gas heat release

$$Q_{gas} = m_{gas} \times C_{P_{gas}} \times (T_{H1} - T_{H2}) \quad (6)$$

$$m_{gas} = \rho_{gas} \times V_{gas} \quad (7)$$

### Total heat release from reactor

$$Q = Q_{oil} + Q_{gas} \quad (8)$$

### Calculate the surface area of the condenser

$$Q = A \times U \times \Delta T_{lm} \quad (9)$$

$$\Delta T_{lm} = \frac{(T_{H1} - T_{C2}) - (T_{H2} - T_{C1})}{\ln \frac{(T_{H1} - T_{C2})}{(T_{H2} - T_{C1})}} \quad (10)$$

### Surface area of the bio-oil condenser

$$A = \frac{Q}{U \times \Delta T_{lm}} \quad (11)$$

### Where:

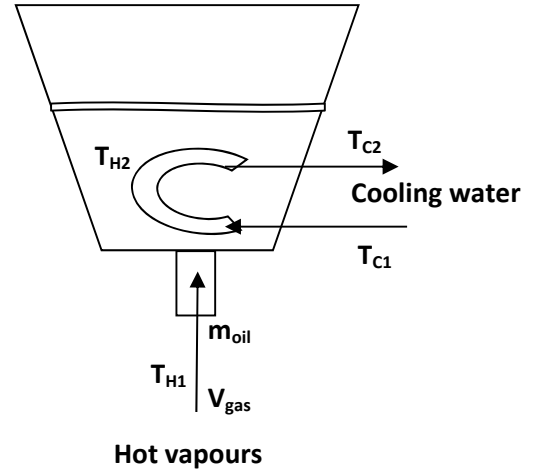
$Q_{oil}$ : Total heat release of bio-oil

$Q_{oil1}$ : Heat release by cooling from  $T_{H1}$  to  $T_{H2}$

$Q_{oil2}$ : Heat release by condensation of the bio-oil from vapor phase to liquid phase

$Q_{gas}$ : Total heat release of gas

$Q$ : total heat release when cooling from  $T_{H1}$  to  $T_{H2}$



$C_{p_{oil}}$ : specific heat capacity of bio-oil

$C_{p_{water}}$ : specific heat capacity of water

$C_{p_{organic}}$ : specific heat capacity of organic oil

$C_{p_{gas}}$ : specific heat capacity of gas

$\delta_{oil}$ : specific heat condensation of bio-oil

$\delta_{water}$ : specific heat condensation of water

$\delta_{organic}$ : specific heat condensation of organic

$m_{oil}$ : mass of bio-oil

$V_{gas}$ : flow rate of recycle gas

$\rho_{gas}$ : density of gas

$T_{H1}$ : inlet temperature of bio-oil

$T_{H2}$ : outlet temperature of bio-oil

$T_{C1}$ : inlet temperature of cooling water

$T_{C2}$ : outlet temperature of cooling water

A: total surface area

U: overall heat transfer coefficient

$\Delta T_{lm}$ : log mean temperature difference

Overall heat transmission coefficient values from various fluids are summarized in Table 1.<sup>1</sup> Water and heavy oil fluids cooler is supposed to be similar with that of water and bio-oil fluids therefore, it is selected to calculate the surface area of the bio-oil condenser. The real parameters of bio-oil have not found in the literature. Thus the specific heat condensation, the specific heat capacity of bio-oil and the overall heat transfer coefficient are investigated in a wide range that cover possibilities in reality to understand how these parameters influence to the surface area. Table 2 shows the parameters using for calculating a base case of surface area of condenser. These parameters are collected from previous PCR pyrolysis experiments and from similar fluids to bio-oil.

Table 1: Overall heat transfer coefficient in heat exchangers<sup>1</sup>

Hot Fluid	Cold Fluid	Overall heat transmission coefficient	
		W/m <sup>2</sup> K	KJ/h.m <sup>2</sup> .K
Organic solvents	water	250 – 750	900 - 2700



Light oils	Water	350 – 700	1260 - 2520
Heavy oil	Water	60 – 300	216 - 1080
Reduced crude	Water	75 – 200	270 - 720
Gases (1 atm)	Gases (1atm)	5 – 35	18 - 126

Table 2: The parameter selected to calculate for base case

Parameter	Value	Note
$T_{H1}$ , °K	773	Collected from cyclone of the PCR set up
$T_{H2}$ , °K	293	Collected from condenser of the PCR set up
$T_{C1}$ , °K	275	Collected from cooling water inlet of the PCR set up
$T_{C2}$ , °K	283	Collected from cooling water outlet of the PCR set up
$\delta_{water}$ , KJ/Kg	395	Table 1
$\delta_{organic}$ , KJ/Kg	270	Select gasoline – Ref 2
$\delta_{oil}$ , KJ/Kg	307.5	Equation 5
$C_{pwater}$ KJ/Kg.K	4.19	Table 1
$C_{porganic}$ KJ/Kg.K	2.3	Select light oil, 300°F – Ref 2
$C_p$ KJ/Kg.K	2.86	Equation 3
Biomass feed rate, kg/h	1	Design capacity for wood pyrolysis
$m_{oil}$ , kg/h	0.7	Assume that 70%*feedstock for wood case
$V_{gas}$ , m3/h	0.84	Collected from the PCR at gas resident time of 0.76 s
$\rho_{gas}$ , kg/m3	1.11	Select combustion products – Ref 2
$m_{gas}$ , Kg/h	0.93	Equation 7
$C_{pgas}$ , KJ/Kg.K	1	Select combustion gas - Ref.2
Qoil1, Kj/h	961	Equation 2
Qoil2, Kj/h	215	Equation 4
Qoil, Kj/h	1176	Equation 1
Qgas, Kj/h	446	Equation 6
Q, Kj/h	1622	Equation 8

$\Delta T_{lm}$ , K	124	Equation 10
U, Kj/h.m <sup>2</sup> .k	216	Select heavy oil – water - Ref. 1
A, m <sup>2</sup>	0.0607	Equation 11

The surface area of condenser is investigated various values of specific heat capacity, the specific heat condensation of bio-oil, gas residence time, log mean temperature difference and overall heat transfer coefficient. The results shown in Figure 1 - 4 have been found that these parameters have an influence to the surface area. The surface area varies from 100 to 800 cm<sup>2</sup>. Thus the surface area is proposed to be about 800 cm<sup>2</sup> for a feeding rate of 1kg/h.

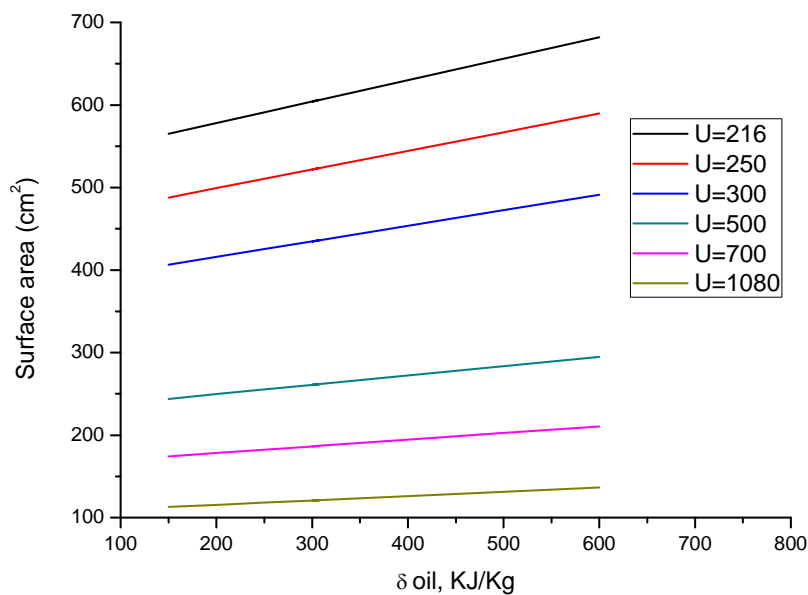


Figure 1: Effects of specific heat condensation of bio-oil ( $\delta_{oil}$ ) and overall heat transfer coefficients (U, Kj/h.m<sup>2</sup>.k) to the surface area of condenser ( $C_p=2.86$  KJ/Kg.K,  $\Delta T_{lm}=124$ K,  $\tau=0.76$ s)

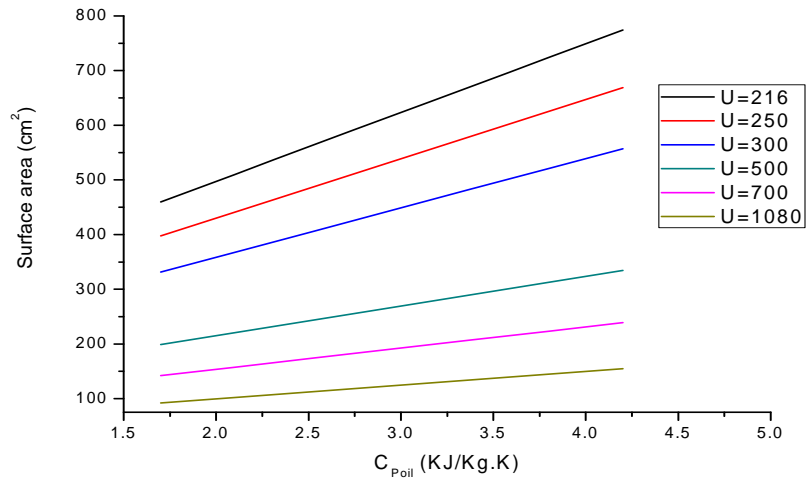


Figure 2: Effects of specific heat capacity of bio-oil ( $C_{p_{oil}}$ ) and overall heat transfer coefficient (U, KJ/( $hm^2K$ )) to the surface area of condenser (at  $\delta_{oil} = 307$  KJ/Kg,  $\Delta T_{lm}=124K$ ,  $\tau=0.76s$ )

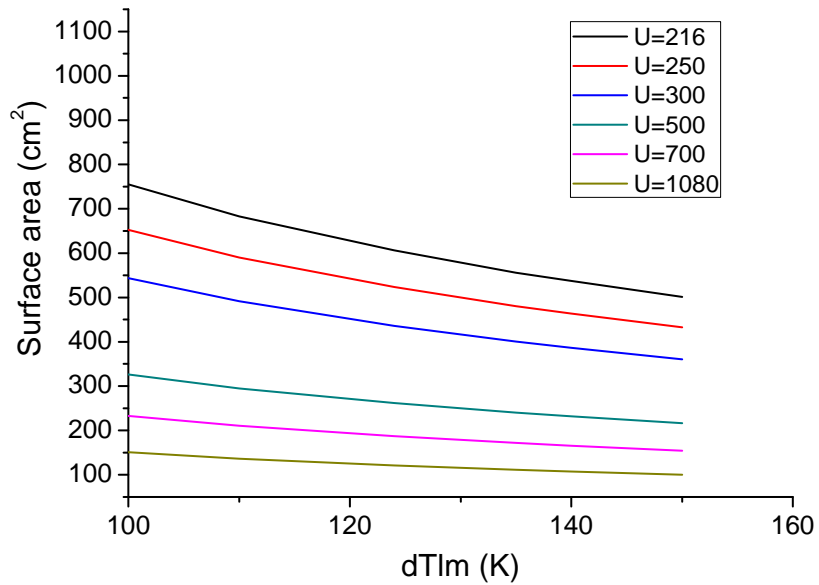


Figure 3: Effects of log mean temperature difference ( $\Delta T_{lm}$ ) and overall heat transfer coefficients (U, KJ/( $hm^2K$ )) to the surface area of condenser (at  $\delta_{oil} = 307$  KJ/Kg and  $C_p=2.86$  KJ/Kg.K,  $\tau=0.76s$ )

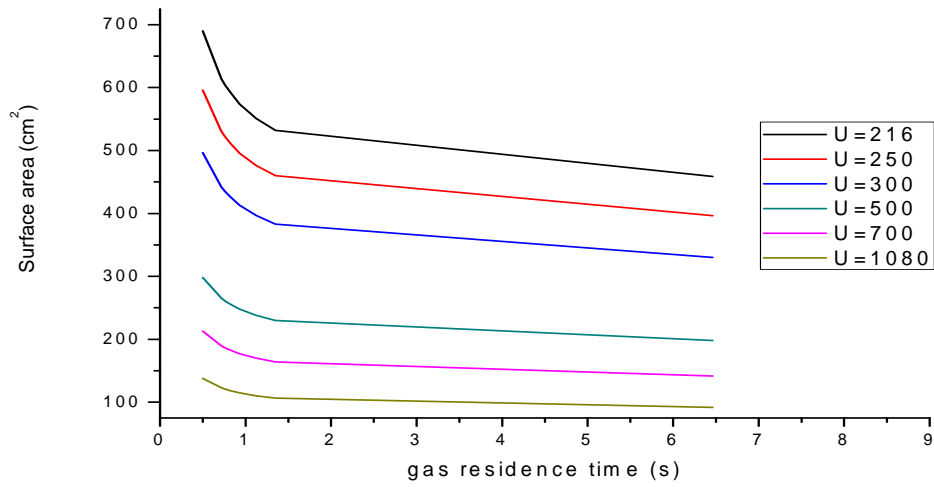


Figure 4: Effects of gas residence time and overall heat transfer coefficients ( $U$ ,  $\text{KJ}/(\text{hm}^2\text{K})$ ) to the surface area of condenser (at  $\delta_{\text{oil}} = 307 \text{ KJ}/\text{Kg}$  and  $C_p = 2.86 \text{ KJ}/\text{Kg.K}$ ,  $\Delta T_{\text{lm}} = 124\text{K}$ ,  $\tau = 0.76\text{s}$ )

References:

1. <http://www.engineeringpage.com/technology/thermal/transfer.html>
2. <http://www.engineeringtoolbox.com/>